IMMUNOACTIVE, ANTIBACTERIAL AND DRUG-CARRYING PROPERTIES OF SELECTIVE SURFACTANTS

Submitted by:

Lyné van Rensburg

MSc.Med.Sci. (Pharmacology) *cum laude*

For the degree of Doctor of Philosophy (PhD)

at Stellenbosch University, Department of Medicine, Division of Clinical Pharmacology

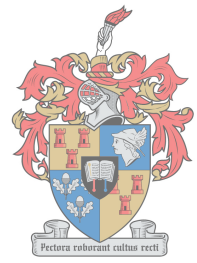

UNIVERSITEIT
iYUNIVESITHI
STELLENBOSCH
UNIVERSITY

Supervisor: Prof J.M. van Zyl

(Division of Clincal Pharmacology, Faculty of Medicine and Health Sciences, Stellenbosch University)

Co-Supervisor: Prof J. Smith

(Department of Pediatrics, Tygerberg Children's Hospital, Faculty of Medicine and Health Sciences, Stellenbosch University)

March 2018

DECLARATION

By submitting this dissertation electronically, I declare that the entirety of the work contained therein is my own, original work, that I am the sole author thereof (save to the extent explicitly otherwise stated) that reproduction and publication thereof by Stellenbosch University will not infringe any third party rights and that I have not previously in its entirety or in part submitted it for obtaining any qualification.

VERKLARING

Deur hierdie proefskrif elektronies in te lewer, verklaar ek dat die geheel van die werk hierin vervat, my eie, oorspronklike werk is, dat ek die alleenouteur daarvan is (behalwe in die mate uitdruklik anders aangedui), dat reproduksie en publikasie daarvan deur die Universiteit van Stellenbosch nie derdepartyregte sal skend nie en dat ek dit nie vantevore, in die geheel of gedeeltelik, ter verkryging van enige kwalifikasie aangebied het nie.

Date/ Datum: .....13 October 2017.....

Lyné van Rensburg

SUMMARY

Surfactant replacement therapy is used the treatment of neonatal respiratory distress syndrome as surfactant's biophysical behaviour helps to maintain proper lung function and reduces the work associated with breathing. Secondly, surfactant associated proteins are important role players in the innate immune response within the pulmonary environment and therefore assist in pulmonary host defence. However, natural and synthetic exogenous surfactants have gained much interest in other areas of therapy such as possibly aiding in dual-drug delivery systems for infectious or inflammatory pulmonary conditions. Both types have been studied extensively in animal models and in clinical trials and have elicited positive and negative effects on lung function. This thesis aims to determine whether a synthetic peptide containing surfactant, Synsurf®, may have potential immunomodulatory effects compared to the naturally derived surfactants, Curosurf® and Liposurf®.

Two formulations of Synsurf®, combined with the antibiotic linezolid were tested for its efficacy as a respirable compound in a pressurised metered dose inhaler. The outcome of these experiments revealed the prospect of Synsurf®'s adaptability as a pulmonary drug carrier. Furthermore, the tuberculosis isolates H37Rv and MDR-X51 displayed enhanced susceptibility to surfactant-drug micro-particle combinations.

The main findings of this study show that the natural surfactants Curosurf® and Liposurf® as well as Synsurf® inhibit secretion of pro-inflammatory cytokines and influence the production of reactive oxygen species in NR8383 alveolar macrophages and therefore influence cell viability. The inhibitory effects on cytokine secretion was displayed in a dose-dependent manner as well as a threshold effect that was seen for all three surfactants. This may result from unique mechanisms of decreasing cell signalling or up-regulating anti-inflammatory activity that was further elucidated by the employment of proteomics.

The findings in this thesis on the comparison of the two natural and one synthetic surfactant led to the following main conclusions: a) Different surfactant compositions modulate the anti-inflammatory activity in lipopolysaccharide stimulated alveolar macrophages via the possible involvement of different signalling pathways. The initial hypothesis regarding the protective nature that is linked to the protein content in natural surfactants is challenged and may be

deemed as “not fully supported” as these new findings suggest non-specific lipid or synthetic peptide protection with alveolar macrophages as seen with Synsurf®. b) Different surfactant compositions effect cell viability and morphology in a time and dose-dependent manner revealing that the treatment of neonatal respiratory distress syndrome may depend upon the specific preparation or dose used. c) All three surfactants displayed an impact on the antibiotic activity of linezolid that holds positive ramifications for drug loaded surfactants. d) The data shows that linezolid in combination with Synsurf® can be aerosolised in desired particle ranges for optimal lung deposition for a possible non-invasive, site-specific, delivery model via pressurised metered dose inhaler.

OPSOMMING

Surfaktantvervangingsterapie word gebruik in die behandeling van neonatale respiratoriese noodsindroom aangesien die biofisiese werking van surfaktant behoorlike longfunksie help handhaaf en die inspanning verbonde aan asemhaling verminder. Tweedens is surfaktantverwante proteïene belangrike rolspelers in die aangebore immuunreaksie in die pulmonêre omgewing, en bevorder dus pulmonêre gasheerverdediging. Tog is daar ook toenemende belangstelling in natuurlike en sintetiese eksogene surfaktante op ander behandelingsgebiede, soos dat dit moontlik dubbele middelleweringstelsels vir infeksie- of inflammatoriese pulmonêre toestande kan ondersteun. Albei tipes surfaktante is reeds omvattend in diermodelle en kliniese proewe bestudeer, en blyk sowel positiewe as negatiewe uitwerkings op longfunksie te hê. Hierdie tesis beoog om te bepaal of ’n surfaktant wat sintetiese peptiede bevat, naamlik Synsurf®, ’n moontlike rol in immuunregulering speel vergeleke met die natuurlik afgeleide surfaktante Curosurf® en Liposurf®.

Twee Synsurf®-formules is in kombinasie met die antibiotikum linezolid getoets vir doeltreffendheid as ’n inasembare verbinding in ’n drukinhalator met afgemete dosisse. Die uitkoms van hierdie eksperimente dui op die moontlike aanpasbaarheid van Synsurf® as ’n draer vir pulmonêre middels. Daarbenewens toon die tuberkulose-isolate H37Rv en MDR-X51 verhoogde vatbaarheid vir mikropartikel surfaktantmiddel kombinasies.

Die hoofbevinding van die studie toon dat die natuurlike surfaktante Curosurf® en Liposurf® sowel as Synsurf® die afskeiding van pro-inflammatoriese sitokiene strem en ’n invloed het op die produksie van reaktiewe suurstofspesies in NR8383- alveolêre makrofage, en dus op sellewensvatbaarheid. Die remmende uitwerking op sitokienafskeiding is op ’n dosisafhanklike manier bewys, sowel as deur ’n drempeleffek vir ál drie surfaktante. Dít kan dalk spruit uit unieke meganismes wat selseine verminder, of die opregulering van anti-inflammatoriese aktiwiteit, wat verder met behulp van proteomika toegelig is.

Die hoofgevolgtrekkings na aanleiding van die bevindinge van hierdie tesis oor die vergelyking van die twee natuurlike en een sintetiese surfaktant is soos volg: a) Verskillende surfaktantsamestellings moduleer anti-inflammatoriese werking in lipopolisakkaried-gestimuleerde alveolêre makrofage deur die moontlike betrokkenheid van verskillende

seinroetes. Die aanvanklike hipotese oor die beskermende funksie van die proteïeninhoud van natuurlike surfaktante word bevraagteken. Aangesien hierdie nuwe bevindinge dui op nie-spesifieke lipied- of sintetiesepeptiedbeskerming by alveolêre makrofage, soos in die geval van Synsurf®, kan die hipotese nie ten volle ondersteun word nie. b) Verskillende surfaktantsamestellings beïnvloed sellewensvatbaarheid en -morfologie op ’n tyd- en dosisafhanklike manier, wat daarop dui dat die behandeling van neonatale respiratoriese noodsindroom moontlik kan afhang van die spesifieke preparaat of dosis wat gebruik word. c) Ál drie surfaktante het oënskynlik ’n impak op die antibiotiese aktiwiteit van linezolid, wat belowend lyk vir surfaktante as middeldraers. d) Die data toon dat linezolid in kombinasie met Synsurf® in ’n gewenste partikelgrote verstuif kan word vir optimale longneerslag in ’n moontlike nie-ingrypende, terreinspesifieke leweringsmodel, deur middel van ’n drukinhalator met afgemete dosisse.

DEDICATION

Ouma Lydia,

Met liefde, eerbied, respek en groot hartseer, herhinder ek ouma se laaste woorde aan my:

"Jy is van goeie hout gesny"

Pretensieloos en rigtingvas het ouma my aangemoedig en in my deursettingsvermoë geglo. Ek is geseënd dat ouma my daaglikse lewe, asook my drome en my vrese kon deel. Ek was bevoorreg en is so dankbaar dat ek na ouma se lewensveranderende verhale kon luister.

Haar onvoorwaardelike liefde het sy vir al haar kleinkinders gegee: allesomvattende liefde - sonder grens, maat of tyd.

Die spore wat sy gelaat het sal nie uitgevee kan word nie.

ACKNOWLEDGEMENTS

The best and worst moments of my doctoral journey have been shared with many people.

First and foremost I would like to thank my supervisor, Prof. Johann van Zyl, for the patient guidance, encouragement and advice he has provided throughout my time as his student. I have been extremely lucky to have a supervisor who cared so much about my work as well as my personal well-being. Together with Prof Johan Smith, they have both routinely gone beyond their duties to fire-fight my worries, concerns, and anxieties, and have worked to instil great confidence in both myself and my work and were always generous with their knowledge. My life is forever richer for having been given the opportunity to work with Synsurf® and the Synsurf® team.

I would like to thank my parents for allowing me to realise my own potential. All the support they have provided me over the years was the greatest gift anyone has ever given me. My dad who taught me the value of hard work and an education – for always encouraging me to pursue "something more". My mother who taught me to never settle for "less" and to strive for excellence in everything I do.

I would like to thank my husband, Ian, for his unremitting encouragement. Put simply, I have never met anyone who believes in me more. Thank you for making me more than I am and always reminding me of how far I have come. You are my sounding board.

My friends, who always took the time to listen, even when I was just complaining. Who sacrificed their time to help me whenever I needed it and offered their knowledge and appreciation of research when I lacked enthusiasm to carry on.

To my fellow post-graduate fellows, Chris-Marie and Kim, our chats in between work and coffee runs have meant so much to me. I wish the both of you much success in your own endeavours and want to thank the both of you for adding so much joy to my professional and personal life when the office seemed to cave in on me.

I would like to thank Dr Annadie Krygsman and the department of Physiological Sciences for making their labs available to me to run experiments as well as always being helpful whenever I needed assistance.

I would like to thank Prof. Pierre Goussard and his team for their assistance regarding the bronchoalveolar lavage sampling.

I would also like to thank the NRF: National Research Foundation for their financial support.

Finally, I would like to thank INNOVUS for their financial and structural support. Without this, the further development and innovation, intellectual property and patenting regarding Synsurf® at the University would not have been possible.

TABLE OF CONTENTS

LIST OF TABLES

LIST OF FIGURES

DISCLAIMER

Any opinion, findings and conclusions or recommendations expressed in this material are those of the author(s) and therefore the NRF does not accept any liability in regard thereto.

1 CHAPTER 1: LITERATURE REVIEW

1.1 Introduction

The development of inhaled drug delivery systems has gained great interest, as it is an attractive route for drug delivery. Supporting reasons for the inhalation route being a preferred means of drug delivery alongside reduced incidence of adverse systemic side effects include: (A) Site-specific drug delivery for locally acting compounds can lead to a rapid onset of action (Timsina, Martin et al. 1994), especially for drugs that undergo extensive first pass metabolism such as hormones, peptides and proteins. Furthermore, potent drugs can be administered at lower dosages (Newhouse, Corkery 2001). (B) The large surface area of the respiratory tract of 70-80 m^2 with a good blood supply also provides excellent conditions for efficient drug absorption (Weibel, Gomez 1962). Moreover, the decreased invasiveness may offer improved patient compliance for infectious pulmonary disease. With the advent of novel macromolecular medications, the horizon of aerosol drug delivery is expanding to include non-respiratory conditions e.g. diabetes, analgesia, thyroid disorders and genetic disease.

Respiratory diseases such as asthma, adult respiratory distress syndrome (ARDS), neonatal respiratory distress syndrome (RDS), chronic obstructive pulmonary disease (COPD), pulmonary tuberculosis (TB), cystic fibrosis, pulmonary arterial hypertension and human immunodeficiency virus (HIV)-related lung pathology, as well as various non-respiratory conditions are all prone to continued use of inhaled drugs. Thus, improvements to inhaled drug delivery systems as well as dual drug delivery tools are very desirable. Designing a successful system for drug delivery to the respiratory tract requires a comprehensive understanding of the disease condition, lung anatomy and physiology, physio-chemical properties of drug alone and the polymeric matrix combined production process of the drug (Mossaad 2014).

1.2 Structure and Function of the Respiratory Tract

The primary function of the respiratory tract (RT) is gas exchange: facilitating the movement of oxygen into the blood from inspired air and removing carbon dioxide from the circulation through a very thin blood-gas barrier in the exchange area (see Figure 1.1). A secondary function appears to be the cleaning and humidifying of the incoming air to prevent damage to this vital organ. The RT is broadly divided into three regions: (1) the upper RT, also called the oropharyngeal region, consists of the mouth, pharynx and larynx. (2) The conducting airways, which include the trachea, bronchi and bronchioles. (3) The lower RT, also called the alveolar or pulmonary region, which extends from the respiratory bronchioles to the distal alveolar sacs and forms about 85% of the total lung volume.

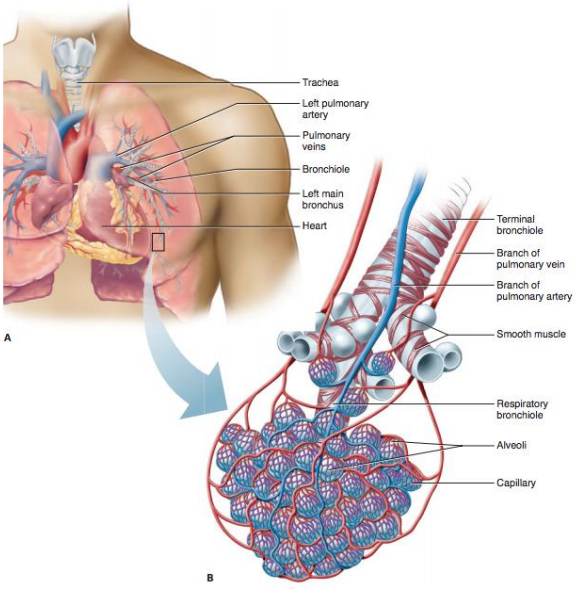

Figure 1.1: Structure of the respiratory system. A) The respiratory system is diagrammed with a transparent lung to emphasize the flow of air into and out of the system. B) Enlargement of boxed area from (A) shows transition from conducting airway to the respiratory airway, with emphasis on the anatomy of the alveoli. Red and blue represent oxygenated and deoxygenated blood, respectively (Barrett, Ganong 2010).

The function of the upper RT is to heat and moisten, as well as remove particulate matter from the inspired air. The inspired air passes down the trachea and through the bronchioles, respiratory bronchioles, and alveolar ducts to the alveoli. The airways divide as many as 23 times between the trachea and the alveolar sacs to form an asymmetric, continuous, dichotomously branching structure. The upper conducting airways form the first 16 divisions

(see Figure 1.2) that transport the air to and from the outside environment (Barrett, Ganong 2010).

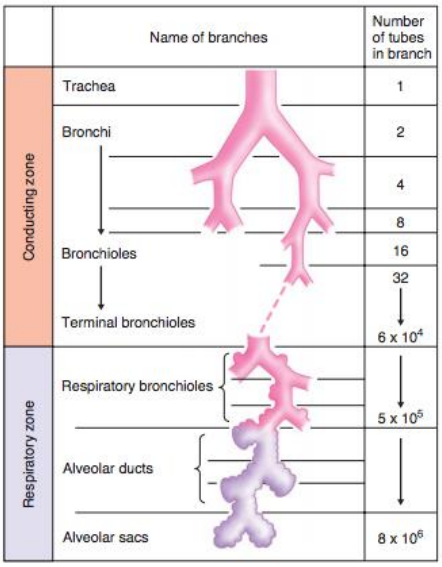

Figure 1.2: The branching patterns of the airway during the transition from conducting to respiratory airway are drawn (not all divisions are drawn, and drawings are not to scale) (Barrett, Ganong 2010).

1.3 Surfactant Replacement Therapy

Surfactant therapy was established from the observation that the lungs of babies dying from RDS lack the surface-active material; and was further based on the assumption that it should be possible to compensate for this deficit by administering the absent material (or an equivalent substance) via the airways. Exogenous surfactant therapy has therefore been an essential part of the routine care of preterm neonates with RDS since the beginning of the 1990s (Robertson, Halliday 1998). However, this is not a new concept. The American pathologist, Peter Gruenwald, conveyed this theory in 1947, which was based on the pressure-volume recordings and histological observations on lungs of babies with RDS. He postulated that `the addition of surface active substances to the air or oxygen which is being spontaneously breathed in or introduced by a respirator might aid in relieving the initial atelectasis of newborn infants' (Gruenwald 1947). Fujiwara and colleagues (1980) undertook the pilot study for the clinical debut of surfactant therapy application, which showed the dramatic improvement of lung function in babies with RDS treated with a large dose of modified natural surfactant instilled directly into the airways. These findings created a historical moment as previous efforts to treat babies with RDS were unsuccessful (Fujiwara, Chida et al. 1980). The reason as to why

previous aerosolized artificial surfactant was ineffective has been attributed to the use of dipalmitoylphosphatidylcholine (DPPC) alone. DPPC is an essential component of pulmonary surfactant, but cannot be used as an effective substitute alone. It is now well known that hydrophobic proteins are required to enhance spreading of the surface-active material in the airspaces and are thus required in exogenous surfactants for appropriate efficiency (Robertson, Halliday 1998). Since then, many randomised controlled studies have demonstrated that surfactant therapy was not only well tolerated, but that it significantly reduced both neonatal mortality and pulmonary air leaks (Ainsworth, Milligan 2002).

1.3.1 Pulmonary Surfactant Composition and Production

Pulmonary surfactant is a lipoprotein complex produced by the Type II alveolar cells, stored in the lamellar bodies and then secreted into the alveolar space. It covers the alveolar epithelial surface and small bronchioles to form a lattice-like structure called 'tubular myelin' (Haagsman, Van Golde 1991, Wright, Dobbs 1991) that is believed to be the precursor to the surfactant monolayer (see Figure 1.3), and is the direct precursor to the surfactant film at the air–liquid interface. The mechanism in which these lamellar bodies are released is unclear (Clements, Oyarzun et al. 1981), although mechanical and humoral mechanisms have been implicated (Goerke, Clements 1986).

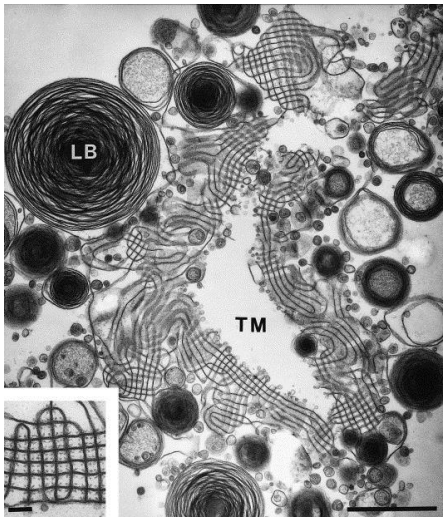

Figure 1.3: Particles in the alveolar sub-phase. In this electron micrograph section of a rat lung, lamellar bodies (LB) are seen forming tubular myelin (TM) (bar at lower right=1.0 μm). The remaining vesicular structures may represent both used and rejected surfactant materials. Inset: detail of tubular myelin at lower left, showing small projections in the corners, thought to represent SP-A (bar=0.1 μm) (Goerke 1998)**.**

β-Adrenergic agents, and changes in ventilatory patterns are some physiological triggers for surfactant secretion from alveolar epithelia, in addition to several other biochemical mediators. As the film compresses it facilitates the reductions in surface tension and is also purified during the breathing cycle as certain protein components are compressed out of the film. As surfactant is actively being secreted, materials are constantly being exchanged from the film and are recycled into the type II epithelial cells (Figure 1.4A); this helps maintain a constant surfactant pool size within the alveolus. Thus, many recycled alveolar surfactant components are transported back to form newly formed lamellar bodies (Glasser, Mallampalli 2012).

The schematic representation of the life cycle of pulmonary surfactant in the normal lung is displayed in Figure 1.4B. It was first discovered 57 years ago when Avery and Mead (1959) found that bronchoalveolar lavage (BAL) fluid of newborns with IRDS (then known as hyaline membrane disease) lowered surface tension less than that of healthy newborns when investigating the pathogenesis of respiratory failure of premature newborns (Avery, Mead 1959, Rosenberg, Seiliev et al. 2006).

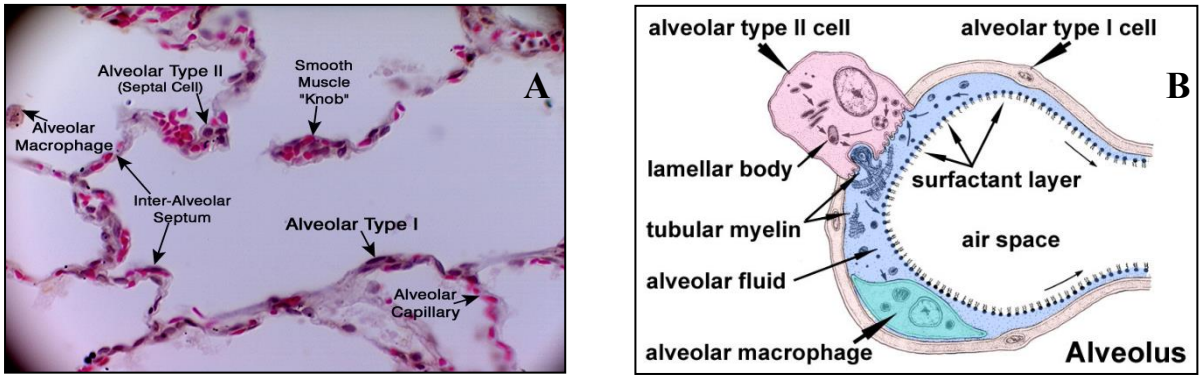

Figure 1.4: A) Several Alveoli. Type I pneumocytes are obvious by their large central nuclei while type II pneumocytes have a 'flattened' nuclei and a cytoplasm that spreads out to the side. An alveolar macrophage can also be noted within the alveolar space (McLeod 2010.) **B)** The Aveolus: Formation and metabolism of Surfactant. Lamellar bodies are formed by type II alveolar epithelial cells and secreted by exocytosis into the fluid lining the alveoli. The released lamellar body material is converted to tubular myelin and it is the source of the phospholipid surface film. Surfactant is taken up by endocytosis into alveolar macrophages and type II epithelial cells (Barrett, Ganong 2010, Hill 2016).

Surfactant isolated from healthy mammals' lung BAL fluid consists of 90% lipids and 8 - 10% proteins (Figure 1.5); however, the composition may vary and is dependent on factors such as age, species, specific lung compartment, disease state, diet and isolation method. Phospholipids

(80%) make up for the majority of the lipid content of which 8 - 10% is neutral. Phosphatidylcholine constitute for 80% of the phospholipids of which 40 - 80% of it is dipalmitoylphosphatidylcholine (DPPC) and 8 - 15% is phosphatidylglycerol (PG) (see Figure 1.6). There may also be small quantities of phosphatidylethanolamine (PE), phosphatidylserine (PS), phosphatidylinositol (PI), and sphingomyelin (SM) (King, Clements 1972., Sanders 1982, Serrano, Pérez-Gil 2006). The presence of PI and the ratio of PI to PG is an indication of lung maturity. For instance, a low PG:PI ratio is a sign of lung immaturity (Ayden, 1999). There are 4 surfactant-associated proteins: SP-A, SP-B, SP-C, and SP-D (see Figure 1.7). SP-C has the exception of being formed in the bronchiolar epithelial cell (Kalina, Mason et al. 1992) and not in the type II alveolar cells like its counterparts. The hydrophilic SP-A (35 kDa) and SP-D (43 kDa) are referred to as collagen-containing C-type (calcium dependent) lectins called collectins, which contribute significantly to surfactant homeostasis and pulmonary immunity (Possmayer 1988, Kishore, Greenhough et al. 2006). The smaller hydrophobic, carbohydrate containing proteins SP-B (8 kDa) and SP-C (4.2 kDa) make up less than 1% of the total protein weight and facilitate the adsorption and spreading of lipid to form the surfactant monolayer at the air-liquid interface (Jobe, Wood 1993).

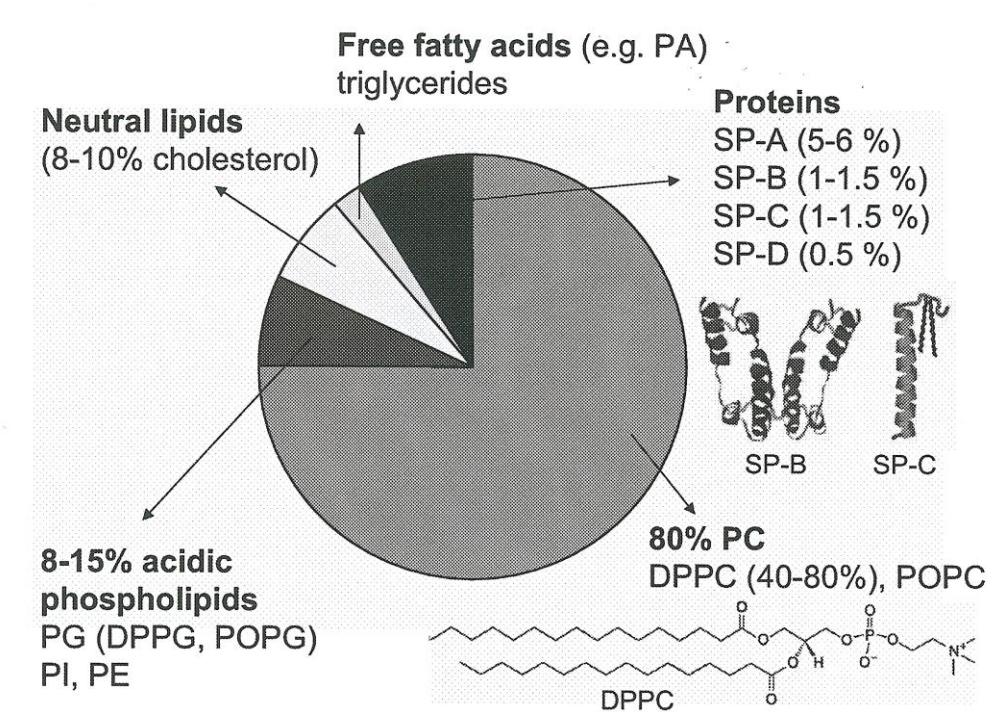

Figure 1.5: Composition of human lung surfactant (Serrano, Pérez-Gil 2006).

The surfactant system, through specific lipid-lipid and lipid-protein interactions, displays how the membrane's condition in several different forms governs biological functions. It sets it apart from understanding its structure alone, but rather understanding the structure-function and interactions present in highly differentiated cells (Pérez-Gil 2008).

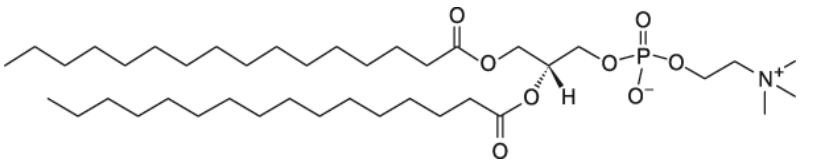

Formula: $C_{40}H_{80}NO_8P$
Molar Mass: 734.039 g/mol

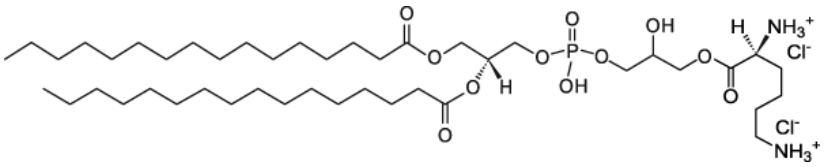

Formula: $C_{38}H_{75}O_{10}P$
Molar Mass: 722.969862 g/mol

Figure 1.6: Structure of **(Above)** DPPC: 1,2-dipalmitoyl-*sn*-glycerol-3-phosphocholine; **(Below)** PG: 1,2-diacyl-sn-glycerol-3-phosphorylglycerol (Avanti Lipids Polar, Inc.).

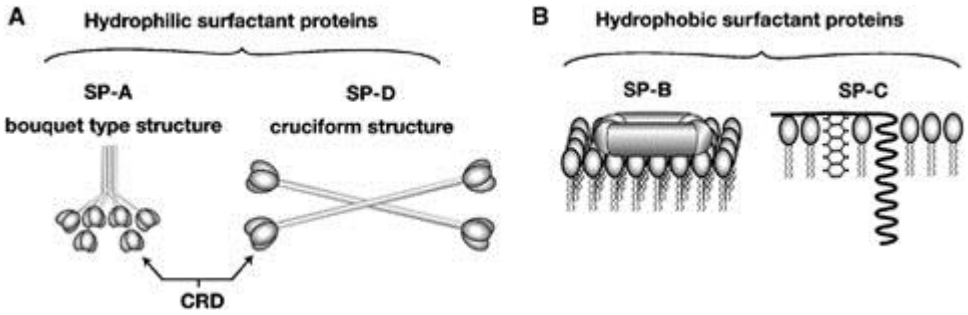

Figure 1.7: Structure of surfactant proteins (SP-A, SP-B, SP-C, and SP-D). **(A)** SP-A and SP-D are hydrophilic surfactant proteins and part of the collectin family. Common structural features are an amino N-terminal, a collagen like domain, a neck region, and a carbohydrate recognition domain (CRD). **(B)** SP-B and SP-C are hydrophobic surfactant proteins and play a role in biophysical surfactant functions. They are found in close association with surfactant phospholipids (Christmann, Buechner-Maxwell et al. 2009).

1.3.2 Physiological Mechanisms of Action of Pulmonary Surfactant

The main function of surfactant is in its biophysical behaviour to help maintain proper lung function; to act as an air–water surface tension lowering agent of a continuous liquid layer that is assumed to line the alveoli and adjacent terminal airways at all times and in this manner, surfactant reduces the work associated with breathing (Ayden 1999). During inspiration and expiration, the alveolar surface size and the area that surfactants covers can similarly alter repetitively. When the alveoli collapse at lower inspiratory pressures, the surfactant allows for their reopening and protects them from future collapse during expiration. The orientation of surfactant molecules is such that the polar heads group in the aqueous phase and the non-polar groups point towards the air. The orientation of the monolayers reduces surface energy/tension. The typical surface tension of water covering glycocalex of alveolar cells is 72 mN/m, surfactant adsorption decreases the surface tension to 23 mN/m or extremely low values to < 5 mN/m; that facilitates the work of breathing and assists with improved respiratory mechanics (Rosenberg, Seiliev et al. 2006).

The first model that was introduced by von Neegaard in 1929 is still known as the "bubble model" and was further developed by Clements in 1962 (Hills 1991). However, there are other models that are in opposition that describe surfactant function within the alveoli such as:

1. The "Totally dry" model by (Colacicco 1985)
2. The "Shell" model/ "Geodesic-Dome" Model by (Morley 1987)
3. The new, discontinuous model by (Hills, Burke et al. 1998, Hills 1999)

These models are outside the scope of this report and will not be discussed further. However, they are discussed, in length by (Hills 1988).

When the phospholipid and protein mixture are secreted, they are quickly adsorbed as a monomolecular film at the air-aqueous interface and is a mixture of saturated and unsaturated phospholipids. This film allows the adjustments of surface tension with area during dynamic expiration and inspiration and thus maintains alveolar stability. This increases lung compliance and resists possible alveolar atelectasis that results in clinically reduced work of breathing (Chimote, Banerjee 2005). The inability to execute these properties is defined as surfactant dysfunction. Thus in surfactant dysfunction, near zero minimum surface tension is not reached.

This results in alveolar collapse, which in turn requires increased breathing efforts to re-expand and stabilise the atelectatic alveoli (Banerjee 2002).

1.3.3 Pulmonary Surfactant Dysfunction and Lung Disease

When surfactant production or function is altered, many respiratory disorders may arise. Many pre-term infants born with surfactant deficiency develop respiratory distress syndrome (RDS) which is the prototypical lung condition characterised by inadequate surfactant production by the immature lungs. Lung inflammation is observed in many of these infants as respiratory failure and is compensated by active support such as mechanical ventilation or increased oxygen concentrations (Chakraborty, McGreal et al. 2010). Surfactant replacement is commonly used today in the clinical management of pre-term and/or new-born babies with RDS both as a prophylactic and rescue therapy, and there is accumulating evidence indicating that this treatment might also be effective in several other forms of lung disease including meconium aspiration syndrome, neonatal pneumonia, acute lung injury (ALI), and the `adult' form of acute respiratory distress syndrome (ARDS) (Robertson, Halliday 1998).The dynamic properties of lung surfactant permit the alveolar surface tension to change with inflation and deflation, thus keeping the smaller sized alveoli from complete collapse. The altered behaviour results in (see Figure 1.8) a reduction in the work of breathing. Loss of surfactant activity thus results in reduced lung compliance, atelectasis, and impaired gas exchange (Wright, Notter et al. 2001).

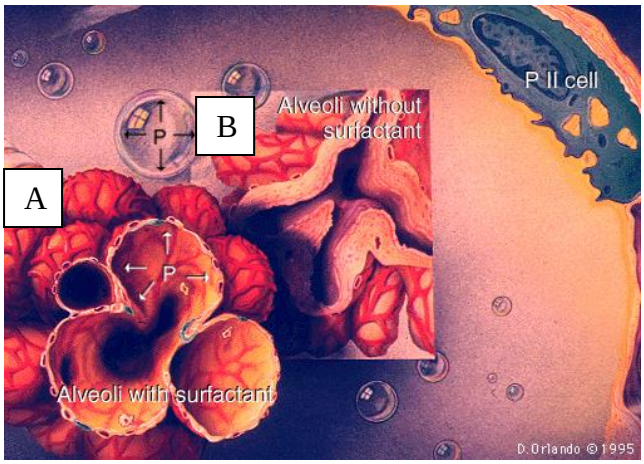

Figure 1.8: Alveoli structure **(A)** with surfactant and **(B)** without surfactant (Johns Hopkins School of Medicine's Interactive Respiratory Physiology) (**Abbreviations:** P, Pressure; P II cell, Type 2 pneumocyte).

There are a number of pathways by which lung surfactant activity can be compromised. The reductions in the content or composition of active large surfactant aggregates have been reported in BAL, oedema fluid, or tracheal aspirates from patients with ALI/ARDS or other diseases involving lung injury (Petty, Reiss et al. 1977, Hallman, Spragg et al. 1982, Seeger, Pison et al. 1990). The one important mechanism of surfactant dysfunction in ALI/ARDS is the physicochemical interactions with substances in the alveoli as a result of permeability oedema or inflammation (see Figure 1.9). There have been many studies documenting lung injury and impairment of surfactant due to inhibitors such as plasma and blood proteins, reactive oxidants, proteases and other lytic enzymes as well as phospholipases (Raghavendran, Willson et al. 2011). It is however important to document that the surface activity deficits from all these mechanisms can be alleviated *in vitro* by exogenous surfactant administration, even if these inhibitor substances remain present (Wang, Holm et al. 2005), thus supporting surfactant supplementation strategies.

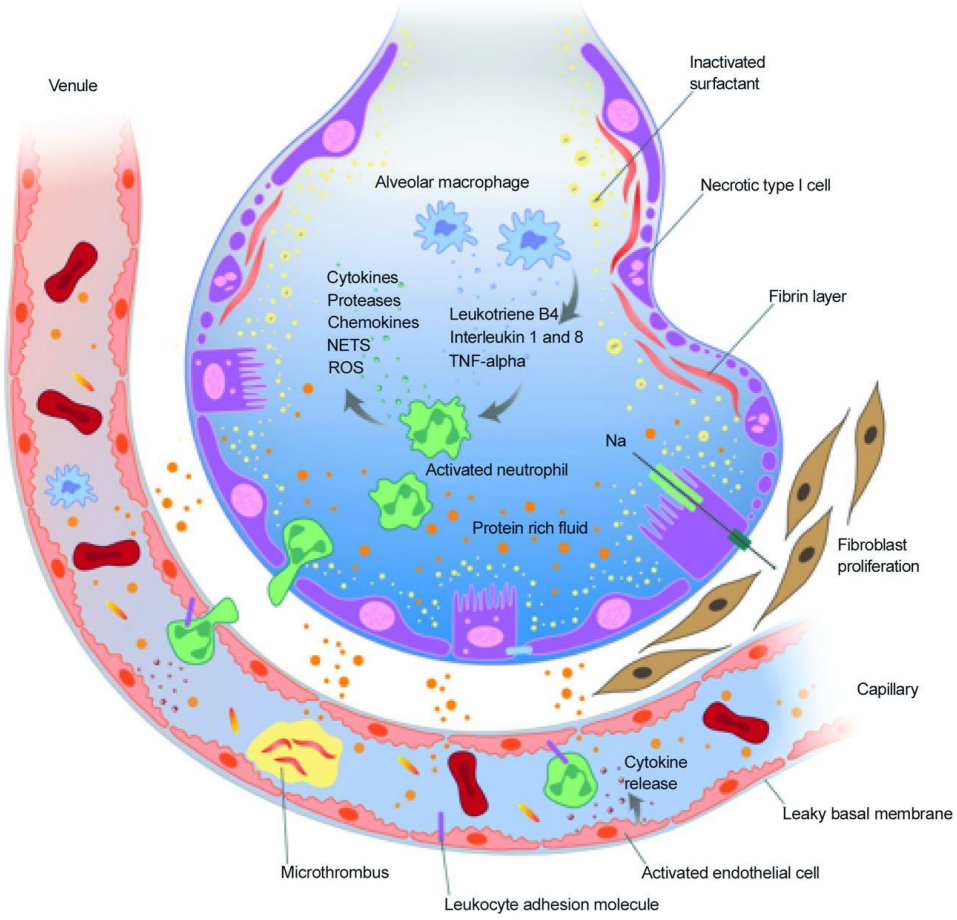

Figure 1.9: Role of surfactant in non-neonatal acute lung injury. Increased pulmonary endothelial permeability, epithelial injury, and apoptosis lead to an influx of protein-rich fluid that inactivates surfactant. Similarly, cytokines, neutrophils, reactive oxygen species (ROS), thrombin, and mechanical stretch contribute to an intense pulmonary inflammatory response, with accumulation of both pro-inflammatory and anti-inflammatory mediators that may inactivate surfactant and decrease surfactant synthesis. Reduction in the production and turnover of surfactant leads to decreased lung compliance, resting lung volume, and functional residual capacity. NETS = neutrophil extracellular traps; TNF-α = tumor necrosis factor alpha. Courtesy Dr Anil Sapru (Willson 2015).

Given the importance of surfactant associated proteins in the function and metabolism of surfactant, inherited deficiencies of specific proteins could potentially cause respiratory diseases (Nogee, deMello et al. 1993). These authors reported a case of congenital pulmonary alveolar proteinosis where the absence of SP-B and its mRNA led to the dysfunction of the surfactant's spreading properties; however, the mechanism is still unclear. Another mutation that leads to abnormalities in surfactant composition and function is the spontaneous deletion on one allele of the SP-C gene that is associated with sporadic interstitial lung disease. This results in the aggregation and misfolding of the SP-C and subsequent cell injury and

inflammation (Hamvas, Nogee et al. 2004). This pulmonary inflammatory response may have further implication on surfactant inactivation as mentioned previously.

Also, infectious diseases may too, in turn, alter the activity of these proteins, or phospholipids, that may result in surfactant dysfunction. Some research groups have also investigated whether the host inflammatory response contributes to respiratory impairment by disrupting the pulmonary surfactant system. One such group's findings demonstrated that the surfactant pathology associated with *Pneumocystis pneumonia* (PCP) is related to the inflammatory process rather than being a direct effect of P. *carinii*. Moreover, they found that the $CD8^+$ lymphocytes were involved in the mechanism leading to surfactant dysfunction (Wright, Notter et al. 2001). It has also been demonstrated that SP-A suppresses the T-cell dependent lung inflammatory response that often occurs in patients (and mice) following allogeneic bone marrow transplant reiterating its secondary immunomodulatory function (Wright, Borron et al. 2001). Another significant pulmonary infection to consider in the role of surfactant dysfunction is pulmonary tuberculosis. The M. *tuberculosis* bacteria tend to reside within the alveolar space and are thus in close proximity with the surrounding surfactant. Mycolic acid, which is moderately surface active, is able to detach from the mycobacterium's cell wall and could possibly interact with the pulmonary surfactant resulting in lung surfactant dysfunction (Chimote, Banerjee 2005).

Given the known contributions of surfactant dysfunction in ILD/RDS and other infectious diseases, it seems likely that surfactant therapy in combination with other agents will ultimately be applicable for at least some adult as well as paediatric patients. A combination therapy approach is considered the most relevant for adults with ALI/ARDS as previous responses to exogenous surfactant delivery have, to date, been unsatisfactory. Thus, it stands to reason that the use of multiple therapeutic agents (biological targets and pharmacologic agents) or interventions based on a mechanistic rationale for synergy may significantly enhance outcomes in patients with complex inflammatory lung injury pathology (Raghavendran, Willson et al. 2011).

1.3.4 Natural extract versus Synthetic Surfactant

Exogenous surfactants may be of animal or synthetic origin and both types have been extensively studied in animal models and in clinical trials to determine the optimum

timing, appropriate dosage, and frequency, route and method of administration (Ainsworth, Milligan 2002).

Bengt Robertson and Tore Curstedt developed a porcine surfactant, Curosurf® (aptly named for their surnames), which was effective in immature animals and was used in a pilot clinical trial that started in 1983. Further trials conducted in pre-term infants with RDS decreased neonatal mortality rates and showed that early treatment was more effective than later administration (Curstedt, Halliday et al. 2015). The surfactant could be manufactured in a reproducible way in large quantities; however, the manufacturing process was very time consuming and for the production of a batch for the treatment of 80–100 preterm infants' lungs, approximately 50 adult pigs were needed (Robertson, Curstedt et al. 1990). Although effective in the treatment of preterm infants with RDS, modified natural surfactants have proven to be expensive and the supplies are limited. There have also been concerns about the potential risk of immunogenic and infectious complications using these preparations and concerns still remain for the administration of animal-derived proteins in more immunocompromised populations, such as children or adults with acute lung injury (Lacaze-Masmonteil 2008). Nevertheless, it is worthy to mention that no adverse effects of this nature have been described in any of the infants previously treated (Kattwinkel 2005, Curstedt, Halliday et al. 2015). On the other hand, synthetic surfactants have the potential to completely eliminate the already very low and hypothetical risks of transmission of viral or unconventional infectious agents (Lacaze-Masmonteil 2008).

The necessity for synthetic surfactant preparations was prompted by the need to expand the indications for surfactant treatment that can be more easily produced, in large quantities, at less batch-batch variation, and at a reasonable cost. As mentioned before, there is a wide variety of commercially available, animal-derived surfactant formulations and some, though limited, synthetic surfactants (see Table 1.1), and both are beneficial as therapy for neonatal RDS. Animal-derived surfactants (Beractant®) and calfactant (Infasurf®) are modified or purified from bovine or porcine lungs and are still preferred over first generation, protein-free synthetic surfactants (e.g, colfosceril palmitate) (Polin, Carlo 2014).

Table 1.1: Composition and Dosage of Surfactants (Polin, Carlo 2014).

Surfactant	Main Phospholipids	Proteins	Phospholipid Concentration	Suggested Dose	Phospholipid per Dose
Animal-derived					
Poractant (Curosurf®) minced porcine lung extract	DPPC and PG	(0.6%) SP-B and (1%) SP-C	80 mg/mL	2.5 mL/kg	100-200 mg/kg
Liposurf® (Bovine lipid extract surfactant suspension)	DPPC and PG	176 – 500 µg of SP-B and SP-C per mL	27 mg/mL	5 mL/kg	135 mg/kg
Beractant (Survanta®) minced bovine lung extract	DPPC and PG	(<0.1%) SP-B and (1%) SP-C	25 mg/mL	4 mL/kg	100 mg/kg
Synthetic					
Colfosceril palmitate (Exosurf®)	DPPC (100%)	None	13.5 mg/mL	5 mL/kg	67.5 mg/kg
Synsurf®	DPPC and PG	P-Lys and P-Glu	60 mg/ml	1.7 mL/kg	100mg/kg
Lucinactant (Surfaxin®)	DPPC and POPG	KL_4 peptide as SP-B	30 mg/mL	5.8 mL/kg	175 mg/kg

Each different component of surfactant has an important function that collectively and independently influences both its primary dynamic surface behaviour (reduction in surface tension) and secondary role in lung defence. The continuous exploration in this field of study has led to the greater understanding of these individual components, particularly the surfactant-associated proteins, which in turn made it possible for the development of newer synthetic surfactants; however, it is not without difficulty (Ainsworth, Milligan 2002, Curstedt, Halliday et al. 2015). The structural complexity and instability of SP-B and SP-C was overcome to a certain extent by the synthesis of more stable and rather simple analogues of SP-B and SP-C (Almlén, Stichtenoth et al. 2008, Almlén, Walther et al. 2010, Curstedt, Halliday et al. 2015). The relatively incomplete knowledge of some phospholipids' function in surfactant, in combination with the limited commercial availability of many synthetic phospholipids, has led to the use of very simple phospholipid mixtures in earlier synthetic surfactant preparations (Curstedt, Halliday et al. 2015). Before protein analogues were introduced or deemed necessary for surfactant

success, the first protein-free synthetic surfactant colfosceril palmitate, also known as Exosurf®, was tested around 1989 for the prophylaxis and treatment of infants at risk for RDS. Since then, the drug was tested in many clinical trials and found to be efficacious, however, it was discontinued firstly, in the United States, and later in the UK (2003). Exosurf® trials have been underpowered in studies where its efficacy was examined against newer surfactants that were making their debut (Kattwinkel 2005). Another protein–free synthetic surfactant, Pumactant, was voluntarily withdrawn from the market in 2000 by the licence holder following the results of a randomized clinical trial which unexpectedly showed higher mortality rates in neonates who were administered Pumactant (Department of Health, United Kingdom 30 August 2000). These findings reiterate the importance of protein analogues within phospholipid surfactant mixtures.

SP-B is essential for lamellar body formation as well as for DPPC configuration at the air-fluid interface (at body temperature). Therefore, the search for a synthetic surfactant preparation that contains a functional synthetic apoprotein that is equivalent or superior to the animal-derived surfactants has continued. Although the molecular structure of SP-B has been synthesised in the laboratory, the molecule however does not configure appropriately (Kattwinkel 2005). Unfortunately, no successful trials with a synthetic SP-B-containing preparation have been published. An analogue of SP-C has been produced and is able to promote film adsorption *in vitro* and has been shown to treat surfactant deficiency in animal models (Davis, Jobe et al. 1998). There has been a trial of this analogue in adult ARDS but it proved unsuccessful (Spragg, Lewis et al. 2004). Again, there have thus far been no published neonatal trials with this analogue.

Recently, a new-generation synthetic surfactant containing both phospholipids and proteins (SP-B and SP-C analogues) has been developed. After preclinical testing in preterm lambs (Sato, Ikegami 2012, Seehase, Collins et al. 2012) and newborn pigs (Salvesen, Curstedt et al. 2014), CHF5633® (developed Chiesi Farmaceutici, Tore Curstedt and Jan Johansson) has undergone a preliminary first study in pre-term infants. CHF5633® was found to be well tolerated and showed a promising clinical efficacy profile. The encouraging data provides a basis for ongoing randomised controlled trials (Sweet, Turner et al. 2017). This study stands testament to the fact that new surfactant preparations could

revolutionise the treatment of preterm infants worldwide as it could be manufactured consistently and safely in almost unlimited quantities.

Advantages of one type of surfactant over another type are usually categorised by the biophysical properties, animal studies and randomised trials in neonatal populations; however, it has only been a recent development to include possible immunological categories as well (Chroneos, Sever-Chroneos et al. 2010, Wright 2005). The choice of surfactant may also be based upon the neonatologist's opinion regarding the necessity for a rapid response or the timing of administration (Halliday, Speer 1995). At present, animal-derived exogenous surfactants are preferred to other surfactants as they have relatively few adverse effects associated with the large and rapid changes in oxygenation during administration; however, with newer protein containing synthetic surfactants emerging this may soon change. Synthetic surfactants have slower response rates and may therefore be favoured for prophylaxis (preventing/worsening RDS rather than treatment of established RDS) whereas natural surfactants may be more suitable for very ill babies at risk of barotrauma and pulmonary air leaks due to their rapid response (Halliday, Speer 1995, Polin, Carlo 2014).

Another synthetic surfactant to be FDA approved, lucinactant (Surfaxin® Discovery Laboratories), contains a 21-amino acid peptide (leucine and lysine repeating units, KL_4 peptide) that mimics SP-B activity and has recently been accepted for the prevention and treatment of RDS in preterm infants (Sinha, Lacaze-Masmonteil et al. 2005, Moya, Sinha et al. 2007). When compared with animal-derived surfactant (beractant or poractant), lucinactant was shown to be an equivalent alternative. Neonatal morbidities (intraventricular hemorrhage, periventricular leukomalacia, pulmonary hemorrhage, sepsis, patent ductus arteriosus, retinopathy of prematurity, necrotizing enterocolitis, and bronchopulmonary dysplasia) were not significantly different between preterm infants treated with animal-derived surfactants and those treated with synthetic surfactants (Polin, Carlo 2014). This prophylactic study also compared the efficacy of lucinactant (Surfaxin®) with colfosceril palmitate (Exosurf®). They concluded that lucinactant is a more effective surfactant preparation than colfosceril palmitate for the prevention of RDS as it reduces the incidence of bronchopulmonary dysplasia (BPD) rates. Therefore, lucinactant was the first of a new class of surfactants containing a functional

peptide of SP-B that proved itself an effective therapeutic option for preterm infants at risk for RDS (Moya, Gadzinowski et al. 2005).

A previous multicenter randomized controlled trial conducted by Hudak and colleagues (1997) compared the efficacy and safety of the protein/peptide free synthetic surfactant colfosceril palmitate (Exosurf®) and a surfactant extract of calf lung lavage (Infasurf®) in the prevention of neonatal respiratory distress syndrome in premature infants. The prophylactic surfactant administration resulted in the animal surfactant-treated infants displaying significantly less air leaks compared to those of the Exosurf® group; however, intraventricular hemorrhage occurred more frequently in the Infasurf® surfactant-treated infants. No decrease in the risk of mortality associated with the prophylactic use of animal-derived surfactant was reported also (Hudak, Martin et al. 1997).

Comparisons of synthetic and animal-derived surfactants have largely been used as rescue strategies in the past where surfactant is given to neonates with established respiratory distress syndrome; the exception to date are the two prophylaxis trials mentioned above. Ainsworth and colleagues (2000) conducted a randomized controlled trial to compare a synthetic surfactant (Pumactant®) with a natural porcine surfactant (poractant alfa, Curosurf®) for the treatment of respiratory distress syndrome in neonates. However, as mentioned previously, the trial was stopped on the recommendation of the data and safety monitoring committee because of concern regarding increased mortality in the group receiving synthetic surfactant (Ainsworth, Beresford et al. 2000, Ardell, Pfister et al. 2015).

Early rescue is defined as surfactant treatment within 1 to 2 hours of birth, and late rescue is defined as surfactant treatment 2 or more hours after birth (Polin, Carlo 2014). A recent meta-analysis of early (within 2 hours) versus delayed surfactant treatment concluded that the risks of mortality, air leak, chronic lung disease, and chronic lung disease or death were significantly decreased in the early administration group (Polin, Carlo 2014). Although there are no statistically significant benefits to prophylactic use of surfactants when compared with prophylactic continuous positive airway pressure (CPAP), several studies have investigated whether administration of surfactant early in the course of respiratory insufficiency improves clinical outcomes (Polin, Carlo 2014). The studies found that using CPAP immediately after

birth with subsequent selective surfactant administration should be considered as an alternative to routine intubation with prophylactic or early surfactant administration in preterm infants.

A synthetic peptide-containing surfactant (Synsurf®) consisting of phospholipids and poly-L-lysine electrostatically bonded to poly-L-glutamic acid has been developed based on the KL_4-surfactant principle by van Zyl *et al.* (2013a). The polymers were added to the phospholipids, in order to mimic the hydrophobic and hydrophilic nature of SP-B in the mixture (Van Zyl, Smith et al. 2013a). Their first pre-clinical study demonstrated that Synsurf®, when compared with Exosurf®, improves oxygenation by lowering pulmonary shunt in New Zealand white rabbits with acute lung injury and surfactant-deficient lung disease. In a following randomized controlled trial, the two surfactants, Synsurf® and Curosurf®, were tested in a respiratory distress preterm lamb model. This prophylactic treatment demonstrated that a novel synthetic peptide-containing surfactant (Synsurf®) resulted in a more sustained, improved oxygenation response compared to that of Curosurf®- or saline-treated premature lambs when treated before first breath. The authors reasoned that the polypeptide poly-L-lysine, which is widely used in membrane research due to its interaction with acidic lipids, was worth studying as a KL_4 alternative (van Zyl, Smith 2013b). Future feasibility study for Synsurf® treatment of pre-term infants at risk for RDS are still being considered; but preliminary animal studies have provided promising data to support future human investigations.

1.4 Surfactant: The Innate and Adaptive Immune System

1.4.1 Lungs and Inflammation

The lungs present an immunological challenge for the host as they are most frequently targeted by pathogens. The respiratory epithelium serves as the surface for gaseous exchange along with its ability to fight inhaled pathogens, pollutants and particles. The lungs are constantly challenged and therefore have several different defence mechanisms in place such as filtration of air in the naso-oropharynx and conducting airways, sneezing and coughing. The epithelium represents a physical barrier that produces mucus, which, along with, mucociliary clearance combats any possible onslaught (Wright 2005).

A variety of cells participate in the pulmonary immune response, and the relative involvement of different cells varies with different diseases and the degree of inflammation. The innate immunity is the first line of defence and it recruits a number of leukocytes including basophils, eosinophils, natural killer (NK) cells, mast cells along with the phagocytic cells macrophages, neutrophils and dentritic cells (DCs). The immune cells recognise the pathogen by relying on a large family of pattern recognition receptors (PRRs) termed pathogen-associated molecular patterns (PAMPs). These immune cells can either engage in phagocytosis to "engulf" pathogens or release inflammatory mediators such as histamine and leukotrines (eicosanoid inflammatory mediators) (Mogensen 2009).

The adaptive immune system is also known as the acquired immune system and it is composed of highly specialised, systemic cells. These cells, when they encounter a pathogen, create an immunological memory with a specific response, which will be enhanced to subsequent encounters with that pathogen. The adaptive immune response involves DCs and T and B lymphocytes (and to a lesser extent macrophages) which are known as professional antigen presenting cells (Mogensen 2009).

1.4.2 Inflammation and Cytokines

Inflammation is a self-protective mechanism initiated by the body's innate immune system against tissue injury or infection; but may elicit an adaptive trait by recruiting cells associated with the system to act in collaboration. It underlines a wide variety of physiological and

pathological processes. The latter aspect restricts the tissue damage at an affected site and is characterised by the secretion of numerous inflammatory mediators, which trigger the recruitment of leukocytes and other proteins. These processes are well appreciated, whilst the physiological functions are yet to be determined. Much progress has been made in understanding the cellular and molecular mechanisms found in the acute inflammatory response to infection and, to a lesser extent, tissue injury. In addition, the events leading up to localised chronic inflammation, particularly that which is associated with chronic infections and autoimmune diseases, are only partially known. Systemic chronic inflammation's causes and mechanisms are much less well understood, but do not seem to be caused by the same activators as those associated with local lung infection and injury. It is rather accompanied by malfunction of tissue. That said; it is the homeostatic imbalance of one of several physiological systems that are not directly related to the function of host defence or tissue repair (Medzhitov 2008). The fundamental function of the inflammatory process is to resolve the infection and repair the damaged tissue in order to return the system back to a state of homeostasis. The effectiveness of this function relies on the system's ability to produce a rapid response, whilst ideally limiting the damage to a specific region. However, chronic inflammation, as seen in COPD, causes more damage to the system than a microbe trigger (Barton 2008).

The innate immune response is the first line of defence against an invading pathogen or infection and is activated within a few hours of exposure. Lipopolysaccharides (LPS) and peptidoglycans from bacterial cell walls are examples of PAMPs that trigger recognition on the PRR in immune cells (Horton 2010). Alongside neutrophils and DCs, macrophages, which link the innate and adaptive immune systems, possess a type of germline-encoded receptor/PRR called Toll-like receptors (TLRs) on their surface and within their cytoplasm. Once the TLRs detect PAMPs, the innate immune system is initiated and the release of pro-inflammatory mediators such as cytokines, chemokines and lipid mediators into the circulation is initiated. It does so in distinctive dynamic pattern and results in the activation, recruitment and/or migration of cells to the site of infection (see Figure 1.10) (Akira, Takeda et al. 2001, Russell 2014).

The IL-1 receptor (IL-1R) family members consist of very wide related receptors, including the TLRs, and are characterised by very different extracellular immunoglobulin-like domains and large intracellular Toll/IL-1R (TIR) domains (Slack, Schooley et al. 2000). When the TLRs

are activated, adapter proteins and kinases, such as MyD88 (Wesche, Henzel et al. 1997) and IRAK (Akira, Takeda 2004), are recruited.

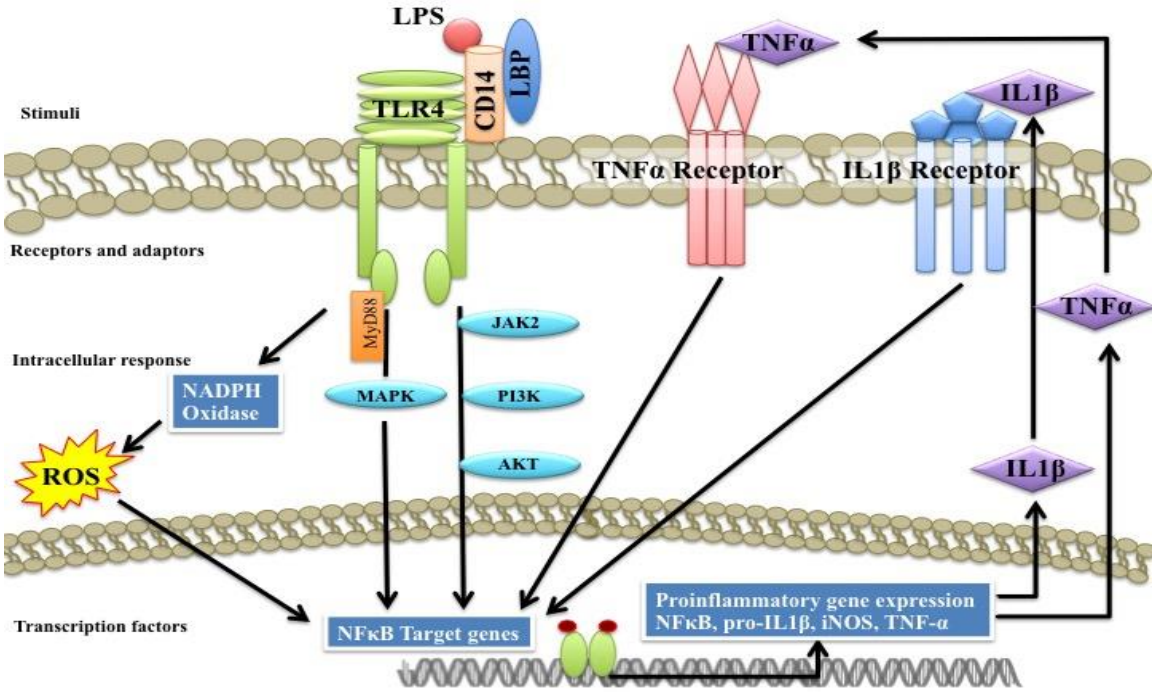

Figure 1.10: The LPS-mediated cellular production of inflammatory cytokines within the macrophage. IL-1β and TNF- α are examples of cytokines that can stimulate their own synthesis. **Abbreviations:** LPS, lipopolysaccharide; ROS, reactive oxygen species; TLR4, toll-like receptor 4; NF-κB, nuclear factor-κB; IL-1β, interleukin 1 beta; iNOS, inducible nitric oxide synthase; TNF-α, tumor necrosis factor alpha

The transcription factors AP-1, CREB, NF-κB and IRF3 are activated through direct or indirect mechanisms after which they are translocated to the nucleus. There, they induce gene transcription of pro-inflammatory factors. The wide variety of target genes regulated by NF-κB includes those encoding cytokines (e.g., IL-1, IL-2, IL-6, IL-12, TNF-α, LTα, LTβ, and GM-CSF), chemokines (e.g., KC/GRO, IL-8, MIP-1α, MCP1, CCL5/RANTES, and eotaxin) (Ghosh, Karin 2002). Interestingly, IL-1 and TNF-α are exploited in a feed forward loop to initiate and intensify the inflammatory response by re-binding to the IL-1Rs. The inflammatory response is driven and maintained by highly integrated gene transcription control within the nucleus of the cell; as well as with multiple steps of post-transcriptional modifiers that modulate mRNA production, transport, translation and posttranscriptional regulation. The rates

of mRNA transport, decay, and translation crucially influences the timing and magnitude of the cellular immune responses (Ishmael, Fang et al. 2007).

Most studies on inflammation have focused on preventing the start of inflammation rather than halting progression of the response. However, as we explore further into finding improved treatments for inflammatory disorders, it is imperative to have a better understanding of the inflammatory mechanisms and the resulting consequences for possible future therapies (Nguyen, Rajaram et al. 2012).

1.4.3 Surfactant Collectins and Immunity

Pulmonary surfactant serves two functions in the lung. Firstly, it is a surface acting agent, initially identified as a lipoprotein complex that lowers surface tension at the air-liquid interface of the alveolar surface. Secondly, the hydrophilic surfactant proteins SP-A and SP-D (also known as collectins) are important components of the innate immune response in the lung and therefore assist in pulmonary host defence. Furthermore; they may also modulate the adaptive immune response. The inflammatory response in the alveolar microenvironment is tightly regulated to avoid damage to the gas-exchanging delicate structures through the concerted efforts of the innate and adaptive immune system.

The phospholipid and protein combination has unique spreading qualities (90% phospholipids and 10% proteins) courtesy of the hydrophobic surfactant proteins B and C (SP-B, SP-C). This promotes lung expansion during inspiration and prevents lung collapse during expiration. They have an essential function in the spreading, adsorption and stability of surfactant lipids (Haagsman, Hogenkamp et al. 2008). Surfactant composition and pool size is controlled by secretion, re-uptake, and recycling by alveolar type II epithelial cells and both alveolar type II epithelial cells and macrophages are responsible for the degradation thereof (Chroneos, Sever-Chroneos et al. 2010).

Earlier studies have provided support for the concept that surfactant might have a role in linking innate and adaptive immunity in the lung by modulating functions of both DCs and T cells. DCs, the most potent antigen-presenting cells in the body, are localised at the host–environment interface, in regions such as the skin and the lung (Havenith, Breedijk et al. 1992). In the lung,

DCs are found in the airway epithelium, the lung parenchyma and the alveolar air-space (Sertl 1986).

On the basis of the observation that lymphocytes, isolated by lung lavage, are hyporesponsive compared with circulating peripheral lymphocytes; Ansfield and co-workers (1979) proposed and showed that surfactant and, in particular, surfactant lipids inhibit lymphocyte function. Subsequent studies by Borron and colleagues (1998) showed that SP-A and SP-D inhibit proliferation of T cells that have been stimulated with plant lectins, CD3-specific antibodies or phorbol esters, by a process that is thought to be mediated (at least, in part) by inhibition of IL-2 production. In addition, both the collagen-like region and the CRD101 of SP-A have been implicated in the inhibition of lymphocyte function, probably owing to inhibition of calcium signalling (Borron, McCormack et al. 1998, Ansfield, Kaltreider et al. 1979).

Although a direct role for SP-A and SP-D in modulating DCs and T-cell functions has been shown *in vivo*, SP-D-null mice have an interesting phenotype with respect to their lymphocytes. Fisher and colleagues reported that SP-D-null mice have peribronchial and perivascular accumulations of lymphocytes in airways and vessels but not in the interstitium. These lymphocytes were activated, as seen by increases in the proportion of both CD4+ and CD8+ T cells that expressed both CD25 and CD69 (Shepherd 2002).

Shepherd (2002) stated in an invited commentary that these studies indicate that SP-D and SP-A might provide an important link between innate and adaptive immunity, by modulation of DCs and T-cell functions. In such a situation, SP-D in the alveolar space would enhance the uptake of pathogens by immature DCs, which are recruited into the alveolar air-space during infection or inflammation. For example, although previous studies have shown that SP-D can bind to *Escherichia coli* (E. *coli*) and enhance its uptake by macrophages (see Figure 1.11), this is the first report showing that SP-D enhances *E.* coli entry into DCs (Brinker, Martin et al. 2001). SP-A would function to inhibit DC maturation, and both SP-A and SP-D would suppress T-cell activation in the alveolar space, which if it occurred, could result in an inflammatory cascade that could damage the lung and impair gas exchange. Additional studies will be required to elucidate the role of surfactant in regulating adaptive immune responses *in vivo*.

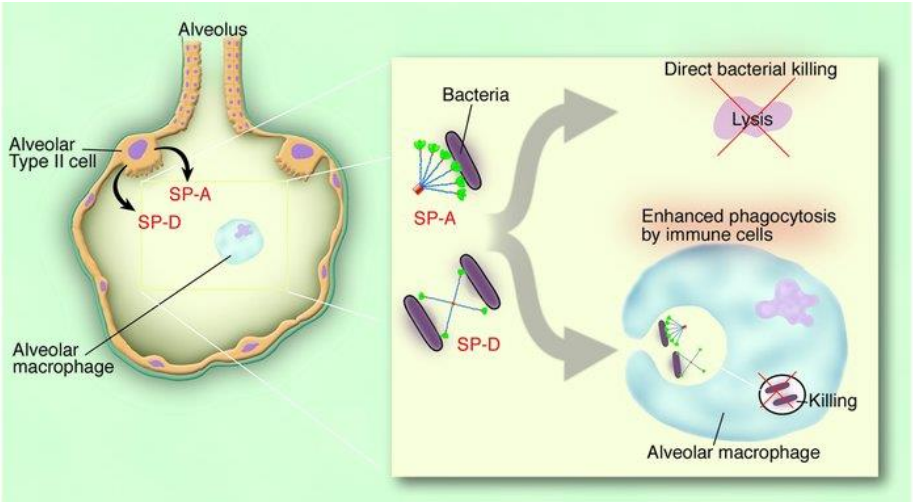

Figure 1.11: Both SP-A and SP-D opsonise pathogens and enhance their phagocytosis by innate immune cells such as alveolar macrophages and neutrophils (Wright 2003).

1.4.4 Surfactant: Effect on Alveolar Macrophages

Harvesting alveolar macrophages (AMs) by bronchoalveolar lavage was first described in 1960 and has since been extensively investigated (Gee, Fick 1980). These cells are critical for host defence as they are the major cell type in recognising infection or injury and innate immunity and comprise 85% of the recovered cells in human lung lavage fluid. They phagocytose particulate matter and invading microorganisms, release cytotoxic reactive oxygen species (ROS) and proteolytic enzymes, and produce nitric oxide (NO) for microbial killing and signalling functions (Fels, Cohn 1986). As previously stated, AMs bring about the pulmonary inflammatory response *via* production of cytokines and chemokines as they are responsive to both specific and nonspecific stimuli; thereby being capable of forming part of both the innate and adaptive immunity. Furthermore, they regulate antigen presentation and opsonisation (Wright 2005). AMs also remove intra-alveolar debris whilst regulating the metabolism and recycling of endogenous surfactant (Kerecman, Mustafa et al. 2008).

As mentioned previously, the two main functions of surfactant are to improve pulmonary mechanics and oxygenation. It (and/or its components) also assists to modulate innate pulmonary immunity and the mechanism of this process lies in the alteration of immune cell function through initiating the inflammatory cascade (Suresh, Soll 2005). Natural surfactant significantly decreased macrophage-mediated neutrophil chemotaxis. Finck and colleagues

(1998) suggested that at low concentrations, surfactant inhibits chemokine release and may reduce pulmonary neutrophil sequestration *in vivo*. It is also well known that alveolar macrophages can be induced to produce nitric oxide (NO) *via* inducible nitric oxide synthase (iNOS) as Lavnikova and collegues (1993) demonstrated with rat alveolar macrophages which produced NO in response to inflammatory stimuli or cytokines, e.g., lipopolysaccharide (LPS) or interferon-γ (IFN-γ) (Lavnikova, Drapier et al. 1993, Finck, Hodell et al. 1998). Furthermore, another study concluded that individual surfactant phospholipids differently modulate the priming of AMs for oxidative responses (Hayakawa, Giridhar et al. 1992).

The natural surfactant's hydrophilic proteins (SP-A and SP-D) have been shown to mediate host defence properties and SP-A specifically decreases TNF-α production, phagocytosis of pathogens and release of ROS (Chroneos, Sever-Chroneos et al. 2010). However, some studies have indicated that exogenous surfactant preparations without measurable hydrophilic proteins also inhibits LPS-stimulated IL-1β and TNF-α secretion and decreases cytokine RNA expression in AMs (Thomassen, Antal et al. 1994). The mechanism by which exogenous surfactants and their components regulate this anti-inflammatory effect is not fully known. However, previous studies by Thomassen and colleagues may offer insight as they demonstrated inhibition of endotoxin-stimulated cytokine secretion from human alveolar macrophages *in vitro* by the synthetic surfactant Exosurf®. They concluded that the suppression was not stimulus specific but Exosurf® reduced both cell associated and secreted TNF-α and IL-1β. This indicates that Exosurf® is not simply blocking cytokine release but, with the observations that with decreased mRNA levels at different time points, it supports the fact that Exosurf® could pre-translationally mediate AM cytokine production (Thomassen, Antal et al. 1994).

There have been some studies that have shown, under different circumstances, that SP-A and SP-D enhance pathogen-dependent activation of pro-inflammatory responses of alveolar macrophages during phagocytosis of SP-A or SP-D-opsonized microbes *in vitro*. Weikert and colleagues (2000) demonstrated this with a study that included bacillus Calmette-Guerin (BCG) organisms grown in the absence of SP-A; where growth increased over a 5-day period whereas inclusion of SP-A dramatically inhibited BCG growth. Inhibition of nitric oxide production blocked BCG killing in the presence and absence of SP-A. It was concluded that the ingestion of SP-A-BCG complexes by rat macrophages leads to production of inflammatory mediators and increased mycobacterial killing (Weikert, Lopez et al. 2000). Barr and

colleagues (2000) studied the effect of SP-A- mediated uptake of respiratory syncytial virus (RSV) on production of TNF-α and interleukin IL-10 by peripheral blood monocytes (PBMC) and alveolar macrophages. Their findings suggested that SP-A is an important opsonin for RSV and that SP-A-mediated uptake of RSV may alter some of the unusual cytokine responses that are postulated to be involved in incomplete immunity to recurrent infection (Barr, Pedigo et al. 2000). Both of these studies are examples of a pro-active clearance mechanism that also operates *in vivo* during initial clearance of experimental pulmonary infections (Chroneos, Sever-Chroneos et al. 2010).

In contrast, other studies have shown that, in contrast, SP-A and SP-D suppress secretion of pro-inflammatory cytokines and oxidant intermediates when macrophages are challenged with components (e.g. LPS). The role of surfactant-associated protein (SP) A in the mediation of pulmonary responses to bacterial LPS was assessed *in vivo* with SP-A gene-targeted [SP-deficient; SP-A(-/-)] and wild-type [SP-A(+/+)] mice in a study performed by Borron *et al.* (2000). The SP-A(-/-) mice produced significantly more TNF-alpha and nitric oxide than SP-A(+/+) mice after LPS treatment. Intratracheal administration of human SP-A to SP-A(-/-) mice restored regulation of TNF-alpha, macrophage inflammatory protein-2, and nitric oxide production to that of SP-A(+/+) mice. This study displays the protective function of SP-A in both *in vivo* animal models and *in vitro* macrophage components as endogenous and/or exogenous SP-A inhibits pulmonary LPS-induced cytokine and nitric oxide production (Borron, McIntosh et al. 2000). It has also been reported that SP-A enhances the secretion of anti-inflammatory IL-10 and induces the secretion of TGF-β when in the presence of mycobacterial cell wall antigen or apoptotic cells (Reidy, Wright 2003).

Therefore, it is necessary to investigate the intracellular events in macrophages treated with exogenous surfactant and assess the possible immunoactive and anti-oxidant properties of said exogenous surfactants in endotoxin-activated and non-activated macrophages. These findings may elucidate the coordination and synchronisation of surfactant metabolism with immune responses within the lung.

1.4.5 Potential Immunogenicity and Immunomodulatory activity of Surfactants

To demonstrate the efficacy and safety of the porcine pulmonary surfactant preparation (Butantan® surfactant) in premature infants, Precioso and colleagues saw it necessary to study its immunogenicity in an adult rabbit model first. This comes directly from the need to study any possible immunogenicity the introduction of the porcine surfactant proteins may elicit in the airway of premature infants. This includes possible antigenic stimuli (linking the innate and adaptive immunity) with a resultant immunological response against those proteins. Their results demonstrated relevance from a clinical as well as an economical point of view concerning the efficacy and safety of Butantan surfactant since it may be a suitable alternative replacement therapy to Curosurf® or Survanta® (Precioso, Sakae et al. 2006).

Various research groups have chemically prepared peptides with sequences based on SP-B such as a KL_4- surfactant, namely Surfaxin®, which was the first synthetic peptide-containing surfactant approved by the FDA (Cochrane, Revak et al. 1996). This surfactant was thought to become an alternative to Curosurf® used as the standard of care in managing RDS; however, Surfaxin® was discontinued in 2015. Based on its design, van Zyl and colleagues developed a polymer-containing surfactant (Synsurf®) consisting of the phospholipids dipalmitoylphosphatidylcholine (DPPC), phosphatidyl glycerol (PG) and poly-L-lysine electrostatically bonded to poly-L-glutamic acid. The polymers were added to the phospholipids in order to mimic the hydrophobic and hydrophilic nature of SP-B or SP-C in the mixture (Van Zyl, Smith et al. 2013a).

Surfactant preparations which have been investigated for therapy differ in composition of their phospholipids, with or without proteins, natural as well as synthetically manufactured surfactants containing peptide constructs (Strayer, Merritt et al. 1989). In this study, we deemed it necessary to establish whether Synsurf® elicits immunomodulatory and immunogenicity characteristics in comparison to other natural surfactants currently in use today. A study conducted by Whitsett and co-workers investigated whether antibodies generated against bovine surfactant proteins, SP-B or SP-C, are detected in serum from infants treated with Survanta®. It was discovered discovered that polyclonal antisera generated in rabbits against the small molecular weight proteins were uniformly reactive with the bovine surfactant test antigens. However, antibodies reacting with the surfactant proteins were never detected by immunoblot analysis with the sera of infants (Whitsett, Hull et al. 1991).

The possibility exists that this study correlates with the findings from a previous study done by Strayer *et al.* (1991) who sought to determine the immunogenicity and the degree of immunologic cross-reactivity of animal pulmonary surfactants because of the expanded use of surfactants to treat neonatal RDS as well as adult RDS. They once again stressed the importance of examining the potential immunologically mediated side effects such as antibody- or immune complex-mediated tissue injury. It is thus critical to recognise the spectrum of injury that is associated with neonatal and adult RDS and its treatment. Therefore, treatment and therapy of RDS should take into consideration the possibility that cross-reactive immunogenic substances may be introduced in patients with RDS. Also, the possibility that effective treatment of RDS may decrease the immune system's exposure to immunogenic endogenous surfactants. This may then mitigate potential future damage due to surfactant immunogenicity (Strayer, Hallman et al. 1991).

1.5 *Mycobacterium Tuberculosis* and Surfactant therapy

1.5.1 Brief history of Tuberculosis

Tuberculosis (TB) is an infectious disease caused by the bacillus *Mycobacterium tuberculosis*. It typically affects the lungs (pulmonary TB) but can affect other sites as well (extrapulmonary TB).By making use of modern day DNA extraction and purification methods, molecular evidence for TB was found in an ancient Egyptian mummy from the New Kingdom which dated back to about 1550 — 1080 BC (Nerlich, Haas et al. 1997). The skeletal remains of Egyptian mummies offered supporting evidence showing that prehistoric humans (4000 BC) had TB, and the tubercular decay in the spines of Egyptian mummies was reported (3000-2400 BC)(Zink, Sola et al. 2003). The German physician Robert Koch was the first to identify and describe the M. *tuberculosis* bacilli in 1882; however, tuberculosis was generally referred to as "consumption" in the poor urban population of Britain and Europe in the early 19th century (Koch 1882). The only treatment available at that time was to stimulate the body's own immune system. Doctors expressed focus on a healthy diet, fresh air, hygiene and the administration of expectorants and purgatives. This led to the opening of the first sanatorium in 1854 in Germany (Rivero 2008).

1.5.2 Epidemiology of Tuberculosis

Worldwide, it was estimated that 9.6 million people were infected with TB in 2014: 5.4 million men, 3.2 million women and 1.0 million children. Globally, 12% of the 9.6 million new TB cases in 2014 were HIV-positive; almost 75% of these cases were in the African Region. These cases led to the deaths of 1.5 million people (1.1 million HIV-negative and 0.4 million HIV-positive) and totalled to 890 000 men, 480 000 women and 140 000 children (World Health Organization 2015). There have been 22 high burden countries (HBC's) identified by the WHO that contribute to 81% of the global TB occurrence. South Africa has been reported to be the sixth highest regarding incidence and the eighth highest regarding estimated prevalence (World Health Organization 2015). Even though the global TB rates have slowly declined (an average of 1.5% per year since 2000); when taking into account the adjustment of population size, from 2012 to 2014, South Africa held its position as having the highest incidence and prevalence of TB among the HBC's (World Health Organization 2012, World Health Organization 2015). South Africa also experienced the largest number of HIV-associated TB cases and the second

largest number of diagnosed multidrug resistant (MDR) TB cases following India. TB remains a global health threat and South Africa has one of the highest rates of TB prevalence (56-66%) driven by HIV (Churchyard, Fielding et al. 2014).

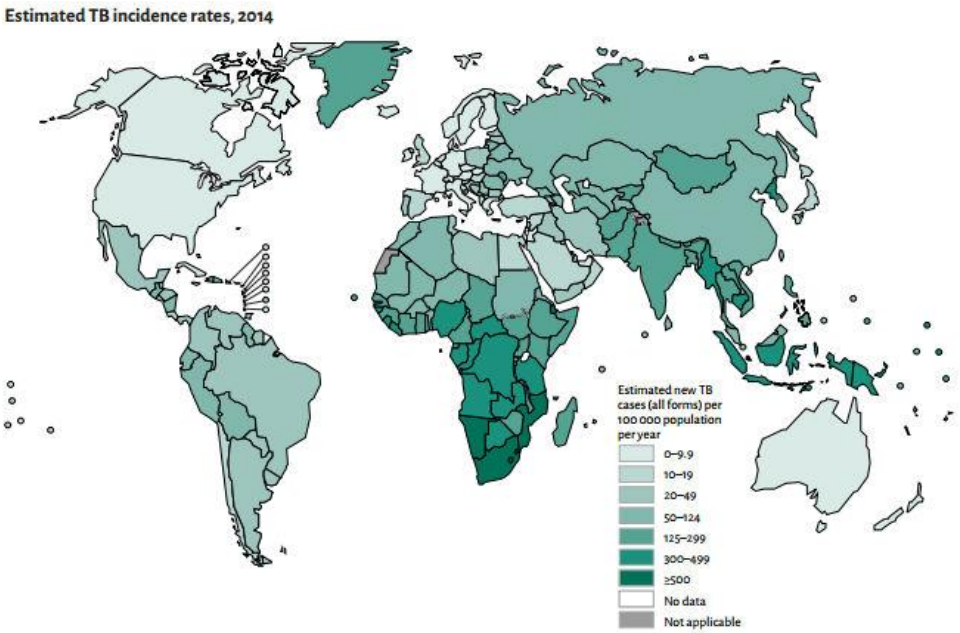

Figure 1.12: Estimated TB incident rates in 2014 (World Health Organization 2015).

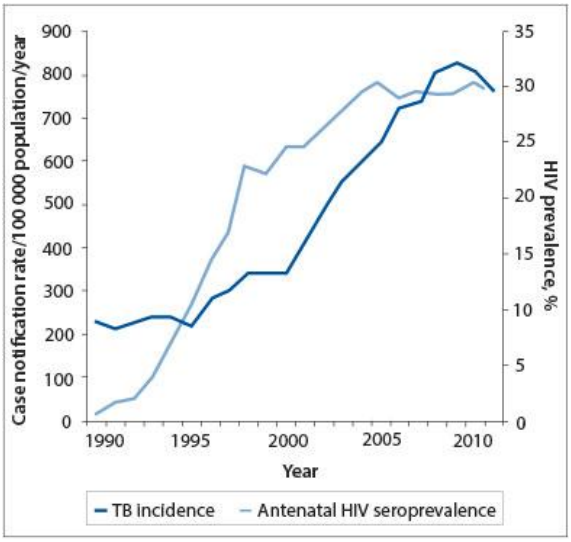

Figure 1.13: Trends in tuberculosis case notification rates and HIV prevalence in South Africa (Churchyard, Fielding et al. 2014).

A person obtains the M. *tuberculosis* (M.*tb*) infection by the inhalation of infected aerosols droplets (2–5 mm in diameter containing as few as 1–3 bacilli) (Koul, Arnoult et al. 2011),

which are produced by people with the active pulmonary disease (Wallis, Pai et al. 2010). When one encounters M.*tb* bacilli (Figure 1.14), three possible outcomes can occur: 1) Clinical symptoms may develop in a few members of the population who develop primary active TB, 2) Latent infection occurs when the majority of infected persons show no disease symptoms but may develop an effective acquired response, 3) it is possible for a portion of latently infected persons to reactivate and develop post-primary active TB (Gideon, Flynn 2011).

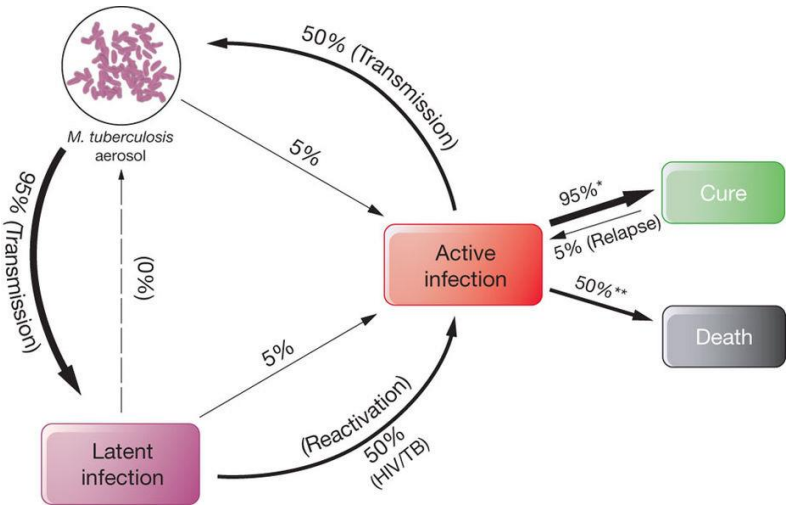

Figure 1.14: Stages of M. *tuberculosis* infection (Koul, Arnoult et al. 2011).

1.5.3 Multi-drug Resistant and Extensively-drug Resistant TB

Multi-drug resistant tuberculosis (MDR-TB) is defined by the WHO as M. *tuberculosis* strains resistant to rifampicin and isoniazid; whereas, extensively resistant tuberculosis (XDR-TB) is defined as MDR-TB that is also resistant to a minimum of three of the six classes of second line drugs (aminoglycosides, polypeptides, fluoroquinolones, thioamides, cycloserine and para-aminosalicylic acid (PAS)). Drug resistance determination is difficult to establish due to the challenges associated with drug-susceptibility testing (DST) such as diagnosis treatment. Therefore, the WHO's XDR-TB Task Force governed in Geneva, Switzerland (October 2006), and modified the definition of XDR-TB. It is now re-defined to XDR-TB as having 'resistance to at least rifampicin and isoniazid (i.e. the definition of MDR-TB), in addition to any fluoroquinolone, and to at least one of the three following injectable drugs used in anti-TB treatment: capreomycin, kanamycin and amikacin' (Migliori, Besozzi et al. 2007).

Estimates of 3.3% of the worldwide new cases and 20% of previously treated cases have MDR-

TB, only about a quarter of these (123 000) were detected and reported. In 2014, there were an estimated 480 000 (360 000–600 000) new cases of global MDR-TB (although there were only 300 000 reported cases, 53% were among new cases and 47% were among previously treated cases) of which 50% of these were in India, China and the Russian Federation. Three-quarters of the 123 000 patients with rifampicin-resistant tuberculosis (RR-TB)/MDR -TB lived in the European Region, India, South Africa or China; equivalent to 41% of the total global MDR-TB burden reported in 2014. Approximately 190 000 (120 000–260 000) deaths resulted from MDR-TB. TB patients co-infected with HIV were estimated at 77% of known TB patients (392 000 people). Of the represented MDR-TB data, XDR-TB amounted to 9.7% portion (World Health Organization 2015). The number of reported MDR-TB and XDR-TB cases in SA increased between 2010 and 2012, with 15 419 and 1 596 cases, respectively, diagnosed in 2012. In 2014, there were 8 640 reported new cases worldwide as well as 32 160 cases of previously diagnosed cases who relapsed to re-treatment (World Health Organization 2012, World Health Organization 2015).

A physician in India identified and reported an alleged incurable form of TB in 2012 which resulted in the first cases of (what was referred to as) totally drug-resistant tuberculosis, TDR-TB (Migliori, Besozzi et al. 2007). More recently, cases have also been reported in Iran, India and South Africa. TDR-TB has been loosely defined as displaying *in vitro* resistance to all first- and second-line drugs tested (rifampicin, isoniazid, streptomycin, ethambutol, pyrazinamide, ethionamide, para-aminosalicylic acid, cycloserine, ofloxacin, amikacin, ciprofloxacin, capreomycin and kanamycin) (Parida, Axelsson-Robertson et al. 2015). This led to the WHO consultative meeting on TDR-TB and in conclusion the committee members did not officially endorse the 'TDR-TB' terminology (Udwadia, Amale et al. 2012). As it still remains to be fully defined, many argue that it is another form of XDR-TB and some rather refer to it as XDR-TB as DST data is 1) limited, 2) not yet established for TDR-TB, or 3) as correlations of DST results and clinical response to treatment have not yet been established. Bedaquiline, delamanid and linezolid are three new drugs that were recently approved by the US Food and Drug Administration (FDA) and the European Medicines Agency. The effectiveness of these drugs against these TDR-TB strains has yet to be considered and they may offer therapeutic solutions for TDR-TB, challenging TDR terminology (Parida, Axelsson-Robertson et al. 2015).

1.5.4 The Evolution of Current TB Chemotherapy

The effective treatment of TB started in 1946 when Streptomycin (SM) was discovered two years prior (Figure 1.15). The Tuberculosis Research Unit of the British Medical Research Council (BMRC) undertook the first clinical trial. However, the frequent emergence of SM resistance led to a second BMRC clinical trial. The combined treatment with SM and para-aminosalicylic acid (PAS) greatly reduced the incidence of SM resistance (Mitchison, Davies 2012). This was then followed by the introduction of isoniazid (INH) in the 1950s, which established the basis of anti-TB chemotherapy until the 1960s. Some regimens explored the possibility of using INH alone. Shortly after this effort, the BMRC headed a national survey in the United Kingdom that led to the discovery that resistant strains were almost always resistant to one of the three available drugs (Fox, Wiener et al. 1957). A combination of SM, INH and PAS formed the first combination TB chemotherapy regimen that was administered over a period of 24 months so that at least two would combat almost any possible resistant strain. Ethambutol (ETH) was substituted for PAS in the early 1960s and treatment duration was shortened by 6 months (Schmitz, Kleine-Allekotte 1960). More than 95% of patients were cured when Rifampicin (RIF) was included in the regime after its discovery in 1965 and the treatment duration was further reduced to 9-12 months. Lastly, Pyrazinamide (PZA) was introduced in the 1980s and shortly thereafter, facilitated the newly WHO launched modern-day short-course treatment; also known as the directly observed treatment, short-course (DOTS) strategy (Nuermberger, Spigelman et al. 2010). DOTS allow patients to consume each dose of anti-TB drugs under supervision to the treatment strategy. It is strongly recommended as this approach maximizes the probability of therapy completion limiting the emergence of possible drug-resistance (Blumberg, Burman et al. 2003).

According to the South African tuberculosis control program, the current standard first line treatment regimen of 2014 consists out of an initial (or intensive) phase and a continuation phase (See Table 1.2). Although treatment of drug-susceptible TB under ideal conditions by DOTS may be successful in 95% of cases, cure rates in the field are often significantly lower (World Health Organization 2012, World Health Organization 2015).

Table 1.2: Treatment regimen for known drug sensitive TB in adults. R – Rifampicin H – Isoniazid Z or PZA– Pyrazinamide E or ETH – Ethambutol (Republic of South Africa: National Department of Health 2014).

Pre- Treatment body weight (kg)	**Intensive phase: 2 months**	**Continuation phase: 4 months**	
	RHZE (150/75/400/275) mg	RH (150/75) mg	RH (300/150) mg
30–37 kg	2 tablets	2 tablets	
38–54 kg	3 tablets	3 tablets	
55–70 kg	4 tablets		2 tablets
≥71kg	5 tablets		2 tablets

The basic principles of treatment and recommended standard anti-TB regimens for adults are also indicated for children. Doses for children are usually extrapolated from adult pharmacokinetic studies, and recent data point to the inadequacy of currently recommended doses of RIF, INH, and ETH. Children eliminate INH faster and require a higher body weight dose (mg/kg) to achieve serum concentrations comparable to those in adults (McIlleron, Willemse et al. 2009).

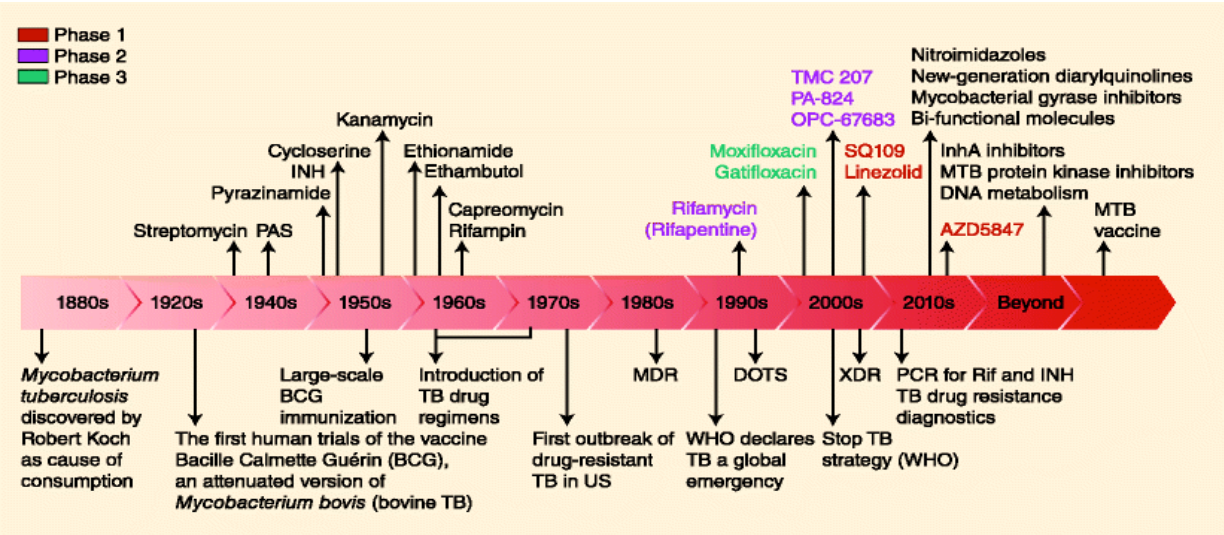

Figure 1.15: Timeline in TB and antitubercular drug development, *DOTS*, directly observed therapy, *MDR* multidrug resistant, M.*tb*, *Mycobacterium, tuberculosis*, TB, tuberculosis, *XDR*, extensively drug resistant (Lalloo, Ambaram 2010).

When treating MDR-TB, consideration of specific resistance gives way to two treatment possibilities. Firstly, a combined treatment plan of aminoglycoside, a fluoroquinolone, PZA, and ethionamide or prothionamide can be used for MDR-TB with resistance to both INH and RIF. However, the second option of an aminoglycoside, fluoroquinolone, PAS, cycloserine, and ethionamide or prothionamide is required for disease with resistance to INH, RIF, ETH and PZA (Nuermberger, Spigelman et al. 2010). Managing MDR-TB is challenging because it requires a prolonged treatment regimen of 24 months that includes second-line drugs, which are more toxic and expensive than first-line drugs. The WHO guidelines for programmatic management of MDR-TB for 2015 has gone unchanged since 2006. For an optimal regimen it should include a fluoroquinolone (ofloxacin, moxifloxacin, ciprofloxacin), an injectable agent (capreomycin, kanamycin, or amikacin), and at least 2 of the following drugs: cycloserine, PAS, and first-line agents other than INH and RIF such as PZA and ETH (World Health Organization 2015).

1.5.5 Prospects and Challenges for Future TB Chemotherapy

Due to the satisfactory cure rates regarding first line drugs in the developing world, research into new anti-tubercular drugs continued to plateau until the late 1990s. The HIV epidemic along with drug-resistant TB drove renewed interest into developing several candidate molecules. This resulted in the synergistic research of newer drugs as well as more effective regimens. The DOTS strategy has revealed that it is difficult to maintain in many national TB control programmes over an extended period of time. Failure to ensure patient compliance is one of the most common reasons for this due to the treatment associated adverse-effects. First line drugs (see Table 1.3) are known to cause nausea, vomiting and drug induced hepatitis. Non-compliance to the recommended chemotherapeutic regimen not only lowers cure rates, but leads to the development of drug-resistant TB, inclusive of the formidable scenarios of MDR-TB and XDR-TB (Zignol, Hosseini et al. 2006, Van Rensburg 2012). The known concern of current TB drugs interactions with the antiretroviral drugs taken by HIV positive people, means that there is an urgent need for new TB drugs. However, new TB drugs should desirably offer: 1) shorter and simpler, but still affordable, multi drug regimens for drug sensitive TB; 2) shorter, more effective, less toxic, and less expensive regimes for drug resistant TB; 3) short, simple, easily tolerable and safe regimes for latent TB; 4) as well as drugs with few drug-drug interactions, so they can be safely provided to patients co-infected with HIV.

Table 1.3: Classification of anti TB drugs (World Health Organization 2015).

First - line	Second - line	Third - line
Rifampicin	Aminoglycosides	Rifabutin
Isoniazid	Amikacin	Macrolides
Ethambutol	Neomycin	Clarithromycin
Pyrazinamide	Polypeptides	Linezolid
	Capreomycin	Thiacetazone
	Viomycin	Thioridazine
	Emviomycin	Arginine
	Flouroquinolones	VitaminD
	Ofloxacin	Perchlorperazine
	Levofloxacin	
	Ciprofloxacin	
	Moxifloxacin	
	Thioamides	
	Ethionamide	
	Prothionamide	
	Para-aminosalicylic acid	

Another pressing concern that needs attention is the availability of paediatric formulations with specific consideration to both individual and fixed drug combinations that offer good bioavailability. There are liquid formulations that are easy to administer to young children, but these bulky and more expensive formulations come with unacceptable toxicity levels. For example, INH syrup causes diarrhoea due to the sorbitol base (Kanabus 2016).

Table 1.4: TB drugs used to treat drug resistant TB according to group (Kanabus 2016).

Group 1 **First Line Oral Agents**	**Group 2** **Injectable Agents**	**Group 3** **Fluoroquinolones**	**Group 4** **Oral Bacteriostatic Second Line Agents**	**Group 5** **Agents with an unclear role in the treatment of drug resistant TB**
pyrazinamide	kanamycin	levofloxacin	para–aminosalicylic acid	clofazimine
ethambutol	amikacin	moxifloxacin	cycloserine	linezolid
rifabutin	capreomycin	ofloxacin	terizidone	amoxicillin/clavulanate
	streptomycin		thionamide	thioacetazone
			protionamide	imipenem/cilastatin
				clarithromycin

Few trials have been carried out on the drugs in Group 5 (see Table 1.4) to see how effective they actually are in the treatment of drug resistant TB. For example, the drug linezolid is an antibiotic usually used to treat severe bacterial infections. The first trial of this drug was led by the National Institute of Allergy and Infectious Diseases to investigate the use of it in treating XDR-TB. It was a small trial but it did show that the drug was effective when added to patients' current treatments, although most of the patients experienced adverse effects (nausea, vomiting, and epigastric pain) (Steenhuysen 2012). Besides linezolid being able to offer a 100% bioavailability and appears to be well tolerated; it has the ability to enter macrophages and thus also has intracellular activity. This is an important feature of this drug when used against mycobacteria that cause chronic infections and require long-term therapy (Wallace, Brown-Elliott et al. 2001).

One prospect that has shown some promise in the advancement of TB chemotherapy is the repurposing of current chemotherapeutic agents; as is the case with linezolid. Drug resistance mainly involves genetic evolution of the pathogen to overcome the toxic effects of the drug and is exacerbated by inappropriate prescription and/or patient non-compliance. Thus, even though research into novel agents and new drugs is important, it is likely that resistance towards these agents will develop in the organism. Thereby, making it more important to work towards

increasing the treatment options that are currently available that target diverse metabolic pathways in the bacilli (Maitra, Bates et al. 2015). However, a concern that one would need to take into consideration when including new derivatives in different drug combinations, is the possibility of cross-resistance (Casenghi, Schoen-Angerer 2006). Another example is a recent study done at Stellenbosch University, called NC001. It involved a new drug combination of an experimental medicine called PA-824 (nitroimidazole derivative) alongside bedaquiline, moxifloxacin and pyrazinamide. This cocktail, dubbed PaMZ, proved to be safe and presented the potential to reduce the time needed to treat drug resistant forms of the disease (Van Rensburg 2012).

The pulmonary collectins, SP-A and SP-D, as previously mentioned, have been reported to bind LPS, opsonize microorganisms, and enhance the clearance of lung pathogens. They enhance the *in vitro* phagocytosis and environmental killing of a variety of pulmonary pathogens by binding to mycobacterial organisms (Wright 2005, Samten, Townsend et al. 2008). Research has shown that most neonates who suffer from surfactant dysfunction are highly susceptible to GBS (group B streptococcal) infection and respiratory failure. Data from animal experiments have indicated that exogenous surfactant improved lung function and diminished bacterial growth in immature rabbits with experimentally induced neonatal GBS pneumonia (Herting, Sun et al. 1997). Therefore, apart from the biophysical properties of surfactant function within the lung, surfactant also plays an important role in the antibacterial defence system of the lung. Thus, the possible use of surfactant as a carrier for antibiotics or specific immunoglobulins is currently an excellent niche for respiratory drug delivery research.

Previous work by Pasula and colleagues (1997) suggest that the attachment of M.*tb* organisms to AMs can be mediated by SP-A. They further stipulated that it is most likely mediated by a carbohydrate-recognition domain on M.*tb* and the SP-A binding appeared to be specific and saturable. Therefore, this data is consistent with the hypothesis that SP-A functions as a "bridge" between the M.*tb* and AMs, facilitating an important first step in the development of infection (Pasula, Downing et al. 1997). Another study by Weikert and colleagues demonstrated how SP-A not only binds to BCG but enhances its uptake by rat AM. Once inside the macrophage, survival of the mycobacteria is dependent on its escaping the bactericidal mechanisms of the host. Rodent macrophages kill ingested mycobacteria through the induction of iNOS and subsequent production of NO. Interference of these systems via iNOS inhibitors have proven

the proliferation of M.*tb* and resulted in disease (Weikert, Lopez et al. 2000). Thus, when considering linezolid's characteristic trait of having intra-macrophage activity, it appears to be a worthy drug for further investigation alongside surfactant therapy due to its desirable properties as a new drug for therapy.

Currently, a common belief to approach the investigation of drug treatment efficacy for tuberculosis lies in exploring novel systems for drug delivery (Mckinney 2000). Local delivery to the lungs by inhalation has emerged as one of the most attractive administration routes to target pulmonary TB infection. Inhaled therapy or the direct administration of antibiotics into a tracheobronchial tree using nebulization or intratracheal instillations, delivers the drug to the diseased organ with a reduction in adverse effects associated with systemic toxicity whilst providing high concentration of drug in a focus of infection (Pandey, Khuller 2005, Parikh, Dalwadi et al. 2014). Administering drugs by the pulmonary route to the lungs allows higher drug concentrations within these lesions. Supplementing conventional therapy with inhaled anti-TB therapy may allow therapeutic concentrations of drug to penetrate locally into lung lesions and treat the resident mycobacteria (Muttil, Wang et al. 2009). The use of exogenous pulmonary surfactant as a vehicle for antibacterial agents has proven its theoretical feasibility to enhance the efficiency of local antimicrobial therapy but this method is still not practised in clinical settings (Kharasch, Sweeney et al. 1991, van't Veen, Mouton et al. 1995).

One such an innovative approach was investigated during the course of this thesis where the feasibility of using various surfactants in drug delivery *in vitro* was investigated.

1.6 Pulmonary Drug Delivery: Aerosol Characteristics and Inhalation Devices

Inhalation therapy has been used for thousands of years as a method for delivering medicine, albeit in a different form and use. Many of the principles used then are still embodied in modern devices still available today (Sanders 2007). Currently with the increase in our understanding of the physiology of the lung and related diseases, pulmonary drug delivery (PDD) is fast becoming an alternative choice to treat local and systemic diseases. The lungs remain an attractive target for drug delivery due to the non-invasive administration as it avoids first-pass metabolism, a more rapid onset of therapeutic action, direct delivery to the site of treatment of respiratory diseases as well as the availability of a huge surface area for local drug action and systemic absorption of drug. Furthermore, while intravenous or oral administration results in high systemic drug concentrations for a short period of time, typically, a relatively low amount actually reaches the lung. A low lung-to-plasma ratio can potentially lead to treatment failure and may increase systemic side effects (Peng, Lin et al. 2016). Focused pulmonary delivery of drugs exposes lung tissue to drug concentration levels significantly higher compared to other routes of administration by reducing systemic toxicity (Meenach, Anderson et al. 2014). The therapeutic applications of pulmonary drugs have extended their borders beyond conventional indications (asthma, COPDs, and cystic fibrosis) to include other inhalable compounds such as antimicrobials and protein therapeutics. Since the physio-chemical properties, dose regimen and patient interface may vary from previous therapies; new formulation techniques and device designs become necessities to explore (see Figure 1.16). There has been an emergence of innovative technologies in aerosol based therapeutics as a result of the recent therapeutic indications that has arisen; which, in turn have sparked studies to ensure optimal aerosolisation performance, therapeutic efficacy and patient adherence (Zhou, Tang et al. 2014).

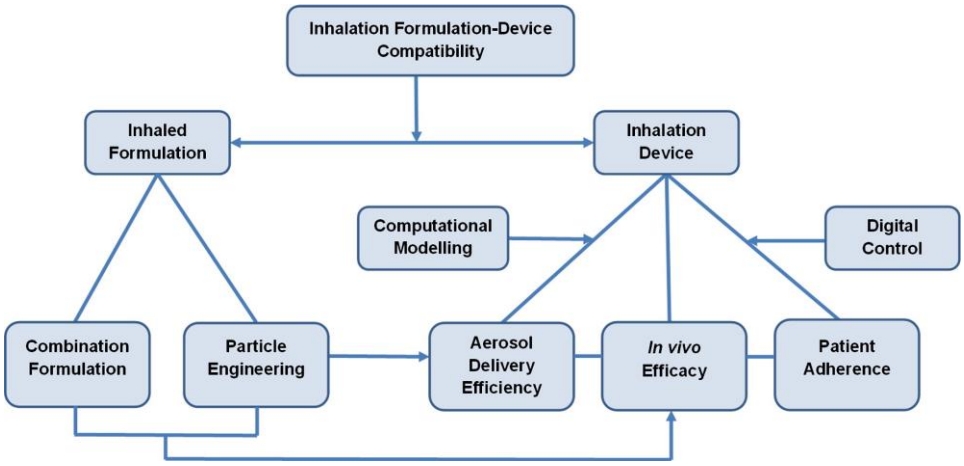

Figure 1.16: Inhalation device design relationships (Zhou, Tang et al. 2014)

Preparations for inhalation are liquid or solid preparations intended for administration as vapours or aerosols to the lung in order to obtain a local or systemic effect. They contain one or more active substances that may be dissolved or dispersed in a suitable vehicle (British Pharmacopoeia 2000). Depending on the type of preparation, they may contain propellants, co-solvents, diluents, antimicrobial preservatives, solubilising and stabilising agents, etc. These excipients are substances formulated alongside the active ingredient and do not adversely affect the functions of the mucosa of the respiratory tract or its cilia but rather act as a therapeutic enhancement facilitating drug absorption, reducing viscosity (Chang 2013), enhancing solubility (Heinemann, Klappoth et al. 2000), or have the purpose of long-term stabilisation (Respaud, Marchand et al. 2014). The selection of appropriate excipients much depends upon the route of administration as well as the dosage form, and the active ingredient itself. Preparations intended to be administered as aerosols (dispersions of solid or liquid particles in a gas) are administered by one of the following devices: nebuliser, breath actuated or pressurised metered-dose inhaler (MDI/ pMDI), or dry-powder inhaler (DPI) (British Pharmacopoeia 2000).

1.6.1 Ideal Aerosols

An aerosol is defined as a relatively stable colloidal suspension of solid or liquid particles in a gas (usually air). There are three major categories of devices currently in clinical use to generate the aerosol particles: nebulizers, MDIs, and DPIs (Mansour, Rhee et al. 2009). The efficacy of the inhaled aerosol depends upon a few factors regarding the particles that comprise the aerosol. The aerosol must be able to reach the desired site of action in the respiratory tract (i.e.

pulmonary region). Drugs administered directly to the lungs in patients with pulmonary diseases may accumulate in central rather than peripheral airways. This may be due to the physiologic properties of fluid dispersion in respiratory pathways and the alterations specific to inflammatory alterations of the airways such as bronchial hyper secretion, bronchoconstriction, and bronchial oedema (Labiris, Dolovich 2003a). For a device or formulation to be practical and effective, therapeutic concentrations of the aerosol particles must first be capable of releasing the drug at the site of action, within a small number of breaths, before clearance mechanisms carry the compound away from the deposition site (Nahar, Gupta et al. 2013).

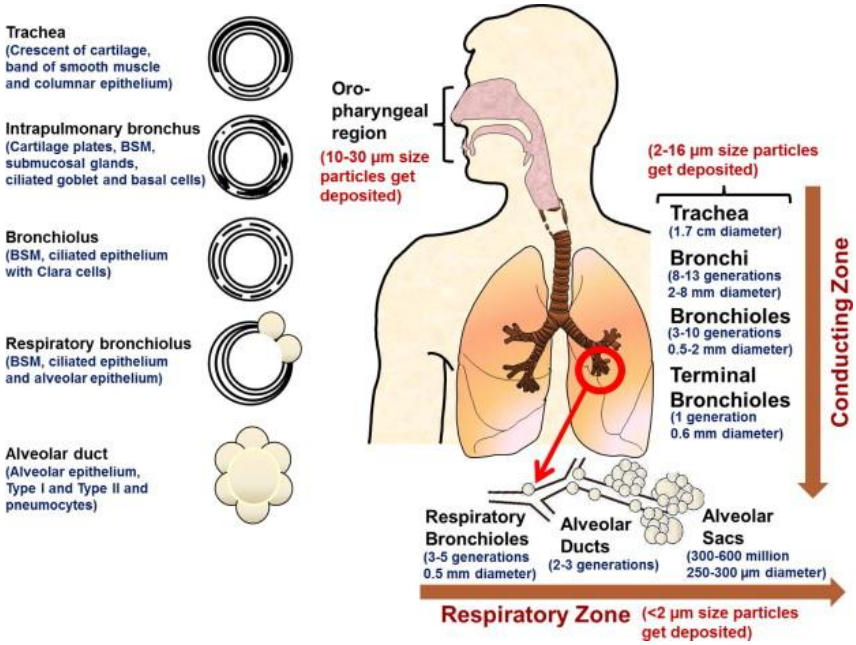

Figure 1.17: The number and dimensions of the airways of the adult lung and structure of the airway wall with the generations as explained by Weibel's tracheo-bronchial tree (Nahar, Gupta et al. 2013).

1.6.2 Nebulisers, Dry Powders and Pressurised Metered-Dose Inhalers

The deposition of therapeutic aerosols occurs by inertial impaction within the oropharynx and large conducting airways whereas the deposition in the small conducting airways and alveoli is due to gravitational sedimentation; however, both are determined by mode of inhalation, particle or droplet size, and the degree of airway obstruction (Lippmann 2011).

There are many devices currently used to deliver aerosolised therapeutic agents. One of the more popular used methods of aerosol drug delivery is the MDI (breath actuation), or pMDI,

due to its reliability and cost effectiveness. Its use is however limited to treating upper airway conditions as deeper lung drug-deposition is challenged with peptide formulations due to inefficient fine particle range and limited delivered dose. Nebulisers employ an aqueous based drug solution through an air jet or an ultrasonic device. This mechanism differed from MDIs as it typically delivers doses over multiple breaths. There have been advances in nebuliser technology that have overcome the conventional limitations of the bulky and costly units; and they still remain an attractive form of independent aerosol inhalation methods that are reasonably easy. If further improvements are made, the nebulising system may very well become an alternative mainstream portable inhaler system rather than a specialty device (Daniher, Zhu 2008).

The pMDIs have, for many years, since being first introduced in the 1950s, led the application form of inhalation therapy as they have many favourable features, such as easy handling, high reliability and accurate metering performance. They currently account for more than 90% of all inhaled asthma therapy (Malcolmson, Embleton 1998). PMDI preparations for inhalation contain the solutions, suspensions or emulsions (alongside propellants or mixtures of liquefied propellants which may act as solvents) supplied in specialised containers equipped with a metering valve and which are held under pressure and enable efficient and consistent dose delivery to the patient (Stein, Sheth et al. 2014). Suitable co-solvents, solubilisers and stabilisers may be added in the excipient if the delivered drug is insoluble or quickly degradable (British Pharmacopoeia 2000). The propellant, which comprises the bulk of the pMDI formulation, is the driving force that atomizes the droplets containing the drug (and excipients); it should be the driving force for ideal lung deposition. The phase-out program of chlorofluorocarbon inhalers (Montreal Protocol on Substances that Deplete the Ozone Layer) allowed for the introduction of more environmentally friendly hydrofluoroalkane propellant based inhalers which paved the way for many improvements to the methods of formulating pMDI drug delivery (U.S. Food and Drug Administration 2015). More attention was indicated to understanding formulation variables, product performance and patient interface, whilst considering the physico-chemical properties of the various excipients and active compounds(Myrdal, Sheth et al. 2013).

The device hardware (see Figure 1.18) includes a canister that is appropriately sized to contain sufficient formulation for the required number of doses. A metering valve is included that is

capable of delivering a consistent amount of drug with each dose delivered (Stein, Sheth et al. 2014).

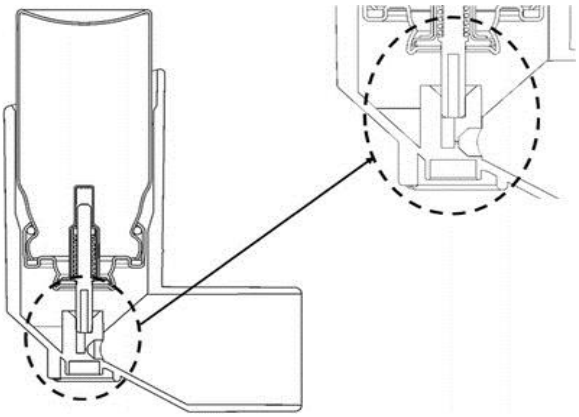

Figure 1.18: Schematic of a pMDI press-and-breathe actuator. Drawing courtesy of 3M Healthcare Ltd (Stein, Sheth et al. 2014).

The pMDI still, 50 years after its invention, remains a mainstay of asthma and COPD therapy worldwide. They are compact and convenient pulmonary drug delivery system that has the advantage of being easily grasped by patients and their multi-dose nature makes them more affordable than competing inhalation delivery systems. The developments of pMDI actuators have been a part of the devise technology improvement that continues to enhance drug delivery efficiency. This stands to prove that innovations that enhance the functionality of pMDIs will be balanced between the advantages of the system and their low cost. This is a crucial component to take into consideration as the expansion of health care in developing countries as well as the increased focus on the costs involved, will ensure that pMDIs remain a cost-effective and crucial pulmonary drug delivery system for treating various lung diseases or conditions (Stein, Sheth et al. 2014).

DPIs have experienced a big increase in development in the last 10 years due to the renowned limitations in other types of inhalation devices. Development of DPIs for the therapy of well-known diseases such as asthma and COPD has led to the increasing realisation of its potential role in other possible therapies that include inhaled antibiotics or peptides and proteins (Newman 2004). Therefore, the investigation of these devices may lead to the optimization of drug delivery. It offers many advantages that include minimal patient hand-lung coordination, portability, and improved stability over liquid aerosols. Due to the absence of a propellant, they

allow for the delivery of compounds that are not water-soluble and that are difficult to deliver as inhaled aqueous solutions via pMDIs or nebulization (Meenach, Anderson et al. 2014). However, improvements in drug formulations need to be taken into consideration. Formulations that, within the inhaled air stream, offer easier dispersion by relatively simple inhaler devices. One can then predict that DPIs could become the device category of choice for a wide range of inhaled therapies, involving both local and systemic drug delivery (Newman 2004). DPIs can be manufactured via spray-drying methods that employ a high throughput engineering method of solid-state particles that allows for microencapsulation of active compounds. This method of particle engineering allows for dry powder formulation designs to benefit regarding improved stability, improved powder dispersibility, controlled release, and/or increased drug permeability. The possibility of sustained release from a therapeutic aerosol may lengthen the drug lodging time within the airways or the alveolar region. This could increase patient compliance and reduce dosing frequency (Meenach, Anderson et al. 2014).

1.6.3 Aerosolised Surfactant as a Pulmonary Drug Delivery Vehicle

When considering surfactant administration, it differs based on manufacturers guidelines for individual surfactants. The dose, frequency of administration, and treatment procedures have been modelled after research protocols. Furthermore, it was found that repeated doses of surfactants given at intervals for predetermined indications have decreased mortality and morbidity compared with placebo or single surfactant doses (Soll, Ozek 2009). However, given the long half-life for surfactant in preterm infants with RDS, re-dosing usually occurs every 12 hours unless the surfactant is inactivated by an infectious process, meconium, or blood (Cogo, Facco et al. 2011). Surfactant administration procedures most commonly involve the endotracheal route, either as bolus, in smaller aliquots or via an adaptor port, and are therefore invasive and may be complicated by transient airway obstruction, oxygen desaturation, bradycardia, and various other physiological impediments (Polin, Carlo 2014, Kendig, Ryan et al. 1998). Many animal models of surfactant administration and small clinical trials of human preterm infants have demonstrated significant differences in clinical outcomes between methods (Zola, Gunkel et al. 1993, Ueda, Ikegami et al. 1994, Valls-i-Soler, López-Heredia et al. 1997). Most of the data collected are conflicting and limited; thus indicating that the optimal method of surfactant administration in preterm infants has yet to be clearly proven. Moreover, the recommended optimal number of doses of surfactant and which body position is best when

surfactant is administered are still two crucial aspects of surfactant therapy which have insufficient evidence (Polin, Carlo 2014).

There are a number of alternative methods to intratracheal administration of surfactant that have been evaluated in clinical trials (Kribs 2011, Abdel-Latif, Osborn 2011, Abdel-Latif, Osborn 2012). The increasing interest and use of non-invasive ventilator support for neonatal RDS and lung injury has motivated clinicians and researchers to look for alternative methods of administering exogenous surfactant. Aerosolised surfactants have been the most attractive route and have received much attention as they may prevent the need for endotracheal intubation. They have already been proven to be efficient and safe in animal models of respiratory distress syndrome by improving both ventilation and lung mechanics, even with minimal lungs deposition (Lewis, Ikegami et al. 1991, Li, Chen et al. 1994, Ellyett, Broadbent et al. 1996, Walther, Hernández-Juviel et al. 2014). However, the therapeutic effects of aerosolised surfactant in human clinical trials have not been convincing as most ultrasonic or jet nebulisers require the patient to have mechanical ventilation to deliver aerosolised surfactants and the improper use of these ventilators may cause or enhance lung injury (Pavone, Albert et al. 2007). It has been found that delivering an aerosolised surfactant by CPAP has beneficial effects in the treatment of NRDS without the need for mechanical ventilation. These results suggest that aerosolised surfactants inhaled by spontaneous breathing may be an attractive alternative method of surfactant-based therapies (Sun, Yang et al. 2009).

In addition, four small clinical studies have been performed to date. The safety and feasibility of these studies were confirmed; however, the effectiveness of this form of treatment requires further study as some groups excluded controls or the intervention was deemed as “too late”. Nebulised Alveofact® showed improvement in oxygenation and alveolar ventilation in preterm infants whereas aerosolised Curosurf® showed no superiority over nasal CPAP alone. These outcomes highlight the need to include optimising the dose of aerosolised surfactant, choosing particle size, developing the best delivery system, and using a surfactant formulation that maintains its integrity and activity once aerosolised (Mazela, Merritt et al. 2007).

Arroe *et al.* conducted a pilot study to estimate whether inhalation of an aerosolised synthetic surfactant (Exosurf®) delivered *via* nasal CPAP in preterm newborns with moderate RDS would improve systemic oxygenation. No adverse effects were noted but no improvement of

clinical substance were seen either (Arroe, Pedersen-Bjergaard et al. 1998). One may speculate that the absence of surfactant proteins contributes to the ineffective aerosolisation as Exosurf® was previously proven to be inefficacious compared to natural surfactants and therefore discontinued (Kattwinkel 2005). However, neither did the aerosolised animal derived surfactant (Curosurf®) display beneficial effects within a nebulised surfactant model for neonatal RDS, which are contrary to the experiments done by Berggren *et al.* (2000). Their findings are indicative to differences in administration techniques and further work is most undoubtedly needed for the optimisation of aerosolised surfactant delivery to the neonatal lung in clinical practice (Berggren, Liljedahl et al. 2000).

An example of an optimisation study is the investigation of an aerosolised form of lucinactant, Surfaxin® performed by Johnsen and colleagues (2006), or in this case Aerosurf®, has shown the feasibility and safety of delivering a peptide-containing synthetic surfactant to newborns with early signs of RDS. This study used a clinically approved device, the Aeroneb Pro (Artemis Medical Ltd, Dartford, Kent, UK) with a specially designed CPAP adaptor, to show the efficacy of such a model (Mazela, Merritt et al. 2007). Moreover, additional detailed analyses showed that the aerosolised lucinactant retained its biochemical activity (Johnson, Mazela et al. 2006, Finer, Merritt et al. 2010).

The use of exogenous pulmonary surfactants as a carrier for drugs (e.g. antibiotics) is a recent concept that has been under investigation as a synergistic approach to pulmonary drug delivery. When considering inhalation administration of drugs or surfactant, the site of maximum deposition within the lung is dependent on the size of the particle, with small particles having maximum penetration but poor deposition and large particles having poor penetration but large deposition. There is always the risk of non-uniform distribution of surfactant administration that may also result in regional atelectasis which hopefully aerosolised surfactant may overcome (Ellyett, Broadbent et al. 1996). However, the potency of some drugs may change with aerosolisation, and therefore may require dose adjustment just as surfactant phospholipid dosage and tidal volume are taken into consideration for inhalation therapy (Willson 2015). Most studies have covered the concept of liposomal drug-surfactant preparations and have proven foundational to optimise other modes of delivery (e.g. nebulisation, DPI, pMDI) (Justo, Moraes 2003, Chimote, Banerjee 2009). Provided that the encapsulated drug-surfactant suspension functions as an excellent surfactant with rapid adsorption, it is hypothesised that it

will improve the distribution of the drugs at the alveolar levels; resulting in atelectatic alveoli expansion. This will allow the chemotherapeutic agents to reach the previously collapsed alveoli, which are likely to be highly infected (Chimote, Banerjee 2009). Moreover, interactions between pulmonary surfactant and antimicrobial agents have been reported. It is therefore crucial to evaluate these interactions before using surfactant-antibiotic mixtures in clinical trials (van't Veen, Mouton et al. 1995).

Although pulmonary drug delivery has been established and proven effective for conditions such as asthma and cystic fibrosis, the concept of antibiotic pulmonary delivery (in combination with exogenous surfactant preparations) is a fairly recent area of study with the long-term goal of preparing inhalable particles for TB therapy. Deep- lung delivery has always been an obstacle, beyond the atelectatic regions, as it has been observed that particles reaching the lungs are phagocytosed rapidly by alveolar macrophages (AM) (Evora, Soriano et al. 1998, Sharma, Saxena et al. 2001). Although phagocytosis and sequestration of inhaled micro-particles may cause complications for drug delivery to other cells comprising lung tissue, it is however, an advantage for chemotherapy of TB as the phagocytosed micro-particles can potentially deliver larger amounts of drug to the AM cytosol where the TB bacilli sometimes reside (Sharma, Saxena et al. 2001).

These new approaches of aerosolised exogenous surfactants for the use of inhalable drug therapy that have reached pre-clinical stage are enumerated. The potential of drug delivery systems to improve and optimise currently available antibiotic therapies (among others) in the context of lung infections supports the need to gain insight into the complex context that surrounds the infection. One also has to gain understanding about the interactions of different fields, such as microbiology, physiopathology, immunology, pharmacokinetics/pharmacodynamics, pharmacology and nanotechnology which in turn opens wider scopes of further research into pulmonary drug delivery (Moreno-Sastre, Pastor et al. 2015).

1.7 References

ABDEL- LATIF, M.E. and OSBORN, D.A., 2012. Nebulised surfactant in preterm infants with or at risk of respiratory distress syndrome. *The Cochrane Library*, (10),.

ABDEL- LATIF, M.E. and OSBORN, D.A., 2011. Laryngeal mask airway surfactant administration for prevention of morbidity and mortality in preterm infants with or at risk of respiratory distress syndrome. *Cochrane Database of Systematic Reviews*, (7),.

AINSWORTH, S.B., BERESFORD, M.W., MILLIGAN, D.W.A., SHAW, N.J., MATTHEWS, J.N.S., FENTON, A.C. and PLATT, M.W., 2000. Pumactant and poractant alfa for treatment of respiratory distress syndrome in neonates born at 25–29 weeks' gestation: a randomised trial. *The Lancet*, **355**(9213), pp. 1387-1392.

AINSWORTH, S.B. and MILLIGAN, D.W.A., 2002. Surfactant Therapy for Respiratory Distress Syndrome in Premature Neonates. *American Journal of Respiratory Medicine*, **1**(6), pp. 417-433.

AKIRA, S. and TAKEDA, K., 2004. Toll-like receptor signalling. *Nature Reviews Immunology*, **4**(7), pp. 499-511.

AKIRA, S., TAKEDA, K. and KAISHO, T., 2001. Toll-like receptors: critical proteins linking innate and acquired immunity. *Nature Immunology*, **2**(8), pp. 675.

ALMLÉN, A., STICHTENOTH, G., LINDERHOLM, B., HAEGERSTRAND-BJÖRKMAN, M., ROBERTSON, B., JOHANSSON, J. and CURSTEDT, T., 2008. Surfactant proteins B and C are both necessary for alveolar stability at end expiration in premature rabbits with respiratory distress syndrome. *Journal of Applied Physiology*, **104**(4), pp. 1101-1108.

ALMLÉN, A., WALTHER, F.J., WARING, A.J., ROBERTSON, B., JOHANSSON, J. and CURSTEDT, T., 2010. Synthetic surfactant based on analogues of SP-B and SP-C is superior to single-peptide surfactants in ventilated premature rabbits. *Neonatology*, **98**(1), pp. 91-99.

ANSFIELD, M.J., KALTREIDER, H.B., CALDWELL, J.L. and HERSKOWITZ, F.N., 1979. Hyporesponsiveness of Canine Bronchoalveolar Lymphocytes to Mitogens: Inhibition of

Lymphocyte Proliferation by Alveolar Macrophages. *The Journal of Immunology*, **122**(2), pp. 542-548.

ARAI, N., YOSHIMOTO, Y., YASUOKA, K. and EBISUZAKI, T., 2016. Self-assembly behaviours of primitive and modern lipid membrane solutions: a coarse-grained molecular simulation study. *Physical Chemistry Chemical Physics*, **18**(28), pp. 19426-19432.

ARDELL, S., PFISTER, R.H. and SOLL, R., 2015. Animal derived surfactant extract versus protein free synthetic surfactant for the prevention and treatment of respiratory distress syndrome. *Cochrane Database of Systematic Reviews*, (8).

ARIAS-DIAZ, J., GARCIA-VERDUGO, I., CASALS, C., SANCHEZ-RICO, N., VARA, E. and BALIBREA, J.L., 2000. Effect of surfactant protein A (SP-A) on the production of cytokines by human pulmonary macrophages. *Shock*, **14**(3), pp. 300-306.

ARROE, M., PEDERSEN-BJERGAARD, L., ALBERTSEN, P., BODE, S., GREISEN, G., JONSBO, F., LUNDSTROM, K., STRUCK, J., WESTERGAARD, M. and PEITERSEN, B., 1998. Inhalation of aerosolized surfactant (Exosurf (R)) to neonates treated with nasal continuous positive airway pressure. *Prenatal and Neonatal Medicine*, **3**(3), pp. 346-352.

AVERY, M. and MEAD, J., 1959. Surface properties in relation to atelectasis and hyaline membrane disease. *A.M.A.Journal of Diseases of Children*, **97**(5), pp. 517-523.

AYDEN, M., 1999. *Aerosolisation and in vitro Deposition of an Artificial Lung Surfactant*, University of Bath.

BACHMANN, M.F. and KOPF, M., 2002. Balancing protective immunity and immunopathology. *Current Opinion in Immunology*, **14**(4), pp. 413-419.

BADAWI, A.M., ISMAIL, D.A., AHMED, S., MOHAMAD, A., DARDIR, M., MOHAMED, D.E., IBRAHEM, A., MANSOUR, N.A. and ASHMAWY, A., 2015. Role of Surfactants in Regulation of Cancer Growth. In: V. GANDHI, K. MEHTA, R. GROVER, S. PATHAK and B.B. AGGARWAL, eds, *Multi-Targeted Approach to Treatment of Cancer*. Cham: Springer International Publishing, pp. 137-149.

BANERJEE, R., 2002. Surface chemistry of the lung surfactant system: techniques for in vitro evaluation. *Current Science*, **82**(4),.

BARR, F.E., PEDIGO, H., JOHNSON, T.R. and SHEPHERD, V.L., 2000. Surfactant protein-A enhances uptake of respiratory syncytial virus by monocytes and U937 macrophages. *American Journal of respiratory Cell and Molecular Biology*, **23**(5), pp. 586.

BARRETT, K.E. and GANONG, W.F., 2010. *Ganong's review of medical physiology*. 23rd ed., International ed. edn. New York: New York : McGraw-Hill Medical.

BARTON, G.M., 2008. A calculated response: control of inflammation by the innate immune system (Review series). *The Journal of Clinical Investigation*, **118**(2), pp. 413.

BEIJA, M., SALVAYRE, R., LAUTH-DE VIGUERIE, N. and MARTY, J., 2012. Colloidal systems for drug delivery: from design to therapy. *Trends in Biotechnology*, **30**(9), pp. 485-496.

BENCZIK, M. and GAFFEN, S.L., 2004. The Interleukin (IL)- 2 Family Cytokines: Survival and Proliferation Signaling Pathways in T Lymphocytes. *Immunological Investigations*, **33**(2), pp. 109-142.

BERGGREN, E., LILJEDAHL, M., WINBLADH, B., ANDREASSON, B., CURSTEDT, T., ROBERTSON, B. and SCHOLLIN, J., 2000. Pilot study of nebulized surfactant therapy for neonatal respiratory distress syndrome. *Acta Paediatrica*, **89**(4), pp. 460-464.

BILLIET, L., FURMAN, C., LARIGAUDERIE, G., COPIN, C., BRAND, K., FRUCHART, J.C. and ROUIS, M., 2005. Extracellular human thioredoxin-1 inhibits lipopolysaccharide-induced interleukin-1beta expression in human monocyte-derived macrophages. *The Journal of Biological Chemistry*, **280**(48), pp. 40310-40318.

BLANK, F., ROTHEN-RUTISHAUSER, B.M., SCHURCH, S. and GEHR, P., 2006. An optimized in vitro model of the respiratory tract wall to study particle cell interactions. . *Journal of Aerosol Medicine*, **19**(3), pp. 392-405.

BLUMBERG, H.M., BURMAN, W.J., CHAISSON, R.E., DALEY, C.L., ETKIND, S.C., FRIEDMAN, L.N., FUJIWARA, P., GRZEMSKA, M., HOPEWELL, P.C., ISEMAN, M.D.,

JASMER, R.M., KOPPAKA, V., MENZIES, R.I., O'BRIEN, R.,J., REVES, R.R., REICHMAN, L.B., SIMONE, P.M., STARKE, J.R. and VERNON, A.A., 2003. American Thoracic Society/Centers for Disease Control and Prevention/Infectious Diseases Society of America: treatment of tuberculosis. *American Journal of Respiratory and Critical Care Medicine*, **167**(4), pp. 603.

BORRON, P., MCINTOSH, J.C., KORFHAGEN, T.R., WHITSETT, J.A., TAYLOR, J. and WRIGHT, J.R., 2000. Surfactant-associated protein A inhibits LPS-induced cytokine and nitric oxide production in vivo. *American Journal of Physiology-Lung Cellular and Molecular Physiology*, **278**(4), pp. L840-L847.

BORRON, P., MCCORMACK, F.X., ELHALWAGI, B.M., CHRONEOS, Z.C., LEWIS, J.F., ZHU, S., WRIGHT, J.R., SHEPHERD, V.L., POSSMAYER, F., INCHLEY, K. and FRAHER, L.J., 1998. Surfactant protein A inhibits T cell proliferation via its collagen-like tail and a 210-kDa receptor. *American Journal of Physiology - Lung Cellular and Molecular Physiology*, **275**(4), pp. L679-L686.

BRINKER, K.G., MARTIN, E., BORRON, P., MOSTAGHEL, E., DOYLE, C., HARDING, C.V. and WRIGHT, J.R., 2001. Surfactant protein D enhances bacterial antigen presentation by bone marrow-derived dendritic cells. *American Journal of Physiology. Lung Cellular and Molecular Physiology*, **281**(6), pp. L1453.

BRITISH PHARMACOPOEIA, 2000. *British Pharmacopoeia Monographs for Inhaled Products.* Medicines & Healthcare products Regulatory agency.

CASENGHI, M. and SCHOEN-ANGERER, T., 2006. *Geneva: Medecins San Frontieres, Campaign for Access to Essential Medicines. Development of new drugs for TB chemotherapy: analysis of the current drug pipeline* 2006.

CHAIRUANGKITTI, P., LAWANPRASERT, S., ROYTRAKUL, S., AUEVIRIYAVIT, S., PHUMMIRATCH, D., KULTHONG, K., CHANVORACHOTE, P. and MANIRATANACHOTE, R., 2013. Silver nanoparticles induce toxicity in A549 cells via ROS-dependent and ROS-independent pathways. *Toxicology in vitro*, **27**(1), pp. 330-338.

CHAKRABORTY, M., MCGREAL, E.P. and KOTECHA, S., 2010. Acute Lung Injury in Preterm Newborn Infants: Mechanisms and Management. *Paediatric respiratory reviews*, **11**(3), pp.162-170.

CHAMPION, J.A., KATARE, Y.K. and MITRAGOTRI, S., 2007. Particle shape: A new design parameter for micro- and nanoscale drug delivery carriers. *Journal of Controlled Release*, **121**(1), pp. 3-9.

CHANG, B.S., 2013. *Protein formulations containing amino acids.* Google Patents.

CHEN, N.Y., LAI, H.H., HSU, T.H., LIN, F.Y., CHEN, J.Z. and LO, H.C., 2008. Induction of apoptosis in human lung carcinoma A549 epithelial cells with an ethanol extract of *Tremella mesenterica*. *Bioscience, Biotechnology, and Biochemistry*, **72**(5), pp. 1283-1289.

CHIBA, H., SANO, H., IWAKI, D., MURAKAMI, S., MITSUZAWA, H., TAKAHASHI, T., KONISHI, M., TAKAHASHI, H. and KUROKI, Y., 2001. Rat mannose-binding protein a binds CD14. *Infection and Immunity*, **69**(3), pp. 1587-1592.

CHIMOTE, G. and BANERJEE, R., 2009. Evaluation of antitubercular drug-loaded surfactants as inhalable drug-delivery systems for pulmonary tuberculosis. *Journal of Biomedical Materials Research Part A*, **89A**(2), pp. 281-292.

CHIMOTE, G. and BANERJEE, R., 2005. Lung surfactant dysfunction in tuberculosis: Effect of mycobacterial tubercular lipids on dipalmitoylphosphatidylcholine surface activity. *Colloids and Surfaces B: Biointerfaces*, **45**(3), pp. 215-223.

CHRISTMANN, U., BUECHNER- MAXWELL, V.A., WITONSKY, S.G. and HITE, R.D., 2009. Role of lung surfactant in respiratory disease: current knowledge in large animal medicine. *Journal of Veterinary Internal Medicine*, **23**(2), pp. 227-242.

CHRONEOS, Z.C., SEVER-CHRONEOS, Z. and SHEPHERD, V.L., 2010. Pulmonary Surfactant: An Immunological Perspective. *Cellular Physiology and Biochemistry*, **25**(1), pp. 13-26.

CHURCHYARD, G.J., FIELDING, K.L., LEWIS, J.J., COETZEE, L., CORBETT, E.L., GODFREY-FAUSSETT, P., HAYES, R.J., CHAISSON, R.E. and GRANT, A.D., 2014. A

Trial of Mass Isoniazid Preventive Therapy for Tuberculosis Control. *New England Journal of Medicine,* **370**(4), pp. 301-310.

CIPOLLA, D., BLANCHARD, J. and GONDA, I., 2016. *Development of Liposomal Ciprofloxacin to Treat Lung Infections.*

CLEMENTS, J.A., OYARZUN, M.J. and BARITUSSIO, A., 1981. Secretion and Clearance of Lung Surfactant: A Brief Review. . In: P. VON WICHERT and H. HERZOG, eds, *Progress in Respiration Research: Clinical Importance of Surfactant Defects.* Vol. 15 edn. Basel: Karger Publishers., pp. 20-26.

COCHRANE, C.G., REVAK, S.D., MERRITT, T.A., HELDT, G.P., HALLMAN, M., CUNNINGHAM, M.D., EASA, D., PRAMANIK, A., EDWARDS, D.K. and ALBERTS, M.S., 1996. The efficacy and safety of KL4-surfactant in preterm infants with respiratory distress syndrome. *American journal of respiratory and critical care medicine,* **153**(1), pp. 404-410.

COGO, P.E., FACCO, M., SIMONATO, M., DE LUCA, D., DE TERLIZI, F., RIZZOTTI, U., VERLATO, G., BELLAGAMBA, M.P. and CARNIELLI, V.P., 2011. Pharmacokinetics and clinical predictors of surfactant redosing in respiratory distress syndrome. *Intensive Care Medicine,* **37**(3), pp. 510-517.

COLACICCO, G., 1985. Arguments against and alternatives for an extracellular surfactant layer in the alveoli of mammalian lung. *Journal of Theoretical Biology,* **114**, pp. 641-656.

COLELL, A., RICCI, J.E., TAIT, S., MILASTA, S., MAURER, U., BOUCHIER-HAYES, L., FITZGERALD, P., GUIO-CARRION, A., WATERHOUSE, N.J., LI, C.W. and MARI, B., 2007. GAPDH and autophagy preserve survival after apoptotic cytochrome c release in the absence of caspase activation. *Cell,* **129**(5), pp. 983-997.

COPLEY SCIENTIFIC, 2017-last update, Introduction to Aerodynamic Particle Sizing [Homepage of Copley Scientific Web Design Wida Group], [Online]. Available: http://issuu.com/pyramidpress/docs/inhaler_brochure_2015_rev4__high_re?e=6944369/13992727 [May, 15, 2017].

CORNFORTH, J.W., HART, P.D., NICHOLLS, G.A., REES, R.J.W. and STOCK, J.A., 1955. Antituberculous effect of certain surface-active polyoxyethylene ethers in mice. *British Journal of Pharmacology and Chemotherapy,* **10**(1), pp. 73-86.

CURSTEDT, T., HALLIDAY, H.L. and SPEER, C.P., 2015. A Unique Story in Neonatal Research: The Development of a Porcine Surfactant. *Neonatology,* **107**(4), pp. 321-329.

DANIHER, D.I. and ZHU, J., 2008. Dry powder platform for pulmonary drug delivery. *Particuology,* **6**(4), pp. 225-238.

DAVIS, A.J., JOBE, A.H., HAFNER, D. and IKEGAMI, M., 1998. Lung function in premature lambs and rabbits treated with a recombinant SP-C surfactant. *American Journal of Respiratory and Critical Care Medicine,* **157**(2), pp. 553-559.

DELIHAS, N., RILEY, L.W., LOO, W., BERKOWITZ, J. and POLTORATSKAIA, N., 1995. High sensitivity of Mycobacterium species to the bactericidal activity by polylysine. *FEMS Microbiology Letters,* **132**(3), pp. 233-237.

DEPARTMENT OF HEALTH, UNITED KINGDOM, 30 August 2000. *Communication to WHO from the* . UK: Medicines Control Agency.

DIBBERT, B., WEBER, M., NIKOLAIZIK, W.H., VOGT, P., SCHÖNI, M.H., BLASER, K. and SIMON, H.U., 1999. Cytokine-mediated Bax deficiency and consequent delayed neutrophil apoptosis: a general mechanism to accumulate effector cells in inflammation. *Proceedings of the National Academy of Sciences,* **96**(23), pp. 13330-13335.

DJAVAHERI-MERGNY, M., JAVELAUD, D., WIETZERBIN, J. and BESANÇON, F., 2004. NF- κB activation prevents apoptotic oxidative stress via an increase of both thioredoxin and MnSOD levels in TNFα- treated Ewing sarcoma cells. *FEBS letters,* **578**(1-2), pp. 111-115.

DOMEJ, W., OETTL, K. and RENNER, W., 2014. Oxidative stress and free radicals in COPD–implications and relevance for treatment. *International Journal of Chronic Obstructive Pulmonary Disease,* **9**, pp. 1207.

DUQUE, G.A. and DESCOTEAUX, A., 2014. Macrophage cytokines: involvement in immunity and infectious diseases. *Frontiers in Immunology,* **5**(491), pp. 1-12.

EISENBERG-LERNER, A., BIALIK, S., SIMON, H.U. and KIMCHI, A., 2009. Life and death partners: apoptosis, autophagy and the cross-talk between them. *Cell Death and Differentiation,* **16**(7), pp. 966-975.

EL HADRI, K., MAHMOOD, D.F.D., COUCHIE, D., JGUIRIM-SOUISSI, I., GENZE, F., DIDEROT, V., SYROVETS, T., LUNOV, O., SIMMET, T. and ROUIS, M., 2012. Thioredoxin-1 promotes anti-inflammatory macrophages of the M2 phenotype and antagonizes atherosclerosis. *Arteriosclerosis, Thrombosis, and Vascular Biology,* **32**(6), pp. 1445-1452.

ELLYETT, K.M., BROADBENT, R.S., FAWCETT, E.R. and CAMPBELL, A.J., 1996. Surfactant Aerosol Treatment of Respiratory Distress Syndrome in the Spontaneously Breathing Premature Rabbit. *Pediatric Research,* **39**(6), pp. 953-957.

ELMORE, S., 2007. Apoptosis: a review of programmed cell death. *Toxicologic Pathology,* **35**(4), pp. 495-516.

EVORA, C., SORIANO, I., ROGERS, R.A., SHAKESHEFF, K.M., HANES, J. and LANGER, R., 1998. Relating the phagocytosis of microparticles by alveolar macrophages to surface chemistry: the effect of 1, 2-dipalmitoylphosphatidylcholine. *Journal of Controlled Release,* **51**(2), pp. 143-152.

FAN, T.J., HAN, L.H., CONG, R.S. and LIANG, J., 2005. Caspase family proteases and apoptosis. *Acta Biochimica et Biophysica Sinica*, **37**, pp. 719-727.

FELS, A.O. and COHN, Z.A., 1986. The alveolar macrophage. *Journal of Applied Physiology (Bethesda, Md.: 1985),* **60**(2), pp. 353.

FERRO, T.J., KERN, J.A., ELIAS, J.A., KAMOUN, M., DANIELE, R.P. and ROSSMAN, M.D., 1987. Alveolar Macrophages, Blood Monocytes, and Density-Fractionated Alveolar Macrophages Differ in Their Ability to Promote Lymphocyte Proliferation to Mitogen and Antigen 1–3. *American Review of Respiratory Disease*, **135**(3), pp. 682-687.

FINCK, C.M., HODELL, M.G., MARX, W.H., PASKANIK, A.M., MCGRAW, D.J., LUTZ, C.J., GATTO, L.A., PICONE, A.L. and NIEMAN, G.F., 1998. Endotoxin-stimulated alveolar macrophage recruitment of neutrophils and modulation with exogenous surfactant. *Critical Care Medicine,* **26**(8), pp. 1414.

FINER, N.N., MERRITT, T.A., BERNSTEIN, G., JOB, L., MAZELA, J. and SEGAL, R., 2010. An open label, pilot study of Aerosurf® combined with nCPAP to prevent RDS in preterm neonates. *Journal of Aerosol Medicine and Pulmonary Drug Delivery*, **23**(5), pp. 303-309.

FLOREA, B.I., CASSARA, M.L., JUNGINGER, H.E. and BORCHARD, G., 2003. Drug transport and metabolism characteristics of the human airway epithelial cell line Calu-3. *Journal of Controlled Release*, **87**(1), pp. 131-138.

FOSTER, K.A., AVERY, M.L., YAZDANIAN, M. and AUDUS, K.L., 2000. Characterization of the Calu-3 cell line as a tool to screen pulmonary drug delivery. *International Journal of Pharmaceutics*, **208**(1), pp. 1-11.

FOX, W., WIENER, A., MITCHISON, D.A., SELKON, J.B. and SUTHERLAND, I., 1957. The prevalence of drug-resistant tubercle bacilli in untreated patients with pulmonary tuberculosis: A national survey, 1955–56. *Tubercle*, **38**(2), pp. 71-84.

FUJIWARA, T., CHIDA, S., WATABE, Y., MAETA, H., MORITA, T. and ABE, T., 1980. Artificial surfactant therapy in hyaline-membrane disease. *The Lancet*, **315**(8159), pp. 55-59.

GALLUZZI, L., MAIURI, M.C., VITALE, I., ZISCHKA, H., CASTEDO, M., ZITVOGEL, L. and KROEMER, G., 2007. Cell death modalities: classification and pathophysiological implications. *Cell Death and Differentiation*, **14**(7), pp. 1237-1243.

GARCÍA, J.E., RODRIGUEZ, F.M., DE CABO, M.R., SALGADO, M.J., LOSADA, J.P., VILLARON, L.G., LOPEZ, A.J. and ARELLANO, J.L.P., 1999. Evaluation of inflammatory cytokine secretion by human alveolar macrophages. *Mediators of Inflammation*, **8**(1), pp. 43-51.

GARDAI, S.J., XIAO, Y.Q., DICKINSON, M., NICK, J.A., VOELKER, D.R., GREENE, K.E. and HENSON, P.M., 2003. By binding SIRPα or calreticulin/CD91, lung collectins act as dual function surveillance molecules to suppress or enhance inflammation. *Cell*, **115**(1), pp. 13-23.

GEE, J.B. and FICK, R.B., 1980. Bronchoalveolar lavage. *Thorax*, **35**(1), pp. 1-8.

GEORGOPOULOS, D., MOULOUDI, E., KONDILI, E. and KLIMATHIANAKI, M., 2000. Bronchodilator delivery with metered-dose inhaler during mechanical ventilation. *Critical Care,* **4**(4), pp. 227-234.

GHOSH, S. and KARIN, M., 2002. Missing Pieces in the NF-κB Puzzle. *Cell,* **109**(2), pp. S81-S96.

GIDEON, H.P. and FLYNN, J.L., 2011. Latent tuberculosis: what the host "sees"? *Immunologic Research,* **50**(2), pp. 202-212.

GLASSER, J.R. and MALLAMPALLI, R.K., 2012. Surfactant and its role in the pathobiology of pulmonary infection. *Microbes and Infection,* **14**(1), pp. 17-25.

GOERKE, J. and CLEMENTS, J.A., 1986. Mechanics of Breathing (Part 1): Alveolar surface tension and lung surfactant, Section 3: The Respiratory System. In: MACKLEM AND J. MEAD, ed, *Handbook of Physiology.* Vol III edn. Bethesda, MD: American Physiological Society, pp. 247-261.

GOERKE, J., 1998. Pulmonary surfactant: functions and molecular composition. *Biochimica et Biophysica Acta (BBA) - Molecular Basis of Disease,* **1408**(2–3), pp. 79-89.

GRAY, R.A., VANDER VELDE,D.G., BURKE, C.J., MANNING, M.C., MIDDAUGH, C.R. and BORCHARDT, R.T., 1994. Delta-sleep-inducing peptide: solution conformational studies of a membrane-permeable peptide. *Biochemistry,* **33**(6), pp. 1323-1331.

GRUENWALD, P., 1947. Surface tension as a factor in the resistance of neonatal lungs to aeration. *American Journal of Obstetrics and Gynecology,* **53**(6), pp. 996-1007.

GUMP, J.M. and THORBURN, A., 2011. Autophagy and apoptosis- what's the connection?. *Trends in Cell Biology,* **21**(7), pp. 387-392.

HAAGSMAN, H.P., HOGENKAMP, A., VAN EIJK, M. and VELDHUIZEN, E.J.A., 2008. Surfactant Collectins and Innate Immunity. *Neonatology,* **93**(4), pp. 288-294.

HAAGSMAN, H.P. and VAN GOLDE, L.M.G., 1991. Synthesis and Assembly of Lung Surfactant. *Annual Review of Physiology,* **53**(1), pp. 441-464.

HAGHI, M., TRAINI, D. and YOUNG, P., 2014. In Vitro Cell Integrated Impactor Deposition Methodology for the Study of Aerodynamically Relevant Size Fractions from Commercial Pressurised Metered Dose Inhalers. *Pharmaceutical research; An Official Journal of the American Association of Pharmaceutical Scientists,* **31**(7), pp. 1779-1787.

HAGHI, M., TRAINI, D., POSTMA, D.S., BEBAWY, M. and YOUNG, P.M., 2013. Fluticasone uptake across Calu-3 cells is mediated by salmeterol when deposited as a combination powder inhaler. *Respirology,* **18**(8), pp. 1197-1201.

HAGHI, M., YOUNG, P.M., TRAINI, D., JAISWAL, R., GONG, J. and BEBAWY, M., 2010. Time- and passage-dependent characteristics of a Calu-3 respiratory epithelial cell model. *Drug Development and Industrial Pharmacy, 2010,* **36;**(10;), pp. 1207-1214.

HALLIDAY, H.L. and SPEER, C.P., 1995. Strategies for surfactant therapy in established neonatal respiratory distress syndrome . *Lung Billogy in the Heath and Disease,* **84**, pp. 443.

HALLMAN, M., SPRAGG, R., HARRELL, J.H., MOSER, K.M. and GLUCK, L., 1982. Evidence of lung surfactant abnormality in respiratory failure. Study of bronchoalveolar lavage phospholipids, surface activity, phospholipase activity, and plasma myoinositol. *Journal of Clinical Investigation,* **70**(3), pp. 973.

HAMVAS, A., NOGEE, L.M., WHITE, F.V., SCHULER, P., HACKETT, B.P., HUDDLESTON, C.B., MENDELOFF, E.N., HSU, F.F., WERT, S.E., GONZALES, L.W. and BEERS, M.F., 2004. Progressive lung disease and surfactant dysfunction with a deletion in surfactant protein C gene. *American Journal of Respiratory Cell and Molecular Biology,* **30**(6), pp. 771-776.

HARCOURT, J.L. and HAYNES, L.M., 2013. Establishing a Liquid-covered Culture of Polarized Human Airway Epithelial Calu-3 Cells to Study Host Cell Response to Respiratory Pathogens In vitro. *Journal of Visualized Experiments,* (72), pp. e50157.

HARTMANN, W. and GALLA, H., 1978. Binding of polylysine to charged bilayer membranes. Molecular organization of a lipid · peptide complex. *BBA - Biomembranes,* **509**(3), pp. 474-490.

HAVENITH, C.E.G., BREEDIJK, A.J. and HOEFSMIT, E.C.M., 1992. Effect of Bacillus Calmette-Guérin Inoculation on Numbers of Dendritic Cells in Bronchoalveolar Lavages of Rats. *Immunobiology*, **184**(4), pp. 336-347.

HAYAKAWA, H., GIRIDHAR, G., MYRVIK, Q.N. and KUCERA, L., 1992. Pulmonary surfactant phospholipids modulate priming of rabbit alveolar macrophages for oxidative responses. *Journal of Leukocyte Biology*, **51**(4), pp. 379.

HEINEMANN, L., KLAPPOTH, W., RAVE, K., HOMPESCH, B., LINKESCHOWA, R. and HEISE, T., 2000. Intra-individual Variability of the Metabolic Effect of Inhaled Insulin Together With an Absorption Enhancer. *Diabetes Care*, **23**(9), pp. 1343.

HELMKE, R., GERMAN, V. and MANGOS, J., 1989. A continuous alveolar macrophage cell line: Comparisons with freshly derived alveolar macrophages. *In Vitro Cellular & Developmental Biology*, **25**(1), pp. 44-48.

HERTING, E., SUN, B., JARSTRAND, C., CURSTEDT, T. and ROBERTSON, B., 1997. Surfactant improves lung function and mitigates bacterial growth in immature ventilated rabbits with experimentally induced neonatal group B streptococcal pneumonia. *Archives of Disease in Childhood - Fetal and Neonatal Edition*, **76**(1), pp. F3.

HERZOG, E., BYRNE, H.J., DAVOREN, M., CASEY, A., DUSCHL, A. and OOSTINGH, G.J., 2009. Dispersion medium modulates oxidative stress response of human lung epithelial cells upon exposure to carbon nanomaterial samples. *Toxicology and Applied Pharmacology*, **236**(3), pp. 276-281.

HILGERS, A.R., CONRADI, R.A. and BURTON, P.S., 1990. Caco-2 cell monolayers as a model for drug transport across the intestinal mucosa. *Pharmaceutical Research*, **7**(9), pp. 902-910.

HILL, M.A., 2016. ***Embryology****Draft 2016.* School of Medical Sciences, Faculty of Medicine, UNSW AUSTRALIA, Sydney 2052 AUSTRALIA: .

HILLEGASS, J.M., SHUKLA, A., LATHROP, S.A., MACPHERSON, M.B., FUKAGAWA, N.K. and MOSSMAN, B.T., 2010. Assessing nanotoxicity in cells in vitro. *Wiley Interdisciplinary Reviews: Nanomedicine and Nanobiotechnology*, **2**(3), pp. 219-231.

HILLS, B.A., 1991. Physiological mechanisms for the action of pulmonary surfactant. In: J.R. BOURBON, ed, *Pulmonary Surfactant: Biochemical, Functional, Regulatory, and clinical Concepts*. Boca Raton: CRC Press, pp. 185-224.

HILLS, B.A., 1988. *The Biology of Surfactant.* Cambridge University Press.

HILLS, B.A., 1999. An alternative view of the role(s) of surfactant and the alveolar model. *Journal of Applied Physiology (Bethesda, Md.: 1985)*, **87**(5), pp. 1567.

HILLS, B., BURKE and THOMAS, K., 1998. Surfactant barrier lining peritoneal mesothelium: lubricant and release agent. *Peritoneal Dialysis International*, **18**(2), pp. 157-165.

HORTON, D.L., 2010. Regulation of cytokines and chemokines during the progression of acute inflammation in the human whole blood model. (Dissertation Summaries)(Report). *Journal of Interferon & Cytokine Research*, **30**(2), pp. 111.

HUANG, T., LIU, Y., SY, C., CHEN, Y., TU, H. and CHEN, B., 2008. In Vitro Activities of Linezolid against Clinical Isolates of Mycobacterium tuberculosis Complex Isolated in Taiwan over 10 Years. *Antimicrobial Agents and Chemotherapy*, **52**(6), pp. 2226.

HUDAK, M.L., MARTIN, D.J., EGAN, E.A., MATTESON, E.J., CUMMINGS, J., JUNG, A.L., KIMBERLIN, L.V., AUTEN, R.L., ROSENBERG, A.A., ASSELIN, J.M., BELCASTRO, M.R., DONOHUE, P.K., HAMM, C.R., JANSEN, R.D., BRODY, A.S., RIDDLESBERGER, M.M. and MONTGOMERY, P., 1997. A Multicenter Randomized Masked Comparison Trial of Synthetic Surfactant Versus Calf Lung Surfactant Extract in the Prevention of Neonatal Respiratory Distress Syndrome. *Pediatrics*, **100**(1), pp. 39-50.

HUSSELL, T. and BELL, T.J., 2014. Alveolar macrophages: plasticity in a tissue-specific context. *Nature Reviews Immunology*, **14**(2), pp. 81-93.

ISHII, H., FUJII, T., HOGG, J.C., HAYASHI, S., MUKAE, H., VINCENT, R. and VAN EEDEN, S.F., 2004. Contribution of IL-1β and TNF-α to the initiation of the peripheral lung response to atmospheric particulates (PM 10). *American Journal of Physiology-Lung Cellular and Molecular Physiology*, **287**(1), pp. L176-L183.

ISHMAEL, F.T., FANG, X., HELLER, N., FAN, J., BLACKSHEAR, P.J., ATASOY, U., CHEADLE, C. and STELLATO, C., 2007. Role of the RNA-binding Protein Tristetraprolin (TTP) in Glucocorticoid (GC)-mediated Gene Regulation. *The Journal of Allergy and Clinical Immunology*, **119**(1), pp. S134-S134.

JANSSEN, W.J., MCPHILLIPS, K.A., DICKINSON, M.G., LINDERMAN, D.J., MORIMOTO, K., XIAO, Y.Q., OLDHAM, K.M., VANDIVIER, R.W., HENSON, P.M. and GARDAI, S.J., 2008. Surfactant proteins A and D suppress alveolar macrophage phagocytosis via interaction with SIRPα. *American Journal of Respiratory and Critical Care Medicine*, **178**(2), pp. 158-167.

JIANG, C., LIU, Z., HU, R., BO, L., MINSHALL, R.D., MALIK, A.B. and HU, G., 2017. Inactivation of Rab11a GTPase in Macrophages Facilitates Phagocytosis of Apoptotic Neutrophils. *The Journal of Immunology*, **198**(4), pp. 1660-1672.

JIANG, S., DUPONT, N., CASTILLO, E.F. and DERETIC, V., 2013. Secretory versus degradative autophagy: unconventional secretion of inflammatory mediators. *Journal of Innate Immunity*, **5**(5), pp. 471-479.

JOBE, A.H. and WOOD, A.J.J., 1993. Pulmonary Surfactant Therapy. *The New England Journal of Medicine*, **328**(12), pp. 861-868.

JOHNS HOPKINS SCHOOL OF MEDICINE'S INTERACTIVE RESPIRATORY PHYSIOLOGY., , Surfactant [Homepage of Copyright © 1995 Johns Hopkins University], [Online]. Available: http://oac.med.jhmi.edu/res_phys/Encyclopedia/Surfactant/Surfactant.HTML [June, 24, 2016].

JOHNSON, M., MAZELA, J. and PEARSON, R., 2006. 8th European Conference on Pediatric and Neonatal Ventilation, *KL4- surfactant (Aerosurf) retains surface activity after aerosolization- Oral presentation*, 29 March- 1 April 2006.

JUSTO, O.R. and MORAES, A.M., 2003. Incorporation of Antibiotics in Liposomes Designed for Tuberculosis Therapy by Inhalation. *Drug delivery*, **10**(3), pp. 201-207.

KALINA, M., MASON, R.J. and SHANNON, J.M., 1992. Surfactant Protein C Is Expressed in Alveolar Type II Cells but Not in Clara Cells of Rat Lung. *American Journal of Respiratory Cell and Molecular Biology*, **6**(6), pp. 594-600.

KANABUS, A., 2016-last update, "Information about Tuberculosis", GHE. TB Statistics for South Africa – National & provincial. Available: http://www.tbfacts.org/tb-statistics-south-africa/ [March, 22, 2016].

KATTWINKEL, J., 2005. Synthetic Surfactants: The Search Goes on. *Pediatrics*, **115**(4), pp. 1075-1076.

KELLEHER, Z.T., SHA, Y., FOSTER, M.W., FOSTER, W.M., FORRESTER, M.T. and MARSHALL, H.E., 2014. Thioredoxin-mediated denitrosylation regulates cytokine-induced nuclear factor κB (NF-κB) activation. *Journal of Biological Chemistry*, **289**(5), pp. 3066-3072.

KENDIG, J.W., RYAN, R.M., SINKIN, R.A., MANISCALCO, W.M., NOTTER, R.H., GUILLET, R., COX, C., DWECK, H.S., HORGAN, M.J., REUBENS, L.J. and RISEMBERG, H., 1998. Comparison of two strategies for surfactant prophylaxis in very premature infants: a multicenter randomized trial. *Pediatrics*, **101**(6), pp. 1006-1012.

KERECMAN, J., MUSTAFA, S., VASQUEZ, M., DIXON, P. and CASTRO, R., 2008. Immunosuppressive properties of surfactant in alveolar macrophage NR8383. *Inflammation Research*, **57**(3), pp. 118-125.

KHARASCH, V.S., SWEENEY, T.D., FREDBERG, J., LEHR, J., DAMOKOSH, A.I., AVERY, M.E. and BRAIN, J.D., 1991. Pulmonary surfactant as a vehicle for intratracheal delivery of technetium sulfur colloid and pentamidine in hamster lungs. *American Review of Respiratory Disease*, **144**(4), pp. 909-913.

KIM, S.U., PARK, Y.H., MIN, J.S., SUN, H.N., HAN, Y.H., HUA, J.M., LEE, T.H., LEE, S.R., CHANG, K.T., KANG, S.W. and KIM, J.M., 2013. Peroxiredoxin I is a ROS/p38 MAPK-dependent inducible antioxidant that regulates NF-κB-mediated iNOS induction and microglial activation. *Journal of Neuroimmunology*, **259**(1), pp. 26-36.

KIM, D.K. and DOBSON, J., 2009. Nanomedicine for targeted drug delivery. *Journal of Materials Chemistry*, **19**(35), pp. 6294-6307.

KING, R.J. and CLEMENTS, J.A., 1972. Surface active materials from dog lung. II. Composition and physiological correlations. *American Journal of Physiology - Legacy Content*, **223,**(3), pp. 715-726.

KISHORE, U., GREENHOUGH, T.J., WATERS, P., SHRIVE, A.K., GHAI, R., KAMRAN, M.F., BERNAL, A.L., REID, K.B.M., MADAN, T. and CHAKRABORTY, T., 2006. Surfactant proteins SP-A and SP-D: Structure, function and receptors. *Molecular Immunology*, **43**(9), pp. 1293-1315.

KITAMURA, H., KAMON, H., SAWA, S.I., PARK, S.J., KATUNUMA, N., ISHIHARA, K., MURAKAMI, M. and HIRANO, T., 2005. IL-6-STAT3 controls intracellular MHC class II αβ dimer level through cathepsin S activity in dendritic cells. *Immunity*, **23**(5), pp. 491-502.

KNOOPS, B., ARGYROPOULOU, V., BECKER, S., FERTÉ, L. and KUZNETSOVA, O., 2016. Multiple roles of peroxiredoxins in inflammation. *Molecules and Cells*, **39**(1), pp. 60-64.

KOCH, R., 1882. Die Atiologie van der Tuberkulose. *Berliner Kliniscben Wocbenshift.*, **15**, pp. 221-230.

KOPITAR-JERALA, N., 2006. The role of cystatins in cells of the immune system. *FEBS Letters*, **580**(27), pp. 6295-6301.

KOUL, A., ARNOULT, E., LOUNIS, N., GUILLEMONT, J. and ANDRIES, K., 2011. The challenge of new drug discovery for tuberculosis. *Nature*, **469**(7331), pp. 483.

KRIBS, A., 2011. How best to administer surfactant to VLBW infants?. *Archives of Disease in Childhood-Fetal and Neonatal Edition*, **96**(4), pp. F238-F240.

LABIRIS, N.R. and DOLOVICH, M.B., 2003a. Pulmonary drug delivery. Part I: Physiological factors affecting therapeutic effectiveness of aerosolized medications. *British Journal of Clinical Pharmacology*, **56**(6), pp. 588–599.

LABIRIS, N.R. and DOLOVICH, M.B., 2003b. Pulmonary drug delivery. Part II: The role of inhalant delivery devices and drug formulations in therapeutic effectiveness of aerosolized medications. *British Journal of Clinical Pharmacology*, **56**(6), pp. 600-612.

LACAZE-MASMONTEIL, T., 2008. Exogenous surfactant therapy: newer developments. *Seminars in Neonatology*, **8**(6), pp. 433-440.

LALLOO, U. and AMBARAM, A., 2010. New Antituberculous Drugs in Development. *Current HIV/AIDS Reports*, **7**(3), pp. 143-151.

LAVNIKOVA, N., DRAPIER, J.C. and LASKIN, D.L., 1993. A single exogenous stimulus activates resident rat macrophages for nitric oxide production and tumor cytotoxicity. *Journal of Leukocyte Biology*, **54**(4), pp. 322.

LEACH, K., BRICKNER, S., NOE, M. and MILLER, P., 2011. Linezolid, the first oxazolidinone antibacterial agent. *Annals of the New York Academy of Sciences*, **1222**(1), pp. 49-54.

LEMOS, M.P., MCKINNEY, J. and RHEE, K.Y., 2011. Dispensability of Surfactant Proteins A and D in Immune Control of Mycobacterium tuberculosis Infection following Aerosol Challenge of Mice. *Infection and Immunity*, **79**(3), pp. 1077-1085.

LEVINE, A. and WHITSETT, J.A., 2001. Pulmonary collectins and innate host defense of the lung. *Microbes and Infection*, **3**(2), pp. 161-166.

LEWIS, J.F., IKEGAMI, M., JOBE, A.H. and TABOR, B., 1991. Aerosolized surfactant treatment of preterm lambs. *Journal of Applied Physiology*, **70**(2), pp. 869-876.

LI, W.Z., CHEN, W.M. and KOBAYASHI, T., 1994. Aerosolized surfactant reverses respiratory failure in lung–lavaged rats. *Acta Anaesthesiologica Scandinavica*, **38**(1), pp. 82-88.

LIPPMANN, M., 2011. Chapter 10 - Respiratory System. In: CANADIAN CENTRE FOR OCCUPATIONAL HEALTH AND SAFETY, ed, *The ILO Encyclopaedia of Occupational Health and Safety*. 4th ed. edn. International labour office, .

LIU, Z., DING, Y., YE, N., WILD, C., CHEN, H. and ZHOU, J., 2016. Direct Activation of Bax Protein for Cancer Therapy. *Medicinal Research Reviews*, **36**(2), pp. 313-341.

LU, J., HOU, R., YANG, Z. and TANG, Z., 2015. Development and characterization of drug-loaded biodegradable PLA microcarriers prepared by the electrospraying technique (poly(L-lactide)) (Report). *International Journal of Molecular Medicine*, **36**(1), pp. 249-254.

LUCAS, R., CZIKORA, I., SRIDHAR, S., ZEMSKOV, E.A., OSEGHALE, A., CIRCO, S., CEDERBAUM, S.D., CHAKRABORTY, T., FULTON, D.J., CALDWELL, R.W. and ROMERO, M.J., 2013. Arginase 1: an unexpected mediator of pulmonary capillary barrier dysfunction in models of acute lung injury.. *Frontiers in Immunology*, **4**(228), pp. 1-7.

MAARSINGH, H., PERA, T. and MEURS, H., 2008. Arginase and pulmonary diseases. *Naunyn-Schmiedeberg's Archives of Pharmacology*, **378**(2), pp. 171-184.

MAINE, G.N., MAO, X., KOMARCK, C.M. and BURSTEIN, E., 2007. COMMD1 promotes the ubiquitination of NF- κB subunits through a cullin- containing ubiquitin ligase. *The EMBO Journal*, **26**(2), pp. 436-447.

MAITRA, A., BATES, S., KOLVEKAR, T., DEVARAJAN, P.V., GUZMAN, J.D. and BHAKTA, S., 2015. Repurposing—a ray of hope in tackling extensively drug resistance in tuberculosis. *International Journal of Infectious Diseases*, **32**, pp. 50-55.

MALCOLMSON, R.J. and EMBLETON, J.K., 1998. Dry powder formulations for pulmonary delivery. *Pharmaceutical Science & Technology Today*, **1**(9), pp. 394-398.

MANSOUR, H.M., RHEE, Y.S. and WU, X., 2009. Nanomedicine in pulmonary delivery. *International Journal of Nanomedicine*, **4**, pp. 299-319.

MANTOVANI, A., BISWAS, S.K., GALDIERO, M.R., SICA, A. and LOCATI, M., 2013. Macrophage plasticity and polarization in tissue repair and remodelling. *The Journal of Pathology*, **229**(2), pp. 176-185.

MANTOVANI, A., SICA, A., SOZZANI, S., ALLAVENA, P., VECCHI, A. and LOCATI, M., 2004. The chemokine system in diverse forms of macrophage activation and polarization. *Trends in immunology*, **25**(12), pp. 677-686.

MARTINEZ, F.O. and GORDON, S., 2014. The M1 and M2 paradigm of macrophage activation: time for reassessment. *F1000Prime Reports*, **6**, pp. 13.

MATHIAS, N.R., TIMOSZYK, J., STETSKO, P.I., MEGILL, J.R., SMITH, R.L. and WALL, D.A., 2002. Permeability Characteristics of Calu-3 Human Bronchial Epithelial Cells: In Vitro - In Vivo Correlation to Predict Lung Absorption in Rats. *Journal of Drug Targeting, 2002,* **10**(1), pp. 31-40.

MAZELA, J., MERRITT, T.A. and FINER, N.N., 2007. Aerosolized surfactants. *Current Opinion in Pediatrics,* **19**, pp. 155-162.

MCGEE, D.J., KUMAR, S., VIATOR, R.J., BOLLAND, J.R., RUIZ, J., SPADAFORA, D., TESTERMAN, T.L., KELLY, D.J., PANNELL, L.K. and WINDLE, H.J., 2006. Helicobacter pylori thioredoxin is an arginase chaperone and guardian against oxidative and nitrosative stresses. *Journal of Biological Chemistry.*, **281**(6), pp. 3290-3296.

MCILLERON, H., WILLEMSE, M., WERELY, C.J., HUSSEY, G.D., SCHAAF, H.S., SMITH, P.J. and DONALD, P.R., 2009. Isoniazid plasma concentrations in a cohort of South African children with tuberculosis: implications for international pediatric dosing guidelines (Clinical report). *Clinical Infectious Diseases,* **48**(11), pp. 1547.

MCKINNEY, J.D., 2000. In vivo veritas: The search for TB drug targets goes live. *Nature Medicine,* **6**(12), pp. 1330.

MCLEOD, A., 2010.-last update, Respiratory Tract Histology [April, 11, 2016].

MEDZHITOV, R., 2008. Origin and physiological roles of inflammation. *Nature,* **454**(7203), pp. 428.

MEENACH, S., ANDERSON, K., HILT, J., MCGARRY, R. and MANSOUR, H., 2014. High-Performing Dry Powder Inhalers of Paclitaxel DPPC/DPPG Lung Surfactant-Mimic Multifunctional Particles in Lung Cancer: Physicochemical Characterization, In Vitro Aerosol Dispersion, and Cellular Studies. *AAPS PharmSciTech; An Official Journal of the American Association of Pharmaceutical Scientists,* **15**(6), pp. 1574-1587.

MEINDL, C., STRANZINGER, S., DZIDIC, N., SALAR-BEHZADI, S., MOHR, S., ZIMMER, A. and FRÖHLICH, E., 2015. Permeation of Therapeutic Drugs in Different Formulations across the Airway Epithelium In Vitro. *PloS one,* **10**(8), pp. e0135690.

MIGLIORI, G.B., BESOZZI, G., GIRARDI, E., KLIIMAN, K., LANGE, C., TOUNGOUSSOVA, O.S., FERRARA, G., CIRILLO, D.M., GORI, A., MATTEELLI, A., SPANEVELLO, A., CODECASA, L.R. and RAVIGLIONE, M.C., 2007. Clinical and operational value of the extensively drug-resistant tuberculosis definition. *The European Respiratory Journal*, **30**(4), pp. 623.

MITCHISON, D. and DAVIES, G., 2012. The chemotherapy of tuberculosis: past, present and future. *The international journal of tuberculosis and lung disease : the official journal of the International Union against Tuberculosis and Lung Disease*, **16**(6), pp. 724.

MOELLERING, R.C., 2003. Linezolid: the first oxazolidinone. *Annals of Internal Medicine*, **138**(2), pp. 135-142.

MOGENSEN, T.H., 2009. Pathogen Recognition and Inflammatory Signaling in Innate Immune Defenses. *Clinical Microbiology Reviews*, **22**(2), pp. 240.

MORENO-SASTRE, M., PASTOR, M., SALOMON, C.J., ESQUISABEL, A. and PEDRAZ, J.L., 2015. Pulmonary drug delivery: a review on nanocarriers for antibacterial chemotherapy. *Journal of Antimicrobial Chemotherapy*, **70**(11), pp. 2945-2955.

MORGAN, M.J. and LIU, Z.G., 2011. Crosstalk of reactive oxygen species and NF-κB signaling. *Cell Research*, **21**(1), pp. 103-115.

MORLEY, C.J., 1987. Ten centre trial of artificial surfactant (artificial lung expanding compound) in very premature babies . *British Medical Journal*, **294**, pp. 991-996.

MOSSAAD, D.M.R., 2014. *"Drug Delivery to the Respiratory Tract Using Dry Powder Inhalers" (2014). Electronic Thesis and Dissertation Repository*, The University of Western Ontario.

MOSSER, D.M., 2003. The many faces of macrophage activation. *Journal of Leukocyte Biology*, **73**(2), pp. 209-212.

MOSSER, D.M., 1999. Receptor mediated subversion of macrophage cytokine production by intracellular pathogens. *Current Opinion in Immunology*, **11**(4), pp. 406-411.

MOYA, F., SINHA, S., GADZINOWSKI, J., D'AGOSTINO, R., SEGAL, R., GUARDIA, C., MAZELA, J. and LIU, G., 2007. One-year follow-up of very preterm infants who received lucinactant for prevention of respiratory distress syndrome: results from 2 multicenter randomized, controlled trials. *Pediatrics,* **119**(6), pp. e1361-e1370.

MOYA, F.R., GADZINOWSKI, J., BANCALARI, E., SALINAS, V., KOPELMAN, B., BANCALARI, A., KORNACKA, M.K., MERRITT, T.A., SEGAL, R., SCHABER, C.J., TSAI, H., MASSARO, J. and D'AGOSTINO, R., 2005. A Multicenter, Randomized, Masked, Comparison Trial of Lucinactant, Colfosceril Palmitate, and Beractant for the Prevention of Respiratory Distress Syndrome Among Very Preterm Infants. *Pediatrics,* **115**(4), pp. 1018-1029.

MURAKAMI, S., IWAKI, D., MITSUZAWA, H., SANO, H., TAKAHASHI, H., VOELKER, D.R., AKINO, T. and KUROKI, Y., 2002. Surfactant protein A inhibits peptidoglycan-induced tumor necrosis factor-α secretion in U937 cells and alveolar macrophages by direct interaction with Toll-like receptor 2. *Journal of Biological Chemistry,* **277**(9), pp. 6830-6837.

MUTTIL, P., WANG, C. and HICKEY, A., 2009. Inhaled Drug Delivery for Tuberculosis Therapy. *Pharmaceutical research; An Official Journal of the American Association of Pharmaceutical Scientists,* **26**(11), pp. 2401-2416.

MYRDAL, P.B., SHETH, P. and STEIN, S.W., 2013. Advances in Metered Dose Inhaler Technology: Formulation Development. *AAPS PharmSciTech,* **15**(2), pp. 434-455.

NAHAR, K., GUPTA, N., GAUVIN, R., ABSAR, S., PATEL, B., GUPTA, V., KHADEMHOSSEINI, A. and AHSAN, F., 2013. In vitro,in vivoandex vivomodels for studying particle deposition and drug absorption of inhaled pharmaceuticals. *European Journal of Pharmaceutical Sciences,* **49**(5), pp. 805-818.

NAKAMURA, T., NAKAMURA, H., HOSHINO, T., UEDA, S., WADA, H. and YODOI, J., 2005. Redox regulation of lung inflammation by thioredoxin. *Antioxidants & redox signaling,* **7**(1-2), pp. 60-71.

NAKATA, K., GOTOH, H., WATANABE, J., UETAKE, T., KOMURO, I., YUASA, K., WATANABE, S., IEKI, R., SAKAMAKI, H., AKIYAMA, H., KUDOH, S., NAITOH, M.,

SATOH, H. and SHIMADA, K., 1999. Augmented proliferation of human alveolar macrophages after allogeneic bone marrow transplantation. *Blood*, **93**(2), pp. 667.

NATHAN, C. and CUNNINGHAM-BUSSEL, A., 2013. Beyond oxidative stress: an immunologist's guide to reactive oxygen species. *Nature Reviews Immunology*, **13**(5), pp. 349-361.

NERLICH, A.G., HAAS, C.J., ZINK, A., SZEIMIES, U. and HAGEDORN, H.G., 1997. *Molecular evidence for tuberculosis in an ancient Egyptian mummy.*

NETEA-MAIER, R.T., PLANTINGA, T.S., VAN DE VEERDONK, F.L., SMIT, J.W. and NETEA, M.G., 2016. Modulation of inflammation by autophagy: consequences for human disease. *Autophagy*, **12**(2), pp. 245-260.

NEWHOUSE, M.T. and CORKERY, K.J., 2001. Aerosols for systemic delivery of macromolecules. *Respiratory care clinics of North America*, **7**(2), pp. 261-75, vi.

NEWMAN, S.P., 2004. Dry powder inhalers for optimal drug delivery. *Expert Opinion on Biological Therapy*, **4**(1), pp. 23-33.

NGUYEN, H.A., RAJARAM, M.V.S., MEYER, D.A. and SCHLESINGER, L.S., 2012. Pulmonary surfactant protein A and surfactant lipids upregulate IRAK-M, a negative regulator of TLR-mediated inflammation in human macrophages. *American Journal of Physiology.Lung Cellular and Molecular Physiology*, **303**(7), pp. L608.

NIEMAND, C., NIMMESGERN, A., HAAN, S., FISCHER, P., SCHAPER, F., ROSSAINT, R., HEINRICH, P.C. and MÜLLER-NEWEN, G., 2003. Activation of STAT3 by IL-6 and IL-10 in primary human macrophages is differentially modulated by suppressor of cytokine signaling 3. *The Journal of Immunology*, **170**(6), pp. 3263-3272.

NOGEE, L.M., DEMELLO, D.E., DEHNER, L.P. and COLTEN, H.R., 1993. Deficiency of pulmonary surfactant protein B in congenital alveolar proteinosis. *New England Journal of Medicine*, **328**(6), pp. 406-410.

NUERMBERGER, E.L., SPIGELMAN, M.K. and YEW, W.W., 2010. Current development and future prospects in chemotherapy of tuberculosis. *Respirology*, **15**(5), pp. 764-778.

OFEK, I., MESIKA, A., KALINA, M., KEISARI, Y., PODSCHUN, R., SAHLY, H., CHANG, D., MCGREGOR, D. and CROUCH, E., 2001. Surfactant protein D enhances phagocytosis and killing of unencapsulated phase variants of Klebsiella pneumoniae. *Infection and immunity,* **69**(1), pp. 24-33.

ONG, H.X., TRAINI, D. and YOUNG, P.M., 2013. Pharmaceutical applications of the Calu-3 lung epithelia cell line. *Expert Opinion on Drug Delivery,* **10**(9), pp. 1287-1302.

PANDEY, R. and KHULLER, G., 2005. Antitubercular inhaled therapy: opportunities, progress and challenges. *Journal of Antimicrobial Chemotherapy,* **55**(4), pp. 430-435.

PARIDA, S.K., AXELSSON- ROBERTSON, R., RAO, M.V., SINGH, N., MASTER, I., LUTCKII, A., KESHAVJEE, S., ANDERSSON, J., ZUMLA, A. and MAEURER, M., 2015. Totally drug- resistant tuberculosis and adjunct therapies. *Journal of Internal Medicine,* **277**(4), pp. 388-405.

PARIKH, R., DALWADI, S., ABOTI, P. and PATEL, L., 2014. Inhaled microparticles of antitubercular antibiotic for in vitro and in vivo alveolar macrophage targeting and activation of phagocytosis. *Journal of Antibiotics,* **67**(5), pp. 387-394.

PASULA, R., DOWNING, J.F., WRIGHT, J.R., KACHEL, D.L., DAVIS JR, T.E. and MARTIN, W.J., 1997. Surfactant protein A (SP-A) mediates attachment of Mycobacterium tuberculosis to murine alveolar macrophages. *American Journal of Respiratory Cell and Molecular Biology,* **17**(2), pp. 209-217.

PATIL-GADHE, A., KYADARKUNTE, A., PEREIRA, M., JEJURIKAR, G., PATOLE, M., RISBUD, A. and POKHARKAR, V., 2014. Rifapentine-proliposomes for inhalation: In vitro and In vivo toxicity (Original Article)(Report). *Toxicology International,* **21**(3), pp. 275.

PAVONE, L.A., ALBERT, S., CARNEY, D., GATTO, L.A., HALTER, J.M. and NIEMAN, G.F., 2007. Injurious mechanical ventilation in the normal lung causes a progressive pathologic change in dynamic alveolar mechanics. *Critical Care,* **11**, pp. R64.

PENG, T., LIN, S., NIU, B., WANG, X., HUANG, Y., ZHANG, X., LI, G., PAN, X. and WU, C., 2016. Influence of physical properties of carrier on the performance of dry powder inhalers. *Acta Pharmaceutica Sinica.B,* **6**(4), pp. 308-318.

PÉREZ-GIL, J., 2008. Structure of pulmonary surfactant membranes and films: The role of proteins and lipid–protein interactions. *BBA - Biomembranes*, **1778**(7), pp. 1676-1695.

PETTY, T.L., REISS, O.K., PAUL, G.W., SILVERS, G.W. and ELKINS, N.D., 1977. Characteristics of Pulmonary Surfactant in Adult Respiratory Distress Syndrome Associated with Trauma and Shock 1–3. *American Review of Respiratory Disease*, **115**(3), pp. 531-536.

POLIN, R.A. and CARLO, W.A., 2014. Surfactant replacement therapy for preterm and term neonates with respiratory distress (Report). *Pediatrics*, **133**(1), pp. 156.

POSSMAYER, F., 1988. Pulmonary Perspective. *The American Review of Respiratory Disease*, **138**, pp. 990.

PRECIOSO, A.R., SAKAE, P.P., MASCARETTI, R.S., KUBRUSLY, F.S., GEBARA, V.C., IOURTOV, D., REBELLO, C.M., VAZ, F.A. and RAW, I., 2006. Analysis of the immunogenicity and stability of a porcine pulmonary surfactant preparation administered in rabbits. *Clinics*, **61**(2), pp. 153-160.

PROCTOR, V.K., 2013. *Signalling Pathways Linking Interleukin 13 Receptor Activation to Lung Epithelial Cell Function. (Doctoral dissertation)*, University of Bath.

RAGHAVENDRAN, K., WILLSON, D. and NOTTER, R.H., 2011. Surfactant Therapy of ALI and ARDS. *Critical Care Clinics*, **27**(3), pp. 525-559.

RAVIKUMAR, B., FUTTER, M., JAHREISS, L., KOROLCHUK, V.I., LICHTENBERG, M., LUO, S., MASSEY, D.C., MENZIES, F.M., NARAYANAN, U., RENNA, M. and JIMENEZ-SANCHEZ, M., 2009. Mammalian macroautophagy at a glance. *Journal of Cell Science*, **122**(11), pp. 1707-1711.

RAY, P.D., HUANG, B.W. and TSUJI, Y., 2012. Reactive oxygen species (ROS) homeostasis and redox regulation in cellular signalling. *Cellular Signalling*, **24**(5), pp. 981-990.

REDDY, P.H., REDDY, T.P., MANCZAK, M., CALKINS, M.J., SHIRENDEB, U. and MAO, P., 2011. Dynamin-Related Protein 1 and Mitochondrial Fragmentation in Neurodegenerative Diseases. *Brain Research Reviews*, **67**(1-2), pp. 103-118.

REIDY, M.F. and WRIGHT, J.R., 2003. Surfactant protein A enhances apoptotic cell uptake and TGF-beta1 release by inflammatory alveolar macrophages. *American journal of physiology.Lung Cellular and Molecular Physiology*, **285**(4), pp. L854.

REPUBLIC OF SOUTH AFRICA: NATIONAL DEPARTMENT OF HEALTH, ed, 2014. *Essential Drugs Programme. Primary Healthcare Standard Treatment Guidelines and Essential Medicines List.* 5th ed. edn. South Africa.

RESPAUD, R., MARCHAND, D., PARENT, C., PELAT, T., THULLIER, P., TOURNAMILLE, J.F., VIAUD-MASSUARD, M., DIOT, P., SI-TAHAR, M., VECELLIO, L. and HEUZÉ-VOURC'H, N., 2014. Effect of formulation on the stability and aerosol performance of a nebulized antibody. *mAbs*, **6**(5), pp. 1347-1355.

RISIN, S.A., HUNTER, R.L., KOBAK, M., ARIEL, B., VISHNEVSKY, B., EROKHIN, V., DEMIKHOVA, O., BOCHAROVA, I. and STOOPS, J.K., 2014. Certain Surfactants Significantly Enhance the Activity of Antibiotics in the Mouse Model of MTB and Drug Resistant MTB Infection and Effectively Remove the Bacteria from a Pulmonary Cavity in Human Ex-Vivo Study. *Annals of Clinical & Laboratory Science*, **44**(2), pp. 117-122.

RIVERO, O.M., 2008. *Cytokines as Immunomodulators in Tuberculosis Therapy.*

ROBERTSON, B., CURSTEDT, T., JOHANSSON, J., JÖRNVALL, H. and KOBAYASHI, T., 1990. Structural and Functional Characterization of Porcine Surfactant Isolated by Liquid-Gel Chromatography. *In Basic Research on Lung Surfactant*, **25**, pp. 237-246.

ROBERTSON, B. and HALLIDAY, H.L., 1998. Principles of surfactant replacement. *Biochimica et Biophysica Acta (BBA) - Molecular Basis of Disease*, **1408**(2–3), pp. 346-361.

ROBINSON, M.W., HUTCHINSON, A.T., DALTON, J.P. and DONNELLY, S., 2010. Peroxiredoxin: a central player in immune modulation. *Parasite Immunology*, **32**(5), pp. 305-313.

RODGERS, J.R. and COOK, R.G., 2005. MHC class Ib molecules bridge innate and acquired immunity. *Nature Reviews: Immunology*, **5**(6), pp. 459.

ROLFE, M.W., KUNKEL, S.L., ROWENS, B., STANDIFORD, T.J., CRAGOE JR, E.J. and STRIETER, R.M., 1992. Suppression of human alveolar macrophage-derived cytokines by amiloride. *American Journal of Respiratory Cell and Molecular Biology*, **6**(6), pp. 576-582.

ROSENBERG, O., SEILIEV, A. and ZHUIKOV, A., 2006. Lung surfactant: correlation between biophysical characteristic, composition, and therapeutic efficacy. *Liposome Technology,* **3**, pp. 317-345.

RÖTH, D., KRAMMER, P.H. and GÜLOW, K., 2014. Dynamin related protein 1- dependent mitochondrial fission regulates oxidative signalling in T cells. *FEBS letters,* **588**(9), pp. 1749-1754.

RUSSELL, K., 2014. *The role of macrophage migration inhibitory factor in airways disease*, London: Imperial College London.

RYAN, M., AKINBI, H., SERRANO, A., PEREZ-GIL, J., WU, H., MCCORMACK, F. and WEAVER, T., 2006. Antimicrobial Activity of Native and Synthetic Surfactant Protein B Peptides. *Journal of Immunology*, **176**(1), pp. 416-425.

SALVESEN, B., CURSTEDT, T., MOLLNES, T.E. and SAUGSTAD, O.D., 2014. Effects of natural versus synthetic surfactant with SP-B and SP-C analogs in a porcine model of meconium aspiration syndrome. *Neonatology,* **105**(2), pp. 128-135.

SAMTEN, B., TOWNSEND, J.C., SEVER-CHRONEOS, Z., PASQUINELLI, V., BARNES, P.F. and CHRONEOS, Z.C., 2008. An antibody against the surfactant protein A (SP-A)-binding domain of the SP-A receptor inhibits T cell-mediated immune responses to Mycobacterium tuberculosis. *Journal of Leukocyte Biology*, **84**(1), pp. 115.

SANDERS, M., 2007. Inhalation therapy: an historical review. *Primary care respiratory journal: journal of the General Practice Airways Group,* **16**(2), pp. 71.

SANDERS, R.L., 1982. The composition of pulmonary surfactant. In: E. FARRELL PM, ed, *Lung Development: Biological and Clinical Perspectives.* Volume 1 edn. New York: New York: Academic Press, (1); 193., pp. 193.

SANG, Y., BRICHALLI, W., ROWLAND, R.R. and BLECHA, F., 2014. Genome-wide analysis of antiviral signature genes in porcine macrophages at different activation statuses. *PloS one*, **9**(2), pp. p.e87613.

SATO, A. and IKEGAMI, M., 2012. SP-B and SP-C containing new synthetic surfactant for treatment of extremely immature lamb lung. *PLoS One*, **7**(7), pp. e39392.

SATRIANO, J., 2004. Arginine pathways and the inflammatory response: interregulation of nitric oxide and polyamines. *Amino acids*, **26**(4), pp. 321-329.

SAUERMANN, R., SCHWAMEIS, R., FILLE, M., LIGIOS, M.L.C. and ZEITLINGER, M., 2009. Cerebrospinal fluid impairs antimicrobial activity of fosfomycin in vitro. *The Journal of Antimicrobial Chemotherapy*, **64**(4), pp. 821.

SAVILL, J., 1997. Apoptosis in resolution of inflammation. *Journal of Leukocyte Biology*, **61**(4), pp. 375-380.

SCHELLER, J., CHALARIS, A., SCHMIDT-ARRAS, D. and ROSE-JOHN, S., 2011. The pro-and anti-inflammatory properties of the cytokine interleukin-6. *Biochimica et Biophysica Acta (BBA)-Molecular Cell Research*, **1813**(5), pp. 878-888.

SCHMITZ, P. and KLEINE-ALLEKOTTE, B., 1960. Treatment of pulmonary tuberculosis with PAS infusions associated with INH and streptomycin. *Die Medizinische Welt*, **42**, pp. 2206-2211.

SCHREIBER, J., JENNER, R.G., MURRAY, H.L., GERBER, G.K., GIFFORD, D.K. and YOUNG, R.A., 2006. Coordinated binding of NF-κB family members in the response of human cells to lipopolysaccharide. *Proceedings of the National Academy of Sciences*, **103**(15), pp. 5899-5904.

SCHRODER, K., HERTZOG, P.J., RAVASI, T. and HUME, D.A., 2004. Interferon-γ: an overview of signals, mechanisms and functions. *Journal of Leukocyte Biology*, **75**(2), pp. 163-189.

SEEGER, W., PISON, U., BUCHHORN, R., OBERTACKE, U. and JOKA, T., 1990. Surfactant abnormalities and adult respiratory failure. *Lung*, **168**, pp. 891-902.

SEEHASE, M., COLLINS, J.J., KUYPERS, E., JELLEMA, R.K., OPHELDERS, D.R., OSPINA, O.L., PEREZ-GIL, J., BIANCO, F., GARZIA, R., RAZZETTI, R. and KRAMER, B.W., 2012. New surfactant with SP-B and C analogs gives survival benefit after inactivation in preterm lambs. *PLoS One,* **7**(10), pp. e47631.

SERRANO, A.G. and PÉREZ-GIL, J., 2006. Protein–lipid interactions and surface activity in the pulmonary surfactant system. *Chemistry and Physics of Lipids,* **141**(1), pp. 105-118.

SERTL, K., 1986. Dendritic cells with antigen-presenting capability reside in airway epithelium, lung parenchyma, and visceral pleura. *The Journal of Experimental Medicine,* **163**(2), pp. 436-451.

SEVER-CHRONEOS, Z., KRUPA, A., DAVIS, J., HASAN, M., YANG, C.H., SZELIGA, J., HERRMANN, M., HUSSAIN, M., GEISBRECHT, B.V., KOBZIK, L. and CHRONEOS, Z.C., 2011. Surfactant protein A (SP-A)-mediated clearance of Staphylococcus aureus involves binding of SP-A to the staphylococcal adhesin eap and the macrophage receptors SP-A receptor 210 and scavenger receptor class A. *The Journal of Biological Chemistry,* **286**(6), pp. 4854-4870.

SHAFER, P.T., 1974. The interaction of polyamino acids with lipid monolayers. *BBA - Biomembranes,* **373**(3), pp. 425-435.

SHAI, Y., 2002. *Mode of action of membrane active antimicrobial peptides.* New York.

SHARMA, R., SAXENA, D., DWIVEDI, A.K. and MISRA, A., 2001. Inhalable Microparticles Containing Drug Combinations to Target Alveolar Macrophages for Treatment of Pulmonary Tuberculosis. *Pharmaceutical Research,* **18**(10), pp. 1405-1410.

SHEN, B.Q., FINKBEINER, W.E., WINE, J.J., MRSNY, R.J. and WIDDICOMBE, J.H., 1994. Calu-3: a human airway epithelial cell line that shows cAMP-dependent Cl-secretion. *American Journal of Physiology-Lung Cellular and Molecular Physiology,* **266**(5), pp. L493-L501.

SHEPHERD, V.L., 2002. Pulmonary surfactant protein D: a novel link between innate and adaptive immunity. *American Journal of Physiology. Lung cellular and Molecular Physiology,* **282**(3), pp. L516.

SILVER, L. and BOSTIAN, K., 1990. Screening of natural products for antimicrobial agents. *The European Journal of Clinical Microbiology & Infectious Diseases,* **9**(7), pp. 455-461.

SILVERMAN, J.A., MORTIN, L.I., VANPRAAGH, A.D.G., LI, T. and ALDER, J., 2005. Inhibition of daptomycin by pulmonary surfactant: in vitro modelling and clinical impact (MAJOR ARTICLE). *Journal of Infectious Diseases,* **191**(12), pp. 2149.

SIMONE, E.A., DZIUBLA, T.D. and MUZYKANTOV, V.R., 2008. Polymeric carriers: role of geometry in drug delivery. *Expert Opinion on Drug Delivery*, **5**(12), pp. 1283-1300.

SINHA, S.K., LACAZE-MASMONTEIL, T., VALLS I SOLER, A., WISWELL, T.E., GADZINOWSKI, J., HAJDU, J., BERNSTEIN, G., SANCHEZ-LUNA, M., SEGAL, R., SCHABER, C.J. and MASSARO, J., 2005. Surfaxin Therapy Against Respiratory Distress Syndrome Collaborative Group. A multicenter, randomized, controlled trial of lucinactant versus poractant alfa among very premature infants at high risk for respiratory distress syndrome. *Pediatrics,* **115**(4), pp. 1030-1038.

SLAATS, J., TEN OEVER, J., VAN DE VEERDONK, F.L. and NETEA, M.G., 2016. IL-1β/IL-6/CRP and IL-18/ferritin: distinct inflammatory programs in infections. *PLoS pathogens,* **12**(12), pp. p.e1005973.

SLACK, J.L., SCHOOLEY, K., BONNERT, T.P., MITCHAM, J.L., QWARNSTROM, E.E., SIMS, J.E. and DOWER, S.K., 2000. Identification of two major sites in the type I interleukin-1 receptor cytoplasmic region responsible for coupling to pro-inflammatory signalling pathways. *The Journal of Biological Chemistry,* **275**(7), pp. 4670.

SOLL, R. and OZEK, E., 2009. Multiple versus single doses of exogenous surfactant for the prevention or treatment of neonatal respiratory distress syndrome. *Cochrane Database Syst Rev.,* **21**(1),.

SONG, J.Y., KIM, K.D. and ROE, J.H., 2008. Thiol-independent action of mitochondrial thioredoxin to support the urea cycle of arginine biosynthesis in Schizosaccharomyces pombe. *Eukaryotic cell,* **7**(12), pp. 2160-2167.

SPORRI, B., KOVANEN, P.E., SASAKI, A., YOSHIMURA, A. and LEONARD, W.J., 2001. JAB/SOCS1/SSI-1 is an interleukin-2–induced inhibitor of IL-2 signalling. *Blood,* **97**(1), pp. 221-226.

SPRAGG, R.G., LEWIS, J.F., WALMRATH, H.D., JOHANNIGMAN, J., BELLINGAN, G., LATERRE, P.F., WITTE, M.C., RICHARDS, G.A., RIPPIN, G., RATHGEB, F. and HÄFNER, D., 2004. Effect of recombinant surfactant protein C–based surfactant on the acute respiratory distress syndrome. *New England Journal of Medicine,* **351**(9), pp. 884-892.

STEENHUYSEN, J., 17 October 2012, 2012-last update, Drug showed promise in clearing drug-resistant tuberculosis [Homepage of Reuters, Life. Published Online], [Online]. Available: https://uk.reuters.com/article/us-tuberculosis-drug-idUKBRE89G1WL20121017 [April, 18, 2016].

STEIN, S.W., SHETH, P., HODSON, P.D. and MYRDAL, P.B., 2014. Advances in Metered Dose Inhaler Technology: Hardware Development. *AAPS PharmSciTech,* **15**(2), pp. 326-338.

STOOPS, J.K., ARORA, R., ARMITAGE, L., WANGER, A., SONG, L., BLACKBURN, M.R., KRUEGER, G.R. and RISIN, S.A., 2010. Certain surfactants show promise in the therapy of pulmonary tuberculosis. *In Vivo,* **24**(5), pp. 687-694.

STOWE, D.F. and CAMARA, A.K., 2009. Mitochondrial reactive oxygen species production in excitable cells: modulators of mitochondrial and cell function. *Antioxidants & Redox Signalling,* **11**(6), pp. 1373-1414.

STRAYER, D.S., HALLMAN, M. and MERRITT, T.A., 1991. Immunogenicity of surfactant. II. Porcine and bovine surfactants. *Clinical & Experimental Immunology,* **83**(1), pp. 41-46.

STRAYER, D.S., MERRITT, T.A., MAKUNIKE, C. and HALLMAN, M., 1989. Antigenicity of low molecular weight surfactant species. *The American Journal of Pathology,* **134**(4), pp. 723.

SUN, H. and PANG, K.S., 2007. Permeability, Transport, and Metabolism of Solutes in Caco-2 Cell Monolayers: A Theoretical Study. *Drug Metabolism and Disposition,* **36**(1), pp. 102-123.

SUN, Y., YANG, R., ZHONG, J., FANG, F., JIANG, J., LIU, M. and LU, J., 2009. Aerosolised surfactant generated by a novel noninvasive apparatus reduced acute lung injury in rats. *Critical Care,* **13**(2), pp. R31.

SURESH, G.K. and SOLL, R.F., 2005. Overview of surfactant replacement trials. *Journal of perinatology : official journal of the California Perinatal Association,* **25**(2), pp. S40.

SWEET, D.G., TURNER, M., STRAŇÁK, Z., PLAVKA, R., CLARKE, P., STENSON, B., SINGER, D., GOELZ, R., FABBRI, L., VAROLI, G. and PICCINNO, A., 2017. A first-in-human clinical study of a new SP-B and SP-C enriched synthetic surfactant (CHF5633) in preterm babies with respiratory distress syndrome. *Archives of Disease in Childhood-Fetal and Neonatal Edition,* , pp. archdischild-2017.

TERGAONKAR, V., CORREA, R.G., IKAWA, M. and VERMA, I.M., 2005. Distinct roles of I [kappa] B proteins in regulating constitutive NF-[kappa] B activity. *Nature Cell Biology,* **7**(9), pp. 921-923.

THOMASSEN, M.J., ANTAL, J.M., CONNORS, M.J., MEEKER, D.P. and WIEDEMANN, H.P., 1994. Characterization of exosurf (surfactant)-mediated suppression of stimulated human alveolar macrophage cytokine responses. *American Journal of Respiratory Cell and Molecular biology,* **10**(4), pp. 399.

THORBURN, A., 2008. Apoptosis and autophagy: regulatory connections between two supposedly different processes. *Apoptosis,* **13**(1), pp. 1-9.

TIMSINA, M.P., MARTIN, G.P., MARRIOTT, C., GANDERTON, D. and YIANNESKIS, M., 1994. Drug delivery to the respiratory tract using dry powder inhalers. *International Journal of Pharmaceutics,* **101**(1), pp. 1-13.

TORTI, F.M. and TORTI, S.V., 2002. Regulation of ferritin genes and protein. *Blood,* **99**(10), pp. 3505-3516.

U.S. FOOD AND DRUG ADMINISTRATION, 29 October, 2015, 2015-last update, Phase-Out of CFC Metered-Dose Inhalers Containing flunisolide, triamcinolone, metaproterenol, pirbuterol, albuterol and ipratropium in combination, cromolyn, and nedocromil - Questions and Answers [Homepage of U.S. Food and Drug Administration], [Online]. Available:

https://www.fda.gov/Drugs/DrugSafety/InformationbyDrugClass/ucm208138.htm [May, 20, 2017].

UDWADIA, Z.F., AMALE, R.A., AJBANI, K.K. and RODRIGUES, C., 2012. Totally drug-resistant tuberculosis in India. *Clinical infectious diseases : an official publication of the Infectious Diseases Society of America,* **54**(4), pp. 579.

UEDA, T., IKEGAMI, M., RIDER, E.D. and JOBE, A.H., 1994. Distribution of surfactant and ventilation in surfactant-treated preterm lambs. *Journal of Applied Physiology*, **76**(1), pp. 45-55.

VAARA, M., 1992. Agents that increase the permeability of the outer membrane. *Microbiological Reviews,* **56**(3), pp. 395-411.

VALLS- I- SOLER, A., LÓPEZ- HEREDIA, J., FERNÁNDEZ- RUANOVA, M.B. and GASTIASORO, E., 1997. A simplified surfactant dosing procedure in respiratory distress syndrome: the "side- hole" randomized study. *Acta Paediatrica,* **86**(7), pp. 74-751.

VAN RENSBURG, L., 2012. *Antimycobacterial agents : a study of Liposomal-Encapsulation, comparitive permeability of bronchial tissue and in vitro activity against mycobacterium tuberculosis isolates.* Stellenbosch : Stellenbosch University.

VAN ZYL, J.M. and SMITH, J., 2013b. Surfactant treatment before first breath for respiratory distress syndrome in preterm lambs: comparison of a peptide-containing synthetic lung surfactant with porcine-derived surfactant. *Drug Design, Development and Therapy*, **7**, pp. 905-916.

VAN ZYL, J.M., SMITH, J. and HAWTREY, A., 2013a. The effect of a peptide-containing synthetic lung surfactant on gas exchange and lung mechanics in a rabbit model of surfactant depletion. *Drug Design, Development and Therapy,* **7**, pp. 139-148.

VAN'T VEEN, A., MOUTON, J.W., GOMMERS, D., KLUYTMANS, J.A., DEKKERS, P. and LACHMANN, B., 1995. Influence of pulmonary surfactant on in vitro bactericidal activities of amoxicillin, ceftazidime, and tobramycin. *Antimicrobial Agents and Chemotherapy,* **39**(2), pp. 329-333.

VENKATARAMAN, S., HEDRICK, J.L., ONG, Z.Y., YANG, C., EE, P.L.R., HAMMOND, P.T. and YANG, Y.Y., 2011. The effects of polymeric nanostructure shape on drug delivery. *Advanced Drug Delivery Reviews,* **63**(14), pp. 1228-1246.

VERDOT, L., LALMANACH, G., VERCRUYSSE, V., HOEBEKE, J., GAUTHIER, F. and VRAY, B., 1999. Chicken cystatin stimulates nitric oxide release from interferon- γ- activated mouse peritoneal macrophages via cytokine synthesis. *The FEBS Journal,* **266**(3), pp. 1111-1117.

VILJOEN, I., 2005. *The role of surfactant in, and a comparison of, the permeability of porcine and human epithelia to various chemical compounds. (Dissertation)*, Thesis (MScMed)-University of Stellenbosch, 2005.

WALLACE, R.J., BROWN-ELLIOTT, B.A., WARD, S., CRIST, C., MANN, L. and WILSON, R., 2001. Activities of linezolid against rapidly growing mycobacteria. *Antimicrobial Agents & Chemotherapy,* **45**(3), pp. 764-767.

WALLACE, W., KEANE, M., MURRAY, D., CHISHOLM, W., MAYNARD, A. and ONG, T.M., 2007. Phospholipid lung surfactant and nanoparticle surface toxicity: lessons from diesel soots and silicate dusts. *Nanotechnology and Occupational Health,* , pp. 23-38.

WALLIS, R.S., PAI, M., MENZIES, D., DOHERTY, T.M., WALZL, G., PERKINS, M.D. and ZUMLA, A., 2010. Biomarkers and diagnostics for tuberculosis: progress, needs, and translation into practice. *The Lancet,* **375**(9729), pp. 1920-1937.

WALTHER, F.J., HERNÁNDEZ-JUVIEL, J.M. and WARING, A.J., 2014. Aerosol delivery of synthetic lung surfactant. *PeerJ,* , pp. e403.

WANG, D., ZHAO, Y., LIU, Z., LEI, H., DONG, M. and GONG, P., 2014. In vitro and intracellular activity of 4-substituted piperazinyl phenyl oxazolidinone analogues against Mycobacterium tuberculosis. *The Journal of Antimicrobial Chemotherapy*, **69**(6), pp. 1711.

WANG, Z., HOLM, B.A., MATALON, S. and NOTTER, R.H., 2005. Surfactant activity and dysfunction in lung injury. In: R.H. NOTTER, J.N. FINKELSTEIN and B.A. HOLM, eds, *Lung injury: Mechanisms, pathophysiology, and therapy.* Boca Raton: Taylor Francis Group, Inc;, pp. 297-352.

WEIBEL, E.R. and GOMEZ, D.M., 1962. Architecture of the Human Lung. *Science*, **137**(3530), pp. 577-585.

WEIKERT, L.F., LOPEZ, J.P., ABDOLRASULNIA, R., CHRONEOS, Z.C. and SHEPHERD, V.L., 2000. Surfactant protein A enhances mycobacterial killing by rat macrophages through a nitric oxide-dependent pathway. *American journal of physiology. Lung cellular and molecular physiology*, **279**(2), pp. L216.

WESCHE, H., HENZEL, W.J., SHILLINGLAW, W., LI, S. and CAO, Z., 1997. MyD88: An Adapter That Recruits IRAK to the IL-1 Receptor Complex. *Immunity*, **7**(6), pp. 837-847.

WHITE, D.C. and FRERMAN, F.E., 1967. Extraction, Characterization, and Cellular Localization of the Lipids of Staphylococcus aureus. *The Journal of Bacteriology*, **94**(6), pp. 1854.

WHITSETT, J.A., HULL, W.M. and LUSE, S., 1991. Failure to detect surfactant protein-specific antibodies in sera of premature infants treated with survanta, a modified bovine surfactant. *Pediatrics*, **87**(4), pp. 505.

WILLSON, D.F., 2015. Aerosolized Surfactants, Anti-Inflammatory Drugs, and Analgesics. *Respiratory care : the official journal of the American Association for Respiratory Therapy*, **60**(6),.

WORLD HEALTH ORGANIZATION, 2015-last update, Global Tuberculosis Report 2015 [Homepage of WHO Press, World Health Organization], [Online]. Available: http://apps.who.int/iris/bitstream/10665/191102/1/9789241565059_eng.pdf [March, 21, 2016].

WORLD HEALTH ORGANIZATION, 2012-last update, Global Tuberculosis Report 2012 [Homepage of WHO Press, World Health Organization], [Online]. Available: http://www.who.int/tb/publications/global_report/gtbr12_main.pdf [March, 21, 2016].

WRIGHT, J.R., 2005. Immunoregulatory functions of surfactant proteins. *Nature Reviews Immunology*, **5**(1), pp. 58-68.

WRIGHT, J.R., 2003. Pulmonary surfactant: a front line of lung host defense. *The Journal of Clinical Investigation*, **111**(10), pp. 1453-1455.

WRIGHT, J.R., BORRON, P., BRINKER, K.G. and FOLZ, R.J., 2001. Surfactant Protein A: regulation of innate and adaptive immune responses in lung inflammation. *American journal of Respiratory Cell and Molecular Biology*, **24**(5), pp. 513-517.

WRIGHT, T.W., NOTTER, R.H., WANG, Z., HARMSEN, A.G. and GIGLIOTTI, F., 2001. Pulmonary inflammation disrupts surfactant function during Pneumocystis carinii pneumonia. *Infection and Immunity*, **69**(2), pp. 758-764.

WRIGHT, J.R. and DOBBS, L.G., 1991. Regulation of Pulmonary Surfactant Secretion and Clearance. *Annual Review of Physiology*, **53**(1), pp. 395-414.

YAMASHITA, C.M., VELDHUIZEN, R.A.W. and GILL, S.E., 2013. Alveolar macrophages and pulmonary surfactant—more than just friendly neighbours. *OA Biology*, **1**(1), pp. 6.

YOO, J.W., DOSHI, N. and MITRAGOTRI, S., 2011. Adaptive micro and nanoparticles: Temporal control over carrier properties to facilitate drug delivery. *Advanced Drug Delivery Reviews*, **63**(14), pp. 1247-1256.

ZANEN, P., GO, L.T. and LAMMERS, J., 1996. Optimal particle size for β2 agonist and anticholinergic aerosols in patients with severe airflow obstruction. *Thorax*, **51**, pp. 977-980.

ZHOU, Q., TANG, P., LEUNG, S.S.Y., CHAN, J.G.Y. and CHAN, H.K., 2014. Emerging inhalation aerosol devices and strategies: Where are we headed? *Advanced Drug Delivery Reviews*, **75**, pp. 3-17.

ZHU, Y.P., BROWN, J.R., SAG, D., ZHANG, L. and SUTTLES, J., 2015. Adenosine 5′-Monophosphate–Activated Protein Kinase Regulates IL-10–Mediated Anti-Inflammatory Signaling Pathways in Macrophages. *The Journal of Immunology*, **194**(2), pp. 584-594.

ZIGNOL, M., HOSSEINI, M.S., WRIGHT, A., LAMBREGTS-VAN WEEZENBEEK, C., NUNN, P., WATT, C.J., WILLIAMS, B.G. and DYE, C., 2006. Global incidence of multidrug-resistant tuberculosis. *Journal of Infectious Diseases*, **194**(4), pp. 479.

ZINK, A.R., SOLA, C., REISCHL, U., GRABNER, W., RASTOGI, N., WOLF, H. and NERLICH, A.G., 2003. Characterization of Mycobacterium tuberculosis Complex DNAs from Egyptian Mummies by Spoligotyping. *Journal of Clinical Microbiology*, **41**(1), pp. 359.

ZOLA, E.M., GUNKEL, J.H., CHAN, R.K., LIM, M.O., KNOX, I., FELDMAN, B.H., DENSON, S.E., STONESTREET, B.S., MITCHELL, B.R., WYZA, M.M. and BENNETT, K.J., 1993. Comparison of three dosing procedures for administration of bovine surfactant to neonates with respiratory distress syndrome. *The Journal of Pediatrics,* **122**(3), pp. 453-459.

1.8 Aims of Study

a) To assess the viability of cell lines after above mentioned time exposure to varying surfactant concentrations within the same time frames using the MTT colorimetric assay for assessing cell metabolic activity.

i. *NR8383 rat alveolar macrophage cell line*

Phalloidin-TRITC staining will be employed to visualize potential stimulation of filamentous actin (F-actin) formation in alveolar macrophages, actin polymerization of NR8383 macrophages; stimulation of cytoskeletal rearrangement, specifically of directed actin-filled filopodia.

ii. *A549 Human Lung carcinoma- Alveolar epithelium cell line*

(For the purpose of an epithelial model)

b) To evaluate the potential anti-inflammatory effects (Cytokine production and Oxidative Burst) of 3 exogenous surfactants (2 animal derived and 1 synthetic surfactant) on un-stimulated and lipopolysaccharide (LPS) stimulated rat alveolar macrophage (AM) cell line NR8383 and human alveolar macrophages derived from BAL (bronchoalveolar lavage) in varying concentrations and time exposure.

1) Curosurf® - Animal derived (porcine)
2) Liposurf® - Animal derived (bovine)
3) Synsurf® - Synthetic

c) Antimicrobial

To evaluate and compare the antimicrobial efficacy of individual drug-surfactant combinations (Curosurf®, Synsurf®, Liposurf®) at concentrations relevant to the MIC_{99} in order to determine their potential drug-MIC lowering capacity using the MGIT 960 system.

Pathogen and drug list:

Mycobacterium tuberculosis – Linezolid

Linezolid was the chosen antibiotic studied due to its potential repurposing for the treatment of MDR-TB.

d) Biophysical

To study the biophysical performance of surfactant-drug combinations in order to allow for a proper evaluation of the significance of the experimental model system, providing a possible non-invasive, site-specific, dual drug delivery model via pMDI (pressurised metered dose inhaler) form. The Calu-3 lung adenocarcinoma cell line (ATCC® HTB-55™) will be investigated as suitable cell-line model for a possible Synsurf® pMDI due to its preferred air-liquid interface characteristics.

i. To develop a novel device for the deposition of aerosolised surfactant-based particles for inhalation onto cultured airway epithelium as well as to validate the compatibility with cells. Furthermore, to characterise the transport of an aerosolised form of the synthetic surfactant Synsurf®.

Synsurf® was investigated as it is an entirely synthetic pulmonary surfactant containing peptides that mimic the action of naturally occurring surfactant proteins SP-B/C and avoids the potential risk of animal-derived pathogen transmission. It is also inexpensive and less complicated to manufacture since it does not rely on protein purification and harvesting from animal sources. Furthermore, pMDI's provide patients with a versatile, reliable, instantly available, self-contained, portable, low cost medical aerosol delivery system.

2 CHAPTER 2: Viability Study

2.1 Introduction

The lungs have become the main targets for the manufacture and processing of pulmonary drug administration. Endogenous pulmonary surfactant cover the bronchioles and alveoli. Inhaled particles encounter surfactant that may lead to particle coating, modification of its epithelial surface chemistry and subsequent cell response (Wallace, Keane et al. 2007, Herzog, Byrne et al. 2009). In turn, this interaction may have consequences for the oxidative potential of the particles. Similarly, administration of exogenous lung surfactant can influence the lung epithelial cell surface as well as the agglomeration state of immune cells within the lung. These are factors of possible exogenous surfactant induced cellular modulation on delicately balanced intracellular pathways. This could potentially play a role in the induction of the respiratory burst and lead to the production of reactive oxygen species (ROS) which, in turn, may induce cell death.

Apoptosis, also called programmed cell death, is a type of cell extinction regulated in an orderly manner by a series of signal cascades in certain situations, and it is an important physical process involved in regulating growth, development, and immune responses (Fan, Han et al. 2005, Chen, Lai et al. 2008). The induction of apoptosis in tumour cells with exogenous surfactant (alongside other treatments) might prove to be an important approach in therapy for cancer and immune system diseases that affect the pulmonary system. This approach is gaining interest. Badawi and co-workers investigated several novel (non-pulmonary) surfactants on the regulation of cancer growth (Badawi, Ismail et al. 2015). Their studies revealed that surfactants may have played a role in the regulation of cancer growth as tin-based surfactants displayed effective antitumor potency.

Assessing the biological activity of surfactants in cell-based experiments of A549 alveolar epithelial carcinoma cells and NR8383 rat alveolar macrophages may indicate a role of oxidative stress in the production of inflammatory cytokines and cytotoxic cellular responses (see Chapter 3). Evaluating the possible *in vitro* induction of biological activity in these cells could perhaps lead to the better understanding of exogenous surfactant administration and the pulmonary response that follow *in vivo*.

The objective of the study was to determine, in the absence of clinical variables, the effect of exogenous surfactants on the biogenesis and metabolism as well as morphological changes in rat alveolar macrophages NR8383 and A549 type II respiratory epithelial cells. The effects of two animal derived and one novel synthetic surfactant were studied at varying concentrations and time intervals for the use in formulations applied on the respiratory epithelium by means of an *in vitro* cytotoxicity assay.

The results obtained by studying known exogenous surfactants can then be compared to the potential toxicity of future exogenous surfactants not yet registered or approved for use in the human respiratory tract. Since it is then possible to determine the cytotoxic potential of new surfactants in relation to other surfactants, surfactant design and development could be tailored to exclude potential toxic components, thus leading to a more rational formulation of the product. The mechanisms of pulmonary surfactants triggering cell death have not yet been investigated in detail. The current study therefore aims to clarify any possible unwanted or unspecific cellular activity exogenous (mammalian-derived and synthetic) lung surfactant may be involved in e.g. the activation of intracellular stress signalling pathways.

2.2 Methods and Materials

Cell Culture

Both the NR8383 and A549 cell lines were successfully established and viability was established 95-98% before each experiment. Both the NR8383 (Rat Alveolar Macrophages, ATCC®, Cat. No. CRL-2192™) and the A549 (Lung Carcinoma, ATCC®, Cat. No. CCL-185™) cell lines were first cultured in 75 cm^2 flasks and maintained in a humidified, 5% CO_2– 95% atmospheric air incubator at 37°C. The NR8383 cell line media comprised of RPMI 1640 (Roswell Park Memorial Institute media) supplemented with 10% fetal calf serum, 1% l-glutamine solution (200 mM), and 1% Penicillin-Streptomycin. The media for the A549 cell line comprised of Advanced DMEM supplemented with 5% fetal calf serum, 1% L-glutamine solution (200 mM), and 1% Penicillin-Streptomycin, and both were routinely changed twice weekly. Cells were seeded to 48-well tissue culture plates at a density of 2.5×10^4 cells/well for NR8383 and 2×10^4 cells/well for A549 respectively. Cell viability before each experiment was assessed by trypan blue exclusion. Equal parts of 0.4% trypan blue dye was added to the cell suspension to obtain a 1 to 2 dilution before cell count. Live cells with intact cell

membranes are not coloured however, if cells take up trypan blue, they are considered non-viable. Cell viability before each experiment was established at ~85-90% before each experiment.

Viability assay

Cell viability was determined by 3-(4,5-Dimethylthiazol-2-yl)-2,5-diphenyltetrazolium bromide (MTT) assay and were performed in triplicate with Curosurf®, Synsurf®, Liposurf® for 30 min, 1, 4, 12 and 24 hours with final phospholipid (DPPC) concentrations of 25 to 1500 µg/ml for both cell lines (see Appendix A). The assay measures the ability of the mitochondria within living cells to reduce the yellow MTT dye to its purple formazan product. This product is then dissolved in isopropanol (1%)/triton (0.1%) solution at a 50:1 ratio; the absorbance reading of the resulting solution is proportional to the number of viable cells.

The cells, when established at 80% confluency after seeding, were stimulated according to the specific experimental procedure. At the end of the experiment, the individual supernatants from the plates containing rat alveolar macrophages were carefully removed and centrifuged and to ensure the collection of all the semi-adherent cells. For the adherent A549 epithelial cell line, the media only needed to be removed. The cells were then incubated (covered in foil) in 250 µl of 2.5 mg/ml MTT solution in phosphate buffered saline (PBS) for 2 hours in a humidified, CO_2 5% – 95% atmospheric air incubator at 37°C. Confirmation of the purple product within the cells was observed using a light microscope. 250 µl of isoproponol (1%)/triton (0.1%) solution was added to each well to lyse cells and dissolve the formazan product. The plates were placed on a slow plate shaker for a few minutes to ensure the product is dissolved. The absorbance at 550 nm was measured using a universal microplate reader, EL800 BioTek Instruments Inc. The effect of treatment on cell viability was calculated as a percentage of optical density relative to the untreated control.

Oxidative Burst

The reactive oxidative intermediate, ROS production, in A549 epithelial cells & AMs, was analysed by flow cytometry (see Appendix C). The respective cell lines were treated in culture with Curosurf®, Liposurf® and Synsurf® (500 - 1500 µg/ml DPPC) for 12 and 24 hours then washed, re-suspended and loaded with the fluorescent probe 2′,7′–dichlorofluorescein acetate

(DCFH-DA, 25 µM) (Sigma Aldrich). Esterase cleaves the acetate groups of DFH-DA, thus the trapped DCFH is converted to the highly fluorescent 2′,7′–dichlorofluorescein (DCF) in the presence of reactive oxygen intermediates. DCFH loaded cells were used as the baseline to measure auto fluorescence. The fluorescence of cells was recorded at an excitation wavelength of 488 nm and green fluorescence from DCF was measured with a 520 nm band pass filter with a 520 nm dichromic mirror. Fluorescence values from cells loaded with DCFH without surfactant treatment were standardised at 100 %. Scattering properties and DCF fluorescence were analysed by FAC-Scan flow cytometer (FACS Calibur, Becton Dickinson). All experiments were repeated at least three times.

Initial gating

To identify the cells, a FSC-A vs SSC-A dot plot was employed and a gate was drawn around the cells to distinguish cells from debris using a polygon gate. All further analysis was performed on the population. To determine fluorescent intensity of DCF, a histogram plot was used and the entire population was gated using an interval gate. Fluorescent intensity values of DCF as analysed as Median Fluorescent Intensity.

DCF was analysed on the BD FACSAria I, on the 488nm laser and detected with the 502LP filter and 530/30 bandpass filter.

Statistical Analysis

One-way analysis of variance (ANOVA) with Tukey's post-test was performed for the comparison of multiple treatments and differences were considered significant when $P \leq 0.05$. The statistical program GraphPad Prism v.5 was used.

Microscopic analysis of F-actin structures of NR8383

Microscopic analysis of F-actin structures of LPS stimulated NR8383 was completed for post-24 h treatment with Curosurf®, Synsurf®, Liposurf® in comparison to control and LPS stimulated control (1 µg/ml) (see Appendix B). Visualization of potential actin polymerization after exposure to surfactants (1) Curosurf®, Synsurf®, Liposurf® with final phospholipid concentrations 750 and 1500 µg/ml DPPC (2) LPS at 1 µg/ml (3) Control- Medium for 24h. Alveolar Macrophages were allowed to adhere to eight-well glass cell culture slides overnight and non-adherent cells were removed before treatment.

Staining Procedure

Cells were washed with warm PBS and fixed with 4% para-formadehyde for 10 minutes and washed three times thereafter for 5 minutes with PBS. Cells were incubated with 0.1% triton X-100 for 6 minutes at 37°C and thereafter washed three times for 5 minutes with PBS. Cells were stained with Phalloidin TRITC (P1951) at 50 μg/ml for 40 minutes at room temperature and washed three times for 5 minutes with PBS. Slides were air-dried and examined using the Zeiss LSM780 ELYRA PS1 confocal microscope.

2.3 Results

Viability assay

NR8383 Rat Alveolar Macrophages

The well-established and commonly used cytotoxicity assay, MTT, was utilised to determine the dose and time dependent toxic effect of three pulmonary surfactants: Curosurf®, Synsurf® and Liposurf® to NR8383 alveolar macrophages. Figures 2.1 - 2.5 show the plots of the cytotoxic response.The results show dose-dependent as well as time (exposure) dependent cytotoxicity of the surfactants. Decrease in cell viability by exposure to higher phospholipid concentrations of surfactants were only recorded from 4h onwards (Figure 2.3). Both Synsurf® and Liposurf® displayed a similar trend in dose-dependent cytotoxicity, however, the decrease in cell viability was not deemed significant. Synsurf® exhibited the same trend for the 12h (Figure 2.4) and 24h (Figure 2.5) time exposure and significant decreases in cell viability were seen at phospholipid concentrations of 1000 µg/ml (*** $P \leq 0.001$) and 1500 µg/ml (** $P \leq 0.01$) for 12 h and again 1000 µg/ml (* $P \leq 0.05$) and 1500 µg/ml (* $P \leq 0.05$) for 24h.

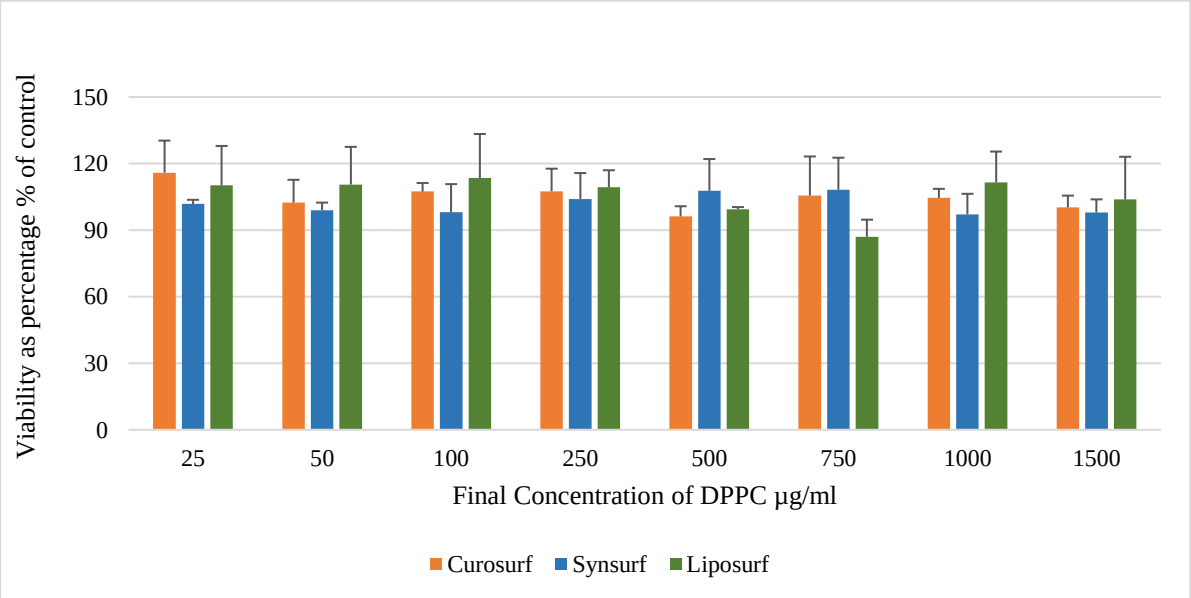

Figure 2.1: The effect of Curosurf®, Synsurf® and Liposurf® on NR8383 cell viability *in vitro*. MTT assay was performed to evaluate the cytotoxic effect of varying surfactants at comparable DPPC concentrations in comparison to untreated NR8383 cells for a 30 min exposure time (n=3). Values represent the percentage to control value (100%).

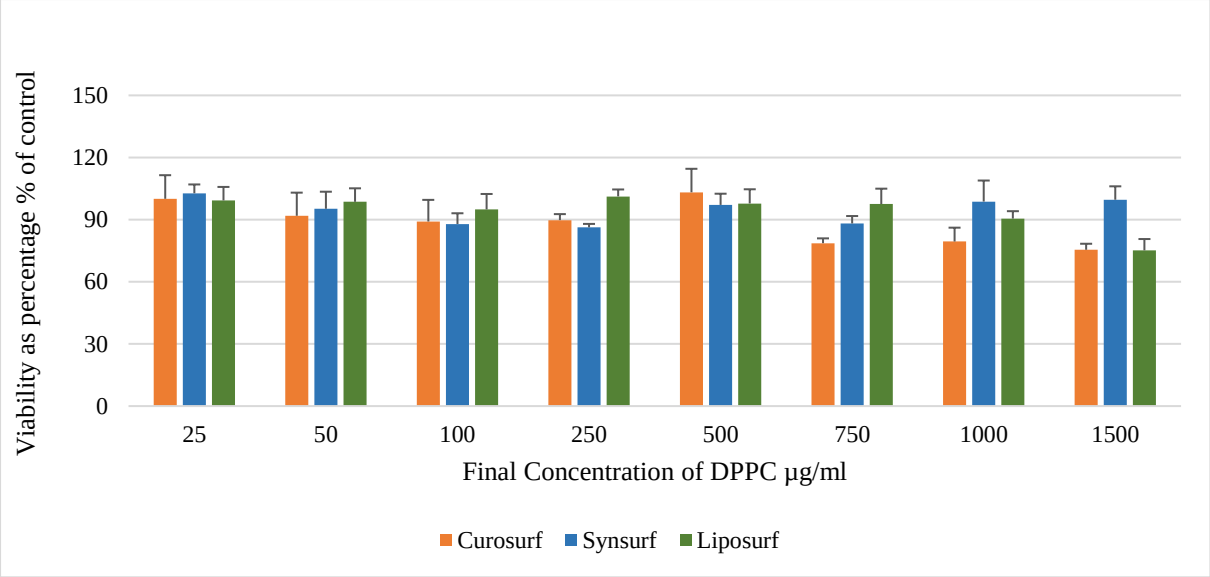

Figure 2.2: The effect of Curosurf®, Synsurf® and Liposurf® on NR8383 cell viability *in vitro*. MTT assay was performed to evaluate the cytotoxic effect of varying surfactants at comparable DPPC concentrations in comparison to untreated NR8383 cells for a 1 h exposure time (n=3). Values represent the percentage to control value (100%).

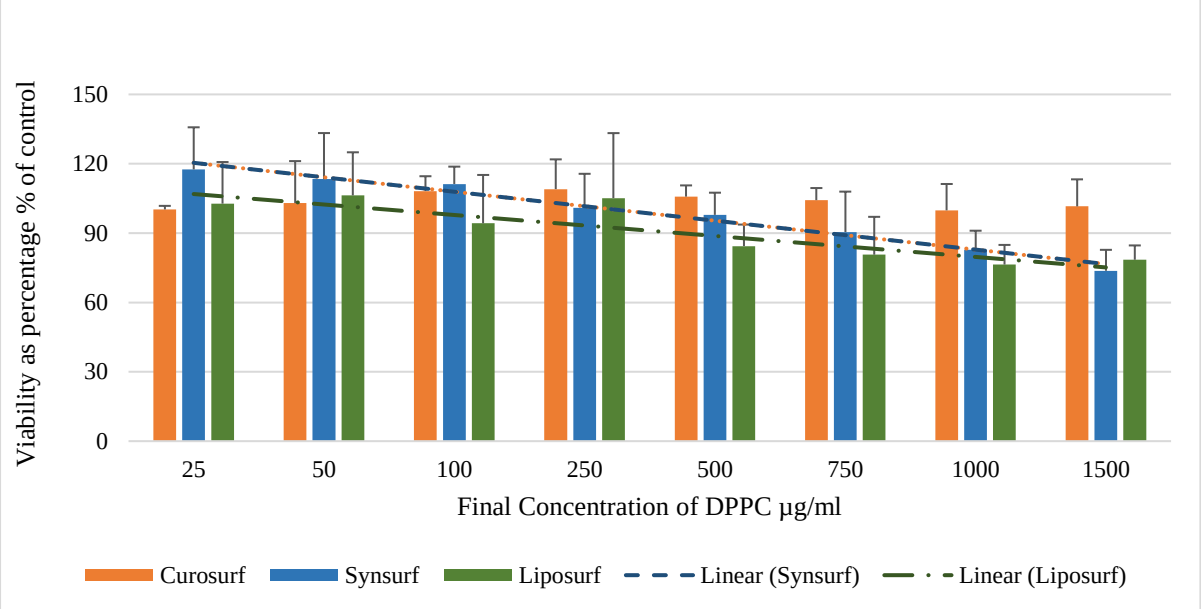

Figure 2.3: The effect of Curosurf®, Synsurf® and Liposurf® on NR8383 cell viability *in vitro*. MTT assay was performed to evaluate the cytotoxic effect of varying surfactants at comparable DPPC concentrations in comparison to untreated NR8383 cells for a 4 h exposure time (n=3). Values represent the percentage to control value (100%) in comparison to control sample.

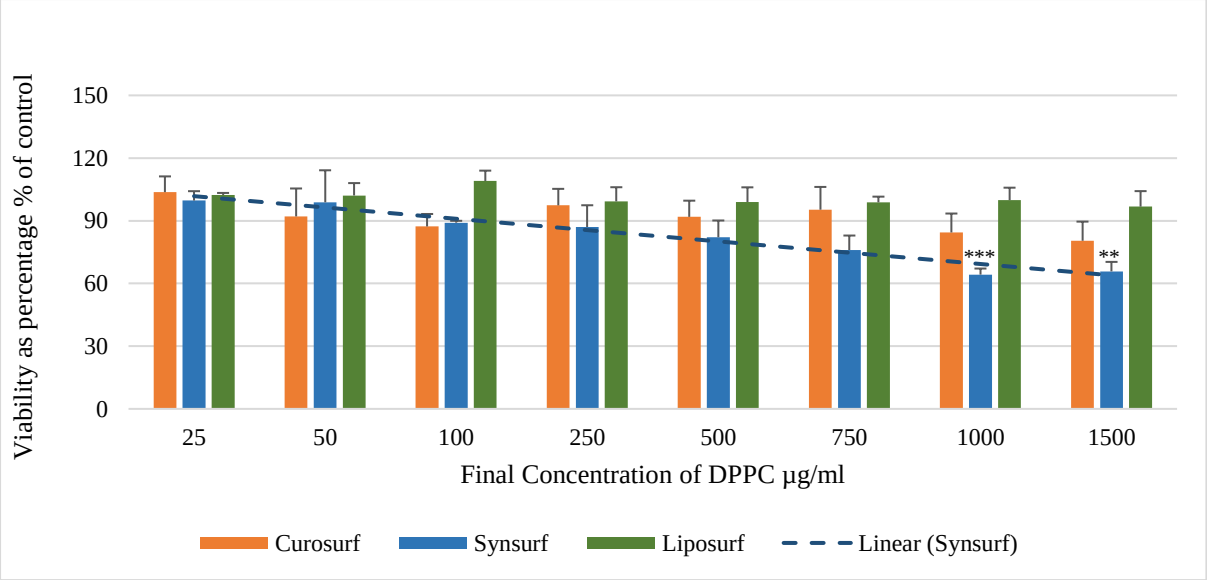

Figure 2.4: The effect of Curosurf®, Synsurf® and Liposurf® on NR8383 cell viability *in vitro*. MTT assay was performed to evaluate the cytotoxic effect of varying surfactants at comparable DPPC concentrations in comparison to untreated NR8383 cells for a 12 h exposure time (n=3). Values represent the percentage to control value (100%) in comparison to control sample. (one-way analysis of variance (ANOVA), Tukey's post-test ** $P \leq 0.01$, *** $P \leq 0.01$

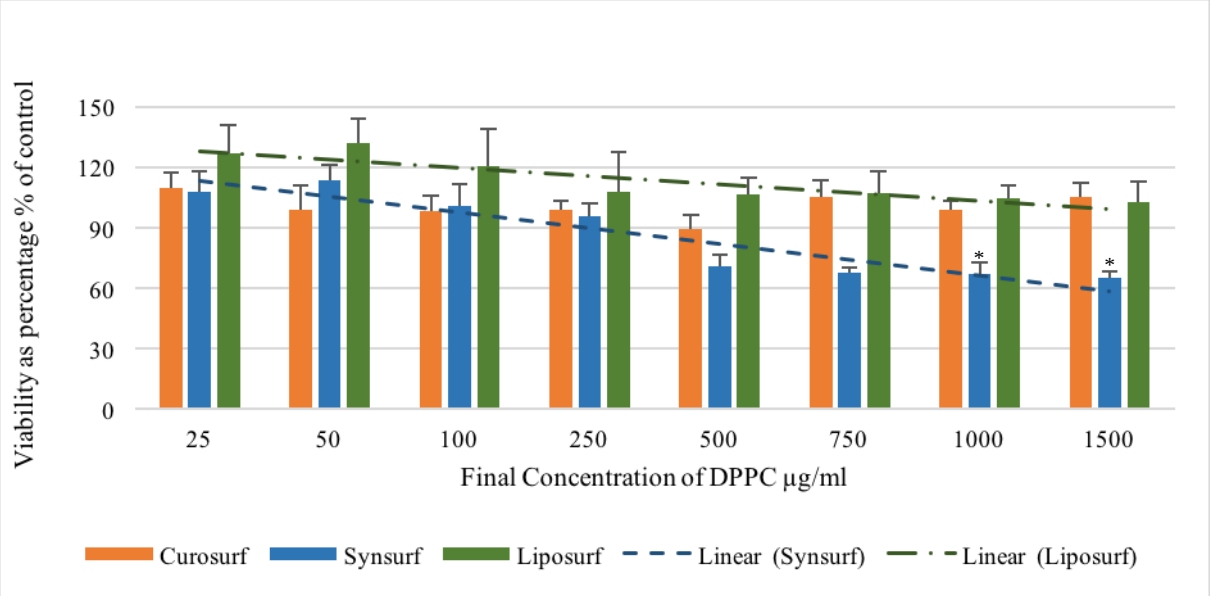

Figure 2.5: The effect of Curosurf®, Synsurf® and Liposurf® on NR8383 cell viability *in vitro*. MTT assay was performed to evaluate the cytotoxic effect of varying surfactants at comparable DPPC concentrations in comparison to untreated NR8383 cells for a 24 h exposure time (n=3). Values represent the percentage to control value (100%) in comparison to control sample. (one-way analysis of variance (ANOVA), Tukey's post-test * $P \leq 0.05$.

A549 Lung Carcinoma

The MTT assay was carried out to determine the dose and time dependent cellular metabolic activity of three pulmonary surfactants: Curosurf®, Synsurf® and Liposurf® to the A549 adenocarcinoma basal epithelial cells. Figures 2.6 - 2.10 show the plots of the cytotoxic response.The results show dose-dependent as well as time (exposure) dependent cytotoxicity of the surfactants. Decrease in cell viability (* $P \leq 0.05$, ** $P \leq 0.01$) by exposure to higher phospholipid concentrations of Curosurf® and Liposurf® were recorded at 1 h (Figure 2.7). Both Synsurf® and Liposurf® displayed a similar trend (not significant) in dose-dependent cytotoxicity at 4 h (Figure 2.8) that was also seen in the NR8383 cell line (Figure 2.3). Synsurf® exhibited the same trend for the 12 h (Figure 2.9) and 24 h (Figure 2.10) exposure time. Significant decrease in cell viability was seen at phospholipid concentrations of 1000 µg/ml (** $P \leq 0.01$) and 1500 µg/ml (*** $P \leq 0.001$) for 12 h and at phospholipid concentrations of 500 µg/ml, 750 µg/ml (*$P < 0.05$), 1000 µg/ml (*** $P \leq 0.001$) and 1500 µg/ml (*** $P \leq 0.001$) for 24h.

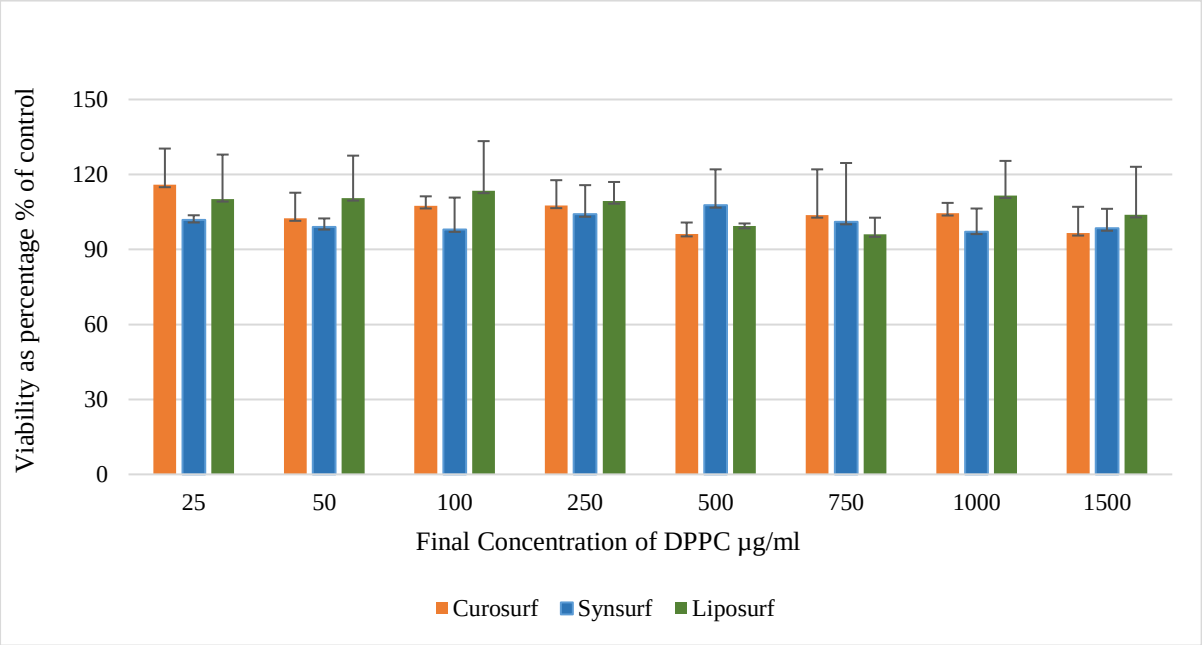

Figure 2.6: The effect of Curosurf®, Synsurf® and Liposurf® on A549 cell viability *in vitro*. MTT assay was performed to evaluate the cytotoxic effect of varying surfactants at comparable DPPC concentrations in comparison to unstimulated A549 cells for a 30 min exposure time (n=3). Values represent the percentage to control value (100%).

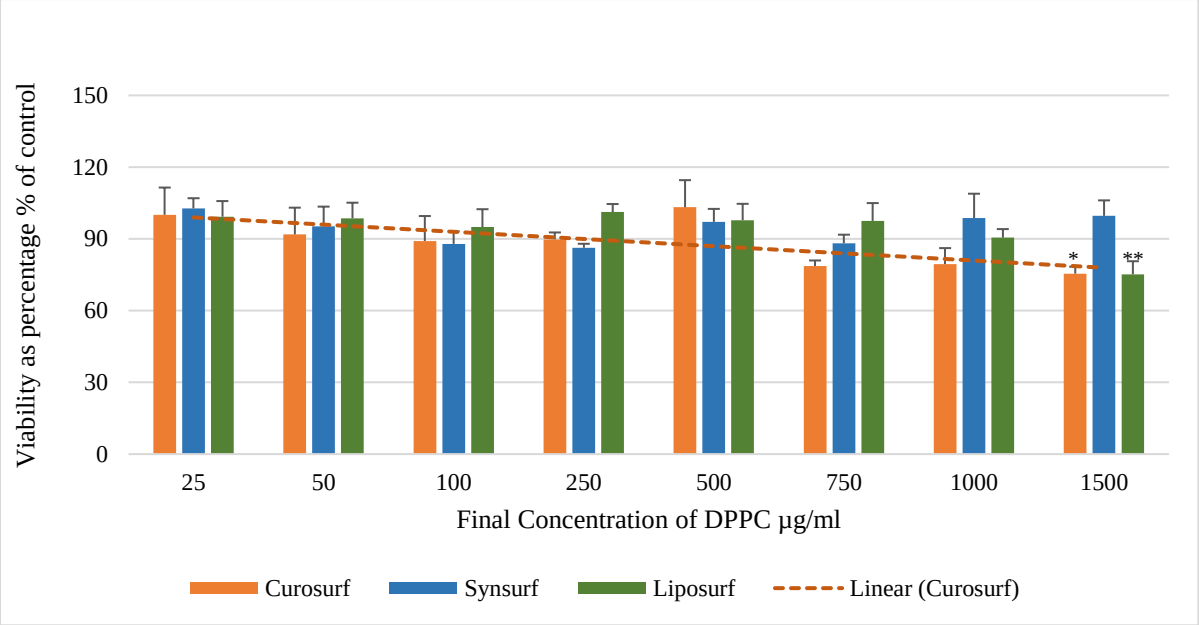

Figure 2.7: The effect of Curosurf®, Synsurf® and Liposurf® on A549 cell viability *in vitro*. MTT assay was performed to evaluate the cytotoxic effect of varying surfactants at comparable DPPC concentrations in comparison to unstimulated A549 cells for a 1 h exposure time (n=3). Values represent the percentage to control value (100%). (one-way analysis of variance (ANOVA), Tukey's post-test * $P \leq 0.05$, ** $P \leq 0.01$ in comparison to the control)

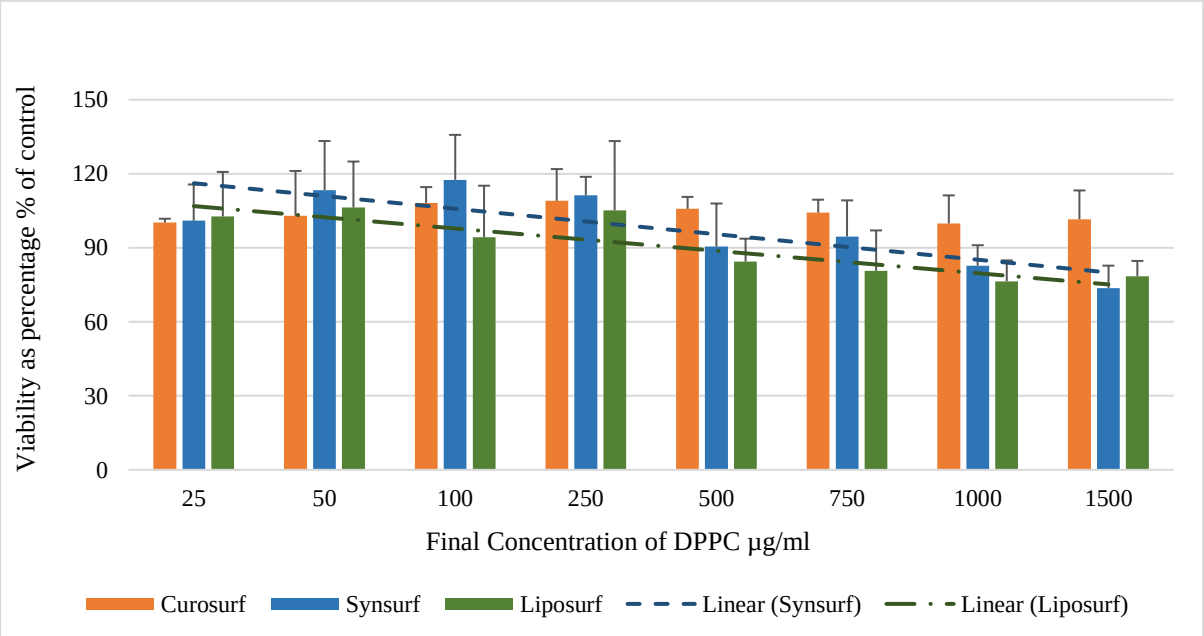

Figure 2.8: The effect of Curosurf®, Synsurf® and Liposurf® on A549 cell viability *in vitro*. MTT assay was performed to evaluate the cytotoxic effect of varying surfactants at comparable DPPC concentrations in comparison to unstimulated A549 cells for a 4 h exposure time (n=3). Values represent the percentage to control value (100%). (one-way analysis of variance (ANOVA), Tukey's post-test).

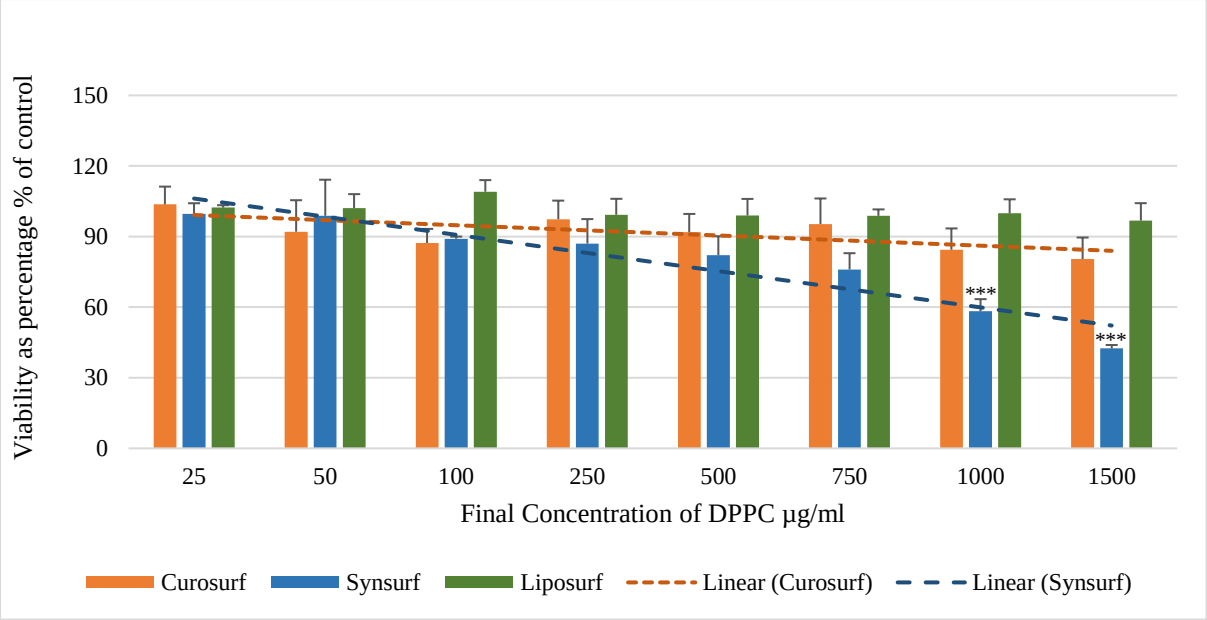

Figure 2.9: The effect of Curosurf®, Synsurf® and Liposurf® on A549 cell viability *in vitro*. MTT assay was performed to evaluate the cytotoxic effect of varying surfactants at comparable DPPC concentrations in comparison to unstimulated A549 cells for a 12 h exposure time (n=3). Values represent the percentage to control value (100%). (one-way analysis of variance (ANOVA), Tukey's post-test, *** $P \leq 0.001$ in comparison to the control).

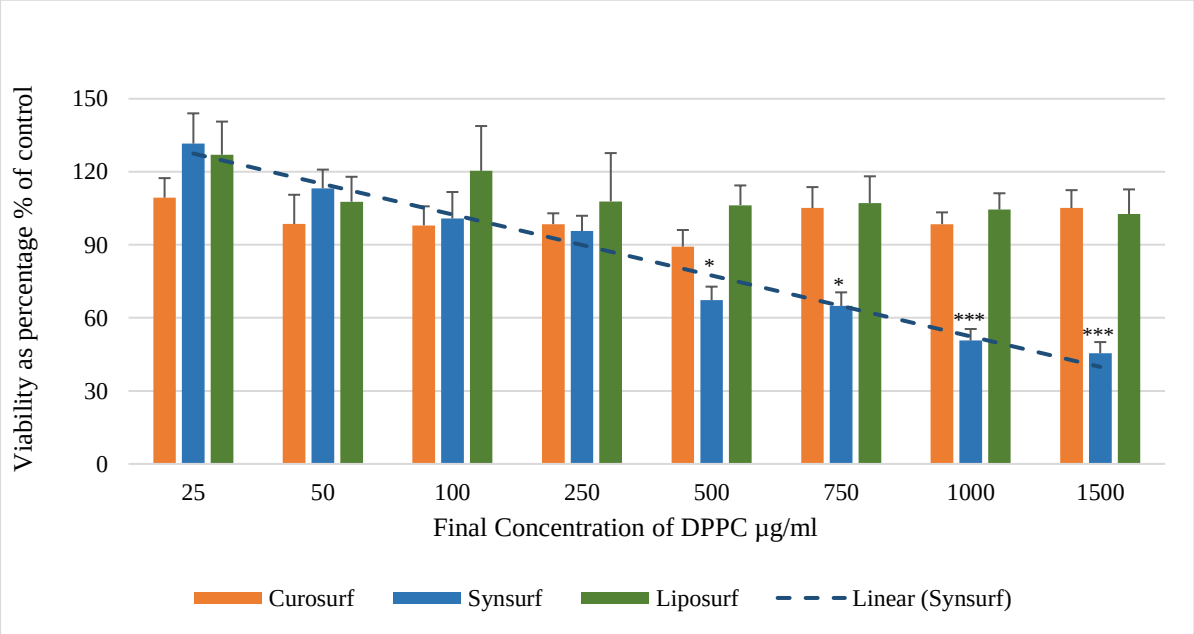

Figure 2.10: The effect of Curosurf®, Synsurf® and Liposurf® on A549 cell viability *in vitro*. MTT assay was performed to evaluate the cytotoxic effect of varying surfactants at comparable DPPC concentrations in comparison to unstimulated A549 cells for a 24 h exposure time (n=3). Values represent the percentage to control value (100%). (one-way analysis of variance (ANOVA), Tukey's post-test * $P \leq 0.05$, *** $P \leq 0.001$ in comparison to the control).

Oxidative Burst

NR8383 Rat Alveolar Macrophages

Both animal derived surfactants significantly decreased basal levels of reactive oxygen intermediates at phospholipid concentrations of 500–1500 µg/ml compared to the un-treated & un-stimulated AMs (Figures 2.11 & 2.12). Curosurf® significantly decreased ($P \leq 0.0001$) ROS production by 90.05 ± 0.45% - 94.75 ± 1.82%, and Liposurf® decreased ($P \leq 0.0001$) ROS production by 89.1 ± 1.20% - 96.16 ± 0.44%. No statistical differences were found among the varying concentrations nor were differences found between the separate surfactants. Synsurf® increased ROS production by 21.6 ± 13.89% at the phospholipid concentration 1500 µg/ml (Figure 2.13) but significantly decreased ($P \leq 0.001$) ROS production by 22.00 ± 3.77% - 80.14 ± 6.30% in a dose-dependent manner at decreasing phospholipid concentration of 750 – 500 µg/ml.

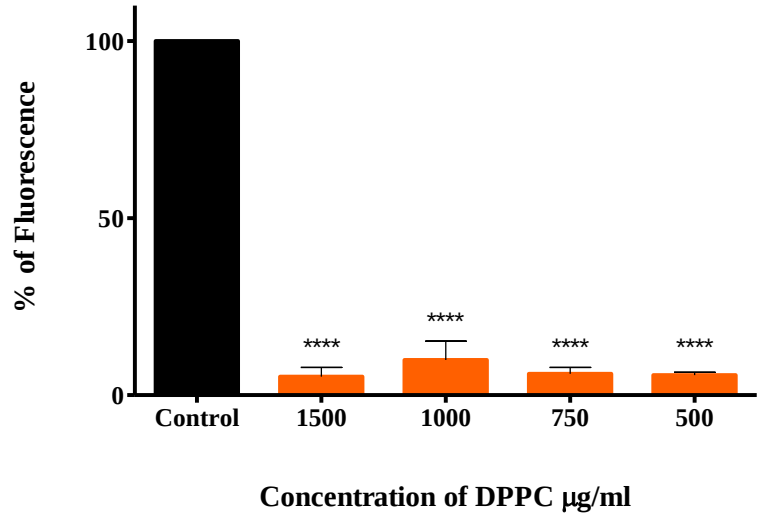

Figure 2.11: The effect of Curosurf®; at 500 – 1500 µg/ml phospholipids on un-stimulated oxidative burst measured by mean channel green fluorescence of DCF-DA. The respective surfactant decreased basal levels of oxidative burst in AMs. Values represent inhibition relative to basal AM fluorescence at 100% vs Control (un-treated & un-stimulated) (n = 5). (one-way analysis of variance (ANOVA), Tukey's post-test **** $P \leq 0.0001$ in comparison to the control).

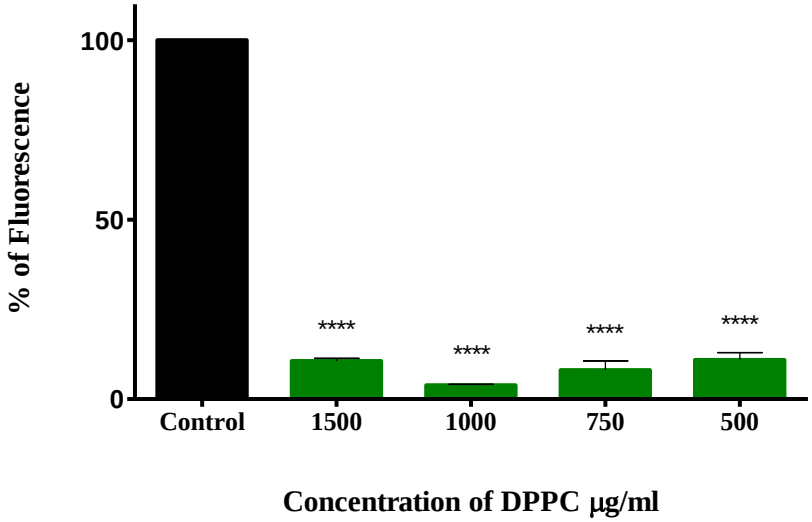

Figure 2.12: The effect of Liposurf®; at 500 – 1500 µg/ml phospholipids on un-stimulated oxidative burst measured by mean channel green fluorescence of DCF-DA. The respective surfactant decreased basal levels of oxidative burst in AMs. Values represent inhibition relative to basal AM fluorescence at 100% vs Control (un-treated & un-stimulated) (n = 5). (one-way analysis of variance (ANOVA), Tukey's post-test **** $P \leq 0.0001$ in comparison to the control).

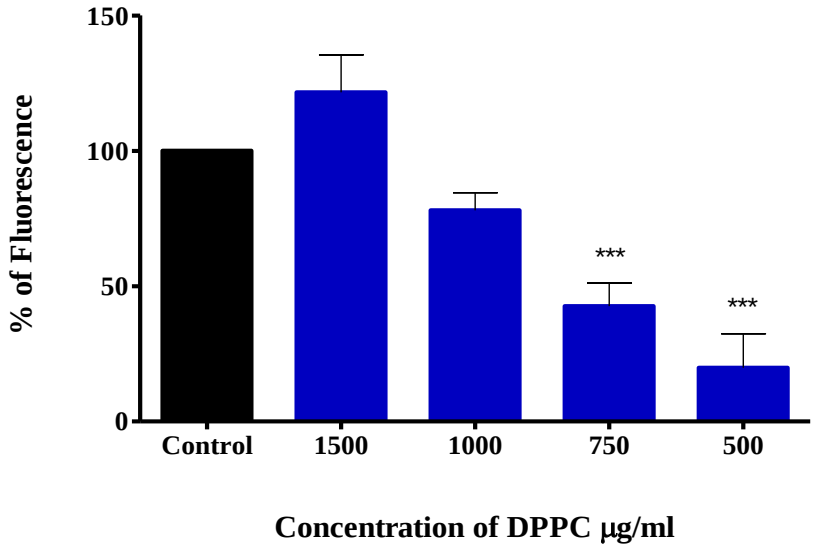

Figure 2.13: The effect of Synsurf®; at 500 – 1500 µg/ml phospholipids on un-stimulated oxidative burst measured by mean channel green fluorescence of DCF-DA. Values represent inhibition relative to basal AM fluorescence at 100% vs Control (un-treated & un-stimulated) (n = 5). (one-way analysis of variance (ANOVA), Tukey's post-test *** $P \leq 0.001$ in comparison to the control).

The animal derived surfactants, Curosurf® and Liposurf®, and the synthetic surfactant (Synsurf®) significantly decreased basal levels of oxidative burst at phospholipid concentration of 500 – 1500 µg/ml compared to the LPS-stimulated AMs (Figures 2.14 – 2.16). Curosurf® (Figure 2.14) significantly decreased ($P \leq 0.0001$) ROS production by 88.53 ± 9.20% - 95.92 ± 0.81%, and Liposurf® (Figure 2.15) decreased ($P \leq 0.0001$) ROS production by 48.17 ± 20.7% - 89.8 ± 0.85% in a dose-dependent manner. No statistical differences among the varying concentrations were found for Curosurf®. However, less inhibition on LPS stimulated ROS production was seen between phospholipid concentrations 1000 µg/ml vs 500 µg/ml for Liposurf® ($P \leq 0.05$). On the other hand, Synsurf® decreased ROS production by 62.43 ± 21.58% - 88.37 ± 055% at phospholipid concentration of 500–1500 µg/ml compared to the LPS-stimulated AMs (Figure 2.16). No statistical differences among the varying concentrations were found thus displaying a threshold effect.

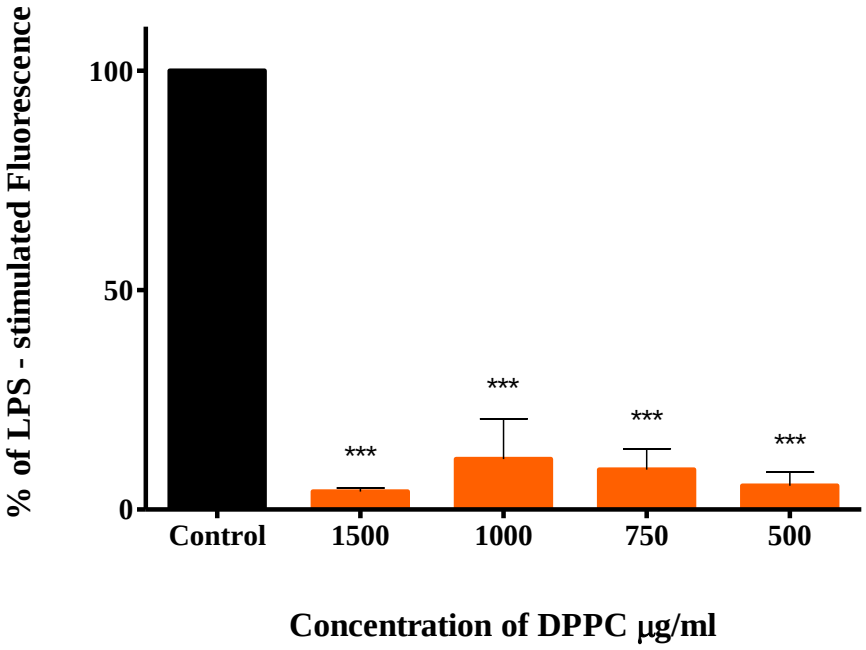

Figure 2.14: The effect of Curosurf® at 500 – 1500 µg/ml phospholipids on LPS-stimulated oxidative burst measured by mean channel green fluorescence of DCF-DA. The respective surfactant decreased LPS levels of oxidative burst. Values represent inhibition relative to LPS-stimulated AM fluorescence at 100%. *** $P \leq 0.001$ vs Control (LPS alone) (n = 3). (one-way analysis of variance (ANOVA), Tukey's post-test *** $P \leq 0.001$ in comparison to the control).

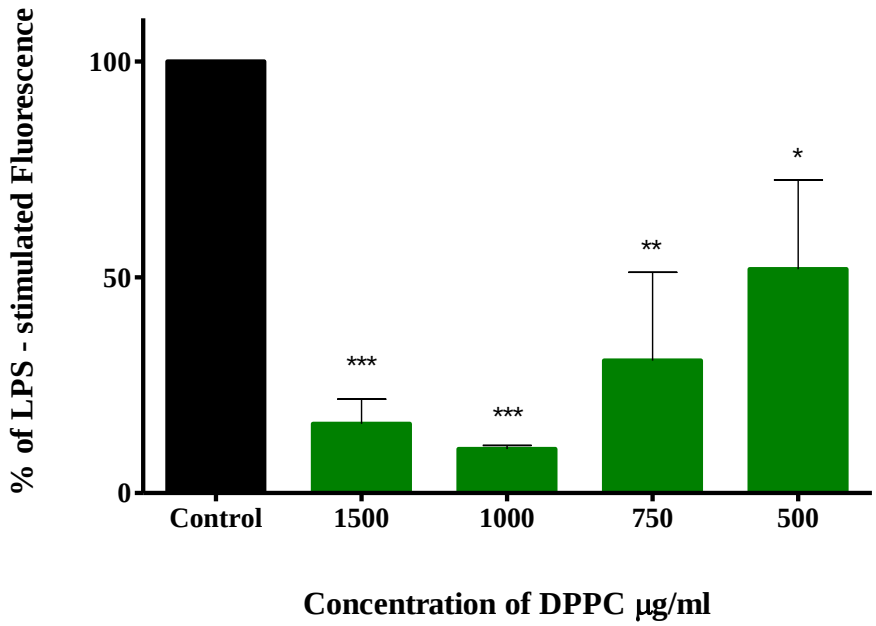

Figure 2.15: The effect of Liposurf® at 500 – 1500 µg/ml phospholipids on LPS-stimulated oxidative burst measured by mean channel green fluorescence of DCF-DA. The respective surfactant decreased LPS levels of oxidative burst. Values represent inhibition relative to LPS-stimulated AM fluorescence at 100%. (one-way analysis of variance (ANOVA), Tukey's post-test * $P \leq 0.05$, ** $P \leq 0.01$, *** $P \leq 0.001$ in comparison to the control (LPS alone) (n = 3).

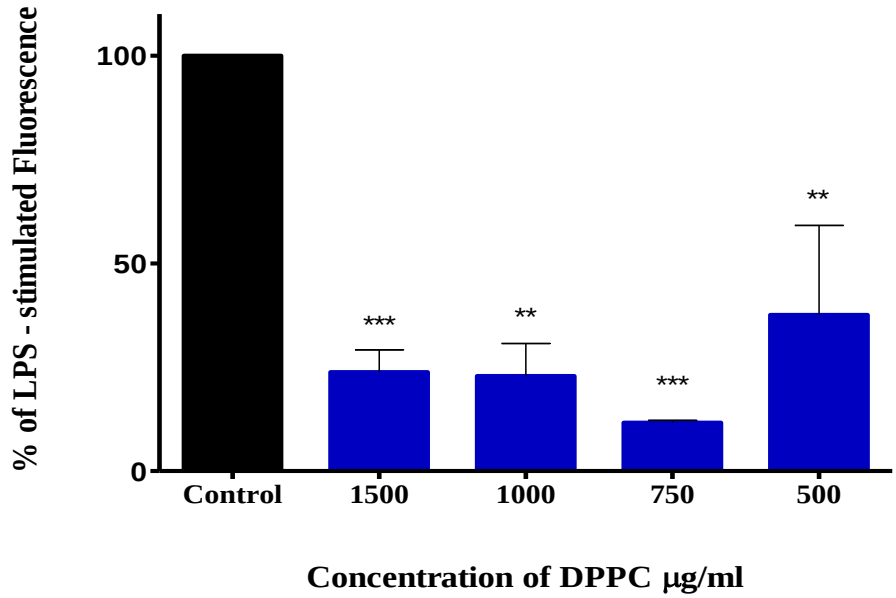

Figure 2.16: The effect of Synsurf® at 500 – 1500 µg/ml phospholipids on LPS-stimulated oxidative burst measured by mean channel green fluorescence of DCF-DA. The respective surfactant decreased LPS levels of oxidative burst. Values represent inhibition relative to LPS-stimulated AM fluorescence at 100%. (one-way analysis of variance (ANOVA), Tukey's post-test ** $P \leq 0.01$,*** $P \leq 0.001$ in comparison to the control (LPS alone) (n = 3).

A549 Lung Carcinoma

All three exogenous surfactants significantly increased basal levels (absence of LPS) of reactive oxygen intermediates at high phospholipid concentrations of 1000 – 1500 µg/ml compared to the un-treated & un-stimulated type II epithelia cells. Curosurf® (Figure 2.17) significantly increased ($P \leq 0.05$) ROS production by 42.14 ± 19.11% at phospholipid concentration of 1500 µg/ml and 55.08 ± 18.16% at phospholipid concentration of 1000 µg/ml ($P \leq 0.01$). Inter-concentration differences were found to statistically significant for 500 µg/ml and 1500 µg/ml ($P \leq 0.001$), 500 µg/ml and1000 µg/ml ($P \leq 0.001$) as well as 500 µg/ml and 750 µg/ml ($P \leq 0.05$). Liposurf® (Figure 2.18) increased ($P \leq 0.01$) ROS production by 49.6 ± 12.16% at phospholipid concentration of 1000 µg/ml and continued that increase to 69.0 ± 2.11% at 750 µg/ml phospholipids ($P \leq 0.001$). Interestingly, at 500 µg/ml phospholipids, ROS significantly decreased by 63.99 ± 10.20% compared to the control ($P \leq 0.001$). Synsurf® (Figure 2.19) increased ($P \leq 0.05$) ROS production by 49.5 ± 14.39% at a phospholipid concentration of 1500 µg/ml and 43.8 ± 16.84% at 1000 µg/ml phospholipids ($P \leq 0.05$) but significantly decreased ($P \leq 0.05$) ROS production by 43.51 ± 9.76% at 500 µg/ml phospholipids compared to the control.

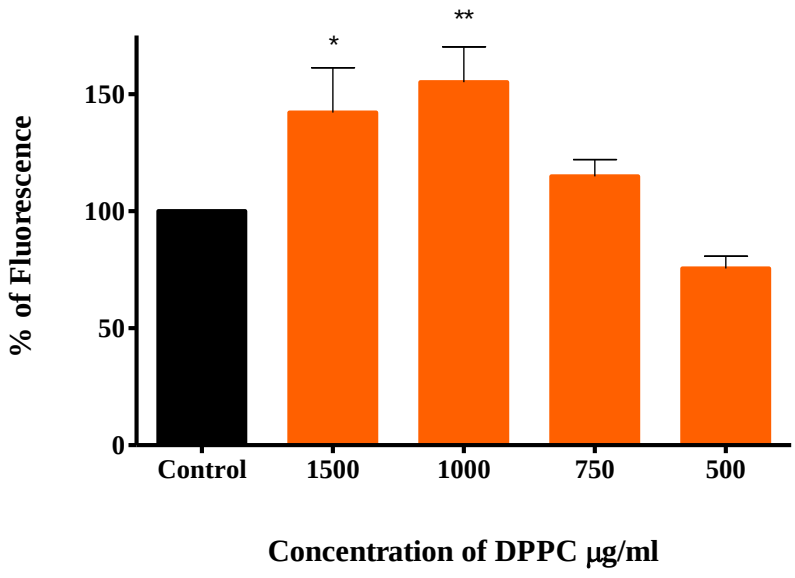

Figure 2.17: The effect of Curosurf® at 500 – 1500 µg/ml phospholipids on un-stimulated oxidative burst measured by mean channel green fluorescence of DCF-DA. Values represent inhibition relative to basal A549 fluorescence at 100%. * $P \leq 0.05$, ** $P \leq 0.01$ vs Control (LPS alone) (n = 3).

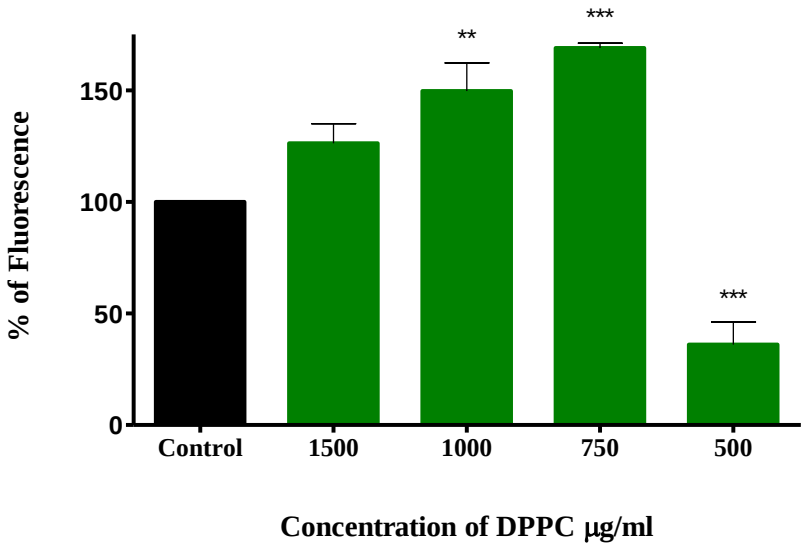

Figure 2.18: The effect of Liposurf® at 500 – 1500 µg/ml phospholipids on un-stimulated oxidative burst measured by mean channel green fluorescence of DCF-DA. Values represent inhibition relative to basal A549 fluorescence at 100%. ** $P \leq 0.01$, *** $P \leq 0.001$ vs Control (LPS alone) (n = 3).

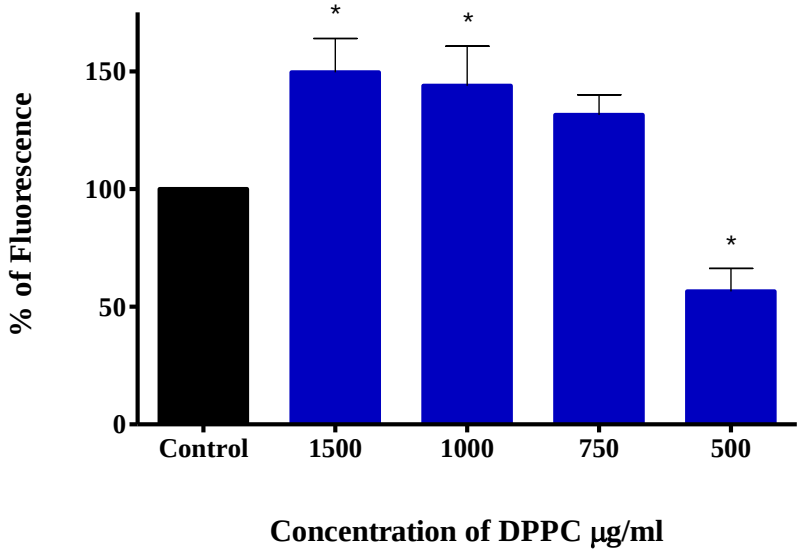

Figure 2.19: The effect of Synsurf®; at 500 – 1500 µg/ml phospholipids on un-stimulated oxidative burst measured by mean channel green fluorescence of DCF-DA. Values represent inhibition relative to basal A549 fluorescence at 100%. * $P \leq 0.05$ vs Control (LPS alone) (n = 3).

Curosurf® (Figure 2.20) and Synsurf® (Figure 2.22) significantly decreased LPS stimulated levels of oxidative burst at a phospholipid concentration 1500 µg/ml by 58.52 ± 5.23 % ($P \leq 0.001$) and 48.05 ± 8.81% ($P \leq 0.01$) respectively compared to the LPS-stimulated type II epithelial cells. The phospholipid concentrations 1000 - 500 µg/ml for both Curosurf® and Synsurf® displayed no effect on LPS stimulated ROS production. On the other hand, Liposurf® decreased ROS production by 41.69 ± 2.58% ($P \leq 0.05$) and 48.63 ± 19.45% ($P \leq 0.05$) respectively at phospholipid concentration of 750 and 500 µg/ml compared to the LPS-stimulated type II epithelial cells (Figure 2.21). No statistical differences were found among the varying concentrations.

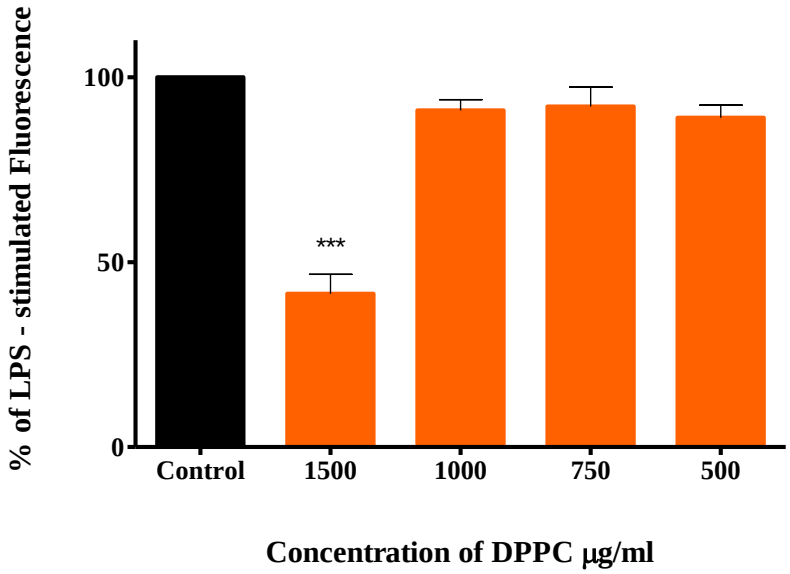

Figure 2.20: The effect of Curosurf® at 500 – 1500 µg/ml phospholipids on LPS-stimulated oxidative burst measured by mean channel green fluorescence of DCF-DA. Values represent inhibition relative to LPS-stimulated A549 fluorescence at 100%. *** $P \leq 0.001$ vs Control (LPS alone) (n = 3).

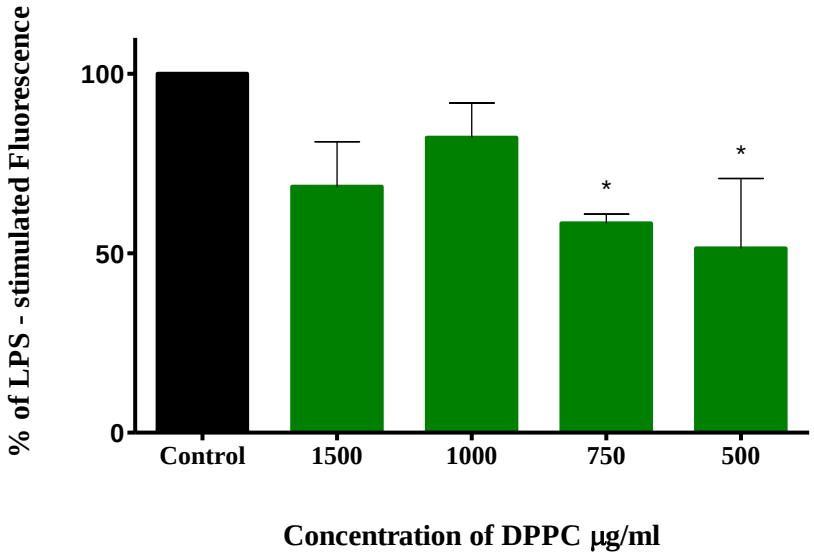

Figure 2.21: The effect of Liposurf® at 500 – 1500 µg/ml phospholipids on LPS-stimulated oxidative burst measured by mean channel green fluorescence of DCF-DA. Values represent inhibition relative to LPS-stimulated A549 fluorescence at 100%. * $P \leq 0.05$ vs Control (LPS alone) (n = 3).

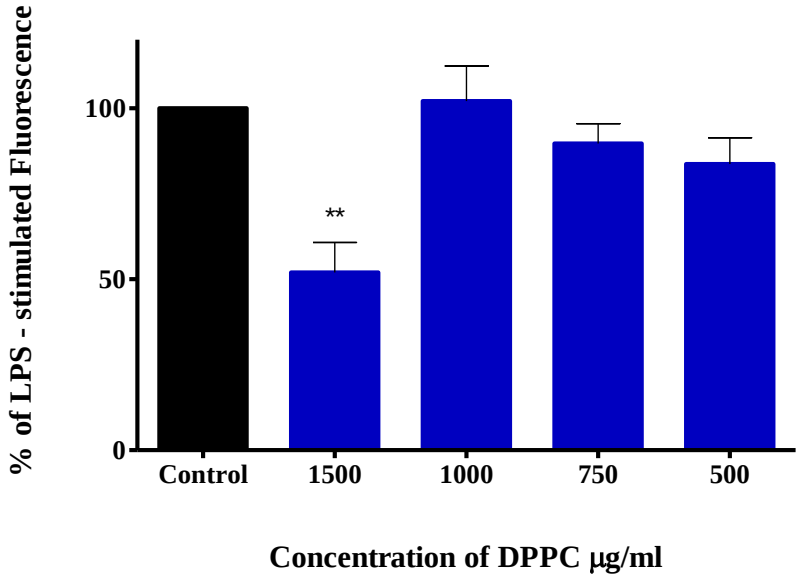

Figure 2.22: The effect of Synsurf® at 500 – 1500 µg/ml phospholipids on LPS-stimulated oxidative burst measured by mean channel green fluorescence of DCF-DA. Values represent inhibition relative to LPS-stimulated A549 fluorescence at 100%. ** $P \leq 0.01$ vs Control (LPS alone) (n = 3).

Correlations

To determine whether the oxidative damage from intracellular ROS production is correlated with cell viability, Pearson's nonparametric correlation was performed (Table 2.1) for the three surfactants at their respective phospholipid concentrations (500 – 1500 µg/ml) following the 24h time exposure.

Graphs were also plotted to correlate the observed increases in the percentages of cells containing high intracellular ROS levels and viable cell percentages. Synsurf® displayed a strong negative relationship between intracellular ROS levels and viable cell percentages for the NR8383 alveolar macrophages. A moderate positive linear relationship was found for Curosurf® in the A549 cell line whereas Synsurf® displayed a strong negative linear relationship between intracellular ROS levels and viable cell percentages.

Table 2.1: Table showing Pearson's Correlation Coefficient between percentage ROS production and percentage cell viability in all three surfactants in both cell lines (unstimulated) at 24h. *r*, correlation coefficient; r^2, squared correlation coefficient; significant correlation established at $P \leq 0.05$.

NR8383	**[*r*]**	**[r^2]**	**Description**	***P* value**
Curosurf®	-0.091	0.008	Weak negative linear relationship	*0.909*
Liposurf®	0.068	0.005	Weak Positive linear relationship	*0.932*
Synsurf®	-0.925	0.856	Strong negative linear relationship	*0.075*
A549				
Curosurf®	0.653	0.426	Moderate positive linear relationship	*0.347*
Liposurf®	-0.102	0.011	Weak negative linear relationship	*0.898*
Synsurf®	-0.761	0.579	Strong negative linear relationship	*0.240*

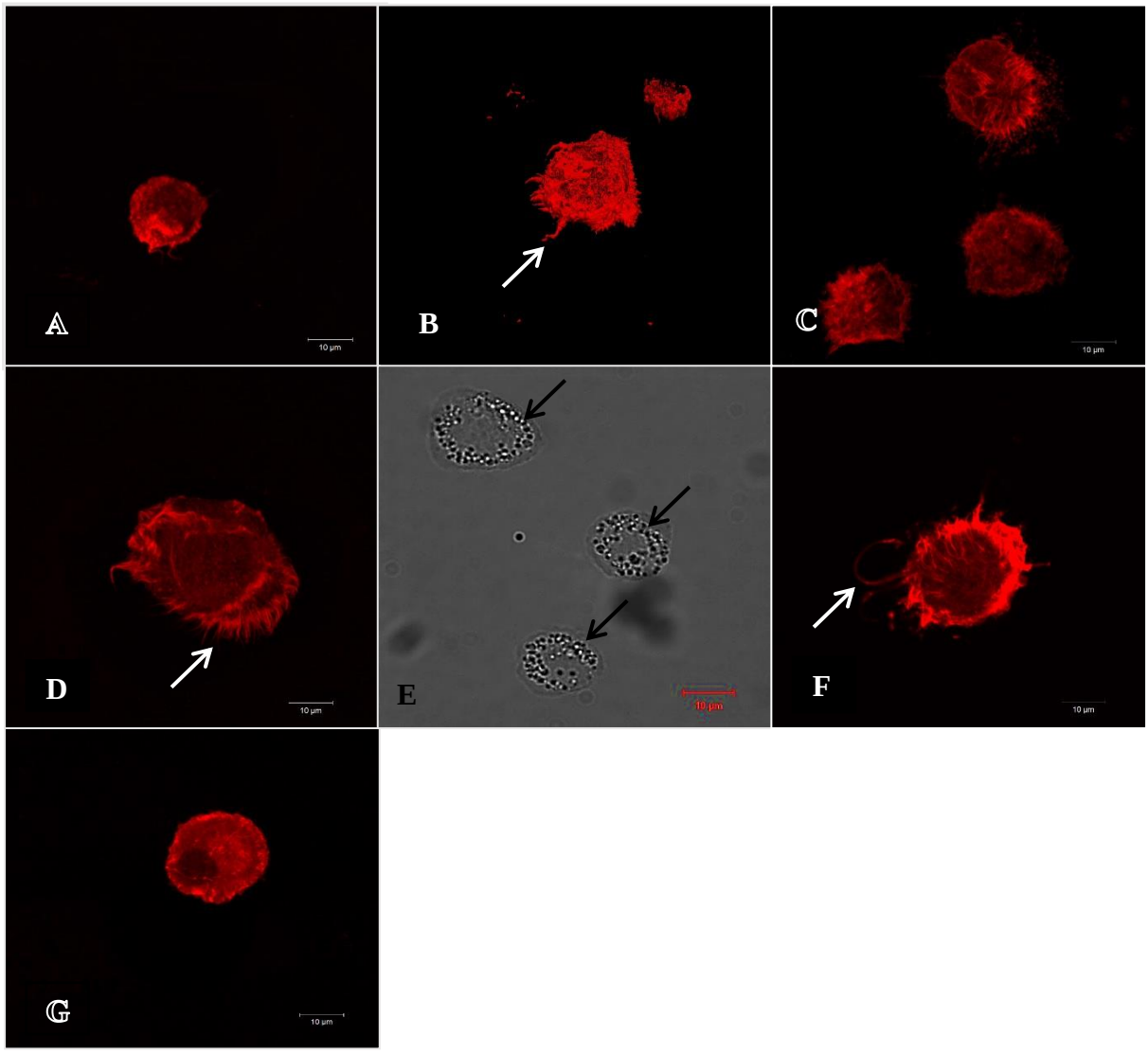

Figure 2.23: Stimulation of Actin Structure Formation and Polymerisation in LPS stimulated Rat Alveolar Macrophage **(A)** Control (**B)** 1 µg/ml LPS Stimulated **(C)&(G)** Synsurf® 1500 µg/ml, 24H **(D)** Curosurf® 1500 µg/ml, 24H **(E)** Curosurf® 1500 µg/ml, 24H Phase-Contrast **(F)** Liposurf® 1500 µg/ml, 24H

In a qualitative visual assay in which deviations from the untreated state were screened, animal derived surfactants stimulated the formation of actin filled structures in a manner similar to that of the LPS stimulated macrophages. In this assay, the large majority of untreated macrophages showed only cortical staining for F-actin with little, or no, actin-filled cellular processes such as filopodia/lamellopodia (Figure 2.23A). Treatment with 1 µg/ml LPS, alveolar macrophages were stimulated to polymerise actin with filopodia emanating from one side of the cell and actin-associated membrane ruffling on the other side around a flattened lamellopodia (Figure 2.23B). On the other hand, Synsurf® treated macrophages (Figure 2.23C) were absent of any

actin polymerisation and displayed similar cortical staining to that of the untreated macrophages. At the same concentration, Curosurf® and Liposurf® treated macrophages responded with non-directional formation of many short actin filled filopodia. Liposurf® (Figure 2.23F) stimulated some long, actin-filled filopodia compared to that of Curosurf®. Furthermore, Curosurf® stimulated these non-directional actin-filled filopodia from the broad non-directional lamellopodia surrounding the cell and presents vacuole formation similar to that of autophagosomes.

2.4 Discussion

Short-term MTTs are metabolic assays that measure the viability of a cell population relative to the control, untreated cells, but do not provide direct information about total cell numbers. Cells are treated with particulates for a predetermined period of time after which soluble yellow tetrazolium salts are added (3-(4, 5-dimethylthiazol-2- yl)-2, 5-diphenyltetrazolium bromide) for 2h at 37°C. During this process, viable cells with active respiratory mitochondrial activity bio-reduce MTT into an insoluble purple formazan product via mitochondrial succinic dehydrogenases. Formazan was subsequently solubilised with a detergent and quantified with a visible light spectrophotometer. Data is presented as optical density (OD)/control group (Hillegass, Shukla et al. 2010). To determine the *in vitro* effects of concentration and exposure-time of surfactant on the viability of cells that exist in the human pulmonary system (A549 and NR8383 cells), cell proliferation and cell viability was determined. The MTT assay of A549 and NR8383 cells revealed that when exposed to certain surfactants at higher phospholipid concentrations for 12h and 24h (Figure 2.4 - Figure 2.5 and Figure 2.9 - Figure 2.10), there was a decrease in cell growth. Our findings show Synsurf® dose dependently inhibited the NR8383 and the A549 cell growth compared to the control cells. The morphological changes in the NR8383 cells did not indicate clear apoptotic bodies for Synsurf®, however, the Curosurf® group did show clear cytoplasmic vesicles (Figure 2.23E) despite having decreased intracellular ROS production and comparative cell viability to the control group, thus indicating that a ROS-independent pathway may be involved (Ray, Huang et al. 2012). After the 4h time exposure, both Synsurf® and Liposurf® resulted in 73.71 ± 9.05% and 78.48 ± 6.20% viability in the NR8383 cell line respectively. However, only Synsurf® at the highest phospholipid concentration of 1500 µg/ml carried on with the same pattern of cell viability for the 12h (65.79 ± 4.5%) and 24h (64.75 ± 3.59%) time exposure. For the A549 cell line, Synsurf® prevented colony formation thus indicating a potential surfactant induced cellular modulation. This finding is linked to the observed increased presence of intracellular ROS. ROS are universal and pleiotropic signalling molecules implicated in the pathogenesis of disease states (Ray, Huang et al. 2012), whilst in physiological states, ROS is normally detected at low levels, required for normal cellular function (Stowe, Camara 2009). ROS is also a common role player in the pathogeneses of a variety of lung disorders such as asthma, COPD, pulmonary fibrosis and cancer (Domej, Oettl et al. 2014).

Our results revealed a decrease in cell viability percentage as the dose of Synsurf® increased. This may suggest that the compounds (phospholipids and polymers of poly-L-lysine bonded electrostatically with poly-L-glutamic acid) may exhibit good interaction with the cellular membranes due to their surface activity. These mechanisms could include interference with enzyme balance, interference with the osmotic balance due to charge density and cationic peptide complex or increase cell membrane permeability (Badawi, Ismail et al. 2015).

Another theory to consider is the cellular uptake of surfactants. Modified surfactant protein uptake, processing and metabolism may result in a low level increase of mitochondrial activity (5 - 10%) in cells exposed to certain surfactants compared to the control as seen in the MTT study. It could also be possible that surfactant components therefore inhibit or block signal transduction, resulting in a transient or 'permanent' switch-off of mitochondrial activity related to surfactant dosage.

It has been observed that apoptotic cell death can occur via a number of pathways in cells via the extrinsic and intrinsic pathways (Elmore 2007). The data suggests that DPPC may influence cellular death pathways as demonstrated by the induction of oxidative stress. The observation that DPPC leads to ROS generation in A549 cells suggests a possible switching from a ROS independent pathway as described by Chairuangkitti and colleagues (2013), causing cell cycle arrest (autophagy) to a ROS dependent pathway culminating in apoptotic cell death (Chairuangkitti, Lawanprasert et al. 2013). It has also been proposed that a two-tiered mechanism of NR8383 cell death, cell cycle arrest and ROS mediated mitochondrial dependant cell death is involved. Previous studies suggest that autophagy protects cells from caspase-independent death that occurs after Mitochondrial Outer Membrane Permeabilisation (MOMP) in the presence of caspase inhibitors (or in this case, DPPC as a permeabilising agent). Interestingly this study showed that as long as cellular respiration can still be generated (in this case by increased glycolysis caused by elevated GAPDH), cells can use autophagy to survive MOMP and the release of cytochrome c and other apoptogenic proteins and recover to continue to grow (Colell, Ricci et al. 2007, Thorburn 2008). Thus, increased levels of autophagy can protect cells from apoptosis and this kind of caspase-independent death. One can therefore speculate that Synsurf® may function via the mitochondrial/caspase pathway due to the decrease in mitochondrial activity in the NR8383. However, Curosurf® may elicit an autophagy pathway as the mitochondrial activity is preserved but rather the presence of

autophagosomes (and not apoptotic bodies) indicate the degradation of organelles. The characterisation of cellular morphology is thus a key to distinguish the associations between the types of cell death. Apoptosis is usually due to caspase cleavage of cytoskeletal and other structural proteins; however, during autophagic cell death the cytoskeleton remains intact and is associated with accumulation of large numbers of autophagic vesicles (degraded organelles). It is therefore not surprising that there would be close connections between the regulatory mechanisms that control autophagy and apoptosis (Galluzzi, Maiuri et al. 2007, Thorburn 2008). Unfortunately, autophagy can also lead to cell death if cellular degradation remains unchecked. Further mechanistic studies are required to determine conclusively if DPPC and/or surfactant protein interactions influence pathway switching. The data further suggests that the onset of cytotoxicity, or rather cellular proliferation cessation, correlates with the activation of two intracellular stress-signalling pathways.

2.5 References

BADAWI, A.M., ISMAIL, D.A., AHMED, S., MOHAMAD, A., DARDIR, M., MOHAMED, D.E., IBRAHEM, A., MANSOUR, N.A. and ASHMAWY, A., 2015. Role of Surfactants in Regulation of Cancer Growth. In: V. GANDHI, K. MEHTA, R. GROVER, S. PATHAK and B.B. AGGARWAL, eds, *Multi-Targeted Approach to Treatment of Cancer*. Cham: Springer International Publishing, pp. 137-149.

CHAIRUANGKITTI, P., LAWANPRASERT, S., ROYTRAKUL, S., AUEVIRIYAVIT, S., PHUMMIRATCH, D., KULTHONG, K., CHANVORACHOTE, P. and MANIRATANACHOTE, R., 2013. Silver nanoparticles induce toxicity in A549 cells via ROS-dependent and ROS-independent pathways. *Toxicology in Vitro,* **27**(1), pp. 330-338.

CHEN, N.Y., LAI, H.H., HSU, T.H., LIN, F.Y., CHEN, J.Z. and LO, H.C., 2008. Induction of apoptosis in human lung carcinoma A549 epithelial cells with an ethanol extract of *Tremella mesenterica*. *Bioscience, Biotechnology, and Biochemistry*, **72**(5), pp. 1283-1289.

COLELL, A., RICCI, J.E., TAIT, S., MILASTA, S., MAURER, U., BOUCHIER-HAYES, L., FITZGERALD, P., GUIO-CARRION, A., WATERHOUSE, N.J., LI, C.W. and MARI, B., 2007. GAPDH and autophagy preserve survival after apoptotic cytochrome c release in the absence of caspase activation. *Cell,* **129**(5), pp. 983-997.

DOMEJ, W., OETTL, K. and RENNER, W., 2014. Oxidative stress and free radicals in COPD–implications and relevance for treatment. *International Journal of Chronic Obstructive Pulmonary disease,* **9**, pp. 1207.

ELMORE, S., 2007. Apoptosis: a review of programmed cell death. *Toxicologic Pathology*, **35**(4), pp. 495-516.

FAN, T.J., HAN, L.H., CONG, R.S. and LIANG, J., 2005. Caspase family proteases and apoptosis. *Acta Biochimica et Biophysica Sinica*, **37**, pp. 719-727.

GALLUZZI, L., MAIURI, M.C., VITALE, I., ZISCHKA, H., CASTEDO, M., ZITVOGEL, L. and KROEMER, G., 2007. Cell death modalities: classification and pathophysiological implications. *Cell Death and Differentiation,* **14**(7), pp. 1237-1243.

HERZOG, E., BYRNE, H.J., DAVOREN, M., CASEY, A., DUSCHL, A. and OOSTINGH, G.J., 2009. Dispersion medium modulates oxidative stress response of human lung epithelial cells upon exposure to carbon nanomaterial samples. *Toxicology and Applied Pharmacology,* **236**(3), pp. 276-281.

HILLEGASS, J.M., SHUKLA, A., LATHROP, S.A., MACPHERSON, M.B., FUKAGAWA, N.K. and MOSSMAN, B.T., 2010. Assessing nanotoxicity in cells in vitro. *Wiley Interdisciplinary Reviews: Nanomedicine and Nanobiotechnology,* **2**(3), pp. 219-231.

RAY, P.D., HUANG, B.W. and TSUJI, Y., 2012. Reactive oxygen species (ROS) homeostasis and redox regulation in cellular signalling. *Cellular Signalling,* **24**(5), pp. 981-990.

STOWE, D.F. and CAMARA, A.K., 2009. Mitochondrial reactive oxygen species production in excitable cells: modulators of mitochondrial and cell function. *Antioxidants & Redox Signalling,* **11**(6), pp. 1373-1414.

THORBURN, A., 2008. Apoptosis and autophagy: regulatory connections between two supposedly different processes. *Apoptosis,* **13**(1), pp. 1-9.

WALLACE, W., KEANE, M., MURRAY, D., CHISHOLM, W., MAYNARD, A. and ONG, T.M., 2007. Phospholipid lung surfactant and nanoparticle surface toxicity: lessons from diesel soots and silicate dusts. *Nanotechnology and Occupational Health,* pp. 23-38.

3 CHAPTER 3: Immunoactive properties of Synsurf®, Curosurf® and Liposurf®

3.1 Introduction

Alveolar Macrophages (AMs) are the key modulators and effector cells in the pulmonary immune response. Their activation influences and creates a cascade response to other divisions of the immune system (Martinez, Gordon 2014). It is essential for AMs to respond efficiently to a broad range of insults. This requirement places a high burden of responsibility on these cells to recognise and respond appropriately to these triggers as to ensure appropriate pro-inflammatory and anti-inflammatory responses (Yamashita, Veldhuizen et al. 2013).

More than 90% of cells lining the alveolar region are AMs. Human lungs are estimated to contain 2.3×10^{10} AMs at a cell density of 17×10^{3} cells/ml in the lower respiratory tract (50 to 100 AMs per alveolus), which places them in a unique sentry position against inhaled environmental antigens. They secrete all the main inflammatory cytokines (IL-1β, TNF-α, IL-6, IL-8 and IL-12) as well as other mediators and chemokines of the pulmonary inflammatory response (IL-2, IFN-γ and GM-CSF) (see Chapter 1 section 4: page 24) (García, Rodriguez et al. 1999, Nakata, Gotoh et al. 1999).

More importantly, macrophages can develop mixed M1/M2 phenotypes (see Figure 3.1) in pathological conditions. Depending on the microenvironment, macrophages can polarise to M1 (inflammatory) or M2 (anti-inflammatory) phenotypes (Helmke, German et al. 1989). This heterogeneity is reflective of the plasticity and versatility of these cells in response to micro-environmental signal exposure. This characteristic makes macrophages key role players in polarised innate and adaptive responses and they do so by orientating adaptive responses in a M1 or M2 direction by expressing specialised and polarised effector functions (Mantovani, Sica et al. 2004). M1 and M2 signatures do not necessarily exclude each other and often coexist in a continuum. Cytokines, chemokines as well as the microenvironment and other immunoregulatory cells, interplay and the resultant mixed phenotype depends on the delicate balance of these activatory and inhibitory activities (Helmke, German et al. 1989).

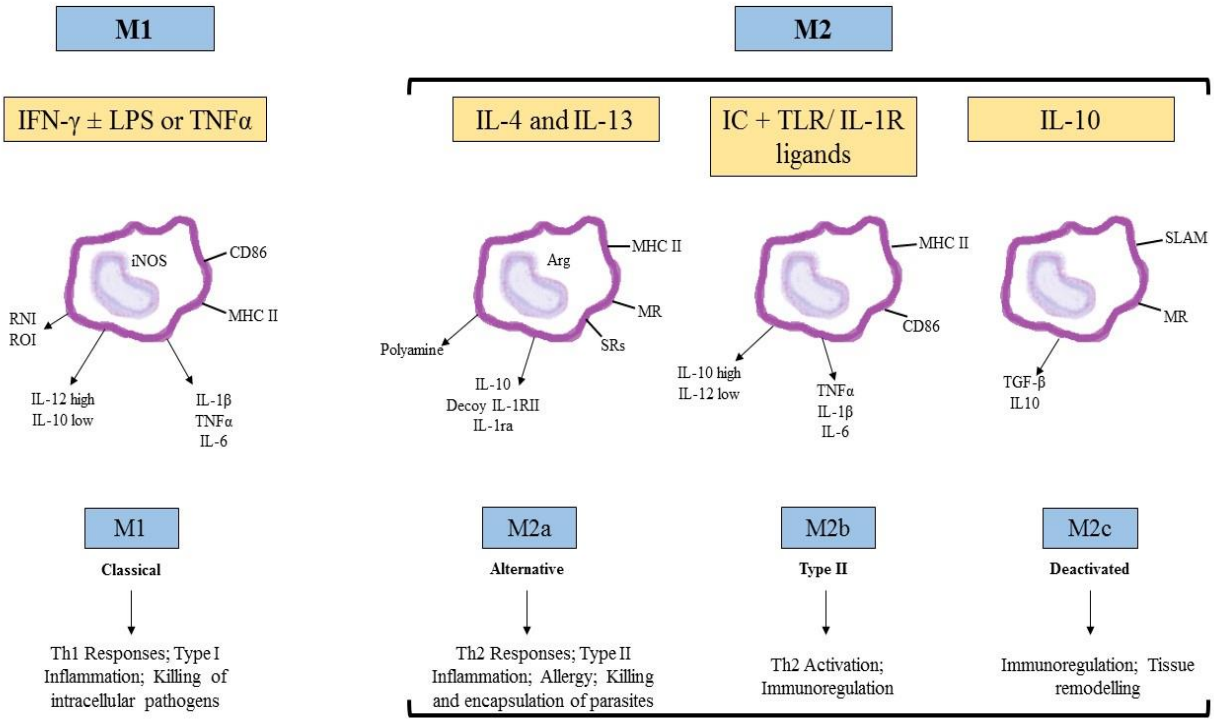

Figure 3.1: A proposed M1-M2 macrophage model, in which M1 included interferon-gamma (IFN-γ) + lipopolysaccharide (LPS) or tumour necrosis factor alpha (TNFα) and M2 was subdivided to accommodate similarities and differences between interleukin-4 (IL-4) (M2a), immune complex + Toll-like receptor (TLR) ligands (M2b), and IL-10 and glucocorticoids (M2c) (Adapted from (Mantovani, Sica et al. 2004)).

Classically M1 macrophages (see Figure 3.2) produce inducible nitric oxide synthase (iNOS) or nitric oxide (NO) as well as reactive oxygen intermediates (ROI) (e.g. ROS) due to arginine metabolism. The alternatively activated M2 macrophages (see Figure 3.3), which are divided further into groups – M2a, M2b and M2c macrophages, are arginase pathway dominant (except M2b) and produce abundant levels of non-opsonic receptors (e.g. the mannose receptor) (Mantovani, Sica et al. 2004).

Furthermore, differential cytokine production is a key feature of M1/M2 macrophages. Since M1/M2 macrophages are found in a continuum state; the M1 phenotype is typically portrayed as exhibiting a IL-12^{high} and IL-10^{low} ratio, whereas M2 macrophages are typically IL-10^{high} and IL-12^{low} ratio. M2 macrophages are generally characterised by low production of pro-inflammatory cytokines (IL-1β, TNFα and IL-6). However, LPS stimulated M2b macrophages are an exception, in that they retain high levels of inflammatory cytokine production with associated high levels of IL-10 and low IL-12 (Mosser 2003). In mice, it was seen that in spite

of their high production of inflammatory cytokines, the M2b macrophages protect mice against LPS toxicity (Mosser 1999).

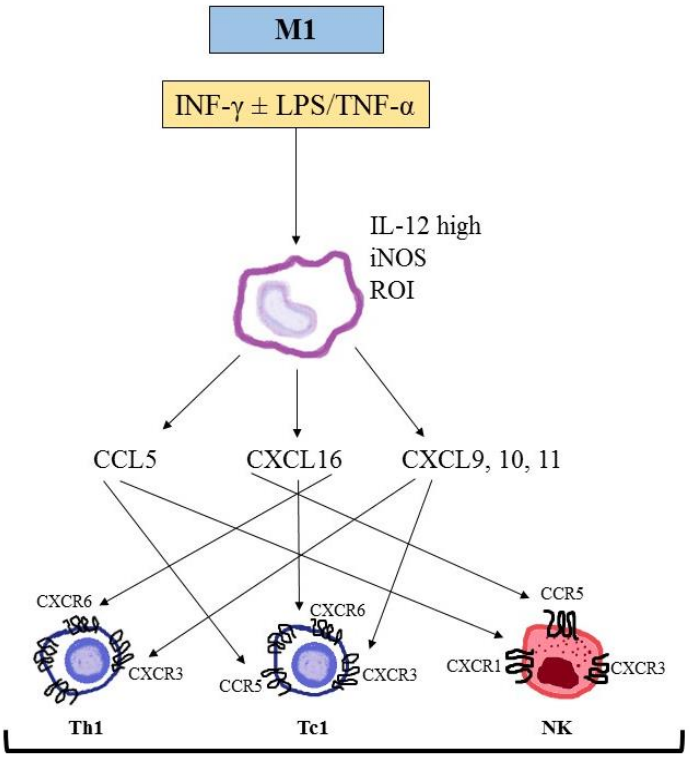

Figure 3.2: The chemokine repertoires of polarised M1 macrophages. M1 polarisation is accompanied by production of inflammatory CC chemokines and IFN-γ-responsive chemokines that recruit Th1, Tc1 and NK cells, and coordinate a type I immune response particularly suited for intracellular pathogen killing. **Abbreviations: IFN-γ**, interferon-γ; **iNOS**, inducible nitric oxide synthase; **NK**, natural killer cells; **ROI**, reactive oxygen intermediates; **Th1**, Type 1 T helper cells (adapted from (Mantovani, Sica et al. 2004)).

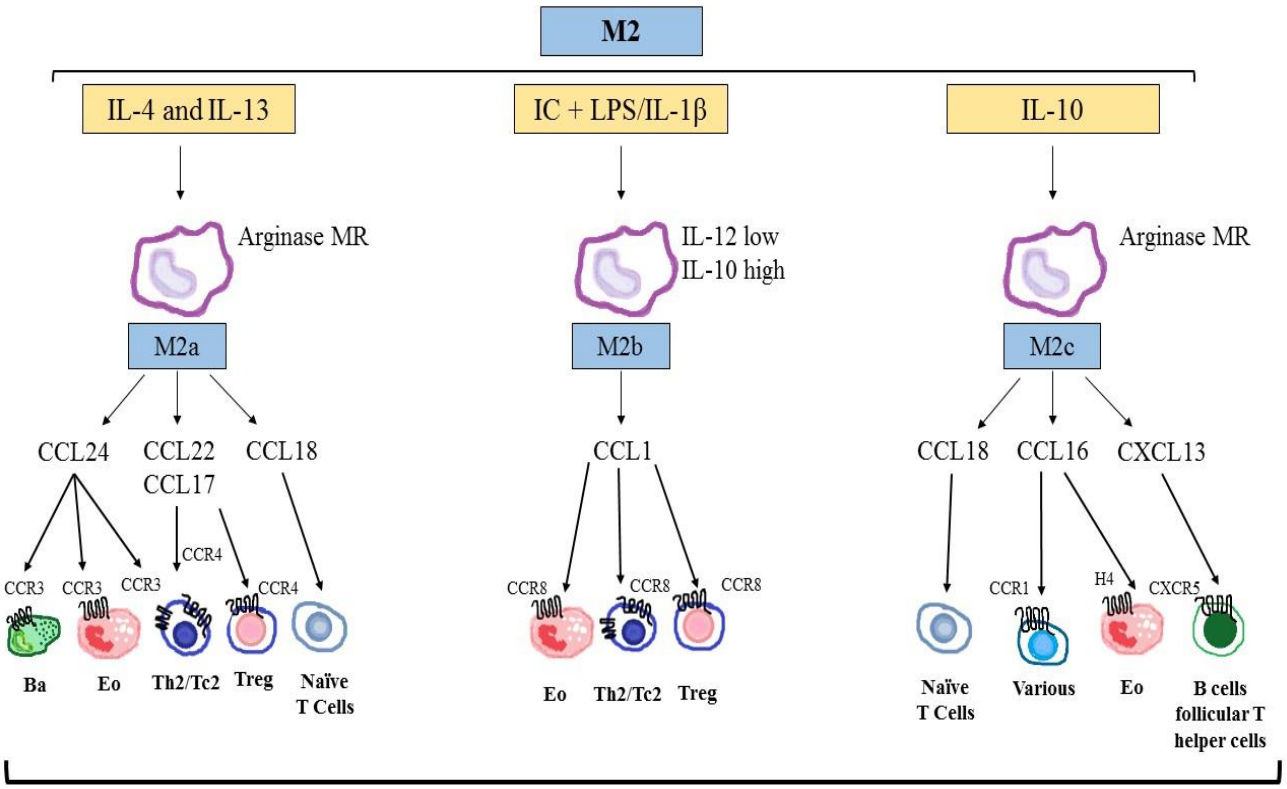

- **Tissue repair**
- **Immunoregulation**
- **Allergy**
- **Tumour Promotion**

Figure 3.3: The chemokine repertoires of polarised M2 macrophages. IL-4 and IL-13 exposure sustains M2a polarisation, which is accompanied by production of chemokine agonists at CCR3, CCR4 and CCR8, consequent recruitment of eosinophils, basophils and Th2 cells, and organization of a type II immune response. M2b polarisation is critically dependent on exposure to immune complexes and TLR or IL-1R agonists, and it is characterised by selective production of CCL1, with consequent recruitment of Tregs and immunoregulation. Exposure to IL-10 drives M2c polarisation, which is characterised by CCL16 and CCL18 production and consequent recruitment of eosinophils and naïve T cells, respectively. Induction of CXCL13 requires co-stimulation by IL-10 and LPS. **Abbreviations: Ba**, basophils; **Eo**, eosinophils; **IC**, immune complexes; **IL-1β**, interleukin-1beta; **IL-4**, interleukin-4; **MR**, mannose receptor; **Treg**, regulatory T cells (adapted from (Mantovani, Sica et al. 2004)).

IL-10 (see Figure 3.4) has been described as a key role player and promoter of macrophage polarization within the M2 populations; however, it is not only limited to inhibiting proinflammatory cytokines. It has been noted that IL-10, in the presence of LPS or alone, can activate four distinctive transcriptional pathways and is thus, more than a mere deactivator. These are specific to (i) control and deactivate inflammation which includes suppressing inflammatory cytokine release and other activator molecules, (ii) the regulation of cytokine/receptor signalling involving the suppressor of cytokine signalling 3 (SOCS3) and PI3-K isoforms, (iii) remodelling the extracellular matrix, (iv) lymphoid tissue neogenesis and B-cell function. Therefore, IL-10-stimulated M2b macrophages are responsible for the regulation of inflammation and immunity (Mantovani, Sica et al. 2004).

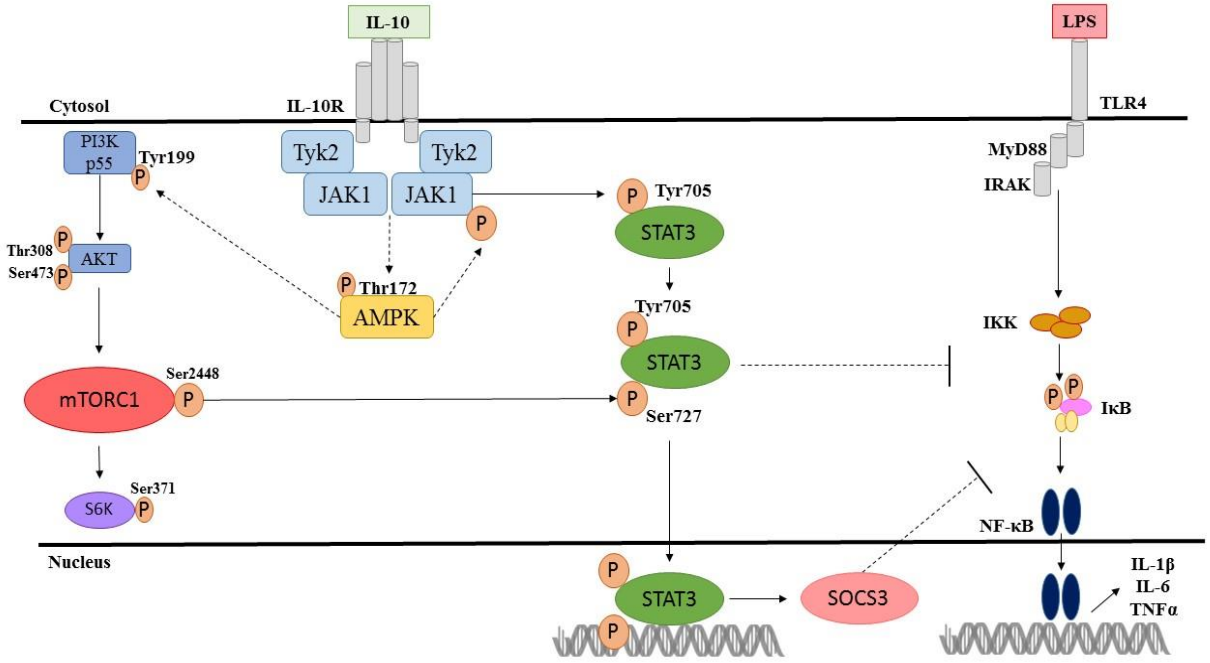

Figure 3.4: IL-10 signalling promotes the rapid phosphorylation of JAK1 in an AMPK-dependent manner. The influence of AMPK on JAK1 phosphorylation is indirect (dotted line). Activation of JAK1 then leads to the phosphorylation and activation of STAT3 (Tyr^{705}), which positively regulates STAT3 (Ser^{727}) phosphorylation. This is critical for SOCS3 production. In addition, AMPK also promotes the activation of PI3K simultaneously by enhancing the phosphorylation of the p55 subunit (indirectly, as indicated by the dotted line). Consequently leading to an increase in mTORC1 activity. MTORC1 activation leads to an increase in phosphorylation of STAT3 (Ser^{727}), which further enhances STAT3 transcriptional activity. It is proposed that STAT3-regulated genes possibly include SOCS3, which in turn suppress TLR-activated inflammatory cytokine production (adapted from (Zhu, Brown et al. 2015). **Abbreviations: JAK/STAT,** Janus Kinase/Signal Transducer and Activator of Transcription; **SOCS3**, Suppressor of cytokine signalling 3.

When considering the surfactant-associated proteins' interactions with macrophages, the mystery becomes speculative regarding how the specific proteins interact with certain surface receptors. The ability of surfactant proteins to interact and modify the downstream cascade action of these proteins may influence alveolar macrophage polarisation. As discussed in Chapter 1, SP-A and SP-D are potent modulators of macrophage function and may also suppress clearance of apoptotic cells through activation of the transmembrane receptor signal inhibitory regulatory protein α (SIRPα) (Janssen, McPhillips et al. 2008).

Nguyen and colleagues reported that short-term (10 min – 2 h) exposure of SP-A to human macrophages decreases TLR-mediated TNF-α production by inhibiting the activity of signalling kinases (Akt and MAPKs) required for NF-κB transcriptional activation (Figure 3.5). These studies model the initial exposure of macrophages to SP-A and do not account for the fact that AMs are constantly exposed to surfactant in the alveolus (Nguyen, Rajaram et al. 2012). This constant exposure results in the constant ligand binding of these surfactant proteins to different receptors on the alveolar macrophage cell surface. Studies have reported that the SP-A and SP-D may act in a dual manner, to enhance or suppress the inflammatory cascade depending on their binding domains on different receptors (Gardai, Xiao et al. 2003).

It has been suggested that the globular heads of SP-A may bind to CD14 and TLR2 (and TLR4) thus suppressing stimulation by LPS (Chiba, Sano et al. 2001, Murakami, Iwaki et al. 2002). The conflicting reports of surfactant proteins' inflammatory mediator induction (Ofek, Mesika et al. 2001) or suppression (Arias-Diaz, Garcia-Verdugo et al. 2000) has become a paradox that is supported by the hypothesis that the orientation of the SP-A and SP-D on their respective receptors determine whether they induce or suppress inflammation; but this is yet to be proven.

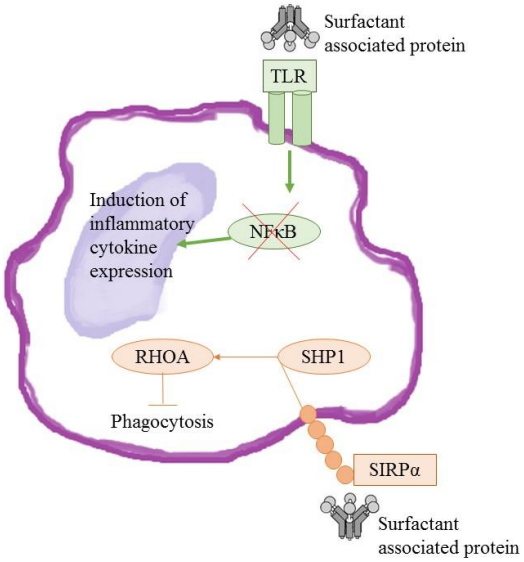

Figure 3.5: Pulmonary surfactant-associated protein A (SP-A) and SP-D are able to block toll-like receptors TLR2 and TLR4 interactions with their respective ligands, as well as their interactions with the TLRs which prevents the activation of nuclear factor-κB (**NF-κB**) and the initiation of the inflammatory response. Binding of surfactant proteins to signal-regulatory protein-α (**SIRPα**) recruits SH2 domain-containing protein tyrosine phosphatase 1 (**SHP1**) and activates Ras homolog gene family, member A (**RHOA**), which inhibits phagocytosis (adapted from (Hussell, Bell 2014).

Both Chiba *et al.* (2001) and Murakami *et al.* (2002) support the model in which both the surfactant proteins A and D bind to signal inhibitory regulatory protein α (SIRPα) activating the downstream blockade of the pro-inflammatory cascade. When taking all of the evidence into consideration, it suggests that SP-A and SP-D help maintain the non- or anti-inflammatory pulmonary environment due to their globular head stimulating the ITIM (immune-receptor tyrosine-based inhibitory motif) -containing SIRPα. In contrast, however, these same domains also interact with PAMPs on the surface of foreign organisms, apoptotic cells and cell debris, which then allows for the presentation of their collagenous tails to the CD91 domains on the AMs. Thus initiating the rearrangement of the AMs' cytoskeleton, ingestion, and the pro-inflammatory cascade (Gardai, Xiao et al. 2003).

This is thus indicative that surfactant associated proteins have unexpected, yet pivotal roles in the regulation of immunomodulatory processes.

3.1 Materials and Methods

3.1.1 NR8383 Cell Culture

The NR8383 AMs were first cultured in 75 cm^2 flasks and maintained in a humidified, 5% CO_2–95% atmospheric air incubator at 37°C. The media, comprised of RPMI 1640 (Roswell Park Memorial Institute media)supplemented with 10% fetal calf serum, 1% L-glutamine solution (200 mM), and 1% Penicillin-Streptomycin (PENSTREP), and was routinely changed twice weekly. Cells were seeded to 12-well tissue culture plates at a density of 2.5×10^5 cells/well. Cell viability before and after each experiment was assessed by trypan blue exclusion. The viability was consistently greater than 95% in all detected samples before seeding as well as after treatment (see Chapter 2: Viability Study page 88). Routine mycoplasma testing was performed to guarantee no contamination risk (see Appendix D).

Inflammatory Cytokines

To evaluate the anti-inflammatory effects of exogenous surfactants, Curosurf®, Liposurf® and Synsurf® were standardised to equivalent phospholipid concentrations, 100 - 1500 µg/ml and incubated with LPS - (1 µg/ml) stimulated and un-stimulated NR8383 AMs over 24 hours.

The changes in cytokines were analysed by using a multiplex (V-PLEX) rat cytokines's electrochemiluminescence-based ELISA kit (Meso Scale Discovery®) as per manufacturer's instructions (**duplicate assay*). The values were first calculated for picogram cytokine per milliliter (pg/ml) of sample, and then converted into microgram (µg/ml) where applicable.

Inflammatory Cytokines

One-way analysis of variance (ANOVA) with Tukey's post-test was performed for the comparison of multiple treatments and differences were considered significant when $P \leq 0.05$. The statistical program GraphPad Prism v.5 was used.

List of Cytokines: IL-1β, TNF-α, IL-6, IL-10, KC-GRO

3.1.2 Detection of protein expression by proteomics

Digests

In-solution Digest

All reagents were analytical grade or equivalent. Samples were reduced by adding 50 mM triscarboxyethyl phosphine (TCEP; Fluka) in 100 mM Triethylammonium bicarbonate (TEAB) (final concentration 5 mM TCEP) for 30 minutes at room temperature. Following reduction, cystein residues were modified to methylthio forms using 200 mM methane methylthiosulphonate (MMTS; Sigma) in 100 mM TEAB (final concentration 20 mM) for 30 minutes. After modification, the samples were diluted to 98 µL with 100 mM TEAB. Proteins were digested by adding 5 µL trypsin (Promega) solution (1 µg/µL) and incubating for 18 hours at 37 °C. The samples were dried down and resuspended in 100 µL 2% acetonitrile (Fluka):water; 0.1% formic acid (FA; Sigma).

Desalting

Residual digest reagents were removed using an in-house manufactured C_{18} stage tip (Empore Octadecyl C_{18} extraction discs; Supelco). The 20 µL sample was loaded onto the stage tip after activating the C_{18} membrane with 30 µL methanol (Sigma) and equilibration with 30 µL 2% acetonitrile:water; 0.05% FA. The bound sample was washed with 30 µL 2% acetonitrile:water; 0.1% FA before elution with 30 µL 50% acetonitrile:water 0.1% FA. The eluate was evaporated to dryness. The dried peptides were dissolved in 20 µL 2% acetonitrile: water; 0.1% FA for LC-MS analysis

Liquid chromatography

Dionex nano-RSLC

Liquid chromatography was performed on a Thermo Scientific Ultimate 3000 RSLC instrument equipped with a 0.5cm x 300µm C_{18} trap column and a 40 cm x 75 µm in-house manufactured C_{18} column (Luna C_{18}, 3.6 µm; Phenomenex) analytical column. The loading solvent system employed was: 2% acetonitrile: water: 0.1% FA; Solvent A: 2% acetonitrile:water: 0.1% FA and Solvent B: 100% acetonitrile:0.1% FA. Samples were loaded onto the trap column using loading solvent at a flow rate of 15 µL/min from a temperature controlled autosampler set at 7 ºC. Loading was performed for 5 min before the sample was eluted onto the analytical column. Flow rate was set to 500 nL/minute and the gradient

generated as follows: 2.0% - 10% B over 5 min; 5% -25% B from 5 - 50 minutes using Chromeleon non-linear gradient 6, 25% - 45% from 50-65 minutes, using Chromeleon non-linear gradient 6. Chromatography was performed at 50°C and the outflow delivered to the mass spectrometer through a stainless steel nano-bore emitter.

Mass spectrometry

Mass spectrometry was performed using a Thermo Scientific Fusion mass spectrometer equipped with a Nanospray Flex ionisation source. The sample was introduced through a stainless steel emitter. Data was collected in positive mode with spray voltage set to 2kV and ion transfer capillary set to 275 °C. Spectra were internally calibrated using polysiloxane ions at m/z = 445.12003 and 371.10024. MS1 scans were performed using the orbitrap detector set at 120 000 resolution over the scan range 350 - 1650 with automatic gain control (AGC) target at 3 E5 and maximum injection time of 40 ms. Data was acquired in profile mode. MS2 acquisitions were performed using monoisotopic precursor selection for ions with charges +2 -+6 with error tolerance set to +/- 10 ppm. Precursor ions were excluded from fragmentation once for a period of 30s. Precursor ions were selected for fragmentation in higher-energy collisional dissociation (HCD) mode using the quadrupole mass analyser with HCD energy set to 32.5%. Fragment ions were detected in the orbitrap mass analyser set to 15 000 resolutions. The AGC target was set to 1E4 and the maximum injection time to 45 ms. The data was acquired in centroid mode.

Data Analysis

The raw files generated by the mass spectrometer were imported into Proteome Discoverer v1.4 (Thermo Scientific) and processed using the SequestHT algorithm included in Proteome Discoverer. Data analysis was structured to allow for methylthio as fixed modification as well as asparagine/glutamine (NQ) deamidation,methionine (M) oxidation. Precursor tolerance was set to 10 ppm and fragment ion tolerance to 0.02Da. The databased used was the rat database obtained from Uniprot. The results files were imported into Scaffold 1.4.4 and identified peptides validated using the X!Tandem search algorithm included in Scaffold. Peptide and Protein validation were done using the Peptide and Protein Prophet algorithms. Protein quantitation were done performing a t-test on the paired data with the Benjamini-Hochberg correction was applied.

Functional Enrichment Analysis

The STRING (Search Tool for the Retrieval of Interacting Genes) database v10.5 used (http://string-db.org) aims to provide a critical assessment and integration of protein–protein interactions, including direct (physical) as well as indirect (functional) associations.

Proteins that were uniquely identified in one particular treatment group were subjected to enrichment analysis using the String database (string-db.org, accessed [27 September 2017]) with the *Rattus norvegicus* whole proteome as the background dataset. Enrichment for GO terms and protein domains was carried out for each set of unique proteins.

In the Enrichment widget, STRING displays every functional pathway/term that can be associated to at least one protein in the network that allows for network visualization and statistical analysis of a user-supplied protein list. The terms were sorted by their enrichment P-value. The P-values were corrected for multiple testing using the method of Benjamini and Hochberg.

3.1.3 Human Bronchoalveolar lavage samples

The bronchoalveolar sampling (BALS) for this study was performed by Prof. Pierre Goussard (Head of Clinical Unit: Paediatric Pulmonology, Department of Paediatrics and Child Health, Stellenbosch University and Tygerberg Children's Hospital. *Ethics Number: N13/07/099*) and collected from children deemed not to have infectious conditions (i.e. Tuberculosis or HIV). The collected samples where from children with structural problems that underwent routine bronchoalveolar sample collection for other investigatory purposes.

After informed consent, BALS collection was performed after topical anesthesia with 4010 lidocaine spray. A flexible fiber optic bronchoscope was introduced through the upper airway and wedged in a segment of the right middle lobe. One 4 - 8 ml of BAL aliquot per patient was aspirated with gentle hand suction and collected for this study.

3.1.4 Isolation and Cultivation of Alveolar Macrophages

Isolated or cultured AMs from bronchoalveolar lavage may have a certain percentage of contaminant cell types; thus, mononuclear cells were isolated by Histopaque-1077 (Sigma, St.

Louis, MO) density gradient centrifugation of whole BALS. After isolation, AMs were allowed to adhere thus separating possible Lymphocytes from the population.

Inflammatory Cytokines

To evaluate the anti-inflammatory effects of exogenous surfactants, Curosurf®, Liposurf® and Synsurf® were standardised to equivalent phospholipid concentrations, 500 - 1500 µg/ml and incubated with LPS- (1 µg/ml) stimulated and un-stimulated human AMs over 24 hours. The changes in cytokines were analysed as previously described by using a multiplex (V-PLEX) human cytokines's electrochemiluminescence-based ELISA kit (Meso Scale Discovery®) as per manufacturer's instructions. The values were first calculated for picogram cytokine per milliliter (pg/ml) of sample, and then converted into microgram (µg/ml) where applicable.

List of Cytokines: IL-1β, IL-2, TNF-α, IL-6, IL-8, INF-γ, GM-CSF, IL-10, IL-12

3.2 Results

3.2.1 Effect of Surfactant on LPS stimulated and non-stimulated NR8383 Alveolar Macrophage Cytokine Secretion

The basal levels of TNF-α from the culture supernatant in the non-stimulated NR8383 AMs supernatant concentrations measured at 24 h in the presence of surfactants are seen in Table 3.1. TNF-α secretion increased in the presence of the three independent surfactants, however, significant increases compared to the control (basal levels) were only found for Liposurf® at phospholipid concentrations of 100 & 500 µg/ml respectively. Curosurf® displayed a concentration dependent decrease in cytokine production whereas Synsurf® displayed a threshold effect (concentrations not exceeding 0.938 ± 0.2120 pg/ml). Liposurf® displayed a statistically significant increase ($P < 0.05$) in TNF-α production at concentrations of 100 & 500 µg/ml phospholipids, compared to the control (Figure 3.6). It was found that Curosurf® significantly decreased ($P < 0.05$) TNF-α release compared to Liposurf® at phospholipid concentrations of 1500 µg/ml. Synsurf® also displayed a significant increase ($P < 0.05$) in TNF-α release compared to Curosurf® at phospholipid concentrations of 750 µg/ml; however, no other differences were seen among the surfactants. Basal levels of IL-1β were found to be below detection. Basal IL-6 pro-inflammatory cytokine levels were only evident in the lower concentration groups for Curosurf® and Synsurf®.

Table 3.1: The mean ± SEM of non-stimulated NR8383 AMs produced TNF-α and IL-6. Supernatant concentrations measured at 24h in the presence or absence of surfactants (100 - 1500 µg/ml total phospholipids) (one-way analysis of variance (ANOVA), Tukey's post-test * $P < 0.05$).

Control	Concentration of DPPC (µg/ml)	Curosurf®	Synsurf®	Liposurf®
		TNF- α (pg/ml)		
Below detection pg/ml	**100**	0.443 ± 0.269	0.690 ±0.176	0.912 ± 0.148*
	250	0.042 ± 0.250	0.737 ±0.051	0.569 ± 0.056
	500	0.051 ± 0.228	0.738 ±0.066	0.923 ± 0.127*
	750	Below detection	0.938 ± 0.212	0.553 ± 0.015
	1000	0.014 ± 0.154	0.914 ± 0.297	0.473 ± 0.309
	1500	0.013 ± 0.001	0.547 ± 0.258	0.791 ± 0.174
		IL-6 (pg/ml)		
Below detection pg/ml	**100**	0.554 ± 0.506	0.416 ± 0.367	Below detection
	250	0.699 ± 0.651	Below detection	Below detection

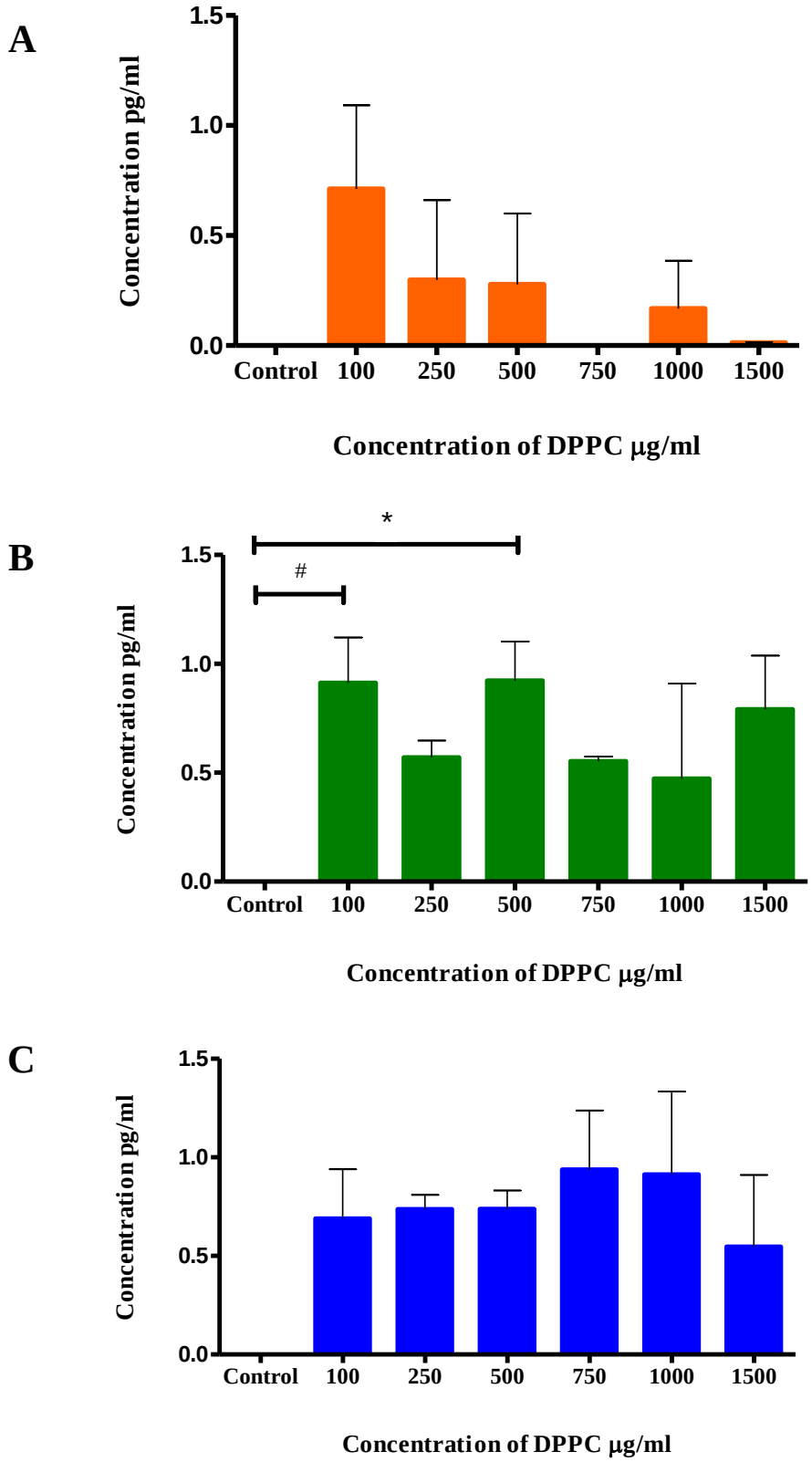

Figure 3.6: Effects of surfactants on non-stimulated TNF-α production. TNF-α in cell supernatant by NR8383 AMs in the presence of A) Curosurf®; B) Liposurf®, & C) Synsurf® at 100 – 1500 µg/ml phospholipids. (One-way analysis of variance (ANOVA), Tukey's post-test **B)** * $P < 0.05$, $^{\#}$ $P < 0.05$).

Table 3.2 displays the LPS (1 µg/ml)-stimulated TNF-α (Figure 3.7) and IL-1β (Figure 3.8) supernatant concentrations measured at 24 h in the presence of surfactants (100 - 1500 µg/ml total phospholipids). Basal supernatant concentrations for TNF-α and IL-1β from LPS-stimulated NR8383 AMs were 3.038 ± 0.0275 ng/ml and 1.317 ± 0.028 µg/ml, respectively. Surfactant-treated cells secreted significantly less (*****$P < 0.0001$) TNF-α and IL-1β at 24 h versus the LPS stimulated un-treated cells at phospholipid concentration of 250 - 1500 µg/ml. The exception was found for TNF-α in the lower phospholipid concentrations (100 and 250 µg/ml), where Curosurf® and Liposurf® displayed no statistical significant difference in cytokine production compared to the control. However, Synsurf® at a phospholipid concentration of 100µg/ml significantly increased (**#***P* < 0.0001) TNF-α secretion (Figure 3.7C) to 4.224 ± 0.040 ng/ml and Curosurf® at a phospholipid concentration of 100µg/ml significantly increased (**#***P* < 0.0001) IL-1β secretion (Figure 3.8C) to 1.95 ± 0.062 ng/ml.

When considering inter-surfactant differences, Curosurf® decreased TNF-α release significantly ($P < 0.001$) more than Liposurf® at phospholipid concentrations 250 - 1000 µg/ml as well as compared to Synsurf® at phospholipid concentration of 100 ug/ml ($P < 0.001$). No differences were seen for Curosurf® vs Synsurf® at phospholipid concentration of 250 µg/ml; however, Synsurf® decreased TNF-α release significantly ($P < 0.001$) more than Curosurf® at phospholipid concentrations 500 - 750 µg/ml and at 1000 - 1500 µg/ml ($P < 0.01$) as well as compared to Liposurf® at phospholipid concentrations 250 - 1500 µg/ml ($P < 0.001$).

Liposurf® IL-1β secretion was significantly less ($P < 0.001$) than Curosurf® for phospholipid concentrations 100, 250, 750, 1000, and 1500 µg/ml but to a lesser extent for 500 µg/ml. Synsurf® IL-1β secretion was also found to be significantly less ($P < 0.001$) than Curosurf® and Liposurf® for all phospholipid concentrations (Table 3.2).

Table 3.2: The mean ± SEM of LPS (1 µg/ml)-stimulated NR8383 AMs production of TNF-α and IL-1β. Supernatant concentrations measured at 24h in the presence or absence of surfactants (100 - 1500 µg/ml total phospholipids) (one-way analysis of variance (ANOVA), Tukey's post-test * $P < 0.05$, *** $P < 0.001$, **** $P < 0.0001$).

LPS Control	Concentration of DPPC (µg/ml)	LPS + Curosurf®	LPS + Synsurf®	LPS + Liposurf®
		TNF- α (ng/ml)		
3.038 ± 0.0275 ng/ml	**100**	2.991 ± 0.159	4.224 ± 0.040	3.182 ± 0.079
	250	1.839 ± 0.162***	1.576 ± 0.110****	2.867 ± 0.078
	500	1.08 ± 0.009****	0.104 ± 0.006****	1.839 ± 0.084****
	750	0.704 ± 0.025****	0.043 ± 0.002****	1.778 ± 0.018****
	1000	0.489 ± 0.025****	0.024 ± 0.002****	1.713 ± 0.0885****
	1500	0.406 ± 0.031****	0.019 ± 0.001****	1.887 ± 0.036****
		IL-1β (ng/ml)		
1.317 ± 0.028 ng/ml	**100**	1.949 ± 0.062****	0.982 ± 0.005****	1.325 ± 0.02
	250	0.778 ± 0.029****	0.469 ± 0.012****	1.215 ± 0.005*
	500	0.406 ± 0.004****	0.102 ± 0.001****	0.498 ± 0.004****
	750	0.371 ± 0.003****	0.048 ± 0.0004****	0.529 ± 0.010****
	1000	0.298 ± 0.010****	Below detection****	0.446 ± 0.010****
	1500	0.387 ± 0.007****	Below detection****	0.597 ± 0.003****

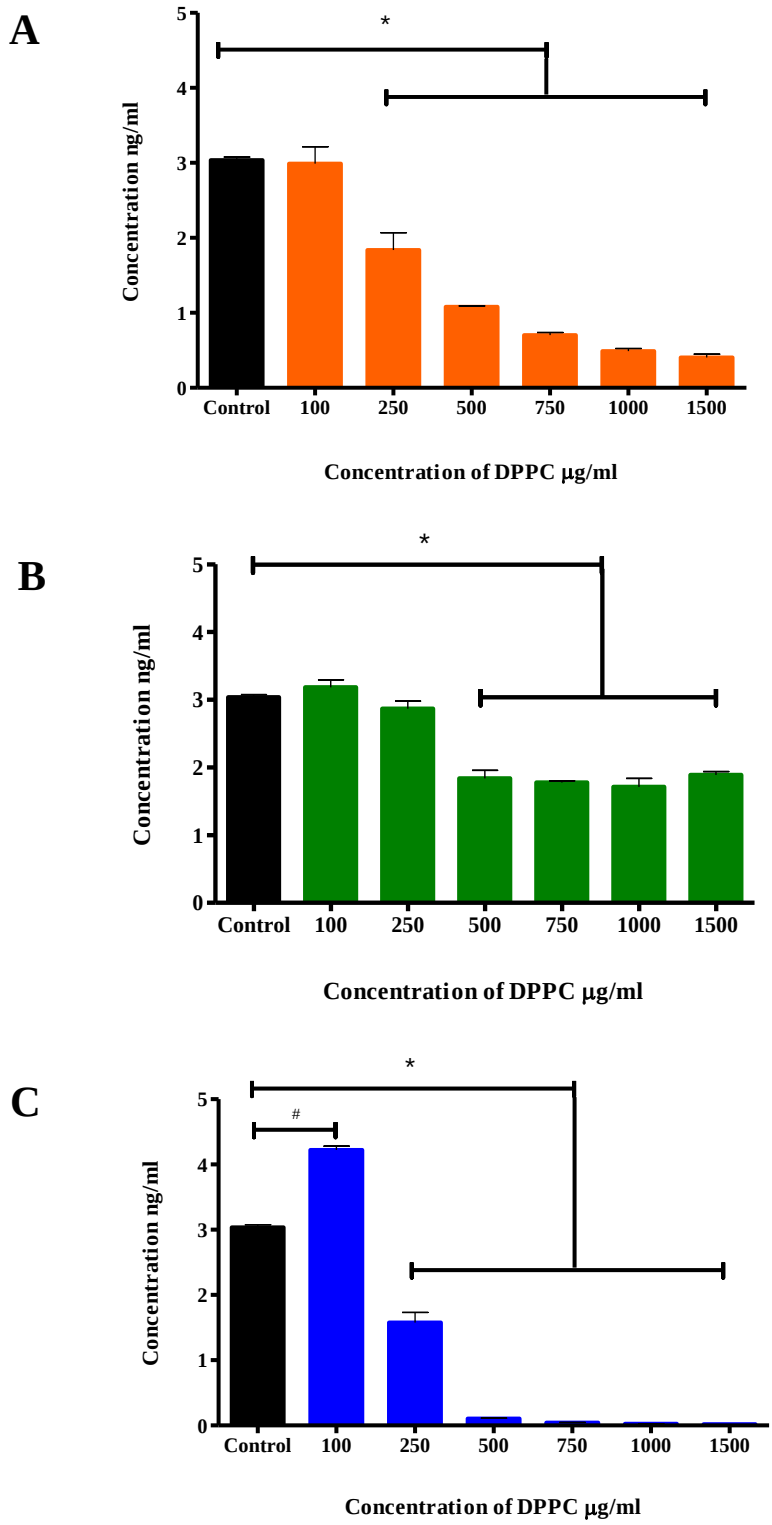

Figure 3.7: Effects of surfactants on LPS-stimulated TNF-α production (ng/ml). TNF-α in cell supernatant by LPS-stimulated NR8383 AMs in the presence of A) Curosurf®; B) Liposurf®, & C) Synsurf® at 100 – 1500 µg/ml phospholipids. (One-way analysis of variance (ANOVA), Tukey's post-test **A)** $^{*}P < 0.0001$ **B)** $^{*}P < 0.0001$, **C)** $^{*}P < 0.0001$, $^{\#}P < 0.0001$.

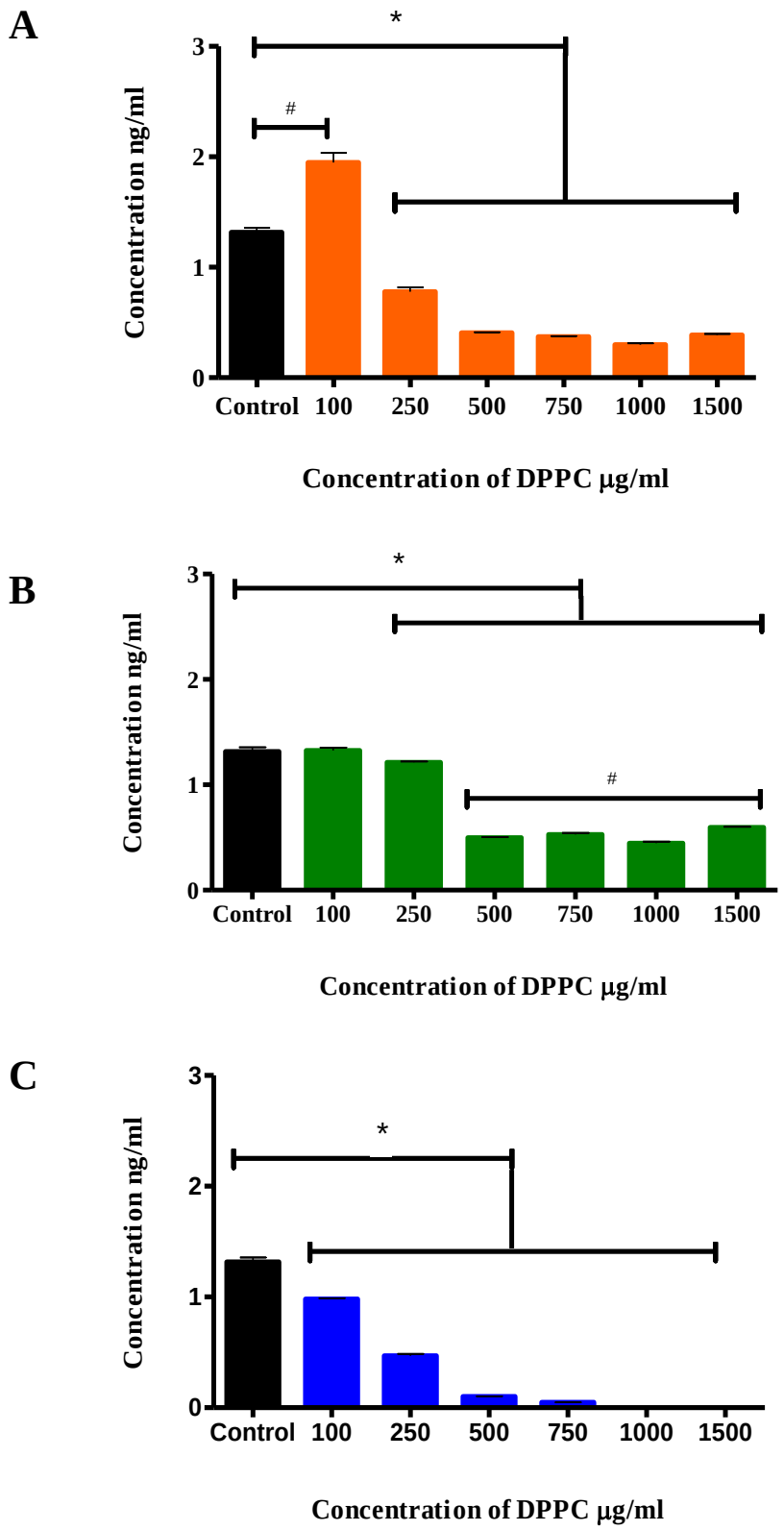

Figure 3.8: Effects of surfactants on LPS-stimulated IL-1β production (ng/ml). IL-1β in cell supernatant by LPS-stimulated NR8383 AMs in the presence of A) Curosurf®; B) Liposurf®, & C) Synsurf® at 100 – 1500 µg/ml phospholipids. (One-way analysis of variance (ANOVA), Tukey's post-test **A)** $^{*}P < 0.0001$, $^{\#}P < 0.0001$ **B)** $^{*}P < 0.05$, $^{\#}P < 0.0001$ **C)** $^{*}P < 0.0001$.

Table 3.3 and Figure 3.9 display the LPS (1 µg/ml)-stimulated NR8383 AM IL-6 supernatant concentrations measured at 24 h in the presence of surfactants (100 - 1500 µg/ml total phospholipids). Basal supernatant concentrations for IL-6 from LPS-stimulated NR8383 AMs was 4.519 ± 0.218 ng/ml. Surfactant-treated cells secreted significantly less IL-6 versus the LPS stimulated un-treated cells (* $P < 0.0001$). In Figure 3.9, Both Liposurf® (B) Synsurf® (C) and displayed a threshold inhibition for stimulated IL-6 production at phospholipid concentration of 500 µg/ml (#, Figure 3.9B & C). Whereas Curosurf® (A) displayed a similar threshold inhibition for LPS-induced IL-6 secretion but a minimal significant difference was seen between 500 - 750µg/ml and 1000 – 1500 µg/ml (# $P < 0.05$, Figure 3.9A).

When considering inter-surfactant differences (Table 3.3), Curosurf® as well as Synsurf® were able to inhibit LPS-induced IL-6 secretion significantly better than that of Liposurf® at phospholipid concentrations 100 - 1500 µg/ml ($P < 0.001$). Synsurf® exposed AMs IL-6 secretion was significantly less ($P < 0.001$) than that of Curosurf® at 100 – 750 µg/ml phospholipids and only minimally significant at 1000 µg/ml ($P < 0.05$). No significant difference was seen in IL-6 secretion for Synsurf® and Curosurf® at 1500 µg/ml phospholipids.

Table 3.3: The mean ± SEM of LPS (1 µg/ml)-stimulated NR8383 AMs production of IL-6. Supernatant concentrations measured at 24h in the presence or absence of surfactants (100 - 1500 µg/ml total phospholipids) (one-way analysis of variance (ANOVA), Tukey's post-test *** $P < 0.001$, **** $P < 0.0001$).

LPS Control	Concentration of DPPC (µg/ml)	LPS + Curosurf®	LPS + Synsurf®	LPS + Liposurf®
		IL-6 (ng/ml)		
4.519 ± 0.218 ng/ml	**100**	2.859 ± 0.05****	2.199 ± 0.019****	3.358 ± 0.122***
	250	0.907 ± 0.048****	0.241 ± 0.0005****	2.009 ± 0.085****
	500	0.413 ± 0.006****	0.004 ± 0.0006****	0.896 ± 0.014****
	750	0.331 ± 0.016****	0.001 ± 0.0003****	0.744 ± 0.006****
	1000	0.177 ± 0.002****	0.001 ± 0.001****	0.646 ± 0.011****
	1500	0.150 ± 0.002****	Below detection****	0.609 ± 0.003****

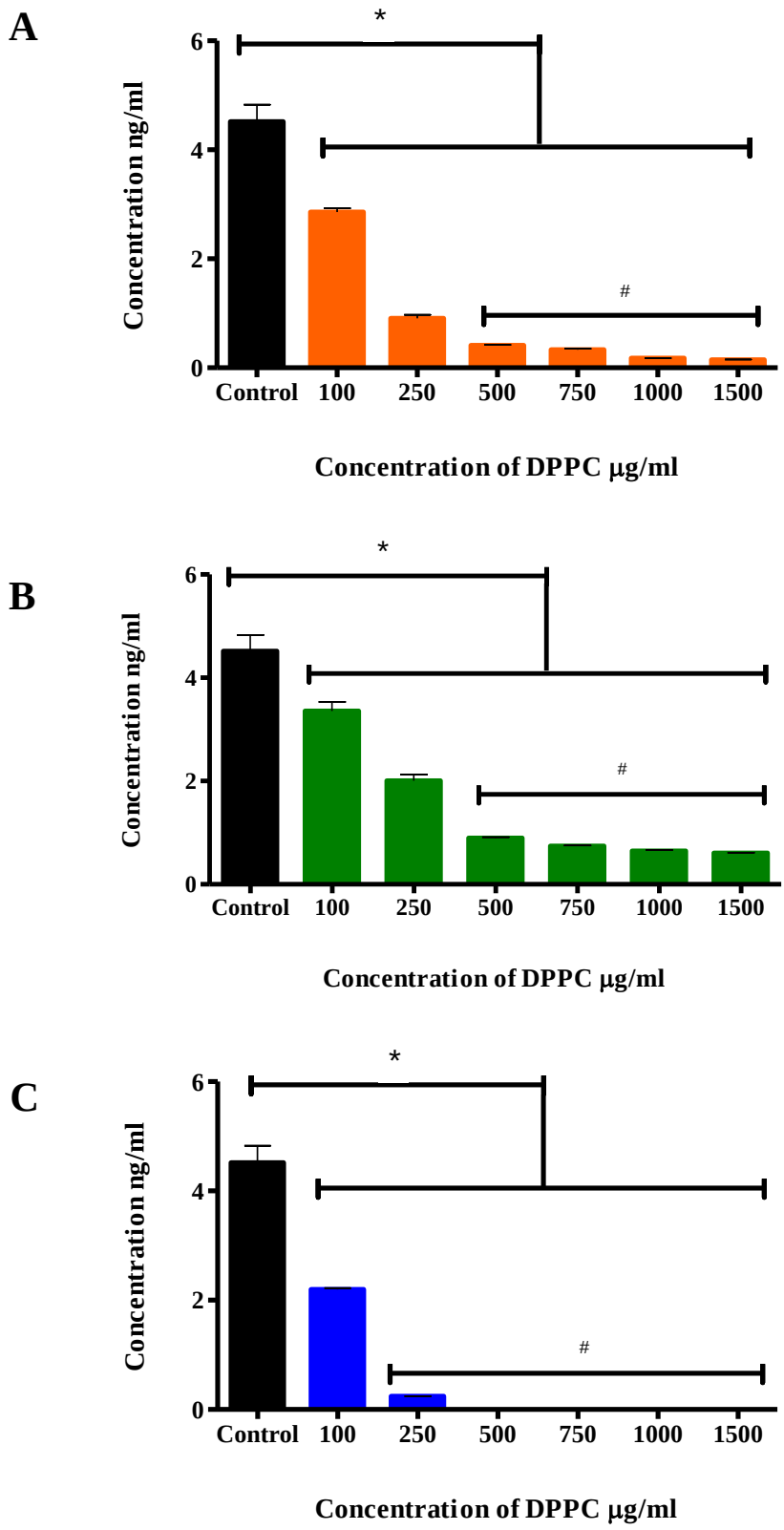

Figure 3.9: Effects of surfactants on LPS-stimulated IL-6 production (ng/ml). IL-6 in cell supernatant by LPS-stimulated NR8383 AM in the presence of A) Curosurf®; B) Liposurf®; & C) Synsurf® at 100 – 1500 µg/ml phospholipids. (One-way analysis of variance (ANOVA), Tukey's post-test **A)** * $P < 0.0001$, $^{\#}P < 0.05$ **B)** $^{*}P <$ 0.05, $^{\#}$*Threshold* **C)** * $P < 0.0001$, $^{\#}$*Threshold*.

Table 3.4 and Figure 3.10 displays the LPS (1 µg/ml)-stimulated KC/GRO (neutrophil chemo-attractant) supernatant concentrations were measured at 24 h in the presence of surfactants (100 - 1500 µg/ml total phospholipids) as seen in Table 3.4. Basal supernatant concentrations for KC/GRO from LPS-stimulated NR8383 AMs was 0.6225± 0.014 ng/ml. Surfactant-treated cells secreted significantly less KC/GRO versus the LPS stimulated un-treated cells (* P < 0.0001). Both Liposurf® (Figure 3.10B) and Synsurf® (Figure 3.10C) displayed a threshold inhibition for stimulated KC/GRO production at phospholipid concentration of 500 µg/ml (# P < 0.0001). Whereas Curosurf® (Figure 3.10A) displayed a similar threshold inhibition for stimulated KC/GRO production at a higher phospholipid concentration of 250 µg/ml (# P < 0.0001).

When considering inter-surfactant differences (Table 3.4), Synsurf® displayed significantly less stimulated KC/GRO secretion compared to both Curosurf® and Liposurf® at phospholipid concentrations 100 - 1500 µg/ml (P < 0.001). Curosurf® and Liposurf® displayed no differences in KC/GRO secretion at phospholipid concentrations 100 - 250 µg/ml as well as 1000 – 1500 µg/ml. However, Liposurf® stimulated less KC/GRO secretion than Curosurf® at phospholipid concentrations 500 (P < 0.001) and 750 µg/ml (P < 0.01).

Table 3.4: The mean ± SEM of LPS (1 µg/ml)-stimulated NR8383 AMs KC/GRO. Supernatant concentrations measured at 24h in the presence or absence of surfactants (100 - 1500 µg/ml total phospholipids) (one-way analysis of variance (ANOVA), Tukey's post-test *** P < 0.001, **** P < 0.0001).

LPS Control	Concentration of DPPC (µg/ml)	LPS + Curosurf®	LPS + Synsurf®	LPS + Liposurf®
		KC/GRO (ng/ml)		
0.623 ± 0.014ng/ml	**100**	0.407± 0.012***	0.210± 0.001****	0.416 ± 0.010****
	250	0.246± 0.024****	0.105± 0.004****	0.272 ± 0.004****
	500	0.241± 0.002****	0.014± 0.001****	0.172 ± 0.001****
	750	0.220± 0.017****	0.004± 0.0003****	0.172 ± 0.002****
	1000	0.200± 0.014****	0.005± 0.00003****	0.166 ± 0.001****
	1500	0.180± 0.004****	Below detection****	0.157 ± 0.010****

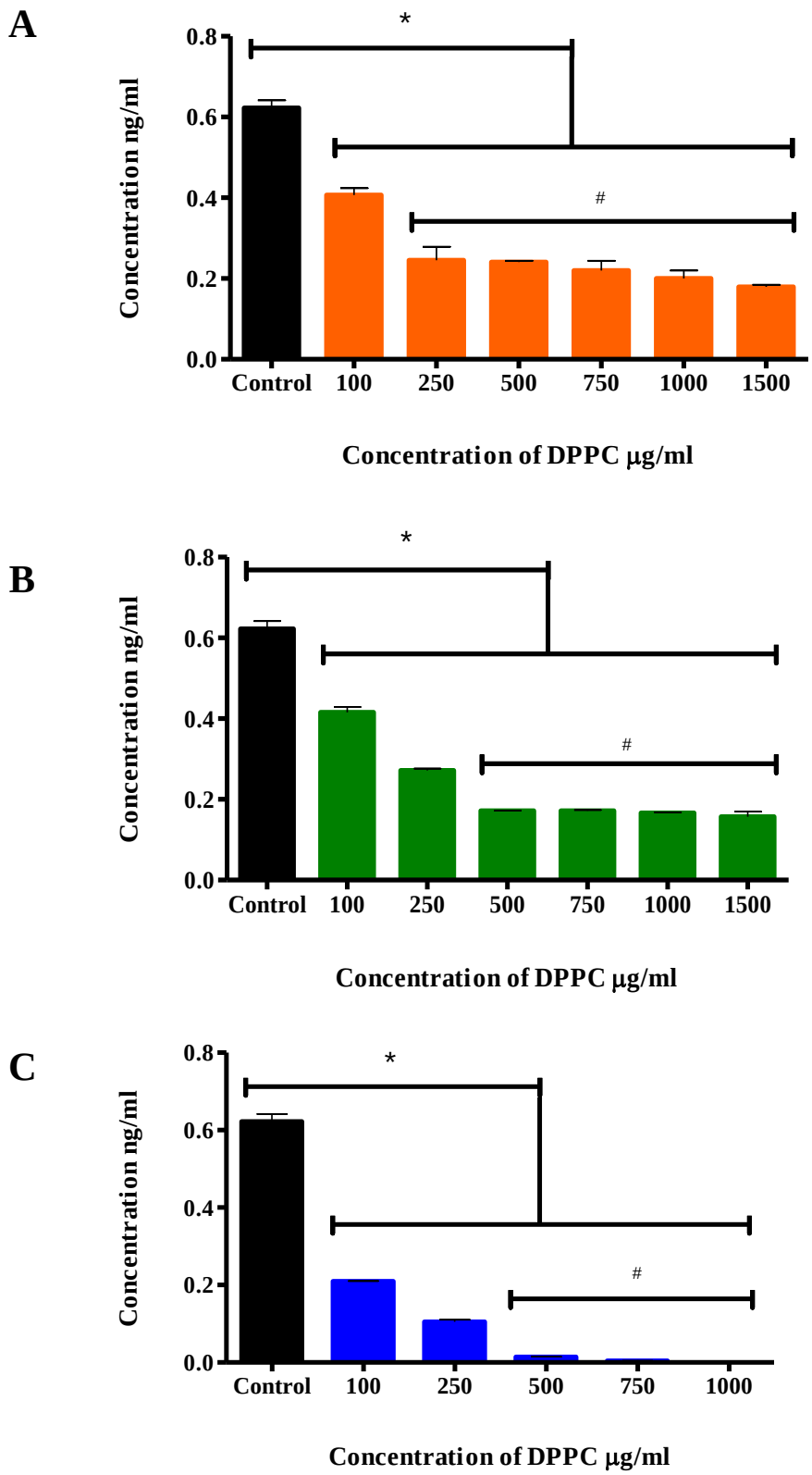

Figure 3.10: Effects of surfactants on LPS-stimulated KC/GRO production (ng/ml) in LPS-stimulated NR8383 AM cell supernatant in the presence of A) Curosurf®; B) Liposurf®, & C) Synsurf® at 100 – 1500 µg/ml phospholipids. (One-way analysis of variance (ANOVA), Tukey's post-test **A)** * $P < 0.0001$, $^{\#}$*Threshold*, **B)** $^{*}P < 0.0001$, $^{\#}$*Threshold*, **C)** * $P < 0.0001$, $^{\#}$*Threshold*.

The anti-inflammatory cytokine IL-10 was also measured in the LPS (1 µg/ml)-stimulated AMs supernatant. Concentrations were measured at 24 h in the presence of the three surfactants (100 - 1500 µg/ml total phospholipids). Only the Liposurf® treated AMs showed detectable signals of IL-10 production at the lower phospholipid concentration of 100 – 500 µg/ml (Figure 3.11) and these were found to be statistically significant ($P < 0.05$) compared to the LPS stimulated un-treated AMs (control) although no differences were found among the concentration groups.

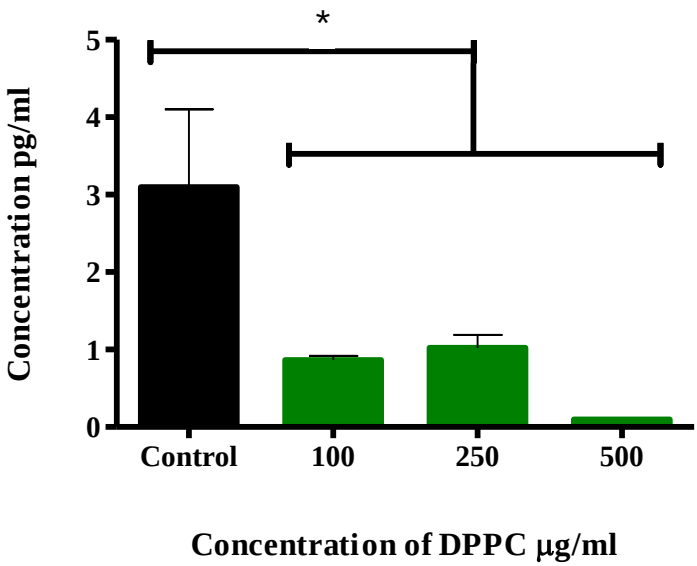

Figure 3.11: Effects of Liposurf® on LPS-stimulated NR8383 AMs production of IL-10 at 100 – 500 µg/ml phospholipids.). (One-way analysis of variance (ANOVA), Tukey's post-test * P < 0.05).

3.2.2 Proteomics

The total protein repertoire with the unique and overlapping protein expression observed in the AMs exposed to Curosurf®, Liposurf®, and Synsurf® is shown in Figure 3.12. Table 3.5 and Figure 3.13 display the total protein repertoire with the statistically significant, overlapping up- and down-regulated expression observed in the AMs. Curosurf® displayed 32 unique protein expressions (Table 3.6), whereas Liposurf® (Table 3.8) and Synsurf® (Table 3.9) displayed 25 and 21 respectively.

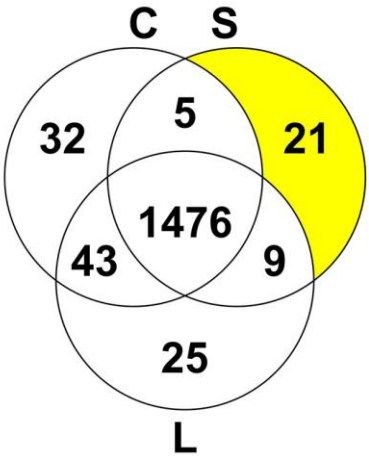

Figure 3.12: The total protein repertoire and the unique and overlapping protein expression observed in AMs exposed to **C**, Curosurf®, **L**, Liposurf®, and **S**, Synsurf® (synthetic surfactant highlighted).

It is noted that these proteins are not all associated with immunomodulatory functions. However, it is imperative to grasp that surfactant exposure to AMs may have more profound effects on other molecular regulatory processes than was initially assumed. Furthermore, it is vital that one takes into consideration the dynamic complexity of protein regulatory processes of which an investigatory attempt such as this only captures a static time frame.

Table 3.5: The number of up- and down-regulated proteins that are differentially expressed for **CTR** (Control), **C** (Curosurf®), **L** (Liposurf®) and **S** (Synsurf®) based on proteomic quantification (n=3). Down-regulated expression , Up-regulated expression , levels unquantified .

Bio View: Identified Proteins	Accession Number	ANOVA Test (P-Value) (p <= 0.05)	Quantitative Profile			
Heme oxygenase 1	HMOX1_RAT	0.0002	CTR high	C high	L high	S low
Heterogeneous nuclear ribonucleoprotein	HNRPD_RAT	0.03	CTR high	C high	L high	S low
Eukaryotic translation initiation factor 6	IF6_RAT	0.042	CTR high	C high	L high	S low
MHC class Ib antigen	O19445_RAT	0.019	CTR high	C high	L high	S low
Voltage-dependent anion-selective channel protein 3	VDAC3_RAT	0.007	CTR high	C high	L high	S low
ATP5H_RAT ATP synthase subunit d, mitochondrial	ATP5H_RAT	0.022	CTR high	C high	L high	S low
Glyceraldehyde-3-phosphate dehydrogenase	G3P_RAT	0.033	CTR low	C high	L high	S high
Cystatin-B	CYTB_RAT	0.005	CTR low	C high	L high	S high
MAP4_RAT Isoform 2 of Microtubule-associated protein 4	Q5M7W5-2	0.014	CTR low	C high	L high	S high
Calcineurin B homologous protein 1	CHP1_RAT	0.021	CTR low	C high	L high	S high
Pcbp2 protein	Q6AYU2_RAT	0.026	CTR high	C low	L high	S high
Embigin	EMB_RAT	0.038	CTR high	C low	L high	S high
Arginase-1	ARGI1_RAT	0.002	CTR high	C high	L low	S low
RNA-binding motif protein, X chromosome retrogene-like	RMXRL_RAT	0.040	CTR high	C high	L low	S low
Cnpy3 protein	B2RYF8_RAT	0.037	CTR high	C high	L low	S low
Protein Tln1	G3V852_RAT	0.006	CTR low	C high	L high	S low
Fructose-bisphosphate aldolase A	ALDOA_RAT	0.001	CTR low	C high	L high	S low
Plectin 6	Q6S3A0_RAT	0.034	CTR low	C high	L high	S low
High density lipoprotein binding protein (Vigilin)	Q3KRF2_RAT	0.032	CTR low	C high	L high	S low
Gamma-enolase	ENOG_RAT	< 0.00010	CTR low	C high	L high	S low
Chaperonin containing Tcp1, subunit 6A (Zeta 1)	Q3MHS9_RAT	0.013	CTR low	C high	L high	S low
Protein Rrbp1	F1M853_RAT	0.013	CTR low	C high	L high	S low

Protein Sptbn1	G3V6S0_RAT	0.027	CTR low	C high	L high	S low
Perilipin	Q5U2U5_RAT	0.001	CTR low	C high	L high	S low
Destrin	DEST_RAT	0.033	CTR low	C high	L high	S low
Spna2 protein	Q6IRK8_RAT	0.021	CTR low	C high	L high	S low
40S ribosomal protein S12	RS12_RAT	0.036	CTR low	C high	L high	S low
Dynamin-1-like protein	DNM1L_RAT	0.014	CTR low	C high	L high	S low
Septin-9 (Fragment)	F1LN75_RAT	0.012	CTR low	C high	L high	S low
Proliferation-associated 2G4	Q6AYD3_RAT	0.026	CTR low	C high	L high	S low
Epithelial protein lost in neoplasm	F1LR10_RAT	0.036	CTR low	C high	L high	S low
Protein Tpd52	F1MAB9_RAT	0.032	CTR low	C high	L high	S low
Single-stranded DNA-binding protein	G3V7K6_RAT	0.031	CTR low	C high	L high	S low
40S ribosomal protein S10	RS10_RAT	0.022	CTR low	C high	L high	S low
Protein Vps4b	Q4KLL7_RAT	0.013	CTR low	C high	L high	S low
ARPC5_RAT Actin-related protein 2/3 complex subunit 5	Q4KLF8	0.011	CTR low	C high	L high	S low
Septin-2	SEPT2_RAT	0.040	CTR low	C high	L high	S low
Protein Chd4	E9PU01_RAT	0.050	CTR low	C high	L high	S low
Fabp4 protein	Q5XFV4_RAT	0.012	CTR low	C high	L high	S low
Isoform Crk-I of Adapter molecule crk	CRK_RAT	0.014	CTR low	C high	L high	S low
Lipoprotein lipase	LIPL_RAT	0.036	CTR low	C high	L high	S low
Crk-like protein	CRKL_RAT	0.016	CTR low	C high	L high	S low
Protein Dhx58	D3ZD46_RAT	0.023	CTR low	C high	L high	S low
Glyceraldehyde-3-phosphate dehydrogenase	D3ZWV2_RAT	0.033	CTR low	C high	L high	S low
cAMP-dependent protein kinase type II-beta regulatory subunit	KAP3_RAT	0.029	CTR low	C high	L high	S low
Granulocyte-macrophage colony stimulating receptor alpha	Q701L2_RAT	0.006	CTR low	C high	L high	S low
SEPT9_RAT Isoform 2 of Septin-9	Q9QZR6-2	0.018	CTR low	C high	L high	S low

D3ZUC9_RAT Oxidative-stress responsive 1 (Predicted)	D3ZUC9_RAT	0.030	CTR low	C high	L high	S low
ELOB_RAT Transcription elongation factor B polypeptide 2	P62870	0.011	CTR low	C high	L high	S low
Small glutamine-rich tetratricopeptide repeat-containing protein	SGTA_RAT	0.001	CTR low	C high	L high	S low
Peroxiredoxin-1	PRDX1_RAT	0.028	CTR low	C high	L low	S high
Protein U2af1	Q3KR55_RAT	0.048	CTR low	C high	L low	S high
Protein Hnrnpa0	F1M3H8_RAT	0.025	CTR low	C high	L low	S high
Elongation factor 1-alpha 1	EF1A1_RAT	0.038	CTR high	C low	L high	S low
Actin-related protein 2	ARP2_RAT	0.006	CTR high	C low	L high	S low
Unconventional myosin-Ic	MYO1C_RAT	0.043	CTR high	C low	L high	S low
HtrA serine peptidase 2	B0BNB9_RAT	0.011	CTR high	C low	L high	S low
Thioredoxin	THIO_RAT	0.019	CTR high	C low	L low	S high
Succinate dehydrogenase [ubiquinone] flavoprotein subunit, mitochondrial	SDHA_RAT	0.035	CTR high	C low	L low	S high
LDLR chaperone MESD	MESD_RAT	0.0003	CTR high	C low	L low	S high
Complement component 1 Q subcomponent-binding protein, mitochondrial	C1QBP_RAT	0.006	CTR high	C low	L low	S high
Cytochrome c oxidase subunit 4 isoform 1, mitochondrial	COX41_RAT	0.018	CTR high	C low	L low	S high
Lymphocyte cytosolic protein 1 OS	Q5XI38_RAT	0.050	CTR low	C low	L high	S high
V-type proton ATPase subunit B, brain isoform	VATB2_RAT	0.033	CTR low	C low	L high	S high
40S ribosomal protein S5	B0BN81_RAT	0.040	CTR low	C low	L high	S high
Catenin (Cadherin associated protein), delta 1 (Predicted), isoform CRA_a	D3ZZZ9_RAT	0.003	CTR low	C low	L high	S high
Heterogeneous nuclear ribonucleoprotein Q	HNRPQ_RAT	0.017	CTR low	C low	L high	S high
Apoptosis regulator BAX	G3V8T9_RAT	0.046	CTR low	C low	L high	S high
Hematopoietic cell specific Lyn substrate 1	Q68FX4_RAT	0.042	CTR low	C high	L low	S low
GTP-binding nuclear protein Ran	RAN_RAT	0.008	CTR low	C high	L low	S low

Ncf4 protein	B2RZ98_RAT	0.012	CTR low	C high	L low	S low
Protein LOC100912427	F1LPL7_RAT	0.019	CTR low	C high	L low	S low
40S ribosomal protein S17	RS17_RAT	0.001	CTR low	C high	L low	S low
Protein Tom1	Q5XI21_RAT	0.010	CTR low	C high	L low	S low
Elongation factor 1-delta	EF1D_RAT	0.028	CTR low	C high	L low	S low
Engulfment and cell motility 1, ced-12 homolog (C. elegans) (Predicted), isoform CRA_a	D3ZY46_RAT	0.005	CTR low	C high	L low	S low
LRRGT00066	Q6TUH8_RAT	0.002	CTR low	C high	L low	S low
Protein Snx6	B5DEY8_RAT	0.010	CTR low	C high	L low	S low
Protein Syap1	Q6AYB6_RAT	0.002	CTR low	C high	L low	S low
Pyrroline-5-carboxylate reductase 3	P5CR3_RAT	0.003	CTR low	C high	L low	S low
AP-1 complex subunit beta-1	G3V9N8_RAT	0.033	CTR low	C high	L low	S low
Prefoldin 5 (Predicted), isoform CRA_a	B5DFN4_RAT	0.047	CTR low	C high	L low	S low
Protein-L-isoaspartate(D-aspartate) O-methyltransferase	PIMT_RAT	0.006	CTR low	C high	L low	S low
Isoform Alpha of Interleukin-18	IL18_RAT	0.046	CTR low	C high	L low	S low
Protein Pin4	M0RCP9_RAT	0.019	CTR low	C high	L low	S low
GrpE protein homolog 1, mitochondrial	GRPE1_RAT	0.002	CTR low	C high	L low	S low
Protein Lsm12	D4A8G0_RAT	0.001	CTR low	C high	L low	S low
ATP-dependent Clp protease proteolytic subunit	M0RAD5_RAT	0.036	CTR low	C high	L low	S low
MAT2B_RAT Methionine adenosyltransferase 2 subunit beta	MAT2B_RAT	0.044	CTR low	C high	L low	S low
AHNAK 1 (Fragment)	Q38PF9_RAT	0.033	CTR low	C high	L low	S low
Mitochondrial import inner membrane translocase subunit Tim13	TIM13_RAT	0.023	CTR low	C high	L low	S low
Coiled-coil domain-containing protein 22	CCD22_RAT	0.026	CTR low	C high	L low	S low
Purine nucleoside phosphorylase	PNPH_RAT	0.025	CTR high	C low	L low	S low
Lipid phosphate phosphatase-related protein type 2	F1LRA5_RAT	0.008	CTR high	C low	L low	S low
Catalase	CATA_RAT	0.049	CTR high	C low	L low	S low
ADP/ATP translocase 2	ADT2_RAT	0.007	CTR high	C low	L low	S low

Interferon-induced GTP-binding protein Mx1	MX1_RAT	< 0.00010	CTR high	C low	L low	S low
Ras-related protein Rab-1A	E9PU16_RAT	0.017	CTR high	C low	L low	S low
N(4)-(Beta-N-acetylglucosaminyl)-L-asparaginase	ASPG_RAT	< 0.00010	CTR high	C low	L low	S low
Guanylate binding protein 2	Q5PQW8_RAT	< 0.00010	CTR high	C low	L low	S low
Interferon-induced protein with tetratricopeptide repeats 3	Q6AYE7_RAT	0.0002	CTR high	C low	L low	S low
26S proteasome non-ATPase regulatory subunit 1	PSMD1_RAT	0.016	CTR high	C low	L low	S low
ADP/ATP translocase 1	Q6P9Y4_RAT	0.007	CTR high	C low	L low	S low
Monocyte differentiation antigen CD14	O88955_RAT	0.022	CTR high	C low	L low	S low
Interleukin-1 alpha	IL1A_RAT	< 0.00010	CTR high	C low	L low	S low
Eukaryotic translation initiation factor 5A-1	IF5A1_RAT	0.048	CTR low	C low	L high	S low
Biliverdin reductase B (Flavin reductase (NADPH))	B5DF65_RAT	0.001	CTR low	C low	L high	S low
Eukaryotic translation initiation factor 2, subunit 2 (Beta)	Q6P685_RAT	0.020	CTR low	C low	L high	S low
Perilipin	M0RA08_RAT	0.039	CTR low	C low	L high	S low
Protein Diap1	F1M775_RAT	0.040	CTR low	C low	L high	S low
Protein Snrpa	Q5U214_RAT	0.013	CTR low	C low	L high	S low
Glutathione S-transferase alpha-3	GSTA3_RAT	0.021	CTR low	C low	L high	S low
Ethylmalonic encephalopathy 1	B0BNJ4_RAT	0.004	CTR low	C low	L high	S low
WW domain binding protein 2, isoform CRA_b	G3V721_RAT	0.019	CTR low	C low	L high	S low
Syntaxin-7	STX7_RAT	0.047	CTR low	C low	L high	S low
Cysteine and glycine-rich protein 1	CSRP1_RAT	0.013	CTR low	C low	L high	S low
LOC684322 protein	B2RZ97_RAT	0.002	CTR low	C low	L high	S low
COP9 signalosome complex subunit 8	CSN8_RAT	0.042	CTR low	C low	L high	S low
Clathrin light chain A	CLCA_RAT	0.003	CTR low	C low	L high	S low
Glia maturation factor beta	GMFB_RAT	0.007	CTR low	C low	L high	S low
Putative phospholipase B-like 2	PLBL2_RAT	0.001	CTR low	C low	L high	S low
Olfactory receptor	Q6ZMA1_RAT	0.0002	CTR low	C low	L high	S low
Voltage-dependent anion-selective channel protein 1	VDAC1_RAT	0.001	CTR low	C low	L low	S high

Synaptic vesicle membrane protein VAT-1 homolog	VAT1_RAT	0.026	CTR low	C low	L low	S high
Ab2-162	Q7TP54_RAT	0.001	CTR low	C low	L low	S high
Protein S100-A10	S10AA_RAT	0.021	CTR low	C low	L low	S high
Ferritin (Fragment)	Q5FVS1_RAT	0.001	CTR low	C low	L low	S high
Protein Itih2	D3ZFH5_RAT	0.015	CTR low	C low	L low	S high
Aldose reductase	ALDR_RAT	0.023	CTR low	C low	L low	S high
Ras-related protein Rab-11B	RB11B_RAT	0.014	CTR low	C low	L low	S high
V-type proton ATPase subunit C 1	VATC1_RAT	0.011	CTR low	C low	L low	S high
NOL1/NOP2/Sun domain family, member 2 (Predicted)	D4A3S8_RAT	0.038	CTR low	C low	L low	S high
Protein Serpinc1	Q5M7T5_RAT	0.038	CTR low	C low	L low	S high
Growth/differentiation factor 15	GDF15_RAT	< 0.00010	CTR low	C low	L low	S high
Anamorsin	CPIN1_RAT	No significance	CTR low	C high	L high	S high
Ubiquitin-like-conjugating enzyme ATG3	ATG3_RAT	No significance				
Annexin	Q6IRJ7_RAT	No significance				
Bcl-x short	Q9WUI5_RAT	No significance				

Figure 3.13: Total protein–protein interaction (PPI) network of surfactant exposed LPS-stimulated NR8383 AMs visualised by STRING v10.5. In this view, only associated proteins are shown and the colour saturation of the edges represents the confidence score of a functional association.

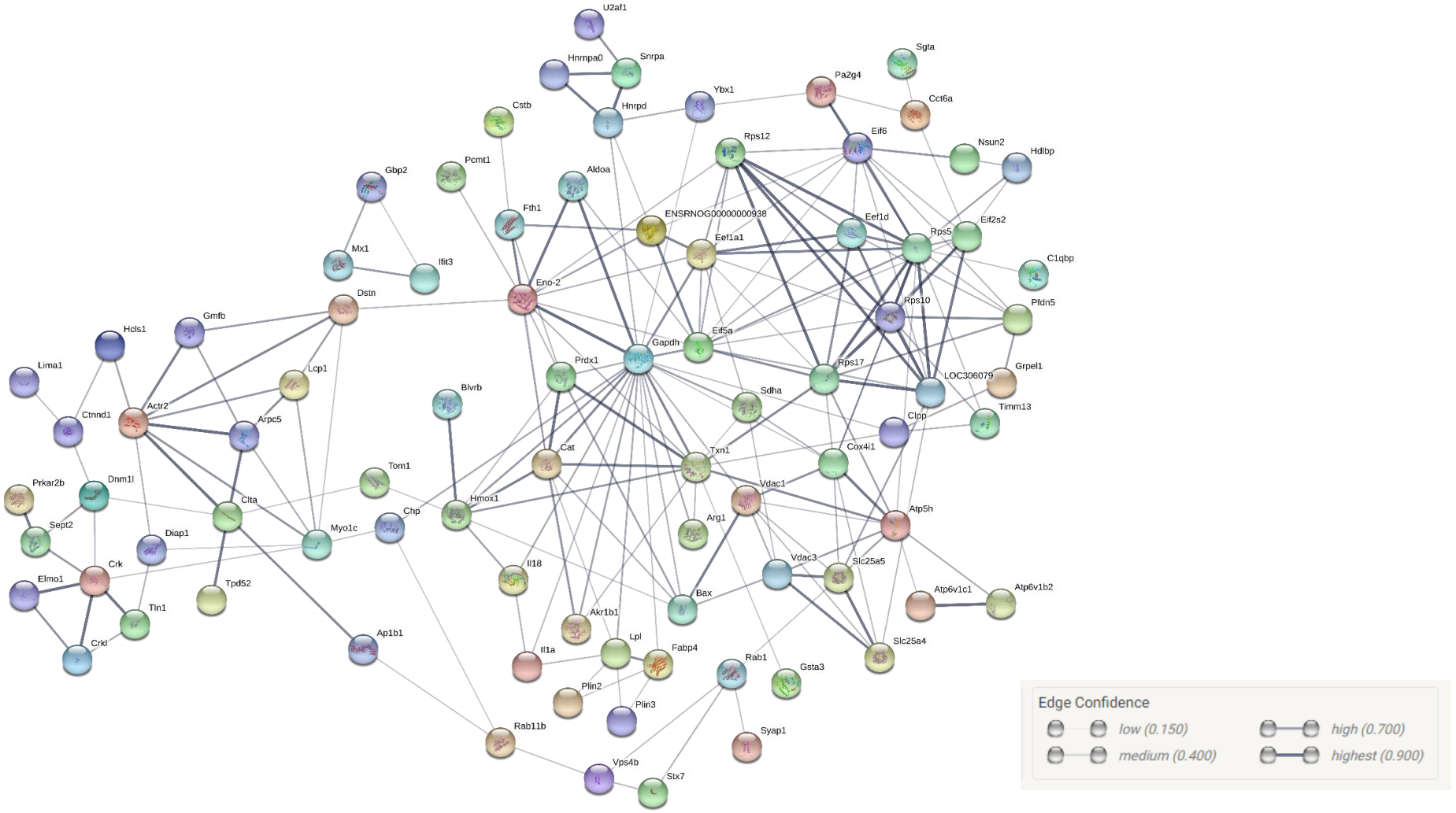

Table 3.6: List of proteins expressed in the Curosurf® exposed LPS-stimulated NR8383 AMs only.

Bio View: Identified Proteins	Accession Number
Glyceraldehyde-3-phosphate dehydrogenase	G3P_RAT
Chaperonin containing Tcp1, subunit 6A (Zeta 1)	Q3MHS9_RAT
Hematopoietic cell specific Lyn substrate 1	Q68FX4_RAT
GTP-binding nuclear protein Ran	RAN_RAT
Interferon-induced GTP-binding protein Mx1	MX1_RAT
Epithelial protein lost in neoplasm	F1LR10_RAT
Ncf4 protein	B2RZ98_RAT
Protein LOC100912427	F1LPL7_RAT
Arginase-1	ARGI1_RAT
40S ribosomal protein S17	RS17_RAT
Protein Tom1	Q5XI21_RAT
MAP4_RAT	MAP4_RAT
Elongation factor 1-delta	EF1D_RAT
Engulfment and cell motility 1, ced-12 homolog (C. elegans) (Predicted), isoform CRA_a	D3ZY46_RAT
LRRGT00066	Q6TUH8_RAT
Protein Snx6	B5DEY8_RAT
Interferon-induced protein with tetratricopeptide repeats 3	Q6AYE7_RAT
RNA-binding motif protein, X chromosome retrogene-like	RMXRL_RAT
Protein Syap1	Q6AYB6_RAT
Pyrroline-5-carboxylate reductase 3	P5CR3_RAT
AP-1 complex subunit beta-1	G3V9N8_RAT
Prefoldin 5 (Predicted), isoform CRA_a	B5DFN4_RAT
Protein-L-isoaspartate(D-aspartate) O-methyltransferase	PIMT_RAT
Isoform Alpha of Interleukin-18	IL18_RAT
Protein Pin4	M0RCP9_RAT
GRPE1_RAT GrpE protein homolog 1, mitochondrial	GRPE1_RAT
Protein Lsm12	D4A8G0_RAT
ATP-dependent Clp protease proteolytic subunit	M0RAD5_RAT
Methionine adenosyltransferase 2 subunit beta	MAT2B_RAT
AHNAK 1 (Fragment)	Q38PF9_RAT
Mitochondrial import inner membrane translocase subunit Tim13	TIM13_RAT
Coiled-coil domain-containing protein 22	CCD22_RAT

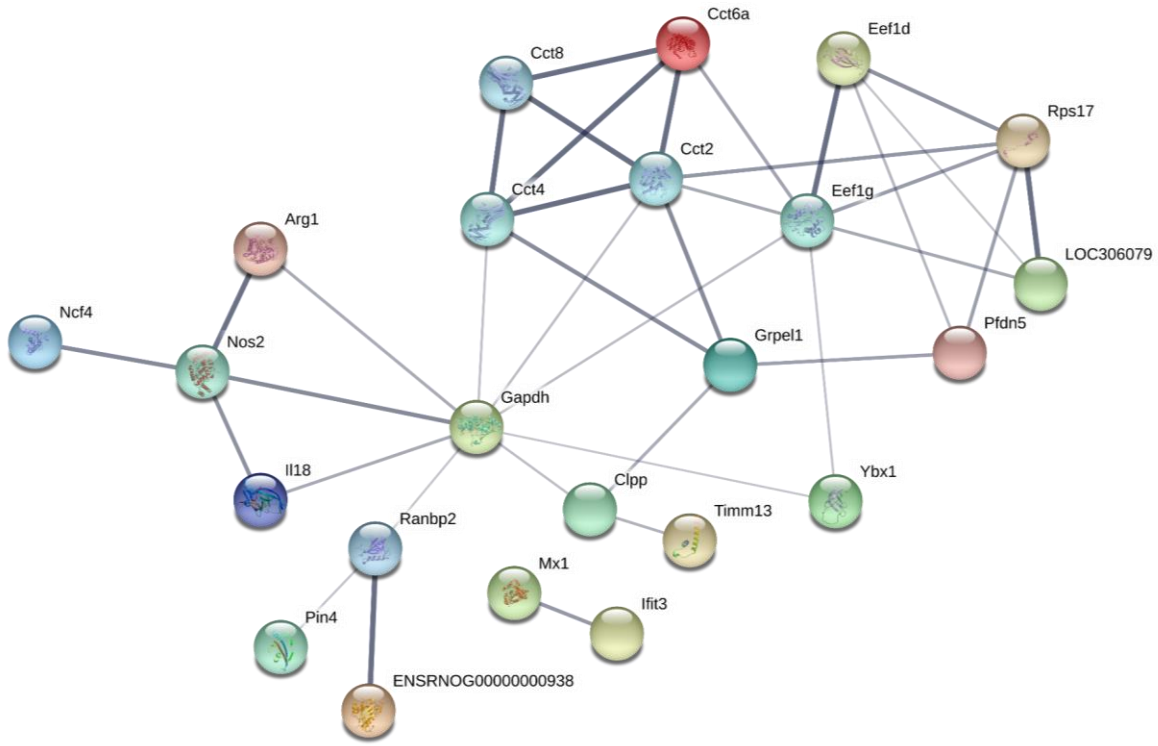

Figure 3.14: Protein–protein interaction (PPI) network visualised by STRING v10.5 for Curosurf® exposed LPS-stimulated NR8383 AMs. In this view, only associated proteins are shown and the colour saturation of the edges represents the confidence score of a functional association.

The above STRING network is visualised from Table 3.6 for Curosurf®. The proposed statistical enrichment analysis in Figure 3.14 of annotated functions for protein–protein interactions (PPI) was investigated further. The functional PPI enrichment (GO terms) for Curosurf® that displayed any significance (*P* value: 5.57 x 10^{-3}) was associated with the molecular function for the biosynthesis of amino acids, but more specifically for arginase activity (arginine metabolism) (False discovery rate (FDR) 6.89E-04). According to this data and the co-expression of IL-18 and IL-6 (albeit decreased) within the Curosurf® population, another PPI enrichment analysis (*P* value: 1.3 x 10^{-6}) was run with these proteins separately (Figure 3.15).

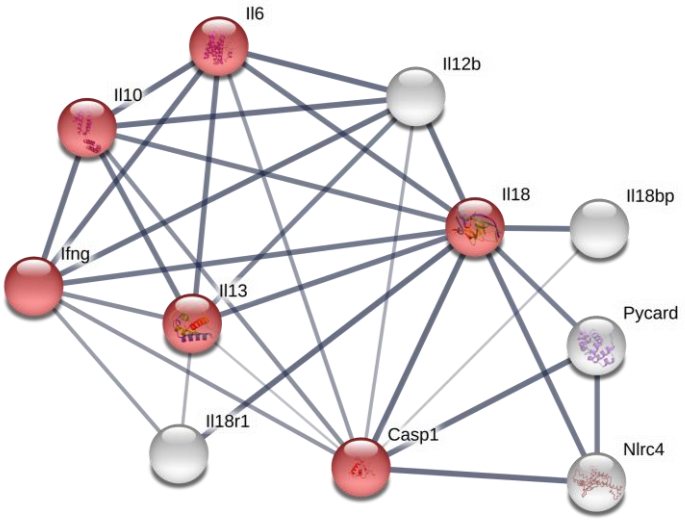

Figure 3.15: Protein–protein interaction (PPI) network visualised by STRING v10.5 for Curosurf® exposed LPS-stimulated NR8383 AMs. In this view, only associated proteins are shown and the colour saturation of the edges represents the confidence score of a functional association. ● Red nodes indicate first shell interactors of direct physical association; ○ White nodes indicate second shell interactors of indirect functional association.

Figure 3.15 displays the STRING network for the selected PPI for Curosurf® exposed LPS-stimulated AMs. The proposed statistical enrichment analysis for Figure 3.15 displayed a PPI enrichment *P* value of 1.3×10^{-6}. The functional PPI enrichment (GO terms) associated with this network can be seen in Table 3.7; all of which are associated with the positive regulation of cytokine production (FDR 5.17E-08) and the positive regulation of apoptotic process (FDR 1.02E-06) (See Chapter 2: Viability Study).

Table 3.7: The GO term (biological process) enrichment analysis for Curosurf® exposed LPS-stimulated NR8383 AMs is seen below. The proposed statistical enrichment analysis of annotated functions for protein–protein interaction (PPI) *P*-value: 1.3 x 10^{-6} and the false discovery rates (FDR) are included relative to presentation that would occur by chance.

#Pathway ID	Pathway description	Observed gene count	False discovery rate	Matching proteins in your network (labels)
GO.0001819	Positive regulation of cytokine production	6	5.17E-08	Casp1, Ifng, Il10, Il13, Il18, Il6
GO.0050670	Regulation of lymphocyte proliferation	5	1.87E-07	Ifng, Il10, Il13, Il18, Il6
GO.0043065	Positive regulation of apoptotic process	6	1.02E-06	Casp1, Ifng, Il10, Il18, Il6, Nlrc4
GO.0050714	Positive regulation of protein secretion	5	1.02E-06	Casp1, Ifng, Il10, Il13, Il6
GO.0050864	Regulation of B cell activation	4	1.02E-06	Ifng, Il10, Il13, Il6
GO.0002700	Regulation of production of molecular mediator of immune response	4	1.99E-06	Ifng, Il10, Il13, Il6
GO.0046427	Positive regulation of JAK-STAT cascade	4	1.99E-06	Ifng, Il10, Il13, Il6
GO.0050671	Positive regulation of lymphocyte proliferation	4	2.05E-06	Ifng, Il13, Il18, Il6
GO.0050707	Regulation of cytokine secretion	4	4.02E-06	Casp1, Ifng, Il10, Il6
GO.0032731	Positive regulation of interleukin-1 beta production	3	5.60E-06	Casp1, Ifng, Il18
GO.0002684	Positive regulation of immune system process	5	1.19E-05	Ifng, Il13, Il18, Il6, Nlrc4
GO.0006954	Inflammatory response	5	1.19E-05	Il10, Il13, Il18, Il6, Nlrc4
GO.0002639	Positive regulation of immunoglobulin production	3	1.26E-05	Ifng, Il13, Il6
GO.0048660	Regulation of smooth muscle cell proliferation	4	1.32E-05	Ifng, Il13, Il18, Il6
GO.0032722	Positive regulation of chemokine production	3	1.46E-05	Ifng, Il18, Il6
GO.2000377	Regulation of reactive oxygen species metabolic process	4	1.60E-05	Ifng, Il10, Il18, Il6
GO.0009617	Response to bacterium	5	2.95E-05	Casp1, Ifng, Il13, Il18, Nlrc4
GO.0050871	Positive regulation of B cell activation	3	2.95E-05	Ifng, Il13, Il6

GO.0050730	Regulation of peptidyl-tyrosine phosphorylation	4	3.02E-05	Ifng, Il13, Il18, Il6
GO.0006955	Immune response	5	3.73E-05	Il10, Il13, Il18, Il6, Nlrc4
GO.0042102	Positive regulation of T cell proliferation	3	4.00E-05	Ifng, Il18, Il6
GO.0050778	Positive regulation of immune response	4	4.11E-05	Ifng, Il13, Il6, Nlrc4
GO.0042035	Regulation of cytokine biosynthetic process	3	4.28E-05	Ifng, Il10, Il6
GO.0001781	Neutrophil apoptotic process	2	4.67E-05	Ifng, Il6
GO.0042531	Positive regulation of tyrosine phosphorylation of STAT protein	3	4.94E-05	Ifng, Il13, Il6
GO.0045321	Leukocyte activation	4	4.94E-05	Casp1, Ifng, Il13, Il6
GO.0043066	Negative regulation of apoptotic process	5	8.33E-05	Il10, Il13, Il18, Il6, Nlrc4
GO.0050715	Positive regulation of cytokine secretion	3	8.61E-05	Casp1, Ifng, Il10
GO.0032680	Regulation of tumor necrosis factor production	3	9.73E-05	Ifng, Il10, Il18
GO.0045428	Regulation of nitric oxide biosynthetic process	3	9.73E-05	Ifng, Il10, Il6
GO.0006952	Defence response	5	0.000101	Ifng, Il13, Il18, Il6, Nlrc4
GO.0001817	Regulation of cytokine production	4	0.000119	Casp1, Ifng, Il13, Il18
GO.0032675	Regulation of interleukin-6 production	3	0.00012	Ifng, Il10, Il6
GO.0051222	Positive regulation of protein transport	4	0.000156	Casp1, Ifng, Il10, Il13
GO.0050708	Regulation of protein secretion	4	0.000169	Casp1, Ifng, Il10, Il13
GO.0001780	Neutrophil homeostasis	2	0.000176	Ifng, Il6
GO.2000379	Positive regulation of reactive oxygen species metabolic process	3	0.000226	Ifng, Il18, Il6
GO.0045073	Regulation of chemokine biosynthetic process	2	0.000268	Ifng, Il6
GO.0045348	Positive regulation of MHC class II biosynthetic process	2	0.000268	Ifng, Il10
GO.0002250	Adaptive immune response	3	0.000281	Ifng, Il18, Il6

Table 3.8: List of proteins expressed in the Liposurf® exposed LPS-stimulated NR8383 AMs only.

Bio View: Identified Proteins	Accession Number
Fructose-bisphosphate aldolase A	ALDOA_RAT
Cystatin-B	CYTB_RAT
Eukaryotic translation initiation factor 5A-1	IF5A1_RAT
Purine nucleoside phosphorylase	PNPH_RAT
Elongation factor 1-alpha 1	EF1A1_RAT
Biliverdin reductase B (Flavin reductase (NADPH))	B5DF65_RAT
Catalase	CATA_RAT
Actin-related protein 2	ARP2_RAT
Eukaryotic translation initiation factor 2, subunit 2 (Beta)	Q6P685_RAT
Protein Vps4b	Q4KLL7_RAT
Perilipin	M0RA08_RAT
Protein Diap1	F1M775_RAT
Protein Snrpa PE=2 SV=1	Q5U214_RAT
HtrA serine peptidase 2	B0BNB9_RAT
Glutathione S-transferase alpha-3	GSTA3_RAT
Ethylmalonic encephalopathy 1	B0BNJ4_RAT
WW domain binding protein 2, isoform CRA_b	G3V721_RAT
Syntaxin-7	STX7_RAT
Cysteine and glycine-rich protein 1	CSRP1_RAT
LOC684322 protein	B2RZ97_RAT
COP9 signalosome complex subunit 8	CSN8_RAT
Clathrin light chain A	CLCA_RAT
Glia maturation factor beta	GMFB_RAT
Putative phospholipase B-like 2	PLBL2_RAT
Olfactory receptor	Q6ZMA1_RAT

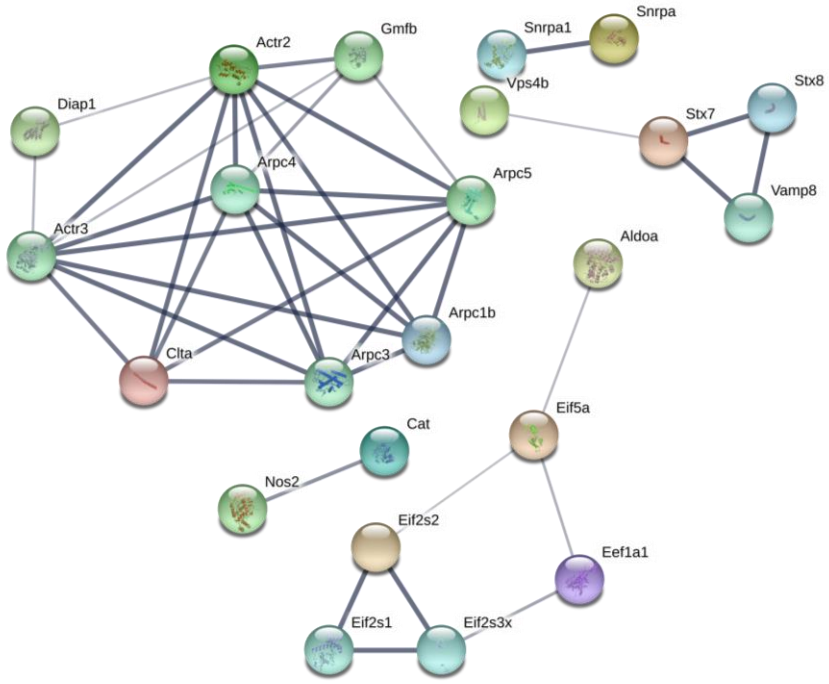

Figure 3.16: Protein–protein interaction (PPI) network visualised by STRING v10.5 for Liposurf® exposed LPS-stimulated NR8383 AMs. In this view, only associated proteins are shown and the colour saturation of the edges represents the confidence score of a functional association.

The above STRING network is visualised from Table 3.8 for Liposurf®. The proposed statistical enrichment analysis in Figure 3.16 of annotated functions for the PPI was investigated further. The functional PPI enrichment (GO terms) for Liposurf® that displayed any significant enrichment value (*P* value: 3.87 x 10^{-4}) was associated with the biological process (GO:0071822; Actr2, Actr3, Aldoa, Arpc5, Cat, Eef1a1, Vamp8) of protein complex subunit organisation (FDR 0.0367) that is linked to actin polymerisation of the structural cytoskeleton (FDR 3.65E-06) and the regulation thereof. This is verified in Figure 2.23F (Chapter 2, page 92) where the rearrangement of the cytoskeleton can be seen via the formation of filopodia/lamellopodia.

Table 3.9: List of proteins expressed in the Synsurf® exposed LPS-stimulated NR8383 AMs only.

Bio View: Identified Proteins	Accession Number
Voltage-dependent anion-selective channel protein 1	VDAC1_RAT
Peroxiredoxin-1	PRDX1_RAT
Synaptic vesicle membrane protein VAT-1 homolog	VAT1_RAT
Ab2-162	Q7TP54_RAT
Thioredoxin	THIO_RAT
Protein S100-A10	S10AA_RAT
Ferritin (Fragment)	Q5FVS1_RAT
Succinate dehydrogenase [ubiquinone] flavoprotein subunit, mitochondrial	SDHA_RAT
LDLR chaperone MESD	MESD_RAT
Protein Itih2	D3ZFH5_RAT
Aldose reductase	ALDR_RAT
Complement component 1 Q subcomponent-binding protein, mitochondrial	C1QBP_RAT
Ras-related protein Rab-11B	RB11B_RAT
V-type proton ATPase subunit C 1	VATC1_RAT
NOL1/NOP2/Sun domain family, member 2 (Predicted)	D4A3S8_RAT
Protein Serpinc1	Q5M7T5_RAT
Cytochrome c oxidase subunit 4 isoform 1, mitochondrial	COX41_RAT
Calcineurin B homologous protein 1	CHP1_RAT
Growth/differentiation factor 15	GDF15_RAT

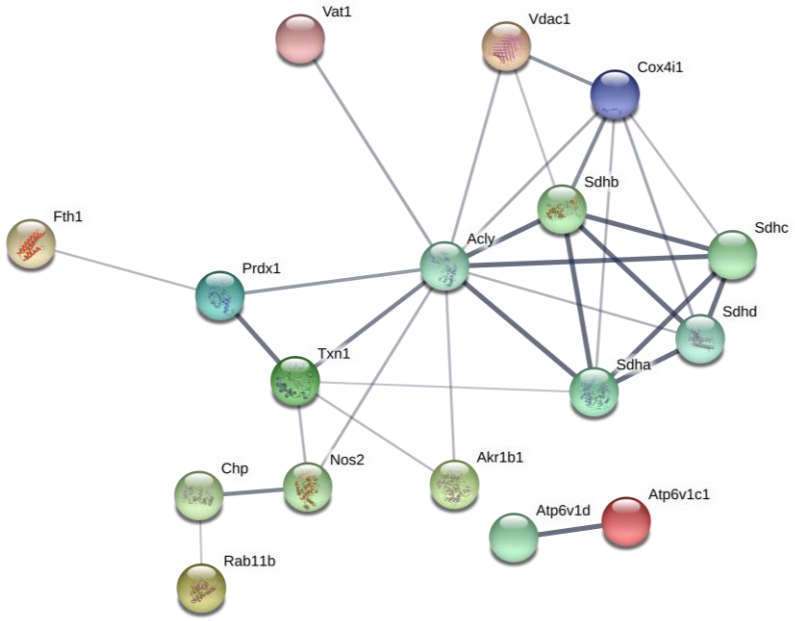

Figure 3.17: Protein–protein interaction (PPI) network visualised by STRING for Synsurf® exposed LPS-stimulated NR8383 AMs. In this view, only associated proteins are shown and the colour saturation of the edges represents the confidence score of a functional association.

The above STRING network is visualised from Table 3.9 for Synsurf®. The proposed statistical enrichment analysis in Figure 3.17 of annotated functions for PPI was investigated further. The functional PPI enrichment (GO terms) for Synsurf® that displayed any significant enrichment value (*P* value: 1.14 x 10^{-6}) was associated with the biological process of oxidation-reduction (GO:0055114) with a FDR of 2.76E-03. This biological process is linked to the molecular function of oxidoreductase activity (GO:0016491) with a FDR of 1.42E-05 and the regulation thereof (Table 3.10).

Table 3.10: The GO term (biological process) enrichment analysis for Synsurf® exposed LPS-stimulated NR8383 AMs is seen below. The proposed statistical enrichment analysis of annotated functions for protein–protein interaction (PPI) *P*-value: 1.14 x 10^{-6} and the false discovery rates (FDR) are included relative to presentation that would occur by chance.

#Pathway ID	Pathway description	Observed gene count	False discovery rate	Matching proteins in your network (labels)
GO:0055114	Oxidation-reduction	7	2.76E-03	Cox4i1, Fth1, Prdx1, Sdha, Sdhb, Txn1, Vat1
GO:0016491	Oxidoreductase activity	8	1.42E-05	Cox4i1, Fth1, Prdx1, Sdha, Sdhb, Sdhd, Txn1, Vat1

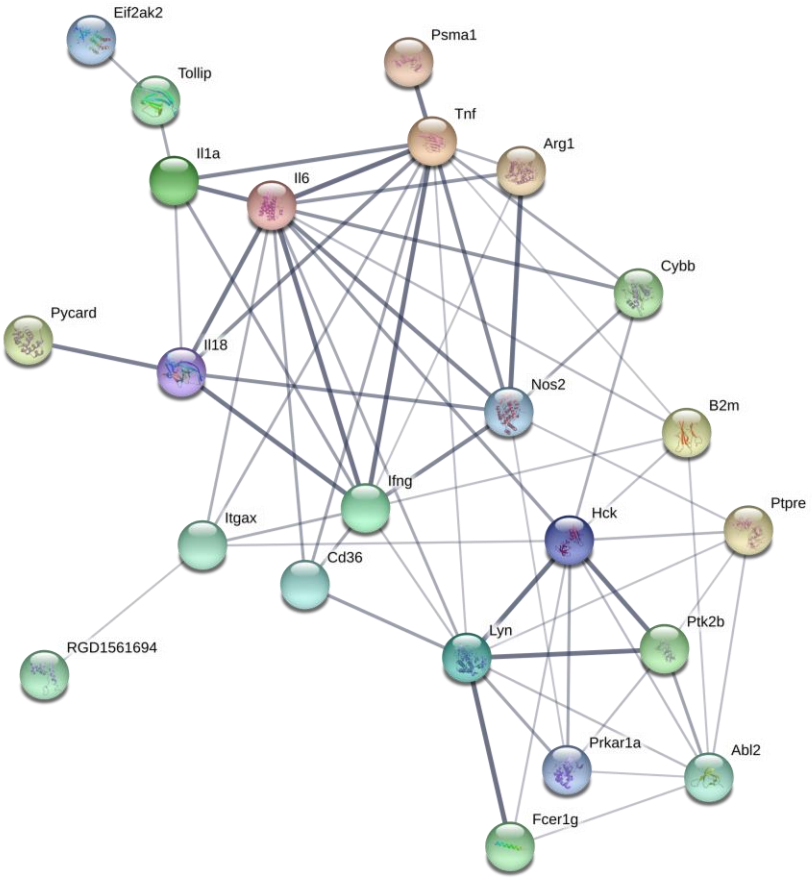

Figure 3.18: The proposed protein–protein interaction (PPI) network visualised by STRING v10.5 for combined surfactant exposed LPS-stimulated NR8383 AMs. In this view, associated proteins are connected and the colour saturation of the edges represents the confidence score of a functional association. STRING displays every functional pathway/term that can be associated. The (biological process) enrichment analysis as seen in Table 3.11.

The proposed PPI interaction for surfactant exposed LPS-stimulated AMs related to the inflammatory process only can be seen in Figure 3.18. The proposed statistical enrichment analysis (*P* value: 1.37 x 10^{-8}) for the annotated functions was investigated further and can be seen in Table 3.11. Although not all proteins were found to be present in the separate surfactant groups, associated proteins are automatically included due to functional regulatory relevance in said pathway. One can therefore assume that these proteins are regulated via association.

Table 3.11: GO term (biological process) enrichment analysis for combined surfactant exposed LPS-stimulated NR8383 AMs (only relevant GO terms are included). Protein–protein interaction (PPI) enrichment analysis *P* value: 1.37 x 10^{-8} and false discovery rate included relative to presentation that would occur by chance.

#Pathway ID	Pathway description	Observed gene count	False discovery rate	Matching proteins in your network (labels)
GO.0002376	Immune system process	19	3.53E-17	Arhgef2, B2m, C1qbp, Card9, Ctsh, Eif2ak2, Fcer1g, Hck, Il1a, Lgals3, Nlrx1, Oasl, Otub1, Pnp, Psma1, Ptk2b, Skap2, Tollip, Trim28
GO.0006955	Immune response	16	1.01E-16	Arhgef2, C1qbp, Card9, Ctsh, Eif2ak2, Fcer1g, Hck, Il1a, Lgals3, Lyn, Nlrx1, Oasl,Pnp, Ptk2b, Tollip, Trim28
GO.0045087	Innate immune response	12	1.06E-13	Arhgef2, C1qbp, Card9, Eif2ak2, Hck, Lgals3, Lyn, Nlrx1, Oasl, Ptk2b, Tollip, Trim28
GO.0006952	Defence response	14	6.58E-12	Arhgef2, C1qbp, Card9, Eif2ak2, Fcer1g, Hck, Il1a, Lgals3, Lyn, Nlrx1, Oasl, Ptk2b, Tollip, Trim28
GO.0002682	Regulation of immune system process	11	1.74E-08	B2m, C1qbp, Card9, Ctsh, Eif2ak2, Fcer1g, Il1a, Pnp, Psma1, Ptpre, Tap1
GO.0002250	Adaptive immune response	6	4.33E-07	C1qbp, Ctsh, Fcer1g, Ifng, Il18, Il6
GO.0042981	Regulation of apoptotic process	12	4.33E-07	C1qbp, Card9, Ctsh, Eif2ak2, Fcer1g, Hck, Ifng, Il18, Lgals3, Lyn, Ptk2b, Tnf

Due to the involvement of NOS and Arginase in L-Arginine metabolism for M2 polarised AMs, it is therefore necessary to include them within their own PPI network (enrichment *P* value: 2.9 x 10^{-2}) which can be seen in Figure 3.19. These PPIs are central in the arginine metabolic process (FDR 1.24E-05) and to the INF-γ cellular response (FDR 1.78E-05). All surfactant exposed LPS stimulated AMs showed NOS2 expression, however, only the Curosurf® group displayed significant upregulated Arginase I.

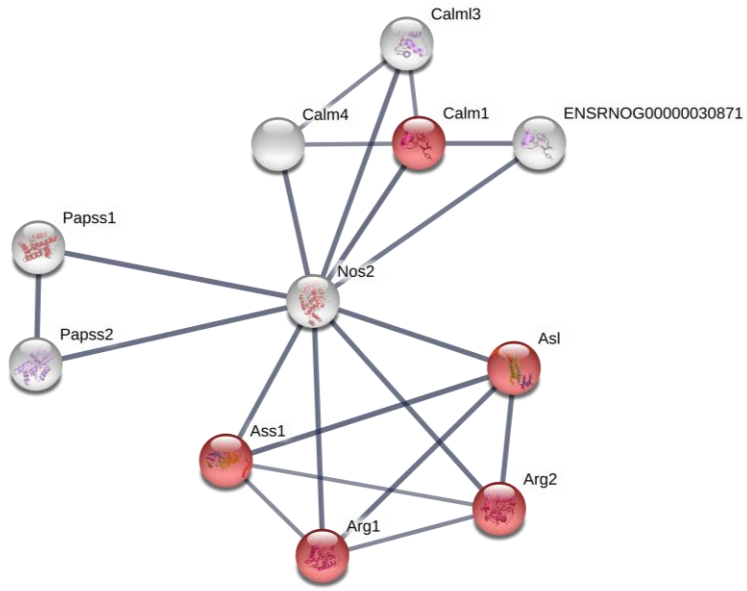

Figure 3.19: Protein–protein interaction (PPI) network visualised by STRING v10.5 for NOS2 and Arg. In this view, associated proteins are connected and the colour saturation of the edges represent the confidence score of a functional association. STRING analysis displays every functional pathway/term that can be associated. ● Red nodes indicate first shell interactors of physical association; ○ White nodes indicate second shell interactors of function association.

3.2.3 Effect of Surfactant on Human BAL derived Macrophages' Cytokine Secretion

After informed consent, a total of 30 paediatric patients' BAL samples were collected. After sample processing and cell counting, the desirable samples were seeded in appropriate densities for the treatment protocol. Other, less desirable cell populations were discarded from the study.

As shown in Figure 3.20, the representative hematoxylin and eosin (H&E) staining indicate different cell populations found in BAL samples. Figure 3.20A & B demonstrated a greater population of neutrophils, such populations were excluded from the current study as macrophage initiated cytokine release was focused on. Figure 3.20C & D indicates the optimal cell population that was used as a standard for the appropriation of the study.

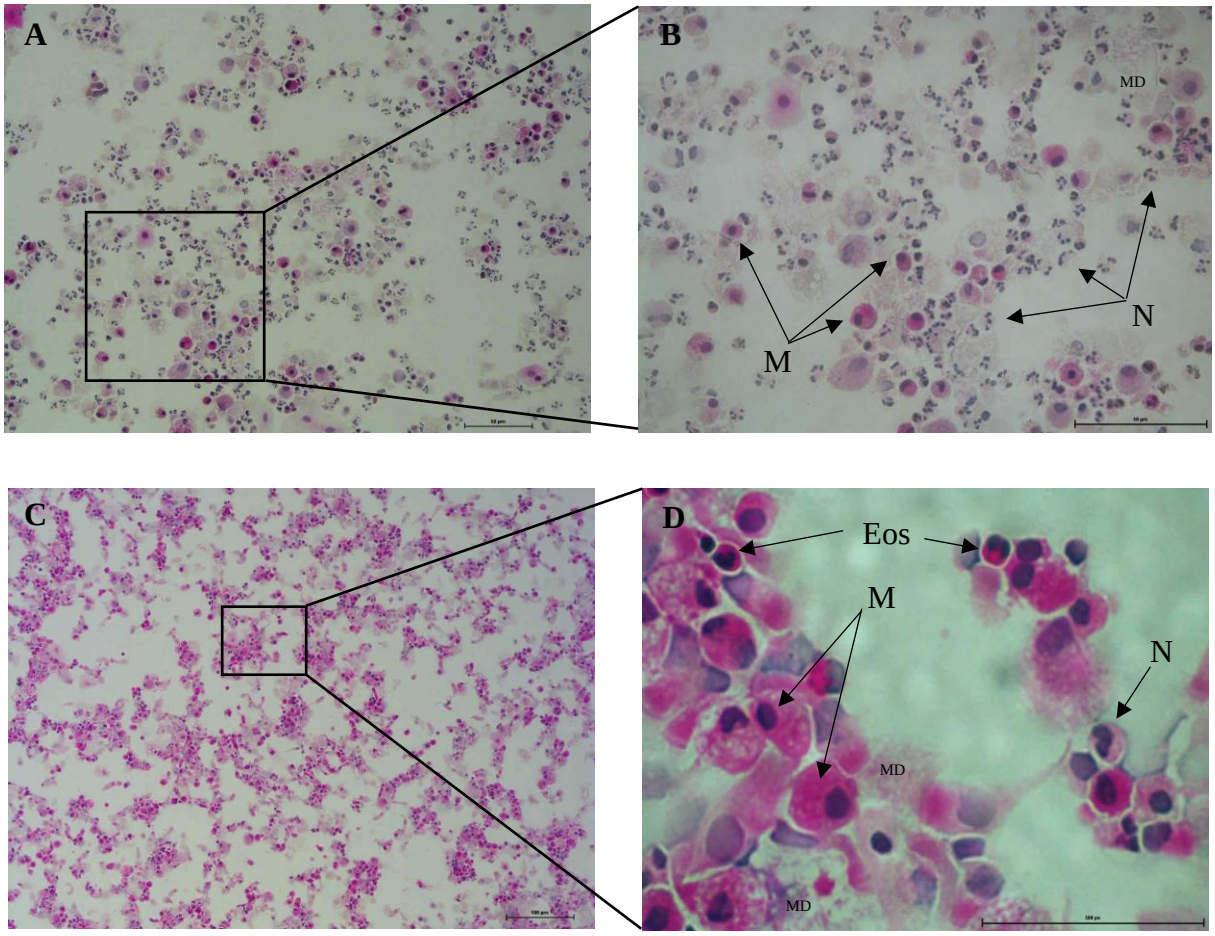

Figure 3.20: H&E staining of human BAL sample after mononuclear cell isolation from patient diagnosed with asthma **(A) & (B)** and a healthy patient with an airway obstruction **(C) & (D)**; **M**: Macrophage, **N**: Neutrophil, **Eos**: Eosinophil, **MD**: Mucus debris. Scale bar represents: **(A) & (B)** 50µm, **(C)** 100 µm, **(D)** 500 px.

Table 3.12 - Table 3.20 represent the results of stimulated macrophage secretion of the nine inflammatory cytokines studied. Comparison of the different surfactants studied with regards to inflammatory and anti-inflammatory cytokine secretion did not reveal significant differences, therefore, data representation is more effective within descriptive statistical analysis.

Although the aim of this determination was to assess spontaneous release of cytokines by LPS-stimulated AM due to surfactant exposure, it should be noted that under these conditions cytokines produced by the actual adherence of AMs to the polystyrene dishes might act as modulatory factors as indicated by the control.

Overall comparison of the secretion of the different cytokines revealed that under LPS stimulated conditions, AMs secrete low amounts of IL-1β (in the 0.25 – 200 pg/10^6 cells range), IL-2 (0.1 - 7 pg/ml) and IFN-γ (5 pg/ml). Increased GM-CSF (100 pg/ml), TNF-α and IL-6 (400 - 600 pg/10^6 cells) and large amounts of IL-8 (3.5 ng/10^6 cells) were seen. The pro-inflammatory cytokine secretion was decreased (compared to control levels) in all three surfactant groups after 24h exposure.

The anti-inflammatory cytokines, IL-10 and IL-12, were also seen to be secreted at low levels under LPS-stimulated conditions but exhibited the opposite nature to the pro-inflammatory cytokines by an increasing in secretion when exposed to surfactants.

Table 3.12: The mean, SD (standard deviation), P25 (25th percentile), P50 (median), & P75 (75th percentile) of LPS (1 µg/ml)-stimulated IL-1βin BAL-derived human alveolar macrophage supernatant concentrations measured at 24h in the presence of surfactants.

IL-1β (pg/ml)				
	Control	**Curosurf®**	**Liposurf®**	**Synsurf®**
N	3	7	7	7
Mean	**176.45**	**168.87**	**118.01**	**97.60**
SD	305.32	292.62	210.07	166.01
P25	0.09	0.30	0.34	0.27
P50	0.25	0.39	1.29	0.60
P75	529	495.5	300.5	332

Table 3.13: The mean, SD (standard deviation), P25 (25th percentile), P50 (median), & P75 (75th percentile) of LPS (1 µg/ml)-stimulated IL-2 in BAL-derived human alveolar macrophage supernatant concentrations measured at 24h in the presence of surfactants.

IL2 (pg/ml)				
	Control	**Curosurf®**	**Liposurf®**	**Synsurf®**
N	3	5	5	7
Mean	**7.61**	**5.16**	**4.38**	**10.91**
SD	1126	7.77	5.84	19.03
P25	0.0170	0.14	0.22	0.14
P50	0.0722	0.38	0.022	0.31
P75	1951	7.25	8.86	27.45

Table 3.14: The mean, SD (standard deviation), P25 (25th percentile), P50 (median), & P75 (75th percentile) of LPS (1 µg/ml)-stimulated IL-6 in BAL-derived human alveolar macrophage supernatant concentrations measured at 24h in the presence of surfactants.

IL6 (pg/ml)				
	Control	**Curosurf®**	**Liposurf®**	**Synsurf®**
N	3	7	6	6
Mean	**650.4**	**452.78**	**321.08**	**265.70**
SD	1126	815.29	634.03	412.02
P25	0.0170	0.17	0.07	0.14
P50	0.0722	0.29	0.18	0.24
P75	1951	1134	341	759.5

Table 3.15: The mean, SD (standard deviation), P25 (25th percentile), P50 (median), & P75 (75th percentile) of LPS (1 µg/ml)-stimulated IL-8 in BAL-derived human alveolar macrophage supernatant concentrations measured at 24h in the presence of surfactants.

IL8 (pg/ml)				
	Control	**Curosurf®**	**Liposurf®**	**Synsurf®**
N	3	7	7	7
Mean	**3588**	**3193.71**	**3139.73**	**3101.79**
SD	6020	5153.64	5081.01	4997.25
P25	55.35	89	84.5	95.75
P50	169.0	249.5	251	198.5
P75	10540	10532.5	10316.5	10273

Table 3.16: The mean, SD (standard deviation), P25 (25th percentile), P50 (median), & P75 (75th percentile) of LPS (1 µg/ml)-stimulated TNF-α in BAL-derived human alveolar macrophage supernatant concentrations measured at 24h in the presence of surfactants.

TNF-α (pg/ml)				
	Control	**Curosurf®**	**Liposurf®**	**Synsurf®**
N	1	6	4	6
Mean	**462**	**120.73**	**110.01**	**56.87**
SD	-	195.09	181.01	99.96
P25	-	0.08	0.10	0.08
P50	-	0.13	30.98	0.13
P75	-	273.5	219.93	95.35

Table 3.17: The mean, SD (standard deviation), P25 (25th percentile), P50 (median), & P75 (75th percentile) of LPS (1 µg/ml)-stimulated INF-γin BAL-derived human alveolar macrophage supernatant concentrations measured at 24h in the presence of surfactants.

INF-γ (pg/ml)				
	Control	**Curosurf®**	**Liposurf®**	**Synsurf®**
N	2	5	4	5
Mean	**5.771**	**1.93**	**3.06**	**1.12**
SD	8.039	2.50	4.80	0.85
P25	0.0864	0.28	0.45	0.55
P50	5.771	0.49	0.82	0.60
P75	11.46	2.57	5.68	1.75

Table 3.18: The mean, SD (standard deviation), P25 (25th percentile), P50 (median), & P75 (75th percentile) of LPS (1 µg/ml)-stimulated GM-CSF in BAL-derived human alveolar macrophage supernatant concentrations measured at 24h in the presence of surfactants.

GM-CSF (pg/ml)				
	Control	**Curosurf®**	**Liposurf®**	**Synsurf®**
N	3	7	7	7
Mean	**114.1**	**84.50**	**61.89**	**62.33**
SD	197.3	157.67	129.10	107.94
P25	0.1176	0.28	0.21	0.06
P50	0.2565	0.35	0.42	0.22
P75	342.0	183	86.3	184

Table 3.19: The mean, SD (standard deviation), P_{25} (25th percentile), P_{50} (median), & P_{75} (75th percentile) of LPS (1 µg/ml)-stimulated IL-10 in BAL-derived human alveolar macrophage supernatant concentrations measured at 24h in the presence of surfactants.

IL10				
	Control	**Curosurf®**	**Liposurf®**	**Synsurf®**
N	1	5	4	5
Mean	**0.186**	**18.05**	**15.58**	**4.88**
SD	-	29.70	29.76	8.36
P25	-	0.1244	0.11435	0.157
P50	-	0.176	1.012	0.1635
P75	-	21.25	31.0475	4.55

Table 3.20: The mean, SD (standard deviation), P25 (25th percentile), P50 (median), & P75 (75th percentile) of LPS (1 µg/ml)-stimulated IL-12 in BAL-derived human alveolar macrophage supernatant concentrations measured at 24h in the presence of surfactants.

IL12				
	Control	**Curosurf®**	**Liposurf®**	**Synsurf®**
N	2	4	4	5
Mean	**2.930**	**20.10**	**15.39**	**16.14**
SD	3.966	39.377	18.07	22.08
P25	0.1259	0.24	0.21	0.34
P50	2.930	0.56	12.74	0.35
P75	5.735	39.95	30.58	33.7

3.3 Discussion

3.3.1 NR8383 Rat Alveolar Cell Line

It has been established that pulmonary surfactant has immunomodulatory properties in addition to its function as a surface tension modulator. As surfactant replacement therapy for premature infants with RDS is standard care, and with its growing interest in other forms of lung diseases as well as its potential role in drug delivery, there is much demand for determining whether exogenous surfactant preparations demonstrate similar anti-inflammatory properties as seen in native surfactants (Kerecman, Mustafa et al. 2008).

The present study demonstrates the effects of two exogenous surfactants from animal sources (Curosurf® and Liposurf®) and a synthetic surfactant (Synsurf®) on pro-inflammatory cytokine (TNF-α, IL-1β, IL-6) and chemokine (KC/GRO) secretion, oxidative burst and protein expression in the NR8383 AM cell line. This AM cell line was chosen as it provides a homogenous source of immune cells that has the ability to display consistent inflammatory responses to stimulation. The results demonstrate that Curosurf®, Liposurf® and Synsurf® decrease secretion of the pro-inflammatory cytokines, TNF-α, IL-1β, and IL-6 in LPS-stimulated AMs in a dose dependent manner. Additionally, all three surfactants inhibit the oxidative burst of stimulated AMs by decreased ROS production (see Chapter 2, page 98). However, there was increased cytokine secretion in the un-stimulated, surfactant treated AMs indicating a detrimental response elicited by lower phospholipid concentrations rather than a protective nature of higher phospholipid concentrations as seen in stimulated AMs. This suggests that surfactant or surfactant components alone, have the ability to modulate the inflammatory cascade within the AMs.

The surfactant-induced decrease in TNF-α and IL-1β levels may represent surfactant binding to LPS or LPS receptors. This inhibition was evident when AMs were treated with surfactant during LPS-stimulation; however, the surfactant-induced increase in the un-stimulated AMs suggests that LPS receptor block does not sufficiently explain the suppression of cytokine secretion.

The mechanisms by which exogenous surfactants modulate the inflammatory cascade in AMs are unclear and are thus critical to elucidate when the complex interplay of interactions among

the inflammatory cytokines (inducer or suppressor effects of one cytokine against another) are involved in inflammatory pulmonary conditions.

3.3.2 Proteomics

Macrophages at the different activation statuses undergo immunometabolic changes to differentially express a series of intracellular markers and secretory cytokines/chemokines. These secretory proteins can be linked to regulation of inflammation, tissue repair, T- and B-cell proliferation, phagocytosis and antimicrobial activity (Sang, Brichalli et al. 2014).

All three surfactant exposed LPS stimulated AMs displayed upregulation of cystatin. Cystatin is implicated in INFγ induced production of NO by activated macrophages. Kitamura and colleagues showed that IL-6-mediated signalling reduced cystatin expression and MHC class II αβ dimer molecule levels (Kitamura, Kamon et al. 2005). However, the MHC class Iβ was found to be upregulated within the Curosurf® and Liposurf® group suggesting natural surfactant interference. In the Synsurf® group, MHC class Iβ was downregulated. The decreased levels of IL-6 within the Synsurf® treated AMs, alongside the cystatin could therefore explain the downregulated MHC class Iβ. These MHC class Iβ molecules presents peptides to T cells, bridging the innate and acquired immunity that provides insight into the origins of acquired immunity (Rodgers, Cook 2005). Verdot and colleagues also suggested that cystatin stimulated TNF-α and IL-10 release by IFN-γ-activated murine peritoneal macrophages (Verdot, Lalmanach et al. 1999). These observations by Verdot and colleagues could be of importance regarding surfactant influence on AM cystatin concentrations involved in the upregulation of TNF-α, IL-10 and NO synthesis; thus, pointing out a new effect-relationship between surfactant induced cystatins, cytokines, inflammation and immune responses (Kopitar-Jerala 2006).

The only statistical functional enrichment for Synsurf® was associated with the oxidation-reduction pathway. ROS is known for being a down-stream by-product of the inflammatory response and contributes to cell viability (See Chapter 2, page 87) but it also serves in the multifaceted regulation of inflammatory processes via physiological roles in signalling. One of the key role role-players that was found to be upregulated in the Synsurf® group was Peroxiredoxin-1 (Prx1). ROS production is critical for appropriate cellular responses to prevent

further oxidative damage and to maintain cell survival; however, when an excessive amount of cell damage has occurred, the cell usually enters a form of cell death (autophagy or apoptosis) (Morgan, Liu 2011). Prx1 belongs to a family of anti-oxidants that protects the cell from metabolically produced ROS that trigger toxic mechanisms within the cell if the signal is exacerbated, continues, or if it occurs at the wrong cell cycle interval and region of the cell (Nathan, Cunningham-Bussel 2013). In this context, a similar trend seen by Robinson and colleagues, Prx1 might have an unanticipated, but yet, a very specific and important role in Synsurf® exposed LPS stimulated macrophages (Robinson, Hutchinson et al. 2010). Prx1 may also contribute to the modulation of immune responses by involving Th2-responses via the induction of alternatively activated macrophages (Knoops, Argyropoulou et al. 2016). It has been proposed by Kim and colleagues that Prx1 may also inhibit NO production by suppressing the ROS/NF-κB/iNOS (NOS2) signalling pathway (Kim, Park et al. 2013). When taking the visualised PPI network for Synsurf® (Figure 3.17) into consideration and the association with NOS2 via Thioredoxin 1 (Trx1), it is then possible to hypothesise that the decrease in cytokine production in the Synsurf® exposed LPS stimulated macrophages occurs via redox signalling by the upregulation of Trx1.

Trx1 is another oxidative, stress-limiting protein that was found to be upregulated within the Synsurf® group. Trx1 is able to scavenge ROS within the cytosol and nucleus of the cell to diminish oxidative stress. However, Trx1 seems to play dual and opposing roles in the activation and repression of NF-κB signalling. It is one of the most important cellular antioxidants with anti-inflammatory and anti-apoptotic properties capable of inhibiting IκB degradation within the cytoplasm (see Figure 3.4) (Djavaheri-Mergny, Javelaud et al. 2004, Morgan, Liu 2011) but is also, in turn, able to regulate NF-κB activation through denitrosylation (-nitrosyl (–SNO)) of the p65 subunit (Kelleher, Sha et al. 2014). Kelleher and colleagues demonstrated quantification of Trx1 protein expression, SNO-p65 formation and NF-κB activity in lung cell lysates and found that Trx1 legitimates cytokine-mediated denitrosylation of p65 and therefore its secondary role in NF-κB activation associated with LPS-induced airway inflammation. Furthermore, by Trx-1's ability to limit nuclear ROS levels it in turn deems itself as a transcription regulatory factor by affecting ROS-associated NF-κB activation (El Hadri, Mahmood et al. 2012).

Trx1 might also promote macrophage differentiation into the macrophage M2 anti-inflammatory phenotype. Thereby significantly reducing the LPS induced inflammatory M1 macrophages as indicated by the Synsurf® dose-dependent decrease TNFα and IL1β

expression. This statement is supported by similar findings by El Hadri *et al.* and Billiet *et al.* Both groups demonstrated the induced downregulation of nuclear translocation of activator protein-1 and Ref-1 via Trx1 that led to the shift in phenotype pattern of lesional macrophages to predominantly M2 over M1 and subsequently the secretion of proinflammatory cytokines (Billiet, Furman et al. 2005, El Hadri, Mahmood et al. 2012). Although no M2 associated cytokines were detected in the Synsurf® exposed macrophages, the up-regulation of Trx1 could be indicative to the promotion of a polarisation switch still to occur thereby repressing transcriptional activation of pro-inflammatory cytokines via the ERK/MAP kinase pathway. It is then practical to assume that Synsurf® exposed LPS stimulated AMs upregulates Trx1 activity thereby prompting Trx-dependent IκB degradation, downregulating the transcription of pro-inflammatory cytokines.

Moreover, Trx can be regarded as an adaptive response as it possibly acts as a chaperone to arginase (utilising L-arginine) by protecting the enzyme from inhibition via reactive oxygen and nitrogen intermediates (Nakamura, Nakamura et al. 2005). Thus maintaining arginase in a catalytically active state, preserves its activity and blunts excessive NOS2 activity (McGee, Kumar et al. 2006, Song, Kim et al. 2008, Lucas, Czikora et al. 2013). Taken together, all of these redox activities could make Synsurf® a potent and versatile mediator of inflammation and can possibly be proposed as a therapeutic candidate for the treatment of several pulmonary inflammatory disorders where Trx1 may ameliorate the cytotoxic response.

Ferritin Heavy Chain (FHC) is the second-most well-known NF-κB target that protects the cell from oxidative damage and Ferritin (Q5FVS1_RAT) was found to be co-upregulated in Synsurf® alongside the above mentioned (Down regulated in Curosurf® and Liposurf®). Due to its characteristic of being an iron storage protein, it cannot scavenge ROS directly but can however, protect the cell from iron-mediated oxidative damage by preventing generation of highly reactive •OH radicals via Fenton reactions (Morgan, Liu 2011). Thus, preventing the generation of more highly reactive species (O2•- and •OH) and promoting the breakdown of H_2O_2 into water by peroxidases and catalases (Torti, Torti 2002). However, in this case, Catalase (CATA_RAT) was downregulated in Synsurf®. Besides its ability to promote cell growth, there have been reports that suggest that catalase could be the target of inhibitory p50 homodimers since its promoter is bound by p50 in unstimulated cells and catalase is down-regulated when NF-κB activation occurs (Schreiber, Jenner et al. 2006, Morgan, Liu 2011). Thus, in this instance, it could be that even though there is evidence that NF-κB activation via stimulated AM is decreased, it is still too high for catalase to be upregulated.

The only statistical functional enrichment for Curosurf® was associated with the biosynthesis of amino acids (KEGG pathway for proline (not included)), but more specifically for arginine metabolism. Arginase-1 converts L-arginine into L-ornithine and urea (Figure 3.21) and is a key enzyme of the urea cycle in the liver but it also has an unexpected role in cells and tissues that lack a complete urea cycle. Arginase-1 is also expressed in the airways where it has the biological function of regulating NO synthesis in bronchial epithelial cells, endothelial cells and AMs (Maarsingh, Pera et al. 2008). It competes with NOS for the utilisation of the common substrate L-arginine in activated M2 macrophages thus supressing the cytotoxic response in these cells.

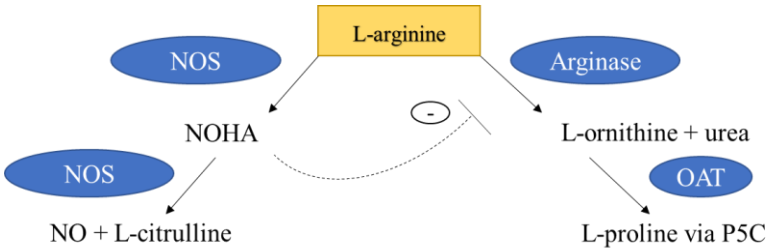

Figure 3.21: L-Arginine metabolism catalysed by arginase and NOS. L-Arginine is a substrate of both NOS, yielding and L-citrulline, and arginase, which in turn produces L-ornithine and urea. Arginase regulates the production of NO by competing with NOS for their common substrate. On the other hand NOHA, an intermediate in the NO synthesis catalysed by NOS, inhibits arginase activity. In addition, the arginase product L-ornithine is the precursor of L-proline. **Abbreviations: NO**, nitric oxide; **NOHA**, N ω N ω -hydroxy-l-arginine; **NOS**, nitric oxide synthase; **OAT**, Ornithine aminotransferase; **P5C**, pyrroline-5-carboxylate (adapted from (Maarsingh, Pera et al. 2008)).

Asthma, chronic obstructive pulmonary disease, cystic fibrosis, and pulmonary hypertension are several lung diseases associated with increased arginase activity suggesting a common feature that underlines these disease's pathophysiologies (Maarsingh, Pera et al. 2008, Lucas, Czikora et al. 2013). With anomalies concerning the delicate homeostasis of NO and exaggerated tissue repair in various inflammatory airway diseases, reduced lung function can occur leading to airway hyper-responsiveness and/or airway remodelling that takes place in the above-mentioned conditions (Maarsingh, Pera et al. 2008).

The presence of upregulated arginase-1 within the Curosurf® exposed AMs (downregulated in the Liposurf® and Synsurf® exposed AM) indicates a proposed M1/M2 phenotypic switch and

M2 polarisation (specifically M2c, see Figure 3.3). This is due to the probable utilisation of L-arginine for the down-stream biosynthesis of proline via L-ornithine that leads to increased cell proliferation (Satriano 2004, Mantovani, Biswas et al. 2013). It is therefore assumed that Curosurf® exposed LPS stimulated AMs upregulates arginase-1 activity and therefore induces M2 phenotypic switch and M2c polarisation; consequently, downregulating the innate M1 phenotype's pro-inflammatory cytokines.

Moreover, Coiled-coil domain-containing protein 22 (CCD22) was found to be upregulated in Curosurf® and Synsurf® exposed LPS stimulated AMs (However, downregulated in Liposurf®), thus suggesting that these two surfactants share a mixed M1/M2 phenotype population. This protein is involved in the regulation of NF-κB signalling by promoting ubiquitination of IκB-kinase subunit IκB thus leading to its subsequent proteasomal degradation and NF-κB activation (see Figure 3.4) (Niemand, Nimmesgern et al. 2003). Since CCD22 is downregulated in Liposurf® and exposed LPS stimulated AMs; and Liposurf® exposed AMs elicited IL10 production (see Figure 3.11), it is therefore acceptable to assume that the NF-κB signalling and subsequent pro-inflammatory cytokine (innate M1 phenotype) is deterred by the JAK/STAT pathway at lower phospholipid concentrations. The proposed subsequent production of SOCS3 interrupts the ubiquitination of the IκB-kinase subunit leading to NF-κB deactivation and halts pro-inflammatory cytokine production (Niemand, Nimmesgern et al. 2003). Contradictory, its function may also involve association with Copper Metabolism Domain Containing 1 (COMMD1) and a Cullin–RING (CUL1) -dependent E3 ubiquitin ligase complex down-regulation of NF-κB activity via degradation of NF-κB subunits by facilitating substrate binding to the ligase and stabilising the interaction between SOCS1 and p65 subunit of NF-κB (Maine, Mao et al. 2007). IκB proteins play an important role in regulating the nuclear pool of NF-κB; however, it is likely that other factors and pathways are involved in this process in cells that are IκB protein deficient (Tergaonkar, Correa et al. 2005, Maine, Mao et al. 2007).

It is also important to mention here that the pleiotropic cytokine, IL-6, elicits pro- and anti-inflammatory properties. All three surfactant exposed LPS stimulated AMs secreted low levels of IL-6 (Figure 3.9); however, Liposurf® exposed AMs secreted significantly more IL-6 than its counterparts (Table 3.3). IL-6 trans-signalling (with soluble IL-6 receptors) could thus be involved within the Liposurf® exposed AMs, explaining the higher TNF-α levels (Figure 3.7) that blunt the anti-inflammatory effects compared to the TNF-α levels of Curosurf® and Synsurf® (Scheller, Chalaris et al. 2011). This may offer the explanation as to the presence of

the anti-inflammatory cytokine IL-10 in the Liposurf® exposed AMs as another mechanism was employed to resolve the upregulated inflammatory cascade.

The second enrichment analysis that displayed significant PPI for upregulated IL-18 and the presence of IL-6 (see Figure 3.15) for Curosurf® exposed AMs is associated with the positive regulation of cytokine production as well as the regulation of the apoptotic process. IL-18 acts as bridge to link the innate immune response by priming Th1 polarisation and priming NK cells (see Figure 3.2) (Slaats, ten Oever et al. 2016). Autophagy is a cellular process that plays a crucial role in environmental adaptation and cellular remodelling and is characterised by the formation of autophagosomes (double-membrane vesicles that capture and transport cytoplasmic material to acidic compartments where material is degraded by hydrolytic enzymes) (Ravikumar, Futter et al. 2009, Duque, Descoteaux 2014). However, it is also been recognised in the mediation of cellular cytokine secretion for those proteins that otherwise do not have a leader peptide as to enter the classical secretory pathway such as IL-1β and IL-18 (Jiang, Dupont et al. 2013). In this case, both the autophagy related protein 3 (Atg3) (not significantly expressed) and Ras-related protein Rab-11b were present but down regulated in all three surfactant exposed AMs groups (except Rab-11b for Synsurf®) indicating causal autophagocytosis in response to the increased cytokine production. These autophagic proteins are essential in regulating immune responses in a "house-keeping" manner by digestion of dysfunctional mitochondria and thereby preventing excess production of mitochondrial ROS. Secondly, autophagy is also responsible for translocating IL-1β and IL18-containing vesicles (inflammasome complexes) for degradation, thus removing unwanted inflammatory proteins. (Duque, Descoteaux 2014, Netea-Maier, Plantinga et al. 2016). Ras-related protein Rab-11b, which was found to be upregulated in Synsurf® exposed LPS stimulated AMs, may initiate a phenotype switch from M1 to M2 macrophages, which secrete anti-inflammatory cytokines such as TGF-β and IL-10 (autophagy inducer), as seen by Jiang and colleagues in the presence of apoptotic neutrophils thereby mediating resolution of inflammation (Jiang, Liu et al. 2017).

The paradox that originates from the complex interactions between the apoptosis and autophagy remains a subject of considerable debate due to the therapeutic potential for cancer treatments. As the autophagic process occurs as cell maintenance and can act as a process for both cell protection and initiate cell death, elucidating the molecular mechanisms and connections between autophagy and apoptosis, may bring to light if one process controls the other (Gump, Thorburn 2011). The apoptosis regulator BAX protein, also known as bcl-2-like protein 4, was found to be upregulated in both the Liposurf® and the Synsurf® exposed LPS

stimulated AMs but down regulated in Curosurf®. Bcl2 family members act as apoptotic regulators; therefore, drugs that activate BAX hold promise as anticancer treatments by inducing apoptosis in cancer cells (Liu, Ding et al. 2016). This suggests that a pulmonary surfactant may be useful as a possible chemotherapeutic drug carrier for site-specific pulmonary cancer treatment. Dibbert and colleagues saw that neutrophils however, expressed little or no Bax under inflammatory conditions and concluded that Bax deficiency occurs at both mRNA and protein levels. Bax deficiency thus appears to be a general hallmark of neutrophils associated with delayed apoptosis via cytokine mediation (Dibbert, Weber et al. 1999). However, AMs in the presence of Synsurf® and Liposurf® seem to overcome this deficiency and thereby apoptotic irregularity. Furthermore, traces of the inhibitor of apoptosis protein (IAP) anamorsin was also present in all three surfactant exposed LPS stimulated AMs groups (not significant). IAPs have anti-apoptotic effects in the cell via the involvement in negative control of cell death upon cytokine withdrawal (via STAT3, see Figure 3.22). These findings create a complicated paradigm where autophagy and apoptosis might be role players in a complex balancing act wherein autophagy alters the extent and kinetics of apoptosis and apoptosis may alter the autophagy occurrence in a stressed cell population thus explaining the presence of both pro- and anti-apoptotic regulators in a cell population. Determining the important interactions in autophagy's regulation of cell death is necessary in therapy when endeavouring to protect healthy cells and to initiate death in diseased cells (Gump, Thorburn 2011).

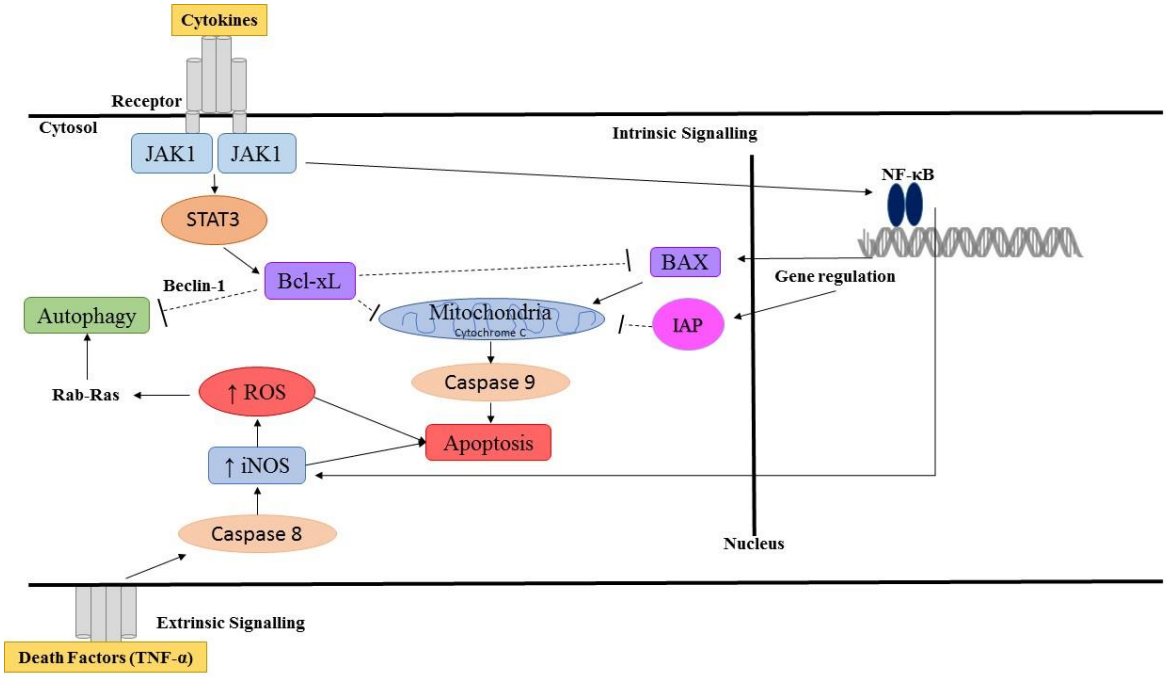

Figure 3.22: The proposed dual autophagy-apoptosis pathway due to surfactant combinational treatment on AMs promoted by the JAK-STAT signalling pathway.

Dynamin-1-like protein (Drp1) (upregulated in Curosurf® and Liposurf®, downregulated in Synsurf®) is involved in several important aspects of mitochondria's morphology and size which are also relevant in T cell signalling. When Drp1 is upregulated, it impairs mitochondrial transport and mitochondrial dynamics (↑ ROS) thus causing mitochondrial dysfunction and fragmentation resulting in apoptosis or aberrant autophagy. The downregulated Drp1 in the Synsurf® exposed LPS stimulated AMs could also have led to reduced ROS production, reducing the transcriptional activity of NF-κB (Reddy, Reddy et al. 2011, Röth, Krammer et al. 2014). It is important to mention that just because a protein regulates autophagy and also affects how efficiently a cell can undergo apoptosis, does not necessarily mean that it was the process of autophagy that affected apoptosis (Thorburn 2008, Eisenberg-Lerner, Bialik et al. 2009). Thus, it is important to underline the very complex participation of signalling pathways in surfactant exposed cells, as cells are programmed to undergo autophagy (apoptosis if autophagic threshold is reached) to limit their pro-inflammatory potential (Savill 1997). The connections between autophagy and apoptosis within surfactant exposed AMs might have more to do with "how" cells die, rather than changing whether or not they do die, thus modestly decreasing toxins and caspase activation. The latter was not detected within the surfactant exposed AMs.

3.3.3 Human BAL derived Macrophages' Cytokine Secretion

Selection of the subjects studied here was based on criteria unanimously accepted in the literature. In particular, the AMs from healthy controls and those from patients with classic types of non-diseased airway obstructions (heterogeneous population). The clinical characteristics together with the data on the BAL of the cases studied were similar to those reported in the literature. Once the present study had been judged suitable, the next step was to standardise the characteristics of cell culture and the concentrations of the different surfactants. Due to the small sample size of healthy patients, a standardised concentration was maintained as to keep statistical integrity regarding pool size. First, the mono-nuclear fraction (macrophages and lymphocytes) was separated of >90% neutrophils, erythrocytes, cellular detritus and dead cells by a density gradient, already reported in the literature for the separation of AMs and adapted accordingly (Ferro, Kern et al. 1987). The next step was to separate AMs from lymphocytes which is mainly due to the capacity of AMs to adhere to polystyrene dishes. Both methods permit the direct study of cytokine production by AMs. However, the results obtained should be interpreted with caution and understanding as adherence itself is able to stimulate the production of these types of inflammatory mediators (Rolfe, Kunkel et al. 1992, García, Rodriguez et al. 1999).

Such an interpretation is featured in the low relationship between LPS stimulated release of IL-1β, IL-2, IL-6 and IL-8 and their spontaneous secretion during prolonged exposure to LPS in combination with surfactant. Synsurf® displayed an approximate two-fold decrease in IL-1β release (97.60 pg/ml) compared to control levels (176.45 pg/ml) whereas both natural surfactants displayed minimal decreases (Table 3.12). After 24h, TNF-α levels (Table 3.16) decreased within the cell supernatant of the surfactant treated AMs. The Curosurf® (120.73 pg/ml) and Liposurf® (110.01 pg/ml) groups displayed an approximate four-fold decrease in TNF-α release compared to control levels (462 pg/ml); whereas, Synsurf® (56.87 pg/ml) displayed a much larger, eight-fold, inhibitory effect on stimulated TNF-α release. TNF-α and IL-1β release by macrophages are "acute response" cytokines that promote neutrophilic and eosinophilic inflammation. Although they are not directly chemo-attractive agents, they may directly or indirectly stimulate the upregulation of relevant secondary cytokines (Table 3.18: GM-CSF) and cell adhesion molecules. The increased presence of TNF-α and IL-1β may synergistically amplify the expression of IL-6 (Table 3.14) and IL-8 (Table 3.15) (Ishii, Fujii

et al. 2004). This being said, it has been seen that peak TNF-α and IL-1β AM release occurs between approximately 8 - 12 h after initial exposure (Kerecman, Mustafa et al. 2008). This may explain the rather low LPS stimulated levels of these cytokines at 24 h compared to that of their downstream-regulated cytokines IL-6 and IL-8 (although both IL-6 and IL-8 are decreased within all three the surfactant groups) which may reach their peak concentrations much later. IL-6 was also found to be at much lower levels compared to IL-8. A previous study witnessed a similar phenomenon and elucidated that the relationship between basal secretion in culture and initial spontaneous release for IL-8 was much higher, intermediate release for IL-6 and low release for TNF-α. This once again suggests that adherence to the plastic culture plate is a very important stimulus in the secretion of IL-8 and, to a lesser extent, that of IL-6 (García, Rodriguez et al. 1999).

Both the natural surfactants decreased secretory levels of IL-2 (Table 3.13) whereas cell supernatant levels of IL-2 where increased when exposed to Synsurf®. It is important note that IL-2 activates several different pathways that mediate the flow of mitogenic and survival-promoting signals (Benczik, Gaffen 2004). Moreover, IL-2 induces JAB/SOCS1/SSI-1 that in turn inhibits IL-2 signalling (Sporri, Kovanen et al. 2001). SOCS1 is involved in the negative regulation of cytokines and initiates an anti-inflammatory response via the regulation of homeostasis. Thus indicating that IL-2 also has anti-inflammatory properties, as does other pro-inflammatory cytokines, such as IFN-γ (Bachmann, Kopf 2002). Levels of IFN-γ secretion (Table 3.17) decreased almost 3-fold when AMs were exposed to Curosurf® and Synsurf®; however, only an approximate 2-fold decrease in the presence of Liposurf® was witnessed. IFN-γ is important for the clearance of bacteria by recruiting many other cells (e.g. NK cells) but some reports indicate that IFN-γ is crucial for the cell cycle arrest in macrophage cell cycles that provides a survival signal, and others suggest that it serves as a pro-apoptotic signal. There have been many advances in the understanding of cell cycle control and apoptosis within isolation; however, the inter-relationship between these intimately related processes concerning protective immunity and immunopathology are yet to be fully understood (Schroder, Hertzog et al. 2004).

3.4 Conclusion

There have been many hypothesises regarding the specific surfactant proteins that may be responsible for the role in blunting the inflammatory response and elicit a protective nature. However, this study shows how Synsurf®, a synthetic peptide containing surfactant, displayed the same "protective" nature, and even more so, to that of animal derived SP-B/C containing surfactants. One can then conclude that the initial hypothesis regarding the protective nature that is linked to the protein content in natural surfactants may be deemed as "not fully supported" as these new findings suggest non-specific lipid or synthetic peptide protection with AMs as seen by Synsurf®. Furthermore, the elucidation of the mechanisms involved in this cyto-protective nature of pulmonary surfactants may offer a window into a patient-specific, individualised treatment option for inflammatory pulmonary disorders.

3.5 References

ARIAS-DIAZ, J., GARCIA-VERDUGO, I., CASALS, C., SANCHEZ-RICO, N., VARA, E. and BALIBREA, J.L., 2000. Effect of surfactant protein A (SP-A) on the production of cytokines by human pulmonary macrophages. *Shock*, **14**(3), pp. 300-306.

BACHMANN, M.F. and KOPF, M., 2002. Balancing protective immunity and immunopathology. *Current Opinion in Immunology*, **14**(4), pp. 413-419.

BENCZIK, M. and GAFFEN, S.L., 2004. The Interleukin (IL)-2 Family Cytokines: Survival and Proliferation Signaling Pathways in T Lymphocytes. *Immunological Investigations*, **33**(2), pp. 109-142.

BILLIET, L., FURMAN, C., LARIGAUDERIE, G., COPIN, C., BRAND, K., FRUCHART, J.C. and ROUIS, M., 2005. Extracellular human thioredoxin-1 inhibits lipopolysaccharide-induced interleukin-1beta expression in human monocyte-derived macrophages. *The Journal of Biological Chemistry*, **280**(48), pp. 40310-40318.

CHIBA, H., SANO, H., IWAKI, D., MURAKAMI, S., MITSUZAWA, H., TAKAHASHI, T., KONISHI, M., TAKAHASHI, H. and KUROKI, Y., 2001. Rat mannose-binding protein a binds CD14. *Infection and Immunity*, **69**(3), pp. 1587-1592.

DIBBERT, B., WEBER, M., NIKOLAIZIK, W.H., VOGT, P., SCHÖNI, M.H., BLASER, K. and SIMON, H.U., 1999. Cytokine-mediated Bax deficiency and consequent delayed neutrophil apoptosis: a general mechanism to accumulate effector cells in inflammation. *Proceedings of the National Academy of Sciences*, **96**(23), pp. 13330-13335.

DJAVAHERI-MERGNY, M., JAVELAUD, D., WIETZERBIN, J. and BESANÇON, F., 2004. NF-κB activation prevents apoptotic oxidative stress via an increase of both thioredoxin and MnSOD levels in TNFα-treated Ewing sarcoma cells. *FEBS letters*, **578**(1-2), pp. 111-115.

DUQUE, G.A. and DESCOTEAUX, A., 2014. Macrophage cytokines: involvement in immunity and infectious diseases. *Frontiers in Immunology*, **5**(491), pp. 1-12.

EISENBERG-LERNER, A., BIALIK, S., SIMON, H.U. and KIMCHI, A., 2009. Life and death partners: apoptosis, autophagy and the cross-talk between them. *Cell Death and Differentiation,* **16**(7), pp. 966-975.

EL HADRI, K., MAHMOOD, D.F.D., COUCHIE, D., JGUIRIM-SOUISSI, I., GENZE, F., DIDEROT, V., SYROVETS, T., LUNOV, O., SIMMET, T. and ROUIS, M., 2012. Thioredoxin-1 promotes anti-inflammatory macrophages of the M2 phenotype and antagonizes atherosclerosis. *Arteriosclerosis, Thrombosis, and Vascular Biology,* **32**(6), pp. 1445-1452.

FERRO, T.J., KERN, J.A., ELIAS, J.A., KAMOUN, M., DANIELE, R.P. and ROSSMAN, M.D., 1987. Alveolar Macrophages, Blood Monocytes, and Density-Fractionated Alveolar Macrophages Differ in Their Ability to Promote Lymphocyte Proliferation to Mitogen and Antigen 1–3. *American Review of Respiratory Disease,* **135**(3), pp. 682-687.

GARCÍA, J.E., RODRIGUEZ, F.M., DE CABO, M.R., SALGADO, M.J., LOSADA, J.P., VILLARON, L.G., LOPEZ, A.J. and ARELLANO, J.L.P., 1999. Evaluation of inflammatory cytokine secretion by human alveolar macrophages. *Mediators of Inflammation,* **8**(1), pp. 43-51.

GARDAI, S.J., XIAO, Y.Q., DICKINSON, M., NICK, J.A., VOELKER, D.R., GREENE, K.E. and HENSON, P.M., 2003. By binding SIRPα or calreticulin/CD91, lung collectins act as dual function surveillance molecules to suppress or enhance inflammation. *Cell,* **115**(1), pp. 13-23.

GUMP, J.M. and THORBURN, A., 2011. Autophagy and apoptosis- what's the connection?. *Trends in Cell Biology,* **21**(7), pp. 387-392.

HELMKE, R., GERMAN, V. and MANGOS, J., 1989. A continuous alveolar macrophage cell line: Comparisons with freshly derived alveolar macrophages. *In Vitro Cellular & Developmental Biology,* **25**(1), pp. 44-48.

HUSSELL, T. and BELL, T.J., 2014. Alveolar macrophages: plasticity in a tissue-specific context. *Nature Reviews Immunology,* **14**(2), pp. 81-93.

ISHII, H., FUJII, T., HOGG, J.C., HAYASHI, S., MUKAE, H., VINCENT, R. and VAN EEDEN, S.F., 2004. Contribution of IL-1β and TNF-α to the initiation of the peripheral lung

response to atmospheric particulates (PM 10). *American Journal of Physiology-Lung Cellular and Molecular Physiology*, **287**(1), pp. L176-L183.

JANSSEN, W.J., MCPHILLIPS, K.A., DICKINSON, M.G., LINDERMAN, D.J., MORIMOTO, K., XIAO, Y.Q., OLDHAM, K.M., VANDIVIER, R.W., HENSON, P.M. and GARDAI, S.J., 2008. Surfactant proteins A and D suppress alveolar macrophage phagocytosis via interaction with SIRPα. *American Journal of Respiratory and Critical Care Medicine*, **178**(2), pp. 158-167.

JIANG, C., LIU, Z., HU, R., BO, L., MINSHALL, R.D., MALIK, A.B. and HU, G., 2017. Inactivation of Rab11a GTPase in Macrophages Facilitates Phagocytosis of Apoptotic Neutrophils. *The Journal of Immunology*, **198**(4), pp. 1660-1672.

JIANG, S., DUPONT, N., CASTILLO, E.F. and DERETIC, V., 2013. Secretory versus degradative autophagy: unconventional secretion of inflammatory mediators. *Journal of Innate Immunity*, **5**(5), pp. 471-479.

KELLEHER, Z.T., SHA, Y., FOSTER, M.W., FOSTER, W.M., FORRESTER, M.T. and MARSHALL, H.E., 2014. Thioredoxin-mediated denitrosylation regulates cytokine-induced nuclear factor κB (NF-κB) activation. *Journal of Biological Chemistry*, **289**(5), pp. 3066-3072.

KERECMAN, J., MUSTAFA, S., VASQUEZ, M., DIXON, P. and CASTRO, R., 2008. Immunosuppressive properties of surfactant in alveolar macrophage NR8383. *Inflammation Research*, **57**(3), pp. 118-125.

KIM, S.U., PARK, Y.H., MIN, J.S., SUN, H.N., HAN, Y.H., HUA, J.M., LEE, T.H., LEE, S.R., CHANG, K.T., KANG, S.W. and KIM, J.M., 2013. Peroxiredoxin I is a ROS/p38 MAPK-dependent inducible antioxidant that regulates NF-κB-mediated iNOS induction and microglial activation. *Journal of Neuroimmunology*, **259**(1), pp. 26-36.

KITAMURA, H., KAMON, H., SAWA, S.I., PARK, S.J., KATUNUMA, N., ISHIHARA, K., MURAKAMI, M. and HIRANO, T., 2005. IL-6-STAT3 controls intracellular MHC class II αβ dimer level through cathepsin S activity in dendritic cells. *Immunity*, **23**(5), pp. 491-502.

KNOOPS, B., ARGYROPOULOU, V., BECKER, S., FERTÉ, L. and KUZNETSOVA, O., 2016. Multiple roles of peroxiredoxins in inflammation. *Molecules and Cells*, **39**(1), pp. 60-64.

KOPITAR-JERALA, N., 2006. The role of cystatins in cells of the immune system. *FEBS letters,* **580**(27), pp. 6295-6301.

LIU, Z., DING, Y., YE, N., WILD, C., CHEN, H. and ZHOU, J., 2016. Direct Activation of Bax Protein for Cancer Therapy. *Medicinal Research Reviews,* **36**(2), pp. 313-341.

LUCAS, R., CZIKORA, I., SRIDHAR, S., ZEMSKOV, E.A., OSEGHALE, A., CIRCO, S., CEDERBAUM, S.D., CHAKRABORTY, T., FULTON, D.J., CALDWELL, R.W. and ROMERO, M.J., 2013. Arginase 1: an unexpected mediator of pulmonary capillary barrier dysfunction in models of acute lung injury. *Frontiers in Immunology,* **4**(228), pp. 1-7.

MAARSINGH, H., PERA, T. and MEURS, H., 2008. Arginase and pulmonary diseases. *Naunyn-Schmiedeberg's Archives of Pharmacology,* **378**(2), pp. 171-184.

MAINE, G.N., MAO, X., KOMARCK, C.M. and BURSTEIN, E., 2007. COMMD1 promotes the ubiquitination of NF-κB subunits through a cullin-containing ubiquitin ligase. *The EMBO journal,* **26**(2), pp. 436-447.

MANTOVANI, A., BISWAS, S.K., GALDIERO, M.R., SICA, A. and LOCATI, M., 2013. Macrophage plasticity and polarization in tissue repair and remodelling. *The Journal of Pathology,* **229**(2), pp. 176-185.

MANTOVANI, A., SICA, A., SOZZANI, S., ALLAVENA, P., VECCHI, A. and LOCATI, M., 2004. The chemokine system in diverse forms of macrophage activation and polarization. *Trends in Immunology,* **25**(12), pp. 677-686.

MARTINEZ, F.O. and GORDON, S., 2014. The M1 and M2 paradigm of macrophage activation: time for reassessment. *F1000Prime Reports,* **6**, pp. 13.

MCGEE, D.J., KUMAR, S., VIATOR, R.J., BOLLAND, J.R., RUIZ, J., SPADAFORA, D., TESTERMAN, T.L., KELLY, D.J., PANNELL, L.K. and WINDLE, H.J., 2006. Helicobacter pylori thioredoxin is an arginase chaperone and guardian against oxidative and nitrosative stresses. *Journal of Biological Chemistry,* **281**(6), pp. 3290-3296.

MORGAN, M.J. and LIU, Z.G., 2011. Crosstalk of reactive oxygen species and NF-κB signaling. *Cell research,* **21**(1), pp. 103-115.

MOSSER, D.M., 2003. The many faces of macrophage activation. *Journal of Leukocyte Biology*, **73**(2), pp. 209-212.

MOSSER, D.M., 1999. Receptor mediated subversion of macrophage cytokine production by intracellular pathogens. *Current Opinion in Immunology*, **11**(4), pp. 406-411.

MURAKAMI, S., IWAKI, D., MITSUZAWA, H., SANO, H., TAKAHASHI, H., VOELKER, D.R., AKINO, T. and KUROKI, Y., 2002. Surfactant protein A inhibits peptidoglycan-induced tumor necrosis factor-α secretion in U937 cells and alveolar macrophages by direct interaction with Toll-like receptor 2. *Journal of Biological Chemistry*, **277**(9), pp. 6830-6837.

NAKAMURA, T., NAKAMURA, H., HOSHINO, T., UEDA, S., WADA, H. and YODOI, J., 2005. Redox regulation of lung inflammation by thioredoxin. *Antioxidants & redox signalling*, **7**(1-2), pp. 60-71.

NAKATA, K., GOTOH, H., WATANABE, J., UETAKE, T., KOMURO, I., YUASA, K., WATANABE, S., IEKI, R., SAKAMAKI, H., AKIYAMA, H., KUDOH, S., NAITOH, M., SATOH, H. and SHIMADA, K., 1999. Augmented proliferation of human alveolar macrophages after allogeneic bone marrow transplantation. *Blood*, **93**(2), pp. 667.

NATHAN, C. and CUNNINGHAM-BUSSEL, A., 2013. Beyond oxidative stress: an immunologist's guide to reactive oxygen species. *Nature Reviews Immunology*, **13**(5), pp. 349-361.

NETEA-MAIER, R.T., PLANTINGA, T.S., VAN DE VEERDONK, F.L., SMIT, J.W. and NETEA, M.G., 2016. Modulation of inflammation by autophagy: consequences for human disease. *Autophagy*, **12**(2), pp. 245-260.

NGUYEN, H.A., RAJARAM, M.V.S., MEYER, D.A. and SCHLESINGER, L.S., 2012. Pulmonary surfactant protein A and surfactant lipids upregulate IRAK-M, a negative regulator of TLR-mediated inflammation in human macrophages. *American Journal of Physiology. Lung Cellular and Molecular Physiology*, **303**(7), pp. L608.

NIEMAND, C., NIMMESGERN, A., HAAN, S., FISCHER, P., SCHAPER, F., ROSSAINT, R., HEINRICH, P.C. and MÜLLER-NEWEN, G., 2003. Activation of STAT3 by IL-6 and IL-

10 in primary human macrophages is differentially modulated by suppressor of cytokine signaling 3. *The Journal of Immunology*, **170**(6), pp. 3263-3272.

OFEK, I., MESIKA, A., KALINA, M., KEISARI, Y., PODSCHUN, R., SAHLY, H., CHANG, D., MCGREGOR, D. and CROUCH, E., 2001. Surfactant protein D enhances phagocytosis and killing of unencapsulated phase variants of Klebsiella pneumoniae. *Infection and Immunity*, **69**(1), pp. 24-33.

RAVIKUMAR, B., FUTTER, M., JAHREISS, L., KOROLCHUK, V.I., LICHTENBERG, M., LUO, S., MASSEY, D.C., MENZIES, F.M., NARAYANAN, U., RENNA, M. and JIMENEZ-SANCHEZ, M., 2009. Mammalian macroautophagy at a glance. *Journal of Cell Science*, **122**(11), pp. 1707-1711.

REDDY, P.H., REDDY, T.P., MANCZAK, M., CALKINS, M.J., SHIRENDEB, U. and MAO, P., 2011. Dynamin-Related Protein 1 and Mitochondrial Fragmentation in Neurodegenerative Diseases. *Brain Research Reviews*, **67**(1-2), pp. 103-118.

ROBINSON, M.W., HUTCHINSON, A.T., DALTON, J.P. and DONNELLY, S., 2010. Peroxiredoxin: a central player in immune modulation. *Parasite immunology*, **32**(5), pp. 305-313.

RODGERS, J.R. and COOK, R.G., 2005. MHC class Ib molecules bridge innate and acquired immunity. *Nature reviews: Immunology*, **5**(6), pp. 459.

ROLFE, M.W., KUNKEL, S.L., ROWENS, B., STANDIFORD, T.J., CRAGOE JR, E.J. and STRIETER, R.M., 1992. Suppression of human alveolar macrophage-derived cytokines by amiloride. *American Journal of Respiratory Cell and Molecular Biology*, **6**(6), pp. 576-582.

RÖTH, D., KRAMMER, P.H. and GÜLOW, K., 2014. Dynamin related protein 1-dependent mitochondrial fission regulates oxidative signalling in T cells. *FEBS letters*, **588**(9), pp. 1749-1754.

SANG, Y., BRICHALLI, W., ROWLAND, R.R. and BLECHA, F., 2014. Genome-wide analysis of antiviral signature genes in porcine macrophages at different activation statuses. *PloS one*, **9**(2), pp. p.e87613.

SATRIANO, J., 2004. Arginine pathways and the inflammatory response: interregulation of nitric oxide and polyamines. *Amino acids*, **26**(4), pp. 321-329.

SAVILL, J., 1997. Apoptosis in resolution of inflammation. *Journal of Leukocyte Biology*, **61**(4), pp. 375-380.

SCHELLER, J., CHALARIS, A., SCHMIDT-ARRAS, D. and ROSE-JOHN, S., 2011. The pro-and anti-inflammatory properties of the cytokine interleukin-6. *Biochimica et Biophysica Acta (BBA)-Molecular Cell Research*, **1813**(5), pp. 878-888.

SCHREIBER, J., JENNER, R.G., MURRAY, H.L., GERBER, G.K., GIFFORD, D.K. and YOUNG, R.A., 2006. Coordinated binding of NF-κB family members in the response of human cells to lipopolysaccharide. *Proceedings of the National Academy of Sciences*, **103**(15), pp. 5899-5904.

SCHRODER, K., HERTZOG, P.J., RAVASI, T. and HUME, D.A., 2004. Interferon-γ: an overview of signals, mechanisms and functions. *Journal of Leukocyte Biology*, **75**(2), pp. 163-189.

SLAATS, J., TEN OEVER, J., VAN DE VEERDONK, F.L. and NETEA, M.G., 2016. IL-1β/IL-6/CRP and IL-18/ferritin: distinct inflammatory programs in infections. *PLoS pathogens*, **12**(12), pp. e1005973.

SONG, J.Y., KIM, K.D. and ROE, J.H., 2008. Thiol-independent action of mitochondrial thioredoxin to support the urea cycle of arginine biosynthesis in Schizosaccharomyces pombe. *Eukaryotic Cell*, **7**(12), pp. 2160-2167.

SPORRI, B., KOVANEN, P.E., SASAKI, A., YOSHIMURA, A. and LEONARD, W.J., 2001. JAB/SOCS1/SSI-1 is an interleukin-2–induced inhibitor of IL-2 signalling. *Blood*, **97**(1), pp. 221-226.

TERGAONKAR, V., CORREA, R.G., IKAWA, M. and VERMA, I.M., 2005. Distinct roles of I [kappa] B proteins in regulating constitutive NF-[kappa] B activity. *Nature Cell Biology*, **7**(9), pp. 921-923.

THORBURN, A., 2008. Apoptosis and autophagy: regulatory connections between two supposedly different processes. *Apoptosis*, **13**(1), pp. 1-9.

TORTI, F.M. and TORTI, S.V., 2002. Regulation of ferritin genes and protein. *Blood*, **99**(10), pp. 3505-3516.

VERDOT, L., LALMANACH, G., VERCRUYSSE, V., HOEBEKE, J., GAUTHIER, F. and VRAY, B., 1999. Chicken cystatin stimulates nitric oxide release from interferon-γ-activated mouse peritoneal macrophages via cytokine synthesis. *The FEBS Journal*, **266**(3), pp. 1111-1117.

YAMASHITA, C.M., VELDHUIZEN, R.A.W. and GILL, S.E., 2013. Alveolar macrophages and pulmonary surfactant-more than just friendly neighbours. *OA Biology*, **1**(1), pp. 6.

ZHU, Y.P., BROWN, J.R., SAG, D., ZHANG, L. and SUTTLES, J., 2015. Adenosine 5′-Monophosphate–Activated Protein Kinase Regulates IL-10–Mediated Anti-Inflammatory Signalling Pathways in Macrophages. *The Journal of Immunology*, **194**(2), pp. 584-594.

4 CHAPTER 4: *In Vitro* Activities of Linezolid in Combination with various Surfactants against *Mycobacterium tuberculosis*

4.1 Introduction

Tuberculosis (TB) infects almost all organs of the human body, but its the most common form is that of pulmonary TB. Worldwide, it was estimated that 9.6 million people were infected with TB in 2014 and South Africa has been reported to be the sixth highest regarding incidence and the eighth highest regarding estimated prevalence (World Health Organization 2015). In cases of pulmonary tuberculosis, pathological variations that have been observed range from crucial regions of alveolar collapse to areas of pneumonia and atelectasis. These pathologies are also associated clinically with lung surfactant dysfunction as seen in cases of adult and neonatal respiratory distress syndrome (Chimote, Banerjee 2005). *Mycobacterium tuberculosis* bacteria (M.*tb*), the causative agents for TB, lodge themselves within the alveolar space and some have the ability to invade, multiply and survive within alveolar macrophages. The alveolar spaces are lined with pulmonary surfactant creating the proximity for possible interactions of the M.*tb* bacilli surface and the surfactant constituents. The major component of the mycobacterial exterior is a lipid rich capsule. Cord factor, or trehalose dimycolate (TDM), forms the thick lipid coat barrier surrounding bacteria. This consequently shields them from the immune system's response and antibiotics. These cell wall lipids have the ability to spontaneously be released into the culture medium or via simple gentle mechanical abrasion. Similarly, these lipids within the cord factor may detached and shed into the pulmonary alveolar space, where they could interact with the pulmonary surfactant system (Ryan, Akinbi et al. 2006) and previous studies have shown that the protective barrier might be compromised by exposing the bacteria to certain surfactants (Stoops, Arora et al. 2010). Although the feasibility of using surfactants for treating M.*tb* infections in mice was demonstrated many years ago, there was a decline in interest in the treatment of the disease as well as other novel treatment possibilities (Cornforth, Hart et al. 1955). However, recent studies investigated the effects of lung surfactant on the bactericidal activity of amoxicillin against *Staphylococcus aureus* and *Streptococcus pneumoniae*, and ceftazidime and tobramycin against *Klebsiella pneumoniae*,

Pseudomonas aeruginosa, *S. aureus*, and *S. pneumonia* (van't Veen, Mouton et al. 1995). This ultimately led to the renewed interest to test the use of exogenous surfactant as a vehicle for antibiotic delivery to the lung. As surfactants have the potential to overcome natural resistance of M.*tb* to antibiotics they can also act as permeabilising agents and allow for better penetration of drugs through mycobacterial barriers. In this regard a study by Risin and colleagues showed that treatment of TB with isoniazid (INH) was enhanced by administering surfactant as an aerosol into the lungs and thus established proof of principle that surfactants alone applied as an aerosol can also reduce the bacterial count in lungs infected with M.*tb* (Risin, Hunter et al. 2014). This may be due to the mycolic acid found on the surface of M.*tb* bacilli that are moderate surface active agents which collapse at surface pressures between 20 and 40 mN/m (Ryan, Akinbi et al. 2006).

When considering oral therapy for TB treatment, there is a significant hepatic metabolism that may lead to insufficient concentration of the anti-TB drugs within the alveolar spaces and macrophages where M.*tb* tend to hide. Therefore, targeted aerosolised antitubercular drug delivery may prove efficient in treating local lung TB infections (Patil-Gadhe, Kyadarkunte et al. 2014). Liposomal dry powder formulations for inhalation (LDPI) have shown many advantages and promising features in localising targeted particles within the respiratory tract; so much so, that the liposomal formulation of inhalable amikacin, named “Arikace”, has been approved as an orphan drug. It received orphan drug status in Europe for the treatment of bronchopulmonary *Pseudomonas aeruginosa* infection in cystic fibrosis (CF) patients in July 2006. Another example of an orphan drug is the use of ciprofloxacin inhalation for the treatment of non-cystic fibrosis bronchiectasis (BE) that has been approved by the US Food and Drug Administration (FDA) (Cipolla, Blanchard et al. 2016). These two inhalation liposomal formulations are currently under phase III and phase IIb clinical trial development stage, respectively (Patil-Gadhe, Kyadarkunte et al. 2014).

Silverman and colleagues (2005), however, reported an inhibition of antibacterial activity of daptomycin alongside pulmonary surfactant interaction *in vitro* for *Streptococcus pneumoniae.* They explained that the interaction between daptomycin and pulmonary surfactant is a direct consequence of its mechanism of action. Daptomycin directly inserts into the membrane of gram-positive bacteria and artificial lipid vesicles. Pulmonary surfactant composition differs to that of most eukaryotic membranes but it does contain approximately 10% PG that is a

prominent component of the gram-positive bacterium's plasma membrane (White, Frerman 1967, Goerke 1998). PC lipid vesicles may allow for more interaction with daptomycin; however, negatively charged PG significantly enhances insertion into the cell membrane. Daptomycin has a direct insertion into the surfactant aggregates *in vitro* due to the calcium dependent surfactant interaction. This evidence supports the model that daptomycin is unable to distinguish between surfactant layers and the small surface area of target pathogens within the lung. Insertion into the surfactant layer is predicted to be an essentially irreversible process resulting in sequestration of the antibiotic(Silverman, Mortin et al. 2005), and therefore rendering it inactive. This may be the first example of a pulmonary surfactant-specific mechanism which results in the failure of an antibiotic whereas further studies otherwise support the opposite. It is therefore important to take the antibiotic target into consideration when aiming to employ surfactant-associated therapy, as membrane targets seem to be disordered whereas nuclear/intracellular targets are not. It is also important to take the characteristics of different infection sites into consideration when one looks at antimicrobial susceptibility as these sites may also affect pharmacodynamics activity of the antibiotics in question (Sauermann, Schwameis et al. 2009).

The oxazolidinones represent a unique class of totally synthetic antimicrobial agents (they are not formed from natural product) that were first discovered in the 1970s but re-investigated in 1996 resulting in linezolid's discovery. For that reason, there are currently no pre-existing specific resistance genes among gram-positive bacteria (Moellering 2003). These agents also have a unique mechanism of action that precludes cross-resistance with currently available agents. Linezolid is the first oxazolidinone developed and approved for clinical use and is an inhibitor of bacterial ribosomal protein synthesis (mRNA synthesis). It prevents the formation of a 70S initiation complex by binding to domain V on the 50S ribosomal subunit near its interface with the 30S unit (Huang, Liu et al. 2008). Many compounds have been tested for their activity *in vitro* against M.*tb* strains; however, intracellular bacteria complicate optimal chemotherapy predictions. This is due to the fact that compounds depend on a series of pharmacokinetic and pharmacodynamic factors such as penetration, accumulation and bioavailability of the drugs inside cells for bacteria to be available to susceptibility.

The recent increasing incidence of multidrug- and extensively drug resistant TB (MDR/XDR-TB) worldwide necessitated the development of novel anti-mycobacterial agents. When

Linezolid was introduced in the treatment of multidrug-resistant *Streptococcus pneumonia* (Silver, Bostian 1990), it also led to its use with other second- and third-line drugs to treat patients with MDR/XDR-TB. Moreover, it has the ability to enter macrophages and thus has intracellular activity (Wang, Zhao et al. 2014).This is an important feature when it is to be used against mycobacteria that cause chronic infections and require long-term therapy (Leach, Brickner et al. 2011).

This study reports the *in vitro* testing of two natural and one synthetic pulmonary surfactant on the anti-mycobacterial effect of Linezolid against a standard H37Rv M.*tb* strain as well as the resistant X51 M.*tb* strain. The approach of investigating an alternative treatment option for pulmonary tuberculosis that alters the bacteria's cell membrane, and therefore its protective barrier, may prove exogenous surfactants as vehicles for drug delivery. The effects of various pulmonary surfactants on the action of the antimicrobial agent Linezolid against M.*tb* have not been described before.

4.2 Materials and Methods

All experiments with infectious material were carried out in a category-3 biosafety laboratory.

(*S*)-*N*-[[3-(3-fluoro-4-morpholinylphenyl)-2-oxo-5-oxazolidinyl]methyl] acetamide	**H37Rv Strain**	**R51 Strain**
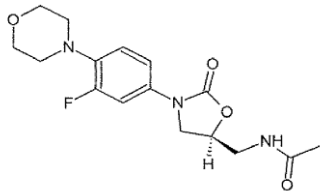 Linezolid	**1 µg/ml**	

Figure 4.1: Minimum Inhibitory Concentration Linezolid.

Linezolid used in this study was obtained as pure substances (Lot #015M4715V (CAT# PZ0014) Sigma-Aldrich Co., St. Louis, MO) and the dilution series was prepared in PBS (pH 7.4).

4.2.1 Mycobacterium species isolates

Clinical isolates of M. *tuberculosis* R51 XDR strain and M. *tuberculosis* H37Rv reference strain, banked in the Department of Medical Biochemistry (SU), was cultured on L-J slant cultures and used for MGIT analysis. Quality control was carried out by coexistent determination of the MICs.

4.2.2 Mycobacterium Culture and Growth Inhibition

For drug-resistant strains from South Africa, mycobacterial growth was measured by using mycobacterial growth indicator tubes (MGIT). Mycobacterial inocula were prepared from cultures of all strains grown on Lowenstein Jensen (LJ) slants. Cell suspensions were prepared in saline and the turbidity adjusted to 0.5 McFarland units. A 1:5 dilution of the bacterial suspension was prepared, and 0.5 ml of the suspension was inoculated into MGIT tubes containing test and control compounds. For mycobacterial growth evaluation, the MGIT 960 system (Becton Dickinson, Sparks, MD) was used, where M. *tuberculosis* growth is observed through fluorescent changes due to oxygen consumption during mycobacterial growth (Rusch-Gerdes *et al.* & Becton Dickinson and Company). One-tenth millilitre of serially diluted

compound was added to the MGIT tube containing 7H9 culture medium, with the final DMSO concentration not exceeding 1.2%. Incubation at 37 °C was continued in the MGIT system, and the growth units (GU) were monitored daily. For MIC_{99} evaluations, a 1% bacterial control culture was prepared in a drug-free MGIT tube and the MIC_{99} of the compound determined relative to the growth units of the control (GU = 400). When the GU of the growth control were 400 and the GU of the drug-containing tube were more than 400, the results were defined as showing resistance, and when the GU of the drug-containing tube were less than 400, the results were considered to show susceptibility.

4.3 Results

Table 4.1: M.*tb* H37Rv clinical isolate drug susceptibility testing with Linezolid at established MIC99 (1 µg/ml) with various exogenous surfactants (R, resistant; S, susceptible). **Abbreviations:** MIC99, minimum inhibitory concentration; PBS, Phosphate-buffered saline.

COMPOUND	CONCENTRATION (µg/ml)	GROWTH UNITS (Day 8)	SUSCEPTIBILITY MIC_{99} (µg/ml)
Control	-	400	
H37Rv with PBS solvent	-	13816	
INH	0.05 µg/ml	0	S
Linezolid	1 µg/ml	377	S
Linezolid	0.5 µg/ml	4674	R
Linezolid	0.25 µg/ml	12878	R
Linezolid	0.125 µg/ml	12030	R
Linezolid + Curosurf®	1 µg/ml	0	S (enhanced)
Linezolid + Curosurf®	0.5 µg/ml	3242	R
Linezolid + Curosurf®	0.25 µg/ml	13276	R
Linezolid + Curosurf®	0.125 µg/ml	12180	R
Linezolid + Synsurf®	1 µg/ml	94	S (enhanced)
Linezolid + Synsurf®	0.5 µg/ml	4773	R
Linezolid + Synsurf®	0.25 µg/ml	12783	R
Linezolid + Synsurf®	0.125 µg/ml	14515	R
Linezolid + Liposurf®	1 µg/ml	143	S (enhanced)
Linezolid + Liposurf®	0.5 µg/ml	3706	R
Linezolid + Liposurf®	0.25 µg/ml	13176	R
Linezolid + Liposurf®	0.125 µg/ml	11228	R
Curosurf® only	1 %	10674	R
Synsurf® only	1 %	17589	R
Liposurf® only	1 %	14252	R

Table 4.2: M.*tb* X51 clinical isolate drug susceptibility testing with Linezolid at established MIC (1 µg/ml) with various exogenous surfactants (R, resistant; S, susceptible). **Abbreviations:** MIC_{99}, minimum inhibitory concentration; PBS, Phosphate-buffered saline.

COMPOUND	CONCENTRATION (µg/ml)	GROWTH UNITS (Day 8)	SUSCEPTIBILITY MIC_{99} (µg/ml)
Control	-	400	
X51 with PBS solvent	-	12861	
Linezolid	1 µg/ml	0	S
Linezolid	0.5 µg/ml	714	R
Linezolid	0.25 µg/ml	6727	R
Linezolid	0.125 µg/ml	9164	R
Linezolid + Curosurf®	1 µg/ml	0	S
Linezolid + Curosurf®	0.5 µg/ml	622	R
Linezolid + Curosurf®	0.25 µg/ml	6131	R
Linezolid + Curosurf®	0.125 µg/ml	10191	R
Linezolid + Synsurf®	1 µg/ml	0	S
Linezolid + Synsurf®	0.5 µg/ml	1255	R
Linezolid + Synsurf®	0.25 µg/ml	6316	R
Linezolid + Synsurf®	0.125 µg/ml	11684	R
Linezolid + Liposurf®	1 µg/ml	0	S
Linezolid + Liposurf®	0.5 µg/ml	301	S (enhanced)
Linezolid + Liposurf®	0.25 µg/ml	5762	R
Linezolid + Liposurf®	0.125 µg/ml	9021	R
Curosurf® only	1 %	12892	R
Synsurf® only	1 %	13420	R
Liposurf® only	1 %	13333	R

4.4 Discussion

Linezolid, in combination with the animal derived surfactants (Curosurf® & Liposurf®) and the synthetic surfactant (Synsurf®), displayed a certain degree of enhanced activity in both strains at certain concentrations compared to their unformulated counterparts *in vitro*. No decrease in Linezolid activity was witnessed when in combination with exogenous surfactant. There have been many suggestions and postulations as to why M.*tb* displays increased susceptibility to drugs when combined with various surfactants. Stoops and colleagues (Stoops, Arora et al. 2010) suggested that surfactants act as "permeabilising agents" and therefore are proficient enough in removing the TDM coat that acts as M.*tb*'s first line of defence. For this reason, increased drug permeability into the intracellular space of the bacteria takes place rather than increasing its own activity. This could be the very reason why Linezolid displays the increased activity in combination with surfactant even at lower MIC concentrations compared to Linezolid alone for both the H37Rv strain (Table 4.1) and the X51 strain (Table 4.2). Taking the surfactant proteins into consideration, SP-A and SP-D may facilitate the clearance of bacteria through numerous mechanisms. SP-A and SP-D may also act as opsonins to enhance bacterial phagocytic removal *in vivo*. Additionally, these collectins appear to exhibit anti-microbial effects on bacteria by potentially increasing the permeability of their membranes (Glasser, Mallampalli 2012). Both SP-A and SP-D bind to LPS, but each interacts with LPS via different mechanisms: SP-D binds to LPS through the core oligosaccharides, whereas SP-A binds to the lipid A domain. SP-D binds Gram-positive bacteria though peptidoglycan and lipoteichoic acid, however, SP-A is unable to interact with these parts but instead utilises the extracellular adhesin protein, Eap, on Gram-positive *S. aureus* for opsonisation as reported by Sever-Chroneos *et al.* (Sever-Chroneos, Krupa et al. 2011). These collectins promote phagocytosis indirectly, by stimulating the activity of alveolar macrophages (Lemos, McKinney et al. 2011). *S. aureus* is opsonized by SP-A, and this allows for the interaction with the recognised SP-A receptor 210 (SP-R210) on alveolar macrophages for phagocytosis (Sever-Chroneos, Krupa et al. 2011). SP-R210, opsonised by SP-A, is also involved in eradicating *Mycobacterium bovis* (bacillus Calmette–Guerin) (Levine, Whitsett 2001). Furthermore, a study performed by Pasula and colleagues suggested that SP-A could mediate M.*tb* attaching to AMs in a Ca^{2+}-dependent manner (Pasula, Downing et al. 1997). However, in a comparative study by Lemos and colleagues (2011), it was reported that the roles of SP-A and SP-D in M.*tb*

infection is not essential for immune control of M.*tb* in a low-dose, aerosol challenge, murine model of TB (Lemos, McKinney et al. 2011).

There have also been reports that SP-B may also, although limited, be a participant in the innate host defence. Ryan *et al.* (2006) reported that SP-B, isolated from human BALF, killed clinical isolates of Gram-positive and Gram-negative bacteria in a dose-dependent manner. They too investigated synthetic peptide derivatives of SP-B, that exhibited a more discerning bactericidal tendency by means of selective lysed bacterial membranes. It was suggested that SP-B interacts with the surface of the lipid bilayer via amphipathic α helices. Therefore, the selectivity between native SP-B and the synthetic peptide derivatives could be due to the mechanism of action that has been proposed for a large number of cationic antibiotic peptides (Chimote, Banerjee 2005). For example, the proposed model by Shai (2002) argues that peptides act on bacterial membranes in four main steps (not discussed here) based on the electrostatic interactions and interfacial hydrophobicity of sufficient levels and accumulation of cationic SP-B peptides (Shai 2002). However, Ryan *et al.*(2006) reported that only the cationic synthetic peptides were attracted to the negatively charged membranes forming permeabilising oligomers; whereas, native SP-B is able to permeabilise both anionic and zwitterionic membranes, even at low protein densities (Ryan, Akinbi et al. 2006).

Synsurf® used in this study, is a synthetic lung surfactant containing polymers of poly-L-lysine electrostatically bonded with poly-L-glutamic acid (~50% neutralisation), to give a cationic peptide complex. The two-stranded polymer containing a percentage of basic lysyl side chains participate in the formation of protein-phospholipid bonds. The construct also has a degree of hydrophobicity in the neutralised double-stranded portion of the molecule forming antiparallel β-sheet aggregates that interacts with the phospholipid bilayer; thus, mimicking some structural and/or functional properties of SP-B (Gray, Vander Velde et al. 1994, van Zyl, Smith 2013b, Shafer 1974, Hartmann, Galla 1978). Moreover, it is known that polycations are able to disrupt outer membranes of bacteria (Vaara 1992). In this regard, it was previously reported that *M. smegmatis* and *M. tuberculosis* display high sensitivity to the bactericidal activity of polylysine on its own (Delihas, Riley et al. 1995). However, our results show that the cationic polymer construct with poly-L-glutamic acid in Synsurf® only displayed antimycobacterial activity in combination with linezolid. This finding is also similar to the results shown with the natural surfactants tested in this study. Although experiments using surfactant in live bacterial cultures

are complex and can be difficult to interpret, we have shown previously that surfactants significantly enhance the permeability of drugs across different epithelia (Viljoen 2005). Taken together, it therefore remains possible that the cationic peptide construct of Synsurf® is able to initiate translocation and cause an increase in membrane permeabilisation in M.*tb* bacilli in order to initiate the enhanced antimycobacterial effect of linezolid.

In summary, the benefit of combining linezolid with a surfactant's antibacterial potential, as indicated in this study, may be useful to improve site-specific drug administration that could allow for lower dosages and minimizing subsequent systemic adverse-effects in the treatment of resistant strains to current chemotherapy regimens.

4.5 Conclusion

The fundamental limitations of this study have to be taken into consideration. Various surfactants were used instead of human surfactant; furthermore, the concentration of the exogenous surfactant used in this study was significantly lower than the concentration of pulmonary surfactant that would be found lining the epithelium. One can therefore conclude that the concentration of pulmonary surfactant, as well as SP-B, *in vivo* may further influence antibiotic activity. However, regardless of concentrations, the surfactants display an impact on the antibiotic activity, the findings of which potentially are of clinical relevance but which must be investigated further in clinical settings. The effects of exogenous surfactants on the microbiology within the human lung *in vivo* have yet to be investigated as well. Although this is only a first step to study the changes in susceptibility of linezolid combined with exogenous surfactants to M.*tb*, the finding holds positive ramifications towards the development of a surfactant loaded with linezolid and other antitubercular drugs in the treatment of one of the most dreaded diseases.

4.6 References

CHIMOTE, G. and BANERJEE, R., 2005. Lung surfactant dysfunction in tuberculosis: Effect of mycobacterial tubercular lipids on dipalmitoylphosphatidylcholine surface activity. *Colloids and Surfaces B: Biointerfaces*, **45**(3), pp. 215-223.

CIPOLLA, D., BLANCHARD, J. and GONDA, I., 2016. *Development of Liposomal Ciprofloxacin to Treat Lung Infections.*

CORNFORTH, J.W., HART, P.D., NICHOLLS, G.A., REES, R.J.W. and STOCK, J.A., 1955. Antituberculous effect of certain surface-active polyoxyethylene ethers in mice. *British Journal of Pharmacology and Chemotherapy*, **10**(1), pp. 73-86.

DELIHAS, N., RILEY, L.W., LOO, W., BERKOWITZ, J. and POLTORATSKAIA, N., 1995. High sensitivity of Mycobacterium species to the bactericidal activity by polylysine. *FEMS Microbiology Letters*, **132**(3), pp. 233-237.

GLASSER, J.R. and MALLAMPALLI, R.K., 2012. Surfactant and its role in the pathobiology of pulmonary infection. *Microbes and Infection*, **14**(1), pp. 17-25.

GOERKE, J., 1998. Pulmonary surfactant: functions and molecular composition. *Biochimica et Biophysica Acta (BBA) - Molecular Basis of Disease*, **1408**(2–3), pp. 79-89.

GRAY, R.A., VANDER VELDE, D.G., BURKE, C.J., MANNING, M.C., MIDDAUGH, C.R. and BORCHARDT, R.T., 1994. Delta-sleep-inducing peptide: solution conformational studies of a membrane-permeable peptide. *Biochemistry*, **33**(6), pp. 1323-1331.

HARTMANN, W. and GALLA, H., 1978. Binding of polylysine to charged bilayer membranes. Molecular organization of a lipid · peptide complex. *BBA - Biomembranes*, **509**(3), pp. 474-490.

HUANG, T., LIU, Y., SY, C., CHEN, Y., TU, H. and CHEN, B., 2008. In Vitro Activities of Linezolid against Clinical Isolates of Mycobacterium tuberculosis Complex Isolated in Taiwan over 10 Years. *Antimicrobial Agents and Chemotherapy*, **52**(6), pp. 2226.

LEACH, K., BRICKNER, S., NOE, M. and MILLER, P., 2011. Linezolid, the first oxazolidinone antibacterial agent. *Annals of the New York Academy of Sciences*, **1222**(1), pp. 49-54.

LEMOS, M.P., MCKINNEY, J. and RHEE, K.Y., 2011. Dispensability of Surfactant Proteins A and D in Immune Control of Mycobacterium tuberculosis Infection following Aerosol Challenge of Mice. *Infection and immunity*, **79**(3), pp. 1077-1085.

LEVINE, A. and WHITSETT, J.A., 2001. Pulmonary collectins and innate host defense of the lung. *Microbes and Infection*, **3**(2), pp. 161-166.

MOELLERING, R.C., 2003. Linezolid: the first oxazolidinone. *Annals of internal medicine*, **138**(2), pp. 135-142.

PASULA, R., DOWNING, J.F., WRIGHT, J.R., KACHEL, D.L., DAVIS JR, T.E. and MARTIN, W.J., 1997. Surfactant protein A (SP-A) mediates attachment of Mycobacterium tuberculosis to murine alveolar macrophages. *American Journal of Respiratory Cell and Molecular Biology*, **17**(2), pp. 209-217.

PATIL-GADHE, A., KYADARKUNTE, A., PEREIRA, M., JEJURIKAR, G., PATOLE, M., RISBUD, A. and POKHARKAR, V., 2014. Rifapentine-proliposomes for inhalation: In vitro and In vivo toxicity (Original Article)(Report). *Toxicology International*, **21**(3), pp. 275.

RISIN, S.A., HUNTER, R.L., KOBAK, M., ARIEL, B., VISHNEVSKY, B., EROKHIN, V., DEMIKHOVA, O., BOCHAROVA, I. and STOOPS, J.K., 2014. Certain Surfactants Significantly Enhance the Activity of Antibiotics in the Mouse Model of MTB and Drug Resistant MTB Infection and Effectively Remove the Bacteria from a Pulmonary Cavity in Human Ex-Vivo Study. *Annals of Clinical & Laboratory Science*, **44**(2), pp. 117-122.

RYAN, M., AKINBI, H., SERRANO, A., PEREZ-GIL, J., WU, H., MCCORMACK, F. and WEAVER, T., 2006. Antimicrobial Activity of Native and Synthetic Surfactant Protein B Peptides. *Journal of Immunology*, **176**(1), pp. 416-425.

SAUERMANN, R., SCHWAMEIS, R., FILLE, M., LIGIOS, M.L.C. and ZEITLINGER, M., 2009. Cerebrospinal fluid impairs antimicrobial activity of fosfomycin in vitro. *The Journal of Antimicrobial Chemotherapy*, **64**(4), pp. 821.

SEVER-CHRONEOS, Z., KRUPA, A., DAVIS, J., HASAN, M., YANG, C.H., SZELIGA, J., HERRMANN, M., HUSSAIN, M., GEISBRECHT, B.V., KOBZIK, L. and CHRONEOS, Z.C., 2011. Surfactant protein A (SP-A)-mediated clearance of Staphylococcus aureus involves binding of SP-A to the staphylococcal adhesin eap and the macrophage receptors SP-A receptor 210 and scavenger receptor class A. *The Journal of Biological Chemistry,* **286**(6), pp. 4854-4870.

SHAFER, P.T., 1974. The interaction of polyamino acids with lipid monolayers. *BBA - Biomembranes,* **373**(3), pp. 425-435.

SHAI, Y., 2002. *Mode of action of membrane active antimicrobial peptides.* New York.

SILVER, L. and BOSTIAN, K., 1990. Screening of natural products for antimicrobial agents. *The European Journal of Clinical Microbiology & Infectious Diseases,* **9**(7), pp. 455-461.

SILVERMAN, J.A., MORTIN, L.I., VANPRAAGH, A.D.G., LI, T. and ALDER, J., 2005. Inhibition of daptomycin by pulmonary surfactant: in vitro modeling and clinical impact (MAJOR ARTICLE). *Journal of Infectious Diseases,* **191**(12), pp. 2149.

STOOPS, J.K., ARORA, R., ARMITAGE, L., WANGER, A., SONG, L., BLACKBURN, M.R., KRUEGER, G.R. and RISIN, S.A., 2010. Certain surfactants show promise in the therapy of pulmonary tuberculosis. *In Vivo,* **24**(5), pp. 687-694.

VAARA, M., 1992. Agents that increase the permeability of the outer membrane. *Microbiological Reviews,* **56**(3), pp. 395-411.

VAN ZYL, J.M. and SMITH, J., 2013b. Surfactant treatment before first breath for respiratory distress syndrome in preterm lambs: comparison of a peptide-containing synthetic lung surfactant with porcine-derived surfactant. *Drug Design, Development and Therapy,* **7**, pp. 905-916.

VAN'T VEEN, A., MOUTON, J.W., GOMMERS, D., KLUYTMANS, J.A., DEKKERS, P. and LACHMANN, B., 1995. Influence of pulmonary surfactant on in vitro bactericidal activities of amoxicillin, ceftazidime, and tobramycin. *Antimicrobial Agents and Chemotherapy,* **39**(2), pp. 329-333.

VILJOEN, I., 2005. *The role of surfactant in, and a comparison of, the permeability of porcine and human epithelia to various chemical compounds. (Dissertation)*, Thesis (MScMed)-University of Stellenbosch, 2005.

WANG, D., ZHAO, Y., LIU, Z., LEI, H., DONG, M. and GONG, P., 2014. In vitro and intracellular activity of 4-substituted piperazinyl phenyl oxazolidinone analogues against Mycobacterium tuberculosis. *The Journal of Antimicrobial Chemotherapy,* **69**(6), pp. 1711.

WHITE, D.C. and FRERMAN, F.E., 1967. Extraction, Characterization, and Cellular Localization of the Lipids of Staphylococcus aureus. *The Journal of Bacteriology,* **94**(6), pp. 1854.

WORLD HEALTH ORGANIZATION, 2015-last update, Global Tuberculosis Report 2015 [Homepage of WHO Press, World Health Organization], [Online]. Available: http://apps.who.int/iris/bitstream/10665/191102/1/9789241565059_eng.pdf [March, 21, 2016].

5 CHAPTER 5: Investigating the Calu-3 cell line as a model for the delivery, deposition and transport of the pMDI form of Synsurf®

5.1 Introduction

There has been considerable effort invested in generating aerosols for pulmonary delivery over the last 10 years. In this regard, administering clinically relevant dosages of inhaled drug and control of lung-regional distribution thereof has proven to be challenging. Moreover, the pharmaceutical industry relies on suitable *in vitro* models for evaluation of drug absorption and metabolism as an alternative to testing in animals. The aim of inhalation of drugs for pulmonary disease therapy is to increase the local drug concentration by avoiding systemic toxicity of said compounds. Three essential variables should therefore be considered. Firstly, precision of the drug targeting specific regions within the lung, preventing drug deposition and loss in the upper respiratory tract. Secondly, uniform drug deposition in the lung that allows for reliable drug dosing, even under varied conditions and diseases. Thirdly, aiming for consistency in that uniform drug deposition occurs throughout the device's life span. When considering these principal pillars of lung deposition of aerosols, improved understanding of the delivery devices and active compounds is required (Georgopoulos, Mouloudi et al. 2000). However, the lung is a complex organ that the functioning of which is regulated by multiple factors such as the structure of the epithelia, the physicochemical properties of the drug as well as the type of delivery system used. Although improved drug deposition remains an important aim, enhanced therapeutic effects do not necessarily follow. Studies of drug deposition *in vitro* may reveal the fate of deposited particles on respiratory epithelia, which may allow for a better understanding of similar happenings *in vivo* (Haghi, Traini et al. 2014). However, the physical features of the respiratory system, as well as its metabolic activity and drug efflux systems constitute a barrier against drug absorption and therefore are vital components for the study of drug transport and potential site for drug toxicity (Florea, Cassara et al. 2003).

The human bronchial adenocarcinoma, Calu-3 cell line, due to its simple reproducible process and similarity *in vivo* physiology, has become the alternative investigatory model for the *in vitro* study of proximal airway respiratory exposure to better understand determinants that

influences pulmonary drug dissolution, absorption, metabolism and efficacy (Ong, Traini et al. 2013, Harcourt, Haynes 2013). Several studies have validated Calu-3 cells as suitable model for investigating drug and ion transport due to their well-formed differentiated, polarised, electrically resistant cell layers (Shen, Finkbeiner et al. 1994, Foster, Avery et al. 2000, Meindl, Stranzinger et al. 2015). From a drug delivery perspective, the objective in this study was to investigate whether the use of two formulations of the synthetic surfactant Synsurf® [S], combined with linezolid, is suitable as a carrier and drug delivery agent for inhalation. Although the idea to use lung surfactant as a carrier agent was proposed several years ago with a tobramycin-surfactant mixture, where it was shown in our previous studies that Synsurf® enhances the permeability of drugs such as 17β-estradiol, hydrocortisone, dexamethasone, zidovudine and isoniazid across porcine bronchial tissue (Viljoen 2005). This new synthetic lung surfactant contains the amphipathic phospholipid DPPC and surface-active phosphatidylglycerol, as well as 1-hexadecanol and tyloxapol and a polymer peptide complex of poly-L-lysine and poly-L-glutamic acid. Although various drugs have been tested in combination with lipid particles, the synthetic lung surfactant Alveofact® was the first liposomal product to reach the market in 15 to 20 years (Beija, Salvayre et al. 2012).

The aim of this study was therefore to test linezolid combined with Synsurf® in a pressurised metered dose inhaler (pMDI) utilising a Calu-3 cell line as target model. To our knowledge, this is an unexplored area with regards to the drug.

5.2 Materials and Methods

Reagents and Standards

HPLC grade acetonitrile (Romil, UK), MilliQ water (Millipore, Milford, MA, USA) and ammonium acetate (Analytical, Merck, Darmstadt, Germany) were used in the mobile phase. The rest of the analyte standards and linezolid were supplied by Sigma Aldrich (St. Louis, MO, USA). Standards were made up volumetrically and appropriately diluted in 50% acetonitrile. The rest of the standards were made up to 0.005 mg/L, 0.05 mg/L, 0.5 mg/L, 2.5 mg/L, 5 mg/L, 25 mg/L, 50 mg/L and 250 mg/L to fall within the expected concentration range that it may occur in samples which had been diluted ten times.

Culture of Calu-3 Cells

The Calu-3 cell line (ATCC® HTB-55™) (passage 33–36) was first cultured as a polarised liquid-covered culture in 75 cm^2 flasks and maintained in a humidified, 5% CO_2–95% atmospheric air incubator at 37°C before subcultured in 12 cm diameter Transwell© inserts (0.33 cm^2 polyester, 0.4 μm pore size) from Costar. Culture medium comprised of Dulbecco's modified Eagle's medium (DMEM) supplemented with 10% fetal calf serum, 1% nonessential amino acid solution (×100), 1% L-glutamine solution (200 mM), and 1% Penicillin-Streptomycin.

Cells cultured on Transwell© supports were seeded at a density of 5×10^5 cells/cm^2 and were introduced into the apical surface of the Transwell© support in 0.2 ml medium with 2 ml medium added to the basolateral chamber. The cells were incubated at 37 °C, 5% CO_2 for 24hrs. For air-liquid interface culture, the cell culture medium was removed on day 2 post-seeding. The cell layers were evaluated through light microscopy with a Nikon TMS Inverted Phase Contrast Microscope (Nikon, Japan). Trans-epithelial electrical resistance (TEER) was measured using an EVOM2 chopstick electrode and EVOM2 Epithelial Voltohmeter (World Precision Instruments, USA). Pre-warmed medium (0.2 ml, 37°C) was added to the apical chamber before returning cells to the incubator to equilibrate for a further 30 min, and then measuring the electrical resistance. TEER was calculated by subtracting the resistance of a cell-free culture insert with correction for the surface area of the Transwell© cell culture support. When the trans-epithelial electrical resistance had reached a value of >700 Ω*cm^2 in submersed culture, it was considered confluent. In air-liquid interface culture, the medium (1.5 ml) in the

basolateral compartment was changed every 2 – 3 days. 0.5 ml and 1.5 ml media were added to the apical and the basolateral compartment respectively for TEER measurements. Prior to the reading cells were equilibrated for 30 min in the incubator.

TEER values were calculated as follows (Equation 1):

TEER ($\Omega * cm^2$) = (Sample – blank resistance, given in Ω) * membrane area, given in cm^2

Blank resistance is defined as the resistance of the membrane without cells and the membrane area for 12-well inserts is calculated to be 1.12 cm^2/well.

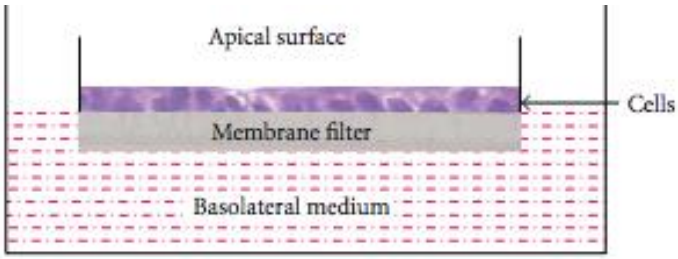

Figure 5.1: Calu-3 air-liquid interface cell culture.

Cell Surface Staining

Alcian blue staining was employed for the detection of glycoproteins. Cell layers were washed twice with 100 ml HBSS and fixed for 10 min by using 2.5% (v/v) glutaraldehyde in 0.1 M sodium cacodylate buffer. The cells were washed again with HBSS and 100 ml alcian blue stain [1% (w/v) alcian blue in 3% (v/v) acetic acid/water at pH 2.5] added for 1 h. The dye was then removed and cell layer washed with HBSS until the rinsate ran clear.

Surfactant preparations

Two synthetic surfactant preparations were used in the study; (i) Synsurf® prepared as described previously by van Zyl and colleagues (prep 1)and (ii) Synsurf® formulated with the addition of 2 wt% cholesterol (prep 2) (Van Zyl, Smith et al. 2013a). Both formulations were then freeze-dried for further use in the pressurized metered dose inhaler (pMDI).

Synsurf® pMDIs

Canisters were filled with a 1:1 ratio of linezolid to Synsurf® (prep 1 & 2). Hydrofluoroalkane (HFA) propellant (Mexichem-Fluor, Runcorn) was added and the canisters were sealed with a

Pamasol Manual Crimper and Filler (DH Industries, Essex, UK). Three canisters were conveyed as: L= linezolid alone, LP1= linezolid + Synsurf® prep 1, and LP2= linezolid + Synsurf® prep 2.

Synsurf® preparation:

Prep1:DPPC 1200.5 mg (♯2); PG 120.5 mg; P-Lys 40.003 mg; P-Glu 12.66 mg; Cet-OH 133.5 mg

Prep 2:DPPC 1202.3 mg (♯2); PG 120.8 mg; P-Lys 40.56 mg; P-Glu 12.98 mg; Cet-OH 132.2 mg; Cholesterol 24.3 mg (2 wt%)

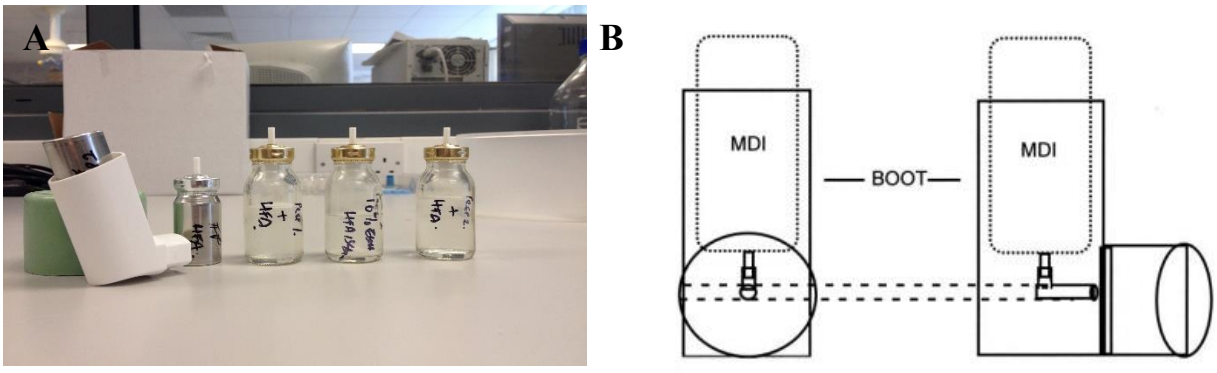

Figure 5.2: (A) pMDI with mouth-piece and canisters containing surfactant and relevant drug. **(B)** Illustration showing that the size of the canister stem and pin hole for the actuator in an albuterol chlorofluorocarbon-propelled metered-dose inhaler (MDI) differs from the hydrofluoroalkane-propelled MDI. The actuator of the chlorofluorocarbon-propelled MDI cannot be used interchangeably with the actuator of a hydrofluoroalkane-propelled MDI, and vice versa. (Illustration courtesy of James B Fink, MSc, RRT, FAARC.) (Georgopoulos, Mouloudi et al. 2000).

Scanning electron microscopy (SEM), cell surface morphology and pMDI drug deposition

The Calu-3 Transwells© were placed in the fixative solution, 2.5% glutaraldehyde and 0.5 g potassium ferrocyanide dissolved in 50 ml normal strength culture media (without serum) post pMDI actuation. The fixative was not added to the apical layer as to avoid possible "emulsion" of surfactant. Rather, the apical side of the Transwell© was covered within a glass dome with fixative solution in neighbouring wells and fixed via gaseous means for 2 hours. Cells were then washed with serum-free media and post-fixed with 1% osmium tetroxide + 1% potassium ferrocyanide for 1 hour at room temperature on the apical and basolateral side. Cells were

washed twice with distilled water over 15 minutes. The membranes were carefully cut out and placed in small glass vials and stained with 2% aqueous uranyl acetate for 1 hour in the dark. Membranes were further washed with acetone 50, 70 and 90% each one over 10 minutes and then twice with 100% acetone, followed by one 15 minute wash with an equal mix of acetone and Hexamethyldisilazane (HMDS) and then two final 15 minute washes with HMDS. They were left partially covered overnight and subsequently sputter coated with gold to achieve a thickness of approximately 20 nm (Edwards Sputter Coater S150B, Edwards High Vacuum, Sussex, UK). Imaging was performed using scanning electron Microscopy (JOEL SEM6480LV system, Tokyo, Japan).

In vitro aerosol deposition studies using a NGI device and dissolution analysis

A multistage cascade Next Generation Impactor™ (Copley Scientific) (NGI), for testing metered-dose inhalers was used. The impaction plates of the NGI were modified to accommodate 6 transwells at 3 stages. This allowed the study of different particle size fractions. The loaded device was connected to the throat of the NGI via a moulded mouthpiece. Testing was performed at a 60L min^{-1} flow rate with a 5 second exposure time after each actuation. A dissolution assay of samples in the basolateral Transwell© was performed upon each actuation (n=2). Samples were vortexed for 30 seconds with HBSS buffer, Sigma Aldrich (St. Louis, MO, USA), containing HEPES (10 mM) and a 0.025% TWEEN and then centrifuged for 10 min at 3000 rpm. Supernatants (±1 ml) were then transferred to HPLC vials. At the end of the experiment, the surface of the Calu-3 cells were washed with buffer and residual apical drug collected for analysis. This allowed for the calculation of total drug deposited via the cumulative sum of all samples.

Figure 5.3: Next Generation Impactor™ (Copley Scientific). **(Right Top)** Stage 1: 1 hole; 14.3 mm. Stage 3: 24 holes; 2.185 mm. Stage 5: 152 holes; 0.608mm. Stage 7: 630 holes; 0.206 mm. **(Right Bottom)** Stage 2: 6 holes; 4.88 mm. Stage 4: 52 holes; 1.207 mm .Stage 6: 396 holes; 0.323 mm. MOC 4032 holes 70 micron

Sample preparation

Samples from dissolution assays were vortexed for 30 seconds, centrifuged on a Hermle Z160M centrifuge (LASEC, SA) for 10 min at 3000 rpm and the supernatant (±1ml) was transferred to an HPLC vial.

Analyses of Linezolid by LC-MS

A Waters Synapt G2 quadrupole time-of-flight mass spectrometer (Waters Corporation, Milford, MA, USA), fitted with a Waters Acquity UPLC and photo diode array detector (PDA) was used for LC-MS analyses. Separation was achieved on a Waters BEH Amide UPLC column (2.1 x 100 mm, 1.7 µm) at a temperature of 35°C. Solvent A consisted of 10mM Ammonium acetate in water, solvent B consisted of 10mM Ammonium acetate in 95% acetonitrile. The gradient consisted of a flow rate 0.25 ml/min, starting with 95% B to 40% B over 9 minutes, applying gradient curve 7, followed by re-equilibration to initial conditions over 5 minutes. Electrospray ionization was done in the negative mode, using a capillary voltage of 2.5 kV, a cone voltage of 15 V, desolvation temperature of 250°C and desolvation gas (N_2) flow of 650 L/h. The rest of the MS settings were optimised for best sensitivity. Data was acquired in MSE mode, consisting of a scan using a low collision energy and a scan using a collision energy ramp from 25-60 V, which has the added advantage of acquiring low energy molecular ion data as well as fragmentation data for all analytes over time. Data was collected using a scan rate of 0.2 seconds over the range m/z 100 - 1000. Leucine enkaphalin was used as lock mass for accurate mass determination on the fly using a lock mass flow rate of 0.002

ml/min, acquiring lock mass data every 20 seconds. Sodium formate was used to calibrate the instrument. The PDA detector was set to scan over the range: 220 - 450 nm.

Drug permeability

The transport of compounds across Calu-3 cells is typically expressed in terms of the apparent permeability coefficient (Papp) measured in the absorptive apical to basolateral (Ap - Bl) direction and is calculated using Equation 5.1:

Equation 5.1:

$$P_{app} = \frac{dQ}{dt} \times \frac{1}{A \times C_0}$$

Where dQ/dt is the linear transport rate of the compound, A is the surface area of the cell layer and C_0 is the initial compound concentration in the donor chamber.

Statistical Analysis

All results are expressed as mean ± standard deviation of at least two replicate experiments. Data were analysed by GraphPad Prism, Version 5, statistical software package (GradPad Software Inc, San Diego, CA, 92130 USA). Analysis of variance (ANOVA) one-way (with Tukey's post hoc analysis) was utilised to test for significance (which was quoted at the level of $P \leq 0.05$) between treatment groups.

5.3 Results

Transepithelial resistance

Calu-3 cells were grown at the air interface to allow monolayer differentiation, and experiments were performed between days 11 and 14 when TEER reached values between 750 - 1000Ω*cm^2 (Figure 5.4). These conditions have previously been established by Haghi *et al.* (Haghi, Young et al. 2010). After the high TEER was determined and thus the presence of tight junction proteins confirmed, the surface properties of Calu-3 cells were studied by SEM pre- and post pMDI impactor actuation. Alcian Blue staining of the Calu-3 cells cultured at air-liquid interface was employed to indicate the presence and increasing concentration of membrane transporter proteins (Figure 5.5).

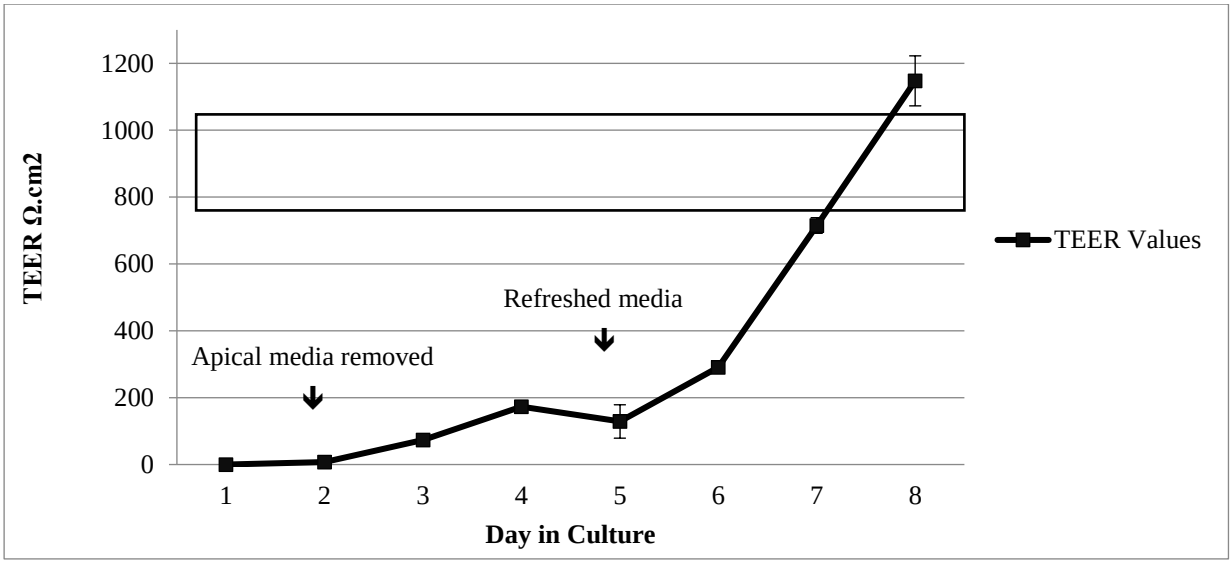

Figure 5.4: Trans-epithelial electrical resistance in Calu-3 cells at ALI.

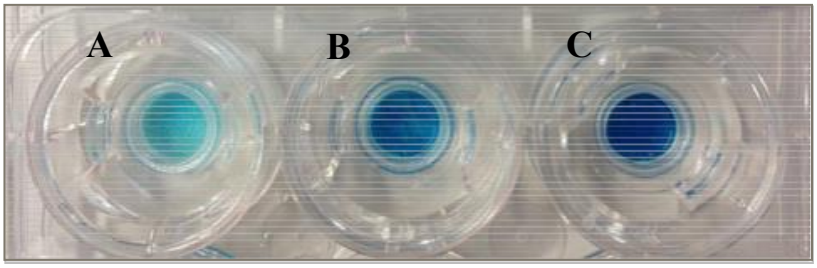

Figure 5.5: Alcian Blue staining of the Calu-3 cells cultured at ALI indicating the presence and increasing concentration of membrane transporter proteins **(A)** Day 1 **(B)** Day 7 **(C)** Day 14.

Transepithelial drug transport

The average particle size (D_{50}) for the NGI™ stages was established as follows: Stage 2: 4.46 µm; Stage 3: 2.82 µm and Stage 4: 1.66 µm at a flow rate of 60 L/min (Copley Scientific 2017). Uptake and transport experiments with linezolid were performed 14 days after seeding and trans-epithelial flux measurements were performed as well as the total amount of trans-epithelial drug transported and cellular uptake were calculated.

Apparent permeability for the three separate preparations in the absorptive direction (apical-to-basal) were determined for 240 minutes (after a 20 min pre-incubation to establish a state of linear flux). Fluxes are expressed as ng/mm^2/min. The passive (paracellular) route across the epithelium was estimated by repeated linezolid flux determinations that indicated steady-state diffusion.

Since these parameters are difficult to control i.e. the amount of recovered sample (start concentration in apical compartment, volume and the amount of samples within each NGI™ chamber), the initial compound concentration (C_0) in the donor chamber was established at the end of each uptake experiment (4 h). The total amount of linezolid collected from the basal compartment, as well as drug remaining on the cell surface and inside the cells were summed to represent total deposited mass (Haghi, Traini et al. 2013).

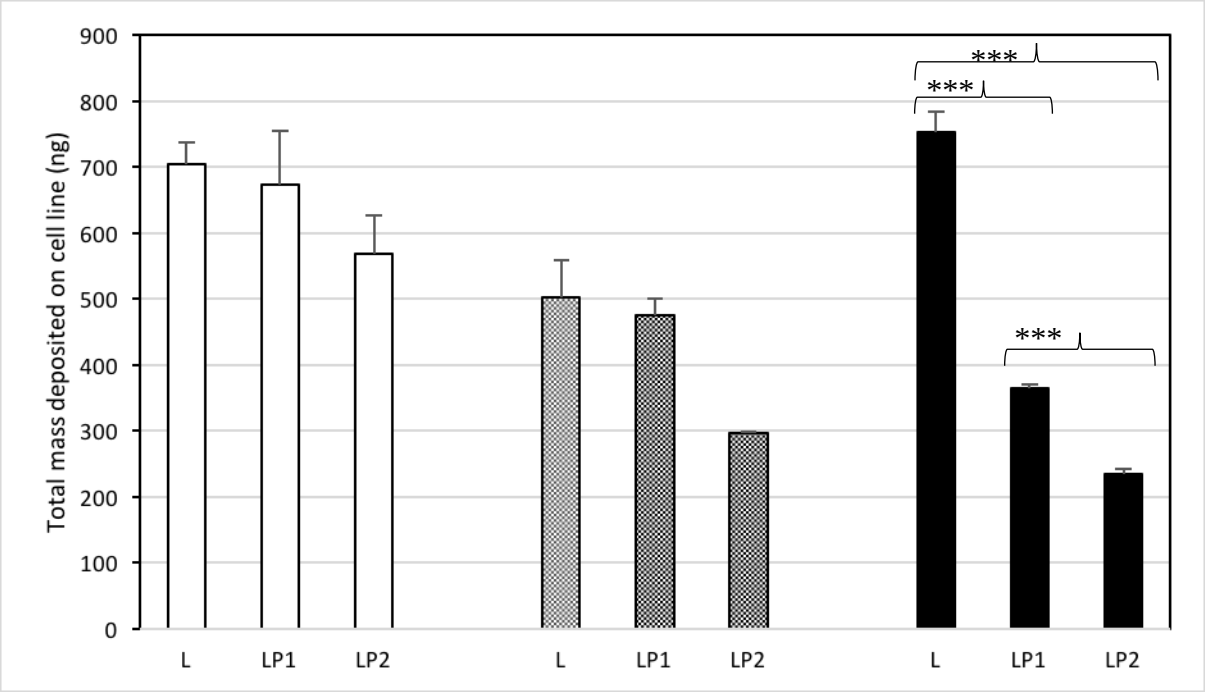

Figure 5.6: Total drug masses deposited on Calu-3 cell monolayer for □, stage 2; ▤, stage 3; and ■, stage 4. ($n = 2$, mean ± standard deviation (SD)) (one-way analysis of variance (ANOVA), Tukey's post-test $P \leq 0.0001$).

Figure 5.6 displays the total drug masses deposited on Calu-3 cell monolayer. One-way analysis of variance showed that the amounts of L deposited in the single preparation and in combination preparations (LP1 & LP2) were similar in stages 2 and 3. However, significant differences in deposited mass was found in stage 4 for L (452.50 ± 32.01 ng) vs. LP1 (363.96 ± 6.18 ng) and L vs. LP2 (235.59 ± 6.05 ng) and LP1 (363.96 ± 6.18 ng) vs. LP2 (235.59 ± 6.05 ng). This could be due to the increased weight/size of the combination preparations and the relative distance travelled to stage 4 (illustrates lower lung deposition) which could indicate the role of impaction rather than sedimentation for larger molecules.

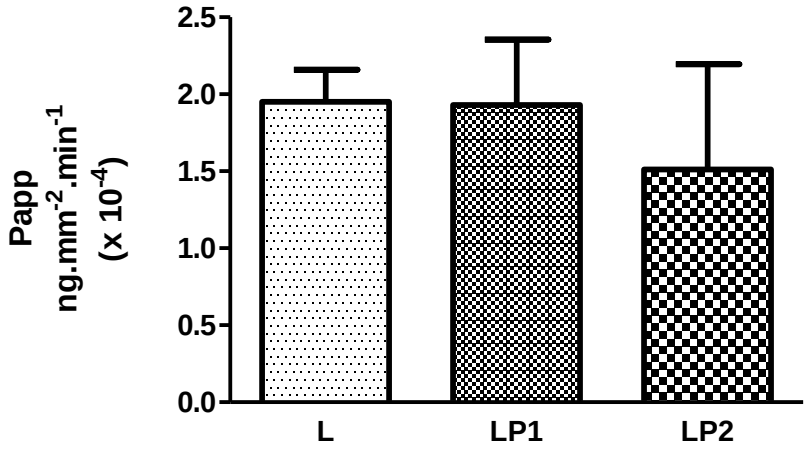

Figure 5.7: The relative transport rate (P_{app}) measured for Linezolid (L), Linezolid + Prep 1 (LP1) and Linezolid + Prep 2 (LP2) across the Calu-3 Transwell© in Stage 2. (one-way analysis of variance (ANOVA), Tukey's post-tests $P \leq 0.05$, no significance seen).

Figure 5.7 displays the relative transport rate (P_{app}) of linezolid measured for L, LP1 and LP2 across the Calu-3 Transwell© in Stage 2. Initial transport rates for L, LP1 and LP2 were found to be similar at P_{app} values of 1.95 x 10^{-4} (±0.30) ng.mm^{-2}.min^{-1}, 1.93 x 10^{-4} (±0.60) ng.mm^{-2}.min^{-1}, and 1.51 x 10^{-4} (±0.96) ng.mm^{-2}.min^{-1} respectively. In Figure 5.8, L and LP1 presented similar initial P_{app} values of 1.64 x 10^{-4} (±0.61) ng.mm^{-2}.min^{-1} and 1.67 x 10^{-4} (±0.01) ng.mm^{-2}.min^{-1} in stage 3 again; whereas LP2 displayed a significantly lower ($P \leq 0.05$) P_{app} value of 5.9 x 10^{-6} (±0.60) ng.mm^{-2}.min^{-1}. Stage 4 represented in Figure 5.9, shows similar initial transport rates for L, LP1 and LP2 at P_{app} values of 2.20 x 10^{-4} (±0.18) ng.mm^{-2}.min^{-1}, 2.02x10^{-4} (±0.41) ng.mm^{-2}.min^{-1},and 1.96 x 10^{-4} (±0.85) ng.mm^{-2}.min^{-1} respectively. These transport rates were also similar to those found in stage 2 (Figure 5.7).

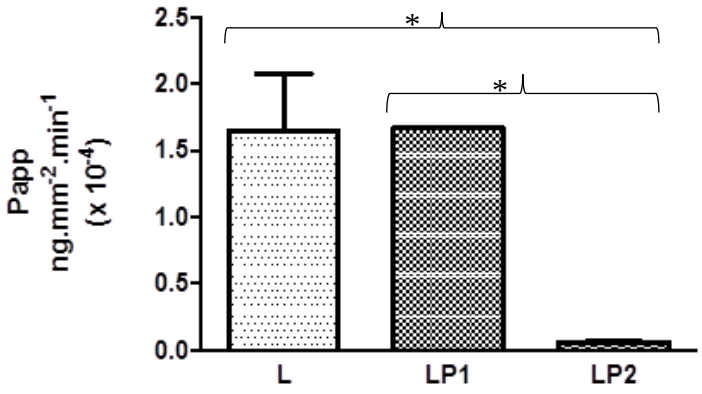

Figure 5.8: The relative transport rate (P_{app}) measured for Linezolid (L), Linezolid + Prep 1 (LP1) and Linezolid + Prep 2 (LP2) across the Calu-3 Transwell© in Stage 3. (one-way analysis of variance (ANOVA), Tukey's post-test * $P \leq 0.05$).

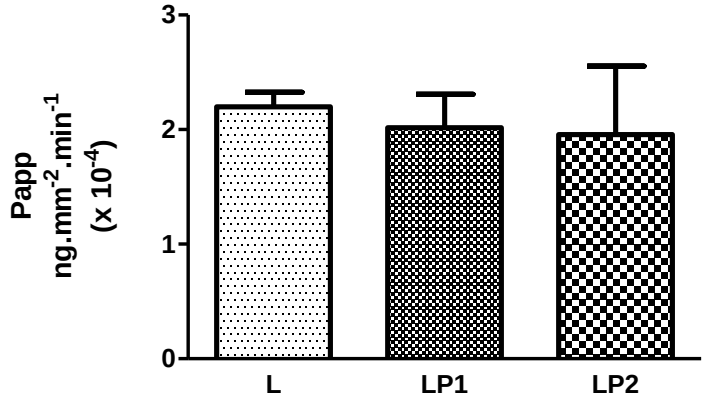

Figure 5.9: The relative transport rate (P_{app}) measured for Linezolid (L), Linezolid + Prep 1 (LP1) and Linezolid + Prep 2 (LP2) across the Calu-3 Transwell© in Stage 4. (one-way analysis of variance (ANOVA), Tukey's post-test $P \leq 0.05$, no significance seen).

Analysis of the transport after 4 h showed that 74.77 ± 9.50% mass percentage of linezolid from the single preparation (L) was detected in the basal chamber for stage 2. The percentage of linezolid detected in the basal chamber from the combination preparation LP1 (92.22 ± 0.25%) was significantly higher than from the combination preparation LP2 (56.42 ± 10.28%) for stage 2 (Figure 5.10). Stage 3 (Figure 5.11) showed very similar mass percentage after transport at 4 h of linezolid in the basal chamber for the single preparation L (86.50 ± 9.75%), and the combination preparations LP1 (72.55 ± 7.92%) and LP2 (88.31 ± 1.32%), respectively. The mass percentage of linezolid detected in the basal chamber for stage 4 (Figure 5.12) after 4 h

showed significant difference between the combination preparations LP1 (90.79 ± 0.55%) and LP2 (71.27 ± 12.98%), however, no difference was seen for the single preparation L (84.05 ± 3.44%).

As seen in Figure 5.10, analysis of the epithelial cell contents revealed that after 4 h, 18.35 ± 11.75% of linezolid from the single preparation (L), 5.00 ± 1.36% from the combination preparation, LP1, and a significant increased amount of 35.75 ± 6.27% from the combination preparation, LP2, were found in the epithelial cells at stage 2. Therefore, at the end of the experiment, 7.84 ± 0.08% of linezolid from L, 2.46 ± 0.97% from the combination preparation LP1, and 7.16 ± 2.4% from the combination preparation LP2, respectively, remained on the surface of the epithelial cells. The amount of linezolid that remained on the surface of the epithelial cells from LP2 significantly increased ($P \leq 0.05$) to that of LP1. The mass percentage remaining of linezolid in the single preparation L was also found to be statistically more than that of LP1 (Figure 5.11).

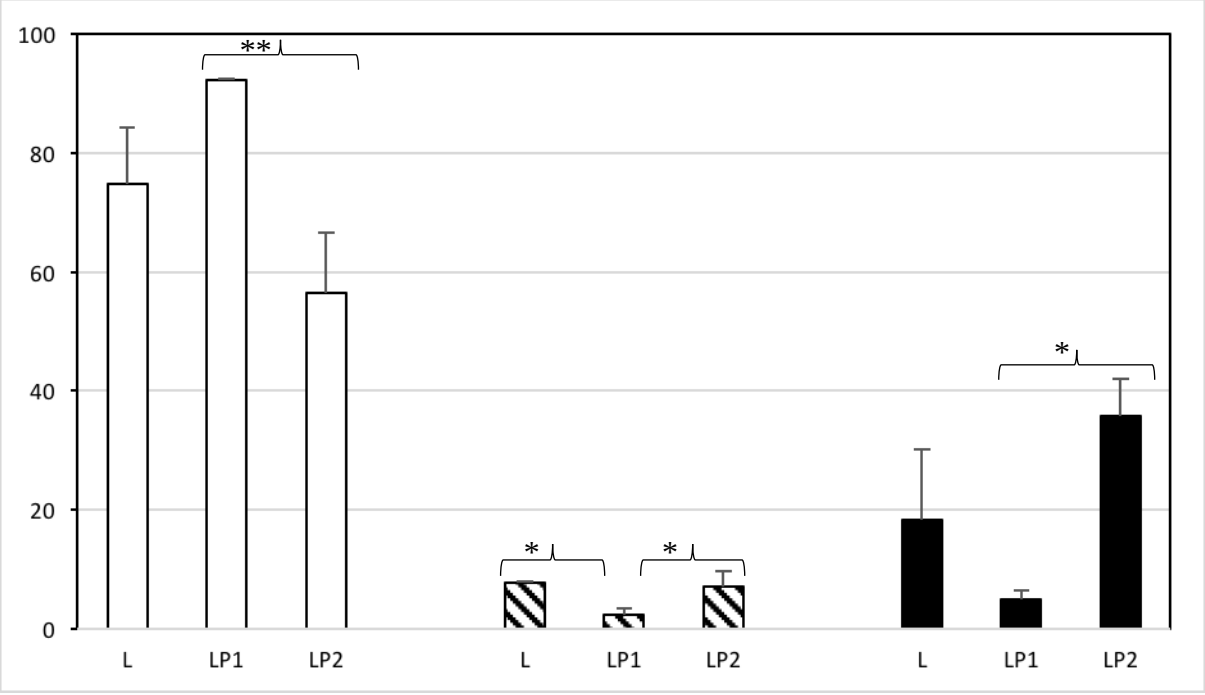

Figure 5.10: Percentage of total drug mass in the basal chamber, remaining on the cell surface, and inside the cells after 4 h after deposition of Linezolid (L), Linezolid + Prep 1 (LP1) and Linezolid + Prep 2 (LP2) at stage 2. (n = 2, mean ± standard deviation (SD)) (n = 3, mean ± SD) (one-way analysis of variance (ANOVA), Tukey's post-tests, * $P \leq 0.05$, ** $P \leq 0.01$). □, % in the basal compartment at 240 min; ▨, % on cells at 240 min; ■, % in cells at 240 min.

The mass percentage of linezolid remaining in the epithelial cell contents after 4 h for stage 3 can be seen in Figure 5.11. Linezolid from LP1 (27.34 ± 10.19 %) was significantly higher than that of linezolid from L (8.31 ± 4.79%) and LP2 (9.72 ± 0.24%), respectively. A similar mass percentage of linezolid remaining on the cell surface of the apical compartment was detected in stages 3 and 4 for all three preparations. The epithelial cell content of linezolid for the single preparation L was similar to stages 2 and 3 at 13.89±1.63 mass percentage at stage 4. The mass percentage (stage 4) of linezolid remaining in the epithelial cell contents from the combination preparation LP2 (22.22 ± 8.37%) was found to be statistically higher than that of linezolid from combination preparation LP1 (8.28 ± 0.27%). Stage 4 (Figure 5.12) showed a similar pattern in the differences of mass percentage for drug remaining within epithelial cell lysate contents for LP1 vs LP2 ($P \leq 0.05$). This direct comparison indicates the effect of drug combination type on cellular uptake and transport.

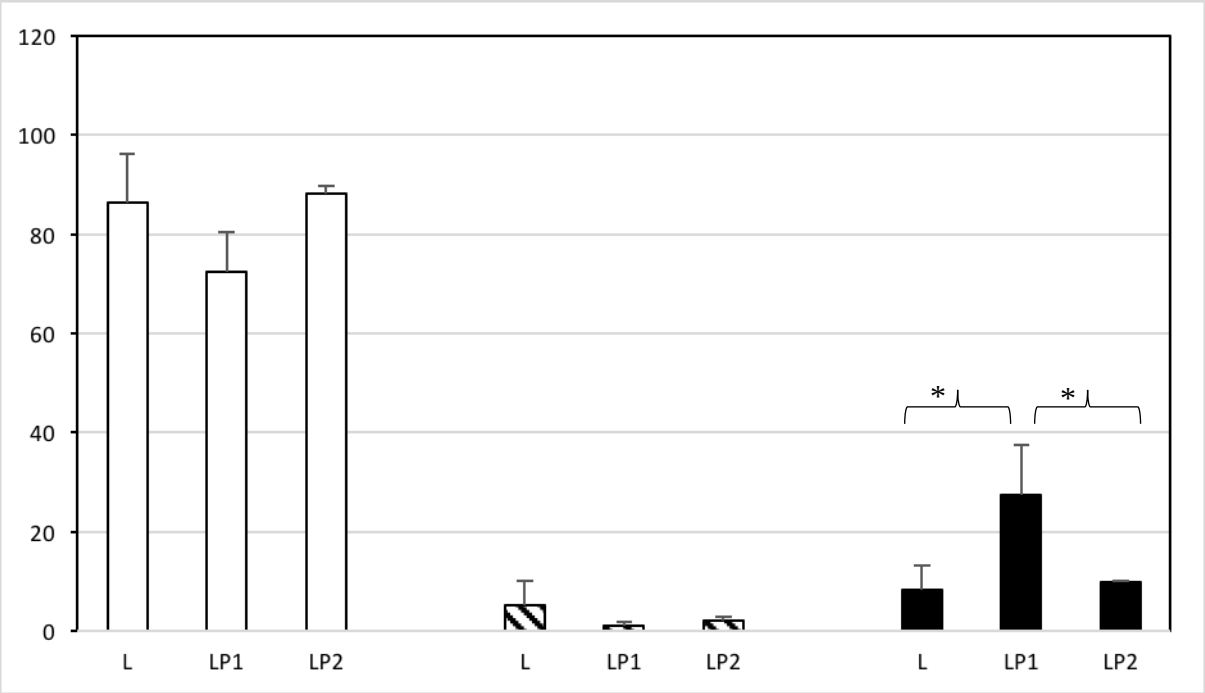

Figure 5.11: Percentage of total drug mass in the basal chamber, remaining on the cell surface, and inside the cells after 4 h after deposition of Linezolid (L), Linezolid + Prep 1 (LP1) and Linezolid + Prep 2 (LP2) at stage 3. (n = 2, mean ± standard deviation (SD)) (n = 3, mean ± SD) (one-way analysis of variance (ANOVA), Tukey's post-tests, * $P \leq 0.05$). □, % in the basal compartment at 240 min; ◪, % on cells at 240 min; ■, % in cells at 240 min.

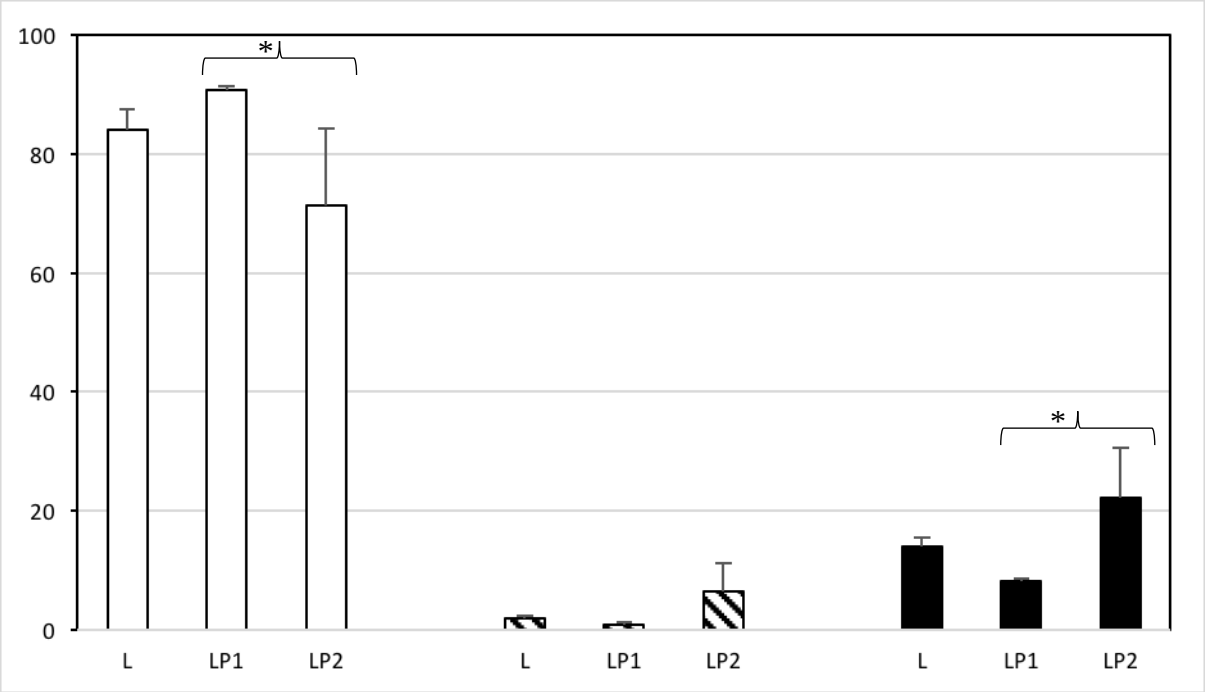

Figure 5.12: Percentage of total drug mass in the basal chamber, remaining on the cell surface, and inside the cells after 4 h after deposition of Linezolid (L), Linezolid + Prep 1 (LP1) and Linezolid + Prep 2 (LP2) at stage 4. (n = 2, mean ± standard deviation (SD)) (n = 3, mean ± SD) (one-way analysis of variance (ANOVA), Tukey's post-tests, * $P \leq 0.05$). □, % in the basal compartment at 240 min; ◪, % on cells at 240 min; ■, % in cells at 240 min.

Surface morphology of Calu-3 cells grown via air-liquid interface (ALI) culture

Scanning electron microscopy was used to study the surface of the cells after 11 days in ALI culture (Figure 5.13), the point at which the TEER maintained its maximum resistance of approximately 750 - 1,000 Ω cm^2 and the cell layer was presumed to be 'intact' with fully formed tight junction proteins accompanied with mucus production. The boundaries between cells were also observed as clearly shown.

Calu-3 cells were clearly shown to express cilia after 7 days in culture (Figure 5.14A & B); a characteristic trait which is only present in a differentiated pseudostratified epithelium. Around 95% of all cells in each sample displayed cilia; however, some cell populations displayed a diverse degree of differentiation. The shape and length of cilia also varied between cells and some displayed a "clumping" characteristic which has also been described by Proctor (Proctor 2013) who reasoned it to be due to the fixing method.

Figure 5.15 displays highly magnified images visualising the particles present on the cell surface post- pMDI fire. Particle size delivered by the pMDI were formulation dependent. The particles have been determined by SEM visualisation and indicated that, in general, the particles were well dispersed 60 seconds post-fire. LP1 displayed a more striated dispersion (Figure 5.16A & B) whereas agglomerates were preferentially seen for LP2. (Figure 5.16C). Images are representative of n=2 independent experiments.

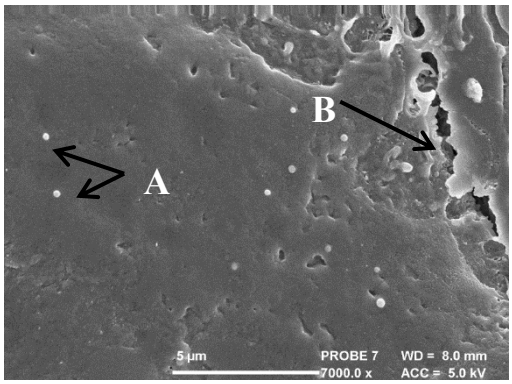

Figure 5.13: (A) Linezolid particles deposited on top of the cells for Stage 2; (B) Examples of tight junction belt fractures after freeze-drying for SEM.

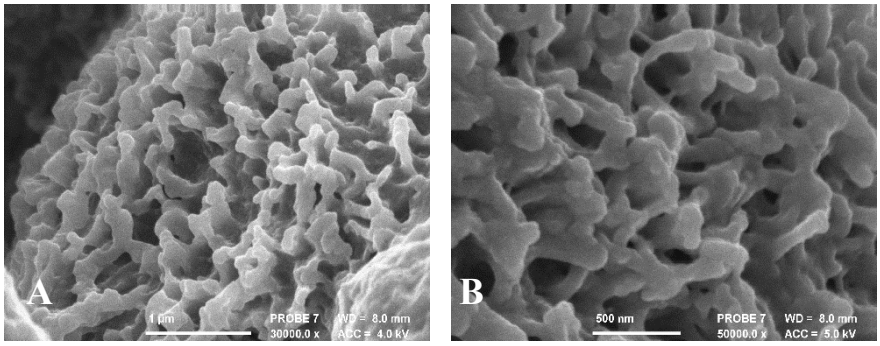

Figure 5.14: SEM images of Calu-3 epithelial layers grown at ALI where cilia on the surface is visible as well as a mucosal layer.

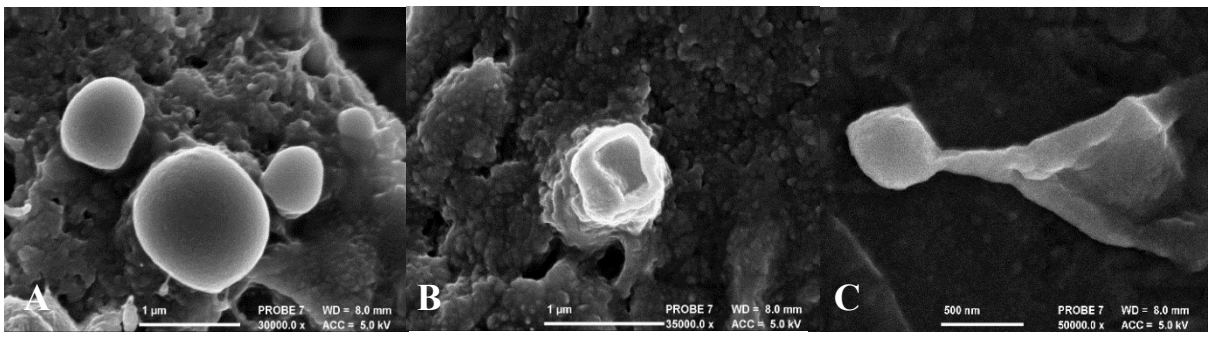

Figure 5.15: SEM images visualising the deposition of Synsurf® and Linezolid on the Calu-3 epithelial layers grown at ALI immediately post pMDI-fire. Droplets were measured between 500 nm and 1 µm.

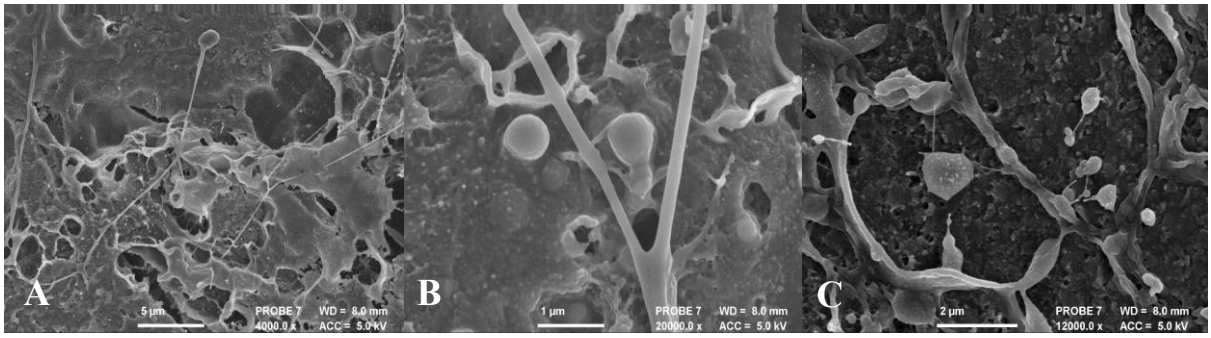

Figure 5.16: SEM images visualising the deposition of Synsurf® on the Calu-3 epithelial layers grown at ALI. Unique spreading properties over the mucosal layers are visible 60 seconds post pMDI-fire for **(A & B)** LP1 and **(C)** LP2.

5.4 Discussion

In this study we compared the diffusion kinetics of linezolid formulated alone and within two preparations of a synthetic surfactant (Synsurf®) based pMDI (LP1 & LP2) across a Calu-3 cell Transwell© culture. The different surfactant drug combinations allow for an evaluation of the significance of the experimental model system, as well as assessment of the formulations providing a possible non-invasive, site-specific, delivery model via pMDI. From a drug delivery perspective this is valuable in the potential development and characterization of a drug-loaded synthetic surfactant.

Under our experimental conditions with a total dose of 500 µg (C_0), fired from the pMDI, the concentration delivered was calculated in the different regions of the lung (Copley Scientific 2017). The same reasoning could be used for the deposition of the compound at the different stages of the NGI^{TM}. In the large conducting airways (Stage 1 of the NGI^{TM}), the potential deposited concentration could amount from 30 to 300 ng/cm^2. The peak concentration in the segmental bronchi (Stage 2) and the small conducting airways (Stage 3) could be 30 ng/cm^2 and in the alveoli, the concentration was shown to be 0.1 – 1 ng/cm^2 (Stage 4-5), which correlated with the total mass deposited on the Calu-3 cell surface (Figure 5.6).

In studies conducted with Caco-2 cells it was shown that the apparent permeability coefficients of compounds with different physicochemical properties and mechanisms of permeation, have a very distinctive effect on the rate of transport. Moreover, drug permeability under Fick's law (Equation 5.1) assumes that the driving force is a concentration gradient difference between the single barrier of the cell monolayer. This either leads to the sequestration of lipophilic drugs into the phospholipid membranes, in transcellular diffusion, or partitioning of hydrophilic drugs into aqueous tight-junctional areas by paracellular diffusion (Mathias, Timoszyk et al. 2002, Hilgers, Conradi et al. 1990). On the other hand, high passive permeability is not necessarily synonymous with high lipophilicity because hydrogen bonding or the presence of an unstirred water layer for a group of compounds can delimit permeability to such an extent that the compounds would exhibit a low permeability (Sun, Pang 2007). This theory may be the explanation for the decreased permeability of linezolid in LP2 containing cholesterol for stage 2 and 3 compared to that of L and LP1. The 2 wt% cholesterol addition to Synsurf® Prep 2, may have contributed to the more lipophilic nature of the compound LP2 as a whole. However,

our data show that LP2 displayed the lowest P_{app} value, albeit not all significant, of all three compounds over all three stages of the NGI™ (Figures 5.7 – 5.9). These findings differ to that from a report by Foster and colleagues that found a linear relationship between the log P_{app} and the log octanol/ water partition coefficient (Foster, Avery et al. 2000). The moderate lipophilicity of linezolid is demonstrated in Figures 5.10 – 5.12 where the remaining concentration values are conveyed for all three pMDI preparations over all 3 stages. Linezolid displays the highest concentration for remaining drug on the surface of the Calu-3 monolayer at stages 2 and 3 compared to that of linezolid in combination with either of the Synsurf® preparations (LP1 & LP2). One can thus speculate that linezolid alone and LP2 has the ability to embed within the cell as their lysate concentration values were found to be similar. In such a situation, electrostatic and hydrophobic interactions are enhanced and may reinforce each other. The different particle sizes among the stages should also to be taken into consideration when deliberating the remaining surface drug of cell lysate concentrations; as there could very well be a higher concentration of drug in a certain particle size distribution and thus more deposited in a certain stage than others.

Synthetic particles of diverse forms have gained increasing attention, as evident from recent studies, which suggested that morphology could influence the mechanisms of drug delivery in many ways (Champion, Katare et al. 2007, Simone, Dziubla et al. 2008, Yoo, Doshi et al. 2011, Kim, Dobson 2009, Venkataraman, Hedrick et al. 2011). In studies conducted by Lu *et al*., it was shown that key parameters such as altering surfactant concentration might alter solution viscoelasticity and surface tension that will change the morphology of the preparation such as filament forming between drops. Instead of filaments breaking up rapidly, they change from a spherical to a spindle-like appearance (Lu, Hou et al. 2015). Under our experimental conditions, we found a more agglomerated and "ribbon-like" nature of LP2 (Figure 5.16C) compared to that of cholesterol-devoid LP1 (Figure 5.16B) that; displayed more perpendicular spreading like characteristics. Moreover, the temperature at which DPPC transitions from the gel phase to the rippled phase (Tp = 36 °C) could also be of significance where DPPC based liposomes form vesicle pearling filaments as seen in Figure 5.16A and B (Lu, Hou et al. 2015, Arai, Yoshimoto et al. 2016). This is reflected for both Synsurf®/linezolid preparations that displayed similar supra-molecular entanglements with the incorporation of droplets and beaded filaments.

The delivered particles and drug dose showed a high dependency from the preparation that has been aerosolised. The Synsurf®/linezolid preparations (LP1 & LP2) showed an assortment of particle ranges from 500 nm to 2 µm in the emitted dose which have been similarly reported by Zanen *et. al.* and other studies (Zanen, Go et al. 1996, Blank, Rothen-Rutishauser et al. 2006, Meindl, Stranzinger et al. 2015). It is generally accepted that to be therapeutically effective, the particles should be in the range of 1 to 5µm since particles > 5µm will generally impact on the mucosa of the oropharynx and be swallowed whereas those < 1µm may remain entrained in the airstream and be exhaled during the next breathing cycle (Copley Scientific 2017). The smaller particles may be deposited peripherally and may be more effective since surfactant is present and functions in the alveolar region. The LP1 and LP2 pMDI particle diameters measured with SEM imaging revealed suitable size distribution to achieve desired lung distribution and still be deemed therapeutically effective. However, fast inhalations (>60 L/min) such as illustrated with a pMDI, result in a reduced peripheral deposition because the aerosol is more readily deposited by inertial impaction in the conducting airway and oropharyngeal regions (Labiris, Dolovich 2003b).

In summary, a synthetic surfactant Synsurf®-based pMDI was investigated to deliver the anti-tubercular drug linezolid. Our data shows that linezolid can be aerosolised in desired particle ranges for optimal lung deposition. The use of the NGI^{TM} and the Calu-3 cell line for the assessment of linezolid dissolution and transport after particle co-deposition has allowed for a more realistic investigation with respect to the *in vivo* situation. This report is the first to studySynsurf® in a pMDI in the evolution of surfactant therapy and drug delivery.

5.5 References

ARAI, N., YOSHIMOTO, Y., YASUOKA, K. and EBISUZAKI, T., 2016. Self-assembly behaviours of primitive and modern lipid membrane solutions: a coarse-grained molecular simulation study. *Physical Chemistry Chemical Physics,* **18**(28), pp. 19426-19432.

BEIJA, M., SALVAYRE, R., LAUTH-DE VIGUERIE, N. and MARTY, J., 2012. Colloidal systems for drug delivery: from design to therapy. *Trends in Biotechnology,* **30**(9), pp. 485-496.

BLANK, F., ROTHEN-RUTISHAUSER, B.M., SCHURCH, S. and GEHR, P., 2006. An optimized in vitro model of the respiratory tract wall to study particle cell interactions. *Journal of Aerosol Medicine,* **19**(3), pp. 392-405.

CHAMPION, J.A., KATARE, Y.K. and MITRAGOTRI, S., 2007. Particle shape: A new design parameter for micro- and nanoscale drug delivery carriers. *Journal of Controlled Release,* **121**(1), pp. 3-9.

COPLEY SCIENTIFIC, 2017-last update, Introduction to Aerodynamic Particle Sizing [Homepage of Copley Scientific Web Design Wida Group], [Online]. Available: http://issuu.com/pyramidpress/docs/inhaler_brochure_2015_rev4__high_re?e=6944369/13992727 [May, 15, 2017].

FLOREA, B.I., CASSARA, M.L., JUNGINGER, H.E. and BORCHARD, G., 2003. Drug transport and metabolism characteristics of the human airway epithelial cell line Calu-3. *Journal of Controlled Release,* **87**(1), pp. 131-138.

FOSTER, K.A., AVERY, M.L., YAZDANIAN, M. and AUDUS, K.L., 2000. Characterization of the Calu-3 cell line as a tool to screen pulmonary drug delivery. *International Journal of Pharmaceutics,* **208**(1), pp. 1-11.

GEORGOPOULOS, D., MOULOUDI, E., KONDILI, E. and KLIMATHIANAKI, M., 2000. Bronchodilator delivery with metered-dose inhaler during mechanical ventilation. *Critical Care,* **4**(4), pp. 227-234.

HAGHI, M., TRAINI, D. and YOUNG, P., 2014. In Vitro Cell Integrated Impactor Deposition Methodology for the Study of Aerodynamically Relevant Size Fractions from Commercial Pressurised Metered Dose Inhalers. *Pharmaceutical research; An Official Journal of the American Association of Pharmaceutical Scientists,* **31**(7), pp. 1779-1787.

HARCOURT, J.L. and HAYNES, L.M., 2013. Establishing a Liquid-covered Culture of Polarized Human Airway Epithelial Calu-3 Cells to Study Host Cell Response to Respiratory Pathogens In vitro. *Journal of Visualized Experiments,* (72), pp. e50157.

HILGERS, A.R., CONRADI, R.A. and BURTON, P.S., 1990. Caco-2 cell monolayers as a model for drug transport across the intestinal mucosa.. *Pharmaceutical Research,* **7**(9), pp. 902-910.

KIM, D.K. and DOBSON, J., 2009. Nanomedicine for targeted drug delivery. *Journal of Materials Chemistry,* **19**(35), pp. 6294-6307.

LABIRIS, N.R. and DOLOVICH, M.B., 2003. Pulmonary drug delivery. Part II: The role of inhalant delivery devices and drug formulations in therapeutic effectiveness of aerosolized medications. *British Journal of Clinical Pharmacology*, **56**(6), pp. 600-612.

LU, J., HOU, R., YANG, Z. and TANG, Z., 2015. Development and characterization of drug-loaded biodegradable PLA microcarriers prepared by the electrospraying technique (poly(L-lactide)) (Report). *International Journal of Molecular Medicine*, **36**(1), pp. 249-254.

MATHIAS, N.R., TIMOSZYK, J., STETSKO, P.I., MEGILL, J.R., SMITH, R.L. and WALL, D.A., 2002. Permeability Characteristics of Calu-3 Human Bronchial Epithelial Cells: In Vitro - In Vivo Correlation to Predict Lung Absorption in Rats. *Journal of Drug Targeting, 2002,* **10**(1), pp. 31-40.

MEINDL, C., STRANZINGER, S., DZIDIC, N., SALAR-BEHZADI, S., MOHR, S., ZIMMER, A. and FRÖHLICH, E., 2015. Permeation of Therapeutic Drugs in Different Formulations across the Airway Epithelium In Vitro. *PloS one,* **10**(8), pp. e0135690.

ONG, H.X., TRAINI, D. and YOUNG, P.M., 2013. Pharmaceutical applications of the Calu-3 lung epithelia cell line. *Expert Opinion on Drug Delivery*, **10**(9), pp. 1287-1302.

SHEN, B.Q., FINKBEINER, W.E., WINE, J.J., MRSNY, R.J. and WIDDICOMBE, J.H., 1994. Calu-3: a human airway epithelial cell line that shows cAMP-dependent Cl-secretion. *American Journal of Physiology-Lung Cellular and Molecular Physiology*, **266**(5), pp. L493-L501.

SIMONE, E.A., DZIUBLA, T.D. and MUZYKANTOV, V.R., 2008. Polymeric carriers: role of geometry in drug delivery. *Expert Opinion on Drug Delivery*, **5**(12), pp. 1283-1300.

SUN, H. and PANG, K.S., 2007. Permeability, Transport, and Metabolism of Solutes in Caco-2 Cell Monolayers: A Theoretical Study. *Drug Metabolism and Disposition*, **36**(1), pp. 102-123.

VENKATARAMAN, S., HEDRICK, J.L., ONG, Z.Y., YANG, C., EE, P.L.R., HAMMOND, P.T. and YANG, Y.Y., 2011. The effects of polymeric nanostructure shape on drug delivery. *Advanced Drug Delivery Reviews*, **63**(14), pp. 1228-1246.

VILJOEN, I., 2005. *The role of surfactant in, and a comparison of, the permeability of porcine and human epithelia to various chemical compounds. (Dissertation)*, Thesis (MScMed)-University of Stellenbosch, 2005.

YOO, J.W., DOSHI, N. and MITRAGOTRI, S., 2011. Adaptive micro and nanoparticles: Temporal control over carrier properties to facilitate drug delivery. *Advanced Drug Delivery Reviews*, **63**(14), pp. 1247-1256.

ZANEN, P., GO, L.T. and LAMMERS, J., 1996. Optimal particle size for β2 agonist and anticholinergic aerosols in patients with severe airflow obstruction. *Thorax*, **51**, pp. 977-980.

6 Concluding Remarks

This study outlined three main themed questions crucial to understanding surfactant pulmonary drug delivery: 1) Is surfactant a suitable inhalable drug carrier within a pMDI, 2) Does surfactant influence anti-tubercular drug activity *in vitro*, and 3) to what extent exogenous surfactants influence alveolar macrophage immunomodulatory characteristics? Moreover, investigating comparable exogenous surfactants indicate that the synthetic surfactant Synsurf® may be a worthy competitor to the natural surfactants, Curosurf® and Liposurf®. Considering this study's unique findings, the elucidation of the possible mechanisms involved in the cyto-protective nature of pulmonary surfactants may offer a window into a patient-specific, individualised treatment option for inflammatory pulmonary disorders.

7 LIST OF ABBREVIATIONS

%	percentage
=	equal
~	approximately
>	greater than
≥	greater than or equal to
<	less than
≤	less than or equal to
±	plus or minus
v/v:	volume per volume
w/v:	weight per volume
w/w:	weight per weight
wt%:	weight percentage
Å	angstrom
°C	degrees Celsius
ε	barrier porosity
μ	micro
ρ	pico
η	viscosity
Ω	ohm
λex	excitation wavelength
λem	emission wavelength
®	registered trademark

ACI:	Andersen cascade impactor
AGC:	Automatic gain control
AIC:	Air interface culture
ALI:	Acute lung injury
AM:	Alveolar Macrophages
ANOVA:	Analysis of variance
APC:	Antigen-presenting cell
APCI:	Atmospheric pressure chemical ionization

API:	Active pharmaceutical ingredient
ARDS:	Adult respiratory distress syndrome
ATCC:	American Type Culture Collection
BAL:	Bronchoalveolar lavage
BALF:	Bronchoalveolar lavage fluid
BCG:	*Mycobacterium bovis* bacille Calmette-Guérin
BE:	Cystic fibrosis bronchiectasis
BMRC:	British Medical Research Council
Ca^{2+}:	Calcium
CCD22:	Coiled-coil domain-containing protein 22
CCL5:	Chemokine (C-C motif) ligand 5
CF:	Cystic fibrosis
CFC:	Chlorofluorocarbon
CFU:	Colony-forming unit
CH_3CN:	Acetonitrile
Cm:	Centimeter
CO_2:	Carbon dioxide
COMMD1:	Copper Metabolism Domain Containing 1
COPD:	Chronic obstructive pulmonary disease
CPAP:	Continuous positive airway pressure
CRD:	Rhodamine dextran concentration
CREB:	cAMP response element binding protein
CUL1:	Cullin–RING
Da:	Dalton
DAN:	2, 3-diaminonaphthalene
DC:	Dendritic cells
DCF:	2′,7′ –Dichlorofluorescein
DCFH-DA:	2′,7′ –Dichlorofluorescein acetate
DDW:	Deionized distilled water
Di:	Diffusion coefficient
DMEM:	Dulbecco’s modified eagle’s medium
DMF:	Dimethylformamide
DMSO:	Dimethyl sulfoxide

DOTS:	Directly observed treatment short-course
DPIs:	Dry powered inhalers
DPPC:	Dipalmitoyl-L-α-phosphatidylcholine
DPI:	Dry powder inhaler
Drp1:	Dynamin-1-like protein
e.g.	For example
EGF:	Epidermal growth factor
ELISA:	Enzyme-linked immunosorbent assay
ESBL:	Extended spectrum β-lactamase-*Klebsiella*
et al.:	And others
EVOM:	EVOM voltohmmeter
F-12:	Dulbecco's Modified Eagle Medium: Nutrient Mixture F-12
FA:	Formic acid
FBS:	Fetal bovine serum
FDA:	US Food and Drug Administration
FDR:	False discovery rate
FHC:	Ferritin Heavy Chain
FP:	Fluticasone propionate
g	Gram
GAPDH	Glyceraldehyde 3-phosphate dehydrogenase
GBS:	Group B streptococcus
GI:	Growth Index
GM-CSF:	Granulocyte macrophage colony stimulating factor
h	Hour
HBSS:	Hank’s buffered salt solution
HCD:	Higher energy collisional dissociation
H&E:	Hematoxylin and Eosin
HEPES:	N-[2-hydroxy-ethyl]piperazine-N’-[2-ethanesulfonic acid]
HFA:	Hydrofluoroalkane
HIV:	Human immunodeficiency virus
HMDS:	Hexamethyldisilazane
HPLC:	High performance liquid chromatography

HPLC-MS/MS: High performance liquid chromatography coupled with tandem mass spectrometry

IAP: Inhibitor of apoptosis protein

ICS: Inhaled corticosteroid

i.e. That is

IL-1β: Interleukin-1 beta

IL-2: Interleukin-2

IL-6: Interleukin 6

IL-8: Interleukin-8

IL-10: Interleukin-10

IL-12: Interleukin-12

IFN-γ: Interferon gamma

INH: Isoniazid

iNOS Inducible nitric oxide synthase

IRAK: Interleukin-1 receptor-associated kinase

IRF3: Interferon regulatory transcription factor

ITIM Immunoreceptor tyrosine-based inhibitory motif

J: Initial rate for mass permeation

JAK/STAT: Janus kinase/Signal transducer and activator of transcription

KC-GRO: Keratinocyte chemoattractant-human growth-regulated oncogene

KEGG: Kyoto encyclopedia of genes and genomes

L: Liter

LDPI: Liposomal dry powder formulations for inhalation

LJ: Lowenstein Jensen

Log P: Octanol-water partition coefficient

LP1: Synsurf®/linezolid preparation 1

LP2: Synsurf®/linezolid preparation 2

LPS: Lipopolysaccharide

LUVs: Large unilamellar vesicles

m: Meter

M: Molarity

M: Methionine

MCP1: Monocyte chemotactic protein 1 (CCL2)

MDR TB:	Multidrug drug-resistant TB
Mg^{2+}:	Magnesium
MGIT :	Mycobacteria Growth Indicator tubes
MIC:	Minimum inhibitory concentration
MIP-1α:	Macrophage Inflammatory Proteins
MLVs:	Multilamellar vesicles
MMTS:	Methane methylthiosulphonate
mN/m:	millinewton/meter
MOMP	Mitochondrial outer membrane permeabilisation
MRNA:	Messenger ribonucliac acid
MRSA:	Methicillin-resistant Staphylococcus aureus
MTB:	Mycobacterium tuberculosis
MTT:	3-(4,5-Dmethylthiazol-2-yl)-2,5-diphenyltetrazolium bromide
MW:	Molecular weight
MyD88:	Myeloid differentiation primary response 88
n:	Nano
NEAA:	Non-essential amino acid
NFκB:	Nuclear factor kappa B
NGI:	Next generation impactor
NK:	Natural killer cells
NO:	Nitric oxide
NQ:	Asparagine/glutamine
nRDS:	Neonatal respiratory distress syndrome
ORAC:	Oxygen radical absorbance capacity
PANPs:	Pathogen-associated molecular patterns
Papp:	Apparent permeability coefficient
PAS:	Para-aminosalicylic acid
PBMC:	Peripheral blood monocytes
PBS:	Phosphate-buffered saline
PC:	Phosphatidylcholine
PCP:	*Pnumocystis pneumonia*
PCS:	Polymer-containing surfactant
PDA:	photo diode array detector

PDD:	Pulmonary drug delivery
PE:	Phosphatidylethanolamin
PENSTREP:	Penicillin-Streptomycin
PG:	Phosphatidyl glycerol
pH:	Negative log of hydrogen ion concentration or activity
PI:	Phosphatidylinositol
pMDI:	Pressurized metered dose inhaler
PPI:	Protein-protein interaction
PRRs:	Pattern recognition receptors
Prx1:	Peroxiredoxin-1
PS:	Phosphatidylserine
Px:	Pixels
PZA:	Pyrazinamide
RANTES:	Regulated on activation, normal T cell expressed and secreted
RDS:	Respiratory distress syndrome
RelA:	Rel-like domain-containing proteins
RHOA:	Ras homolog gene family, member A
RIF:	Rifampicin
RNA:	Ribonucleic acid
ROI	Reactive oxygen intermediates
ROS	Reactive oxygen species
Rpm:	Revolutions per minute
RPMI-1640:	Roswell Park Memorial Institute medium 1640
RR-TB:	Rifampicim-resistant tuberculosis
RSV:	Respiratory syncytial virus
RT:	Respiratory tract
s:	Second
SD:	Standard deviation
SE:	Standard error
SEM:	Scanning electron microscopy
SEM:	Standard error of the mean
SIRPα:	Signal inhibitory regulatory protein α
SM:	Sphingomyolin

SM:	Streptomyocin
SNO:	Denitrosylation
SOCS1:	Suppressor of cytokine signalling 1
SOCS3:	Suppressor of cytokine signalling 3
SP-A:	Surfactant protein A
SP-B:	Surfactant protein B
SP-C:	Surfactant protein C
SP-D:	Surfactant protein D
SPDE:	Monoclonal Mouse anti-SFTPD / Surfactant Protein D Antibody
STRING	Search Tool for the Retrieval of Interacting Genes
SU:	Stellenbosch University
SUVs:	Small unilamellar vesicles
TB:	Tuberculosis
TBS:	Tris buffered saline
TC:	T cells
TCEP:	Triscarboxyethyl phosphine
TDM:	Trehalose dimycolate
TDR-TB:	Totally drug-resistant tuberculosis
TEAB:	Triethylammonium bicarbonate
TEER:	Transepithelial electrical resistance
TLR:	Toll-like receptor
TM:	Trade mark
TNF-α:	Tumor necrosis factor alpha
Tp:	Temperature
Trx1:	Thioredoxin 1
V:	Volt
vs.:	Versus
WHO:	World Health Organization
XDR-TB:	Extensively drug-resistant TB

8 APPENDIX A: MTT Cell Viability Assay Protocol

Method:

Three independent experiments were conducted in triplicate.

- An Isopropanol solution (1%): containing 1 ml concentrated HCl and 99 ml Isopropanol was made.
- Triton solution (0.1 %): 0.1 ml Trition-X-100 + 99 ml dH_20
- An Isopropanol / Triton solution was made in a 50:1 ratio, where 50 ml of 1% Isopropanol was added to 1 ml of 0.1% Triton
- MTT (0.01 g/1 ml PBS) solution was made up just before use. MTT is photosensitive, thus the solution was covered in foil.
- Medium was removed from treated cells.
- PBS (1.5 ml) and MTT (500 µl) was added and allowed to incubate, in 6 well plates covered with foil for 2 hours at 37ºC.
-

NOTE: 0.01g/1 ml PBS (+3 ml PBS) ---> 4mL PBS

4 mL is enough for 8 wells of a 24-well (500 µl per well)

24 wells x 9 plates = 216 wells

216 wells / 8 wells = 27 mL PBS

0.01 x 27 = 0.27g in 27 ml PBS

Then FILTER

Then add another 81 mL PBS

Reference:

Mosmann, T., 1983. Rapid colorimetric assay for cellular growth and survival: application to proliferation and cytotoxicity assays. *Journal of immunological methods*, *65*(1-2), pp.55-63.

9 APPENDIX B: Phalloidin Staining Protocol

Sigma Aldrich Phalloidin from Amanita phalloides – TRITC (P1951)

Emission: 540-545 nm

Excitation: 570-573 nm

Storage: -20^{0}C (Freezer in Histology)

Light sensitive – keep in brown bottle, covered with foil

Stock solution:

- **1mg** made up to **0.5 mg/ml** in **2ml** methanol
- Vortex and store in freezer

Working solution: 50 µg/ml

For 1 ml:

- 100µl stock solution of Phalloidin (10x diluted)
- 10µl DMSO (1%)
- 890 µl PBS (89%)

Stainingprocedure:

- **Wash** cells with PBS
- **Fix cells** for 10 min in 3.7-4% paraformaldehyde made up in PBS
- **Wash** cells 3 x 5 min with PBS
- **Permeabilise** cells for 6 min with 0.1 % Triton X-100 in PBS
- **Wash** cells 3 x 5 min in PBS
- **Blocking** (optional): 5% goat serum – 30 min / overnight in fridge (4ºC)
- **Wash** cells 3 x 5 min with PBS
- **Stain** with Phalloidin-TRITC (50 µg/ml) for 40 min @ room temperature
- **Wash**3 x 5 min with PBS
- Add **Hoechst** (1:8000) for 5 min @ room temperature
- **Wash** 3 x 5 min with PBS
- Let slides **air dry** for a few minutes
- **Mount** upside down on microscope slides (moviol / fluorescent mounting media)
- **Air dry** slides for at least an hour before freezing (Histology freezer).

10 APPENDIX C: ROS Flow Cytometry Protocol

General ROS - DCF (Sigma):

Fluorescent probe 2′,7′ –dichlorofluorescein acetate (DCFH-DA, final concentration 25 µM).

MW: 401.20 g/mol

1. Culture cells in T75 flasks and plate in 12 well plates

2. When cells are 70-80% confluent, begin treatment protocol

3. At the end of treatment protocol, remove media

4. Trypsinise all wells, aspirate in eppi's and centrifuge @ 1500 rpm for 3 min

5. Re-suspend in (300-500 µl) of PBS

(**Note:** the amount of PBS you re-suspend in should be confirmed with CAF staff prior to your experiment:± 1 x 10^6 cells per mL)

6. Add required amount of dye to the PBS cell suspension (5 µl)

7. Incubate cells for 15 mins before taking cells to CAF unit for analysis.

Make a 2 mM concentration of stock solution by weighing out the dye and dissolving in PBS.

Dissolve 0.02g of solute in 25 mL to yield 2mM (or 0.04012g in 50mL)

Therefore 5 µl in 250 µl cell sample to yield 25µM

**DCF is light sensitive so wrap in foil when working with it.*

11 APPENDIX D: Mycoplasma Testing Protocol

When to test: All new cell lines (e.g. gifts from other labs) should be tested as soon as possible (preferably before freezing down to build up stock – might be wasting time and consumables). Frozen stock that has not yet been tested should also be tested once thawed. With continuous culture, routine testing should be performed. This can vary, every 1 - 3 months, and can depend on the amount of work being done – e.g. maybe test just before performing a set of important experiments. Also, important to remember, the more people working in a lab, the greater the risk for contamination.

To test cells, maintain a separate flask in antibiotic-free media – maintain and passage flask 2-3 times. This will allow a "low infection" to proliferate, making it easier to identify.

Day 1

Plate cells:

- Place a clean coverslip (UV sterilised, or dipped in EtOH and allowed to air-dry) in a 35mm dish (or in a well of 6-well plate, however the dish will be easier to handle)
- Seed cells into dish in antibiotic-free media – avoid seeding cells to dense, there should still be spaces between cells on day 3

Day 3

Fixing cells:

- Add 1ml of fixing solution (Metanol:Acetic Acid 3:1) to dish (don't remove media)
- Wait 10 sec, pour off into waste bottle
- Add another 1 ml fixing solution
- Wait 10 sec, pour off into waste bottle
- Rinse 3x gently with dH_20
- Place dish upside down on a paper towel to dry

Stain cells:

- Make sure the coverslip is dry
- Add 100 – 200 µl (just enough to cover coverslip) of Hoechst stain and incubate (covered) for 10 min
- Pour off staining solution

- Rinse 3x gently with dH_20

Mount:

- Place one drop of mounting fluid on a glass microscope slide
- Pick up coverslip with tweezers and dab side on paper towel to remove excess H_20. Place upside down on glass slide

View under fluorescent microscope under blue filter (Ex 360 nm, Em 430 – 490 nm, on Leica Microscope use filter A) – first use 10x then 40X (actual 100x and 400x).

Example: a) clean vs. b) infected

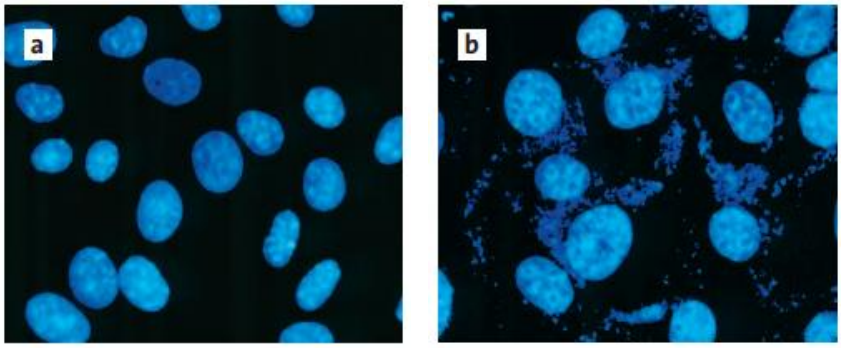

12 APPENDIX E: List of conference contributions, publications and awards

2017 **Faculty of Medicine and Health Sciences 60th Academic Year Day**

Oral Presentation Title: Investigating the Possible Immunoactive and Immunomodulatory properties of various Surfactants

L van Rensburg[1], J van Zyl[2], and J Smith[3]

1, 2. Division of Clinical Pharmacology, Department of Medicine, Faculty of Medicine and Health Sciences, Stellenbosch University, Tygerberg, 3. Department of Pediatrics and Child Health, Tygerberg Children's Hospital, Faculty of Medicine and Health Sciences, Stellenbosch University

2016 **Faculty of Medicine and Health Sciences 60th Academic Year Day**

Poster Presentation Title: Investigating the Possible Immunoactive and anti-mycobacterial properties of various Surfactants

L van Rensburg[1], J van Zyl[2], and J Smith[3]

1, 2. Division of Clinical Pharmacology, Department of Medicine, Faculty of Medicine and Health Sciences, Stellenbosch University, Tygerberg, 3. Department of Pediatrics and Child Health, Tygerberg Children's Hospital, Faculty of Medicine and Health Sciences, Stellenbosch University

2016 **Golden Key honorary society member (Stellenbosch Chapter)**

2016 **International Conference: 2016 All Africa Congress on Pharmacology and Pharmacy**

Misty Hills Hotel and Conference Centre, Muldersdrift, Gauteng, South Africa.

Oral Presentation Title: Investigating the Possible Immunoactive and anti-mycobacterial properties of various Surfactants

2015 **National Conference: South African Society of Basic and Clinical Pharmacology (SASBCP) and Toxicology SA (ToxSA)**, held atThe Wits Club, Johannesburg hosted by The Wits Division of Pharmacology.

Oral Presentation Title: Establishing the Calu-3 Cell line: A model for the investigation of the delivery and deposition of a Surfactant-drug based pressurised metered-dose inhaler (pMDI)

L van Rensburg[1], J van Zyl[2], and J Smith[3]

1, 2. Division of Clinical Pharmacology, Department of Medicine, Faculty of Medicine and Health Sciences, Stellenbosch University, Tygerberg, 3. Department of Pediatrics and Child Health, Tygerberg Children's Hospital, Faculty of Medicine and Health Sciences, Stellenbosch University

2015 **Faculty of Medicine and Health Sciences 59th Academic Year Day**

Poster Presentation Title: Establishing the Calu-3 Cell line: A model for the investigation of the delivery and deposition of a Surfactant-drug based pressurised metered-dose inhaler (pMDI)

L van Rensburg[1], J van Zyl[2], and J Smith[3]

1, 2. Division of Clinical Pharmacology, Department of Medicine, Faculty of Medicine and Health Sciences, Stellenbosch University, Tygerberg, 3. Department of Pediatrics and Child Health, Tygerberg Children's Hospital, Faculty of Medicine and Health Sciences, Stellenbosch University

2015-2016 **NRF Doctoral Freestanding, Innovation, Scarce Skills Scholarship award**

2014 **IUPHAR's 17th World Congress of Basic and Clinical Pharmacology (WCP2014)**

Poster Presentation Title: Drug Susceptibility testing of *Mycobacterium tuberculosis* to Isoniazid and fluoroquinolone entrapped 1,2 Dipalmitoyl-L-α-phosphatidylcholine liposomes

Lyné van Rensburg[1], Johann van Zyl[2], I anWiid[3]

[1´2]Division of Pharmacology, [3]Division Molecular Biology and Human Genetics Faculty of Medicine and Health Sciences, Stellenbosch University, Tygerberg, 7505, South Africa

2014 **University of Bath Global Partner Research scholarship award**
Completed a 6-month research visit to the University of Bath (United Kingdom) under the supervision of Prof. Robert Price.

Peer-reviewed Papers

Pressurised Metered Dose inhaler (pMDI) Deposition of Linezolid combined with a synthetic surfactant Synsurf®: A Calu-3 Model

Lyné van Rensburg[1], Johann M van Zyl[2], and Johan Smith[3]
1, 2. Division of Clinical Pharmacology, Faculty of Medicine and Health Sciences, Stellenbosch University, Tygerberg, 7505, South Africa; 3. Department of Pediatrics, Tygerberg Children's Hospital, Faculty of Medicine and Health Sciences, Stellenbosch University, Stellenbosch University, Tygerberg, 7505, South Africa

Submitted to Drug Design, Development and Therapy, DovePress

The Comparative Effect of Pulmonary Surfactants in combination with Linezolid on the Susceptibility of Mycobacterium tuberculosis *in vitro*.

Lyné van Rensburg[1], Johan M van Zyl[2], Andile H Ngwane[3], and Johan Smith[4]
[1, 2] Division of Clinical Pharmacology, Faculty of Medicine and Health Sciences, Stellenbosch University, Tygerberg, 7505, South Africa; [3] DST/NRF Centre of Excellence for Biomedical Tuberculosis Research/MRC Centre for Tuberculosis Research, Division of Molecular Biology and Human Genetics, Faculty of Medicine and Health Sciences, Stellenbosch University, Tygerberg, 7505, South Africa. [4] Department of Pediatrics, Tygerberg Children's Hospital, Faculty of Medicine and Health Sciences, Stellenbosch University, Stellenbosch University, Tygerberg, 7505, South Africa

Submitted to Experimental and Therapeutic Medicine, Spandidos Publications

Immunoactive properties of Synsurf®, Curosurf® and Liposurf®

Lyné van Rensburg[1], Johann M van Zyl[2], and Johan Smith[3]

[1, 2] Division of Clinical Pharmacology, Faculty of Medicine and Health Sciences, Stellenbosch University, Tygerberg, 7505, South Africa; [3] Department of Pediatrics, Tygerberg Children's Hospital, Faculty of Medicine and Health Sciences, Stellenbosch University, Stellenbosch University, Tygerberg, 7505, South Africa

Submitted to Frontiers in Pharmacology, Inflammation Pharmacology.

Patents

Further Medical Use of Synsurf® Surfactant - PCT International Patent Application *No. PCT/IB2017/056119*